The MIT bag model in nuclear and particle physics.

Evguenii N. Rodionov

Thesis submited for the degree of
Doctor of Philosophy
at
The University of Adelaide
(Department of Physics and Mathematical Physics)
1997

Acknowledgements

First of all I am deeply grateful to my supervisor, Professor Thomas, for his excellent guidance which made it possible for me to undertake research in the theoretical physics most fruitfully. His inspiration in reaching new ideas in the field of physics always encouraged me to investigate the basics of the construction of the world. The feeling of his high professionalism stimulated me in my work and made it possible to keep a constant progress in my study. The successful completion of this thesis is also due to his invaluable assistance.

Further thanks go to Wally Melnitchiouk for his help on the very first stage of my study. I am also indebted to Dr. Crewther for numerous discussions on the most fundamental topics in theoretical physics.

I am especially grateful to Heath O'Connell for all discussions and for being not only my colleague but also an perfect friend and would like to take this opportunity to thank him and Andy Rowlinson for their help in the preparation of this thesis. I am also grateful to Jim McCarthy for his comments and criticism on one of my works.

Acknowledgments must also be made of Profs. Guichon, Londergan, Liu and Saito for very useful collaboration and for countless discussions that I have had for these years.

My understanding of theoretical physics is also partially due to numerous visitors that passed through the University of Adelaide during my studying there and among them Alexander Dorochov. I am thankful to Prof. McKellar for providing me with the computer facilities in Melbourne University.

I want to thank all postgraduate students of the Department of Physics for making up a good company.

Finally, I acknowledge with thanks the financial support of the Australian Government and the University of Adelaide through the award of an Overseas Postgraduate Research Scholarship, without which my study would not have been possible.

Statement

This thesis contains no material which has been accepted for the award of any other degree or diploma in any University and that, to the best of my knowledge and belief, contains no material previosly published or written by another person, except where due reference is made in the text.

I give consent to this copy of my thesis being made avalable for photocopying if applicable, provided due acknowledgement is given.

Signed: Date: 18/8/1997

Abstract

The central subject of this thesis is the application of the MIT bag model to nuclear and particle physics. We investigate the question of symmetry breaking in parton distributions and consider the Drell-Yan process for its experimental verification. The Quark Meson Coupling Model is constructed and applied to finite nuclei to test its validity and reveal possible new directions in the development of nuclear physics.

Contents

List of Figures

1 Introduction

It was the year 1964 when physics took a new step in its development. This year Gell-Mann, Ne'eman [4] and Zweig [5] investigated the symmetry of the known hadrons and found that they can be considered as made up of 3 basic particles, which later were called *up*, *down* and *strange* quarks. Quarks are considered to be elementary particles with size less than 10^{-7} fm [6]. The possible compositeness of quarks was also considered in works [6]-[15] but it was found to be very unlikely.

After the experimental confirmation of the existence of quarks in deep inelastic scattering [16]-[18] particle physics was intensively explored in order to explain the properties of hadrons and the principles of their interactions.

The development of physics based on the quark structure of hadrons went along 3 basic directions:

1. the explanation of the properties of hadrons
2. the prediction of new hadrons
3. the physics of interactions of nucleons.

The bag model played important role in all three cases. It is quite simple by its nature yet very powerful even 30 years after it was introduced. In its elementary representation, the bag model is three quarks in a cavity and it can be enhanced as one wishes: introduce interactions between quarks, insert all sorts of potentials etc..

The earliest of the applications of the bag model was the explanation of the properties of hadrons. In one of the first works on this subject DeGrand et al. [1] managed to find the masses of the light particles, their magnetic moments, weak decay constants and charge radii.

The prediction of new particles is certainly one of the most attractive and beautiful elements in the whole physics. Given a set of quarks and their possible states within a bag anyone can "create" new systems of 2 and 3 quarks. The difficulty is, however, in the calculation of the properties of these hadrons and it was found that the bag model provides a sound base for such investigations.

The physics of the interactions of nucleons is probably the oldest of the puzzles that tortured the minds of scientists from the beginning of 20th century. Almost all the time physicists moved half-intuitively, introducing new particles (π, ρ) and new types of interactions to explain the fact of the attraction between nucleons. By the mid70's the non-relativistic theory of these interactions was perfected [2]. Nevertheless, in addition to an obvious disagreement with some experimentally observed quantities, the fundamental question remained unanswered: what is the basic phenomenon that makes nucleons interact the way they do?

Recently the non-relativistic theory of nucleon interactions was surpassed by a much more powerful model which is based on such fundamental degrees of freedom as quarks and mesons. Even the first analysis showed the powerful potential of this newborn theory and what is important to note here is that the bag model has played a very important role in it.

This thesis has centered around the applications of the bag model to some of the problems in nuclear and particle physics. Part I serves as an introduction to the bag model. In Section 2.1 we review its origin in 1967 followed by seven-years period of absence and its later reemergence in the world of physics as the MIT bag model. We present a short overview of the mathematics of the bag model, and briefly review its role in the modern development of nuclear physics (Section 2.2). In the last Section we concentrate on the method of the calculation of the properties of finite nuclei which we use later in Part III.

As we have mentioned, the experimental observation of quarks was made in deep inelas-

tic scattering (DIS). DIS is certainly the most obvious way of extracting the information on the internal structure of particles. One of the numerous purposes it is used for is the investigation of the quark sub-structure. The experimental results had very poor theoretical support until the attempt was made to use the power of the bag model. In the beginning of Part II we make estimates of charge symmetry breaking in parton distributions, finding values that significantly exceed those expected. We investigate all the possible sources of difference between the distributions of down quarks in the proton and up quarks in the neutron, such as the mass difference between the nucleons, the differences of masses of intermediate states, etc..

In Chapter 7 we discuss the problems of the numerical evolution of structure functions by analyzing and comparing many methods - e.g. those based on Bernstein polynomials, the Altarelli-Parisi equations and approximations of the type $q(x) = c(d+x)^a(1-x)^b$.

Apart from DIS we consider another quite powerful way of studying hadronic substructure - the Drell-Yan process. A thorough investigation of its possibilities in Chapter 8 led us to the idea of an experimental measurement of the value of charge symmetry violation (which we discuss in Section 6.2) in the pion and the nucleon.

Although valence quark distributions are very well determined in numerous experiments there definitely is some shortage of precise data on sea-quark distributions. Continuing the investigation of the advantages of the Drell-Yan process in Section 8.3, we found that by using the combination of π^+ and π^- measurements on deuterium it is possible to extract the pion sea distribution. We also study the role of charge symmetry violation to see if its contribution is sufficiently small that it does not interfere with this determination.

Lastly, the third part of this work is completely devoted to the application of the bag model to nuclear physics. The phenomenon of the interaction of nucleons is, certainly, one of the fundamental questions in this field and the efforts of scientists over the last 80 years led finally to the development of a new theory - the Quark Meson Coupling Model [3], which is based on quark degrees of freedom and at the moment is the most realistic such model. We continue the investigation of the QMC model in an attempt to describe the properties of finite nuclei.

Finally we review all the achievements that we have managed to reach within this work and take a glance at the directions in which it can be continued.

Part I
The MIT bag model

2 The bag model in particle physics.

2.1 Origins of the model

The first description of the bag model appeared in 1967 with the publication of the work by P.N. Bogoliubov titled "Sur un modéle à quarks quasi-indépendants"[1] [19]. In this model, Bogoliubov considered three massless quarks in a vacuum cavity of radius R with a finite, spherical, square well potential, which finally was set to infinity. The radius, R, of the cavity was chosen so as to relate the energy of the 3 quarks to the mass of the hadron. Although this model has a few defects, the major one being the violation of the energy-momentum conservation, it was quite surprising that the estimate of the mass of the nucleon with one of its quarks excited from $1s_{1/2}$ to $2s_{1/2}$ state yielded 1.446 GeV, in comparison with the experimental value of 1.412 GeV[2]. It seems that because the paper was written in French it was not well-known, and with the passing years was almost forgotten.

Seven years later, in 1974, a group of five scientists from the Massachussets Institute of Technology "reinvented" the bag model [22] and it was only after this that they learned about Bogoliubov's paper. Nowadays their model, which is essentially an enhanced version of Bogoliubov's, is referred to as MIT bag model. The problem of the violation of energy-momentum conservation was solved by the inclusion of the phenomenological "confining pressure", while provided a mechanism for "natural" confinement[3] and also cast the model in a Lorentz-covariant form (see Fig 1). It has become possible to calculate properties of nucleons, such as charge radii, axial-vector charges and the gyromagnetic ratios [23] and even now, 20 years later, the MIT bag model is used in many calculations.

But the MIT bag model also has its limitations. When applied to nuclear physics it revealed its main drawback - the violation of chiral symmetry. This problem was non-trival and took the efforts of quite a few scientific groups [25]-[28] to solve it. The developments of the bag model over time have been wide ranging, to the extent that bag models are useful and versatile for the investigation of nucleons and we could cite many more publications on this topic [29]-[36], among which are works on such important questions as the incorporation of the sigma-field (soliton bag model) [30]-[33].

[1] "On the model of quasi-independent quarks."

[2] This process is known as Roper resonance.

[3] As a matter of fact the physics of the phenomenon of confinement started developing only few years ago. In 1991 V.N. Gribov suggested the "Possible solution of the problem of quark confinement" [20, 21], where he came to the conclusion that the mechanism of stability of supercharged nuclei, which is primarily due to the Pauli principle, "seems to be the unique possibility to bind a particle in a small region of space".

2.2 Mathematics of the bag model

We begin our investigation of the bag model by reviewing its basic mathematical structure. We present here the deriviation of the formulae of the model with emphasis on further application in this work, but one can find more thorough discussions of some of the questions in Ref. [19]-[24]. A clear understanding of the mathematics of the bag model is crucial for its further application in the theories of nuclear, particle and any other fields of physics which use the bag model, and the results of the present Chapter will be used throughout this work.

To describe the bag model, we consider a system of 3 quarks, each of mass m_q, in a scalar potential U, providing the confinement of quarks in a cavity (and which in reality is a gluonic field) and external fields[4]. In the most general case there are 5 different sorts of fields. Their form can be found from the consideration of the bilinear forms that can be constructed from the components of ψ and ψ^*. The fact that ψ and ψ^* have 4 components each implies the existence of 16 independent quantities, namely:

$\bar{\psi}\psi$	**S**$calar$	(1)	σ
$\bar{\psi}\gamma^5\psi$	**P**$seudoscalar$	(1)	π
$\bar{\psi}\gamma^\mu\psi$	**V**$ector$	(4)	ω, ρ electromagnetic field
$\bar{\psi}\gamma^\mu\gamma^5\psi$	**A**$xialvector$	(4)	
$\bar{\psi}\sigma^{\mu\nu}\psi$	$second-rank$ **T**$ensor$	(6)	

where in the right colomn examples are given of the physical particles which possess the properties of these fields. The Dirac equation which describes system of three quarks in a cavity with vector, V_V and scalar, V_S, external fields has the form:

$$[\gamma_\mu(\hat{p}^\mu + V_V^\mu) - (m_q + V_S + U)]\psi = 0 \tag{1}$$

with

$$\hat{p^\mu} \equiv (i\frac{\partial}{\partial t}, -i\vec{\nabla}). \tag{2}$$

At the moment we do not take care of the signs of the potentials, as we are interested in general solution. Later on we shall work with the Dirac equation containing real fields

$$[\gamma_\mu(\hat{p}^\mu + V_\omega^\mu + \frac{1}{2}\tau^z V_\rho^\mu) - (m_q - V_\sigma + U)]\psi = 0 \tag{3}$$

where

$$\begin{aligned} V_\sigma &= g_\sigma\sigma \\ V_\omega^\mu &= g_\omega\omega^\mu \\ V_\rho^\mu &= g_\rho b^\mu \end{aligned} \tag{4}$$

describe the interaction of quarks with the fields σ, ω and $b(\equiv \rho)$ through the quark-meson coupling constants g_σ, g_ω and g_ρ and τ^z is the third component of the Pauli isospin matrices.

Our task is to find the parameters of the motion of the confined particle, i.e. its energy eigenvalues and wavefunctions and we start by outlining how this is done. In the case of

[4]It is possible to show that a vector type potential is unable to provide the confinement of a fermion in a cavity [37]. This was the reason for using scalar potentials even before the invention of gluons. An example of the application of vector fields can be found in the description of the motion of an electron in an atom [38].

a fermion[5] with energy ε, total angular momentum quantum number j and projection m onto some direction, the solution of the Dirac equation for a free particle

$$(\gamma\hat{p} - m_q)\psi = 0 \tag{5}$$

involves two spatial wave functions corresponding to two different possible values l for a given j and in the standard representation[6] it can be written as

$$\psi_{pjlm} = N \begin{pmatrix} \sqrt{1 + m_q/\varepsilon}\, R_{pl}\Omega_{jlm} \\ \sqrt{1 - m_q/\varepsilon}\, R_{pl'}\Omega_{jl'm} \end{pmatrix} \tag{6}$$

with $l = j \pm 1/2$ and $l' = 2j - l$. The un-normalized radial functions R_{pl} are just spherical Bessel functions[7] $j_l(pr)$:

$$R_{pl} = j_l(pr) \tag{7}$$

obeying the condition of orthogonality[8]

$$\int_0^\infty r^2 R_{p'l'} R_{pl} dr = 0 \tag{8}$$

when $p' \neq p$ or $l' \neq l$.

The spherical spinors, Ω_{jlm}, involve the spin of the particle and can be represented as[9]

$$\begin{aligned} \Omega_{j,j-1/2,m} &= \begin{pmatrix} \sqrt{\frac{j+m}{2j}}\, Y_{j-1/2,m-1/2} \\ \sqrt{\frac{j-m}{2j}}\, Y_{j-1/2,m+1/2} \end{pmatrix} \\ \Omega_{j,j+1/2,m} &= \begin{pmatrix} -\sqrt{\frac{j-m+1}{2j+2}}\, Y_{j+1/2,m-1/2} \\ \sqrt{\frac{j+m+1}{2j+2}}\, Y_{j+1/2,m+1/2} \end{pmatrix}. \end{aligned} \tag{10}$$

We can simplify the expression for the wave function (6) by the use of the relation between the spherical spinors

$$\Omega_{jl'm} = i^{(l-l')} \vec{n}\vec{\sigma}\Omega_{jlm} \tag{11}$$

$$\vec{n} = \frac{\vec{r}}{r} \tag{12}$$

---

[5] An example of a boson confined in a cavity can be found in [39, 40], where the authors found the eigenvalues of gluons in a bag.

[6] In the standard representation, the wave function is represented as $\psi = \begin{pmatrix} \varphi \\ \chi \end{pmatrix}$ where φ and χ are chosen such that for the particle at rest it has the form $\psi_{\vec{p}=0} = \begin{pmatrix} \varphi \\ 0 \end{pmatrix}$. In this representation γ-matrices have the form $\gamma^0 \equiv \beta = \begin{pmatrix} 1 & 0 \\ 0 & -1 \end{pmatrix}$, $\vec{\gamma} = \begin{pmatrix} 0 & \vec{\sigma} \\ -\vec{\sigma} & 0 \end{pmatrix}$.

[7] First two of them are $j_0 = \frac{\sin x}{x}$, $j_1 = \frac{\sin x}{x^2} - \frac{\cos x}{x}$.

[8] We take the functions R, and Ω without normalizing them, being interested only in the normalization of the wave function ψ_{pjlm}.

[9] First few spherical functions Y_{ij} are

$$Y_{00} = \frac{1}{\sqrt{4\pi}}, \qquad Y_{10} = \frac{i\sqrt{3}}{\sqrt{4\pi}}\cos\Theta, \qquad Y_{1,\pm1} = \mp\frac{i\sqrt{3/2}}{\sqrt{4\pi}}\sin\Theta e^{\pm i\varphi}, \quad \ldots \tag{9}$$

and then the wave function aquires the convenient form which is most often used in the literature:

$$\psi_{pjlm} = N \begin{pmatrix} \sqrt{1+m_q/\varepsilon}\, R_{pl}\Omega_{jlm} \\ \sqrt{1-m_q/\varepsilon}\, R_{pl'} i^{(l-l')} \vec{\boldsymbol{n}}\vec{\boldsymbol{\sigma}}\Omega_{jlm} \end{pmatrix}. \tag{13}$$

The wave function for confined particles can be written, without loss of generality, as

$$\psi_{pjlm} = N \begin{pmatrix} g(r)\Omega_{jlm} \\ f(r) i^{(l-l')} \vec{\boldsymbol{n}}\vec{\boldsymbol{\sigma}}\Omega_{jlm} \end{pmatrix} \tag{14}$$

(we could preserve coefficients $\sqrt{1 \pm m_q/\varepsilon}$, but we'll see how they will reappear).

As it is easy to see, it is not possible to solve (1) for arbitrary fields V_i. For practical purposes however, this is not really necessary and this is why we now impose some conditions that will allow us to come to reasonable results:

1. We shall suppose that the non-perturbative gluon field U is much stronger than all other fields (as a consequence we shall neglect the role of all other fields in the confinement of a quark).

2. Fields V_i do not change too fast at the distances of order of 1 fm (this will allow us to consider first order approximations).

Both of these assumptions seem to be consistent with other phenomenology.

3. When considering nuclear matter we shall use the so called "mean - field" approximation[10], where the meson fields (or rather their operators) are replaced by their expectation values, i.e. classical fields and so only V_i^0 will survive out of $V_i^0, V_i^1, V_i^2, V_i^3$. This approximation is better for cases of high nuclear density.

To begin our analysis of confined particles, we shall rewrite Eq. (1) by multiplying -γ^0 on the left (with $V^\mu = \delta_{\mu 0} V^0$)

$$\begin{gathered} -\gamma^0(i\gamma^0\frac{\partial}{\partial t} + i\vec{\gamma}\vec{\nabla} + \gamma^0 V^0 - (m_q^* + U))\psi = 0 \\ m_q^* = m_q + V_S \end{gathered} \tag{15}$$

and making the use of the expressions

$$(\gamma^0)^2 = \mathbf{1}, \qquad \gamma^0\vec{\gamma} = \vec{\alpha} = \begin{pmatrix} 0 & \vec{\sigma} \\ \vec{\sigma} & 0 \end{pmatrix} \tag{16}$$

to get it in the form

$$[-i\frac{\partial}{\partial t} + \vec{\boldsymbol{\alpha}}\hat{\vec{\boldsymbol{p}}} - V^0 + \beta(m_q^* + U)]\psi = 0, \tag{17}$$

whence one can find the expression for the Hamiltonian

$$\begin{aligned} i\frac{\partial\psi}{\partial t} &= \hat{H}\psi \\ &= [\vec{\boldsymbol{\alpha}}\hat{\vec{\boldsymbol{p}}} - V^0 + \beta(m_q^* + U)]\psi. \end{aligned} \tag{18}$$

In the static state, the Hamiltonian does not depend on time explicitly and this allows us to rewrite (18) as

$$i\frac{\partial\psi}{\partial t} = \hat{H}\psi = \varepsilon_n\psi, \tag{19}$$

[10]The mean field approximation was introduced by Walecka [50] in order to simplify the Lagrangian of the system of mesons and nucleons. Before that, the system of integro-differential equations resulting from that Lagrangian could not be solved.

so that the time dependence of the wave function is

$$\psi_n(\vec{r},t) = \psi(\vec{r})e^{-i\varepsilon_n t}. \tag{20}$$

If now we define

$$\varepsilon_n^* = \varepsilon_n + V^0, \tag{21}$$

then (19) becomes

$$[\vec{\alpha}\hat{\vec{p}} + \beta(m_q^* + U)]\psi = \varepsilon_n^*\psi. \tag{22}$$

For the wave function $\psi = \begin{pmatrix} \varphi \\ \chi \end{pmatrix}$, Eq. (22) splits into two equations

$$\begin{cases} (\varepsilon_n^* - m_q^* - U)\varphi = \vec{\sigma}\hat{\vec{p}}\chi \\ (\varepsilon_n^* + m_q^* + U)\chi = \vec{\sigma}\hat{\vec{p}}\varphi \end{cases} \tag{23}$$

Substitution of the functions φ and χ from (14) gives the system (24), where the second equation takes on this form after being multiplied by $(\vec{\sigma}\vec{n})$ and using the relation $(\vec{\sigma}\vec{n})(\vec{\sigma}\vec{n}) = \vec{n}^2 = 1$:

$$\begin{cases} (\varepsilon_n^* - m_q^* - U)g\Omega_{jlm} = i^{(l-l')}(\vec{\sigma}\hat{\vec{p}})(\vec{n}\vec{\sigma})f\Omega_{jlm} \\ (\varepsilon_n^* + m_q^* + U)f\Omega_{jl'm} = i^{(l'-l)}(\vec{n}\vec{\sigma})(\vec{\sigma}\hat{\vec{p}})g\Omega_{jl'm} \end{cases} \tag{24}$$

Further algebraic manipulations can be performed. First, it is possible to rewrite expressions of the form $(\vec{\sigma}\hat{\vec{p}})(\vec{n}\vec{\sigma})$ and $(\vec{n}\vec{\sigma})(\vec{\sigma}\hat{\vec{p}})$ in a more convenient form[11], namely

$$\begin{aligned} (\vec{\sigma}\hat{\vec{p}})(\vec{n}\vec{\sigma}) &= (\hat{\vec{p}}\vec{r} + i\vec{\sigma}[\hat{\vec{p}}\vec{r}])\tfrac{1}{r} = -i\Big(\vec{\nabla}\vec{r} + (\vec{r}\vec{\nabla}) + \vec{\sigma}[\vec{r}\hat{\vec{p}}]\Big)\tfrac{1}{r} \\ (\vec{n}\vec{\sigma})(\vec{\sigma}\hat{\vec{p}}) &= \tfrac{1}{r}(\vec{r}\hat{\vec{p}} + i\vec{\sigma}[\hat{\vec{p}}\vec{r}]) = -i\tfrac{1}{r}\Big((\vec{r}\vec{\nabla}) - \vec{\sigma}[\vec{r}\hat{\vec{p}}]\Big) \end{aligned} \tag{25}$$

where $[\vec{r}\hat{\vec{p}}] \equiv \vec{r} \times \hat{\vec{p}}$.

Second, considering that

$$\vec{\sigma}[\vec{r}\hat{\vec{p}}] = \vec{\sigma}\hat{\vec{l}} = 2\hat{\vec{l}}\vec{s} \tag{26}$$

and that the eigenvalues of $2\hat{\vec{l}}\vec{s}$ are

$$2\vec{l}\vec{s} = \vec{j}^2 - \vec{l}^2 - \vec{s}^2 = j(j+1) - l(l+1) - \frac{3}{4} = \begin{cases} j - 1/2, & l = j - 1/2 \\ -j - 3/2, & l = j + 1/2 \end{cases} \tag{27}$$

we introduce the variable ϖ:

$$\varpi = \begin{cases} -(j+1/2) = -(l+1), & j = l + 1/2 \\ +(j+1/2) = l, & j = l - 1/2 \end{cases} \tag{28}$$

whereupon (24) becomes

$$\begin{cases} (\varepsilon_n^* - m_q^* - U)g\Omega_{jlm} = -i^{(l-l'+1)}\Big[\frac{3f}{r} + (f' - \frac{f}{r}) - (1+\varpi)\frac{f}{r}\Big]\Omega_{jlm} \\ (\varepsilon_n^* + m_q^* + U)f\Omega_{jl'm} = -i^{(l'-l+1)}\Big[g' + (1+\varpi)\frac{g}{r}\Big]\Omega_{jl'm} \end{cases} \tag{29}$$

[11] $(\vec{\sigma}\vec{a})(\vec{\sigma}\vec{b}) = (\sigma_i a_i)(\sigma_j b_j) = a_i(\sigma_i\sigma_j)b_j = a_i(ie_{ijk}\sigma_k + \delta_{ij})b_j = -ia_i e_{ijk}\sigma_j b_k + \delta_{ij}a_i b_j = -i\vec{a}[\vec{\sigma}\vec{b}] + \vec{a}\vec{b} = i\vec{\sigma}[\vec{a}\vec{b}] + \vec{a}\vec{b}$.

This can be rearranged as

$$\begin{cases} f' + \frac{1-\varpi}{r} f + i^{-(l-l'+1)}(\varepsilon_n^* - m_q^* - U)g = 0 \\ g' + \frac{1+\varpi}{r} g - i^{(l-l'+1)}(\varepsilon_n^* + m_q^* + U)f = 0 \end{cases} \tag{30}$$

For convenience we define the function $\tilde{f}$ as

$$\tilde{f} \equiv i^{(l-l'+1)} f \tag{31}$$

and this gives us a system of equations for the unknown functions $g(r)$ and $f(r)$ in the simplest form

$$\begin{cases} \tilde{f}' + \frac{1-\varpi}{r} \tilde{f} + (\varepsilon_n^* - m_q^* - U)g = 0 \\ g' + \frac{1+\varpi}{r} g - (\varepsilon_n^* + m_q^* + U)\tilde{f} = 0 \end{cases} \tag{32}$$

Equation (32) cannot be solved without specifying ϖ and in our further development we shall consider the case of $\varpi = -1$ which corresponds to $s_{1/2}$ state. Now the solution of this system can be found in a standard way. First, we extract the function $\tilde{f}(r)$ from the second equation

$$\tilde{f} = \frac{1}{\varepsilon_n^* + m_q^* + U} g' \tag{33}$$

and substitute it into the first one to find the differential equation of second order for $g(r)$

$$g'' + \frac{2}{r} g' + (\varepsilon_n^{*2} - (m_q^* + U)^2)g = 0 \tag{34}$$

with the obvious conditions that the functions $f(r)$ and $g(r)$ be

$$\text{1) finite :} \qquad \begin{cases} g(r \to 0) \neq \infty \\ g(r \to \infty) \neq \infty \end{cases} \tag{35}$$

and

$$\text{2) continuous :} \qquad \begin{cases} g(R_{-0}) = g(R_{+0}) \\ \tilde{f}(R_{-0}) = \tilde{f}(R_{+0}) \end{cases}$$

It is easy to find the general solution for $g(r)$:

$$g(r) = \frac{1}{r}(c_1 e^{-\sqrt{-\varepsilon_n^{*2} + (m_q^* + U)^2}\, r} + c_2 e^{\sqrt{-\varepsilon_n^{*2} + (m_q^* + U)^2}\, r}), \tag{36}$$

which we expand in a Taylor Series about $r = 0$

$$g(r \to 0) = \frac{c_1 + c_2}{r} + \sqrt{-\varepsilon_n^{*2} + (m_q^* + U_1)^2}\,(-c_1 + c_2) + \frac{\left(-\varepsilon_n^{*2} + (m_q^* + U_1)^2\right)(c_1 + c_2)\, r}{2} + \mathrm{O}(r)^2 \tag{37}$$

to find that $c_1 = -c_2$ for g to be finite at $r = 0$. Fields U_1 and U_2 that we use here represent the scalar field inside and outside the bag shell.

Now we define k_1 and k_2 as

$$\begin{aligned} k_1 &= +\varepsilon_n^{*2} - (m_q^* + U_1)^2 \\ k_2 &= -\varepsilon_n^{*2} + (m_q^* + U_2)^2 \end{aligned} \tag{38}$$

and $g(r)$ becomes for $r < R$

$$\begin{aligned} g(r)_{r<R} &= \frac{1}{r}c_1(e^{-\sqrt{-\varepsilon_n^{*2}+(m_q^*+U_1)^2}r} - e^{\sqrt{-\varepsilon_n^{*2}+(m_q^*+U_1)^2}r}) \\ &= \frac{1}{r}c_1(e^{-i\sqrt{k_1}r} - e^{i\sqrt{k_1}r}) \\ &= \frac{i2c_1}{r}c_1 \sin\sqrt{k_1}r. \end{aligned} \tag{39}$$

As for the large distances from the center of the bag, $g(r)$ behaves like

$$g(r \to \infty) = \frac{c_4}{r}e^{\sqrt{k_2}r}\Big|_{r\to\infty} \tag{40}$$

implying $c_4 = 0$.

The condition of continuity for $g(r)$ at r=R leads to the equation

$$\begin{aligned} g(R_{-0}) &= \frac{2\mathrm{i}}{R}(a_1 + ia_2)\sin\sqrt{k_1}R \\ = g(R_{+0}) &= \frac{1}{R}(b_1 + ib_2)(e^{-\sqrt{k_2}R}) \end{aligned} \tag{41}$$

where we took into account the fact that, in general, the coefficients c_1 and c_3 are complex

$$\begin{aligned} c_1 &= a_1 + ia_2 \\ c_3 &= b_1 + ib_2 \end{aligned} \tag{42}$$

and this gives us the link between coefficients:

$$\begin{aligned} 2a_1\sin(\sqrt{k_1}R) &= b_2e^{-\sqrt{k_2}R} \\ -2a_2\sin(\sqrt{k_1}R) &= b_1e^{-\sqrt{k_2}R} \end{aligned} \tag{43}$$

From the similar condition for function $\tilde{f}$

$$\begin{aligned} \tilde{f}(R_{-0}) &= (a_1 + ia_2)\frac{i}{\varepsilon_n^* + (m_q^* + U_1)}\Big[\frac{1}{R}\sqrt{k_1}\cos(\sqrt{k_1}R) - \frac{1}{R^2}\sin(\sqrt{k_1}R)\Big] \\ = \tilde{f}(R_{+0}) &= (b_1 + ib_2)\frac{1}{\varepsilon_n^* + (m_q^* + U_2)}\Big[-\frac{1}{R^2}e^{-\sqrt{k_2}R} - \frac{1}{R}\sqrt{k_2}e^{-\sqrt{k_2}R}\Big], \end{aligned} \tag{44}$$

we find the equation for determining the possible values of energy by equating the real and imaginary parts[12]

$$\begin{aligned} &\sqrt{\frac{\varepsilon_n - m}{\varepsilon_n + m}}\cos(\sqrt{k_1}R) - \frac{\sin(\sqrt{k_l}R)}{(\varepsilon_n^* + (m_q^* + U_1))R} \\ &+\sin(\sqrt{k_1}R)\Big[\sqrt{\frac{-\varepsilon_n^* + (m_q^* + U_2)}{\varepsilon_n^* + (m_q^* + U_2)}} + \frac{1}{(\varepsilon_n^* + (m_q^* + U_2))R}\Big] = 0. \end{aligned} \tag{45}$$

[12]In the case of vector fields we have $\sqrt{\frac{-\varepsilon_n^* + (m_q^* - U_2)}{\varepsilon_n^* + (m_q^* + U_2)}}$, instead of $\sqrt{\frac{-\varepsilon_n^* + (m_q^* + U_2)}{\varepsilon_n^* + (m_q^* + U_2)}}$, with the sign change in the square root implying the impossibility of confinement by vector fields.

As a first approximation to the real picture we set $U_1 = 0$ and $U_2 = \infty$, in which case $g(r)$ and $f(r)$ are

$$g(r) = A\sqrt{\varepsilon_n^{*2} - m_q^{*2}}\frac{\sin\sqrt{\varepsilon_n^{*2} - m_q^{*2}}r}{\sqrt{\varepsilon_n^{*2} - m_q^{*2}}r} = A\sqrt{\varepsilon_n^{*2} - m_q^{*2}}j_0(\sqrt{\varepsilon_n^{*2} - m_q^{*2}}r) \tag{46}$$

$$\begin{aligned} f(r) &= -i^{-(l-l'+1)}\frac{A}{\varepsilon_n^* + m_q^*}\Big[\frac{\sin\sqrt{\varepsilon_n^{*2} - m_q^{*2}}r}{(\varepsilon_n^{*2} - m_q^{*2})r^{*2}} - \frac{\cos\sqrt{\varepsilon_n^{*2} - m_q^{*2}}r}{\sqrt{\varepsilon_n^{*2} - m_q^{*2}}r}\Big](\varepsilon_n^{*2} - m_q^{*2}) \\ &= -i^{-(l-l'+1)}A(\varepsilon_n^* - m_q^*)j_1(\sqrt{\varepsilon_n^{*2} - m_q^{*2}}r) \end{aligned} \tag{47}$$

with the arbitrary coefficient A which, for convenience, we shall take as

$$A = \frac{1}{\sqrt{\varepsilon_n^*(\varepsilon_n^* - m_q^*)}} \tag{48}$$

and the equation for possible eigenvalues becomes

$$j_0(\sqrt{\varepsilon_n^{*2} - m_q^{*2}}R) = \sqrt{\frac{\varepsilon_n^* - m_q^*}{\varepsilon_n^* + m_q^*}}j_1(\sqrt{\varepsilon_n^{*2} - m_q^{*2}}R). \tag{49}$$

For example, the solution of (49) with $m_q^* = m_q = 0$, $e^* = e$ and x from Eq. (52) is 2.04, 5.40, 8.58, -3.80, -7.00 etc.. $x = 2.04$ corresponds to the $1S_{1/2}$ state, $x = 5.40$ - to the state $2S_{1/2}$ and so on. Negative values correspond to the states of another parity: $x = -3.80$ is the $P_{1/2}$ state. The fact that the positive and negative eigenvalues x differ in magnitude is of pure relativistic origin.

The last parameter to find is the normalization constant N in Eq. (14), which can be extracted from the condition that no quarks penetrate through the boundary of the cavity, i.e.

$$\int_{\text{cavity}} \psi^\dagger(r)\psi(r)d\vec{\boldsymbol{r}} = 1. \tag{50}$$

Finally we present the wavefunction $\psi_{p\frac{1}{2}0m}$ in the form[13]

$$\psi_{p\frac{1}{2}0m} = N\begin{pmatrix} \sqrt{1 + m_q^*/\varepsilon_n^*}j_0(x\frac{r}{R}) \\ i\sqrt{1 - m_q^*/\varepsilon_n^*}j_1(x\frac{r}{R})\vec{\boldsymbol{n}}\vec{\boldsymbol{\sigma}} \end{pmatrix}\Omega_{\frac{1}{2}0m} \tag{55}$$

$$x = R\sqrt{\varepsilon_n^{*2} - m_q^{*2}} \tag{56}$$

$$N^{-2} = 4\pi R^2 j_0^2(x)\frac{2\varepsilon_n^*(\varepsilon_n^* - 1/R) + m_q^*/R}{\varepsilon_n^*(\varepsilon_n^* - m_q^*)} \tag{57}$$

[13]Sometimes it is more convenient to use another representation for the wave function (see for example ref. [41]) and, in fact, we shell use it in the part III.

$$\psi_{p\frac{1}{2}0m} = \frac{N}{\sqrt{4\pi}}\begin{pmatrix} j_0(x\frac{r}{R}) \\ i\beta j_1(x\frac{r}{R})\vec{\boldsymbol{n}}\vec{\boldsymbol{\sigma}} \end{pmatrix}\Omega_{\frac{1}{2}0m} \tag{51}$$

$$x = R\sqrt{\varepsilon_n^{*2} - m_q^{*2}} \tag{52}$$

$$N^{-2} = 2R^4 j_0^2(x)\frac{\varepsilon_n^*(R\varepsilon_n^* - 1) + m_q^*/2}{x^2} \tag{53}$$

$$\beta = \sqrt{\frac{\varepsilon_n^* - m_q^*}{\varepsilon_n^* + m_q^*}} \tag{54}$$

In principle, one can also get Eq. (49) from the consideration of the boundary conditions. Suppose that n_μ is the normal to the sphere. Then the condition of no quark current crossing the boundary implies

$$n_\mu j^\mu \equiv n_\mu \bar{\psi}\gamma^\mu\psi = 0. \tag{58}$$

This can be satisfied in the following two cases

$$\pm i\gamma n\psi = \psi. \tag{59}$$

As a consequence, we come up with the equalities at the boundary

$$\begin{gathered} \mp i\bar{\psi}\gamma n = \bar{\psi} \\ \bar{\psi}\psi = (\mp\bar{\psi}\gamma n)\psi = \bar{\psi}(\mp i\gamma n\psi) = -\bar{\psi}\psi \end{gathered} \tag{60}$$

which imply

$$\bar{\psi}\psi = 0 \tag{61}$$

$$n_\mu\bar{\psi}\gamma^\mu\psi = 0. \tag{62}$$

Substituting the wave function (56) into (59) gives the desired equation for energy eigenvalues, but the problem is, however, that the ambiguity in the sign in Eq. (59), which effects the eigenenergies, cannot be resolved without the detailed investigation we presented above.

The simplest application of the results we have just derived is, probably, the calculation of the mass of a nucleon. In Bogoliubov's model this is just the total kinetic energy

$$M(R) = \frac{3x}{R}\,, \tag{63}$$

but as we have mentioned, this simplified approach leads to the violation of energy-momentum conservation. The MIT bag model introduced in addition a pressure outside the bag, which provides the confinement of quarks

$$M(R) = \frac{3x}{R} + \frac{3\pi}{4}R^3B \tag{64}$$

with the radius of the cavity found from the condition of equilibrium

$$\frac{\partial M(R)}{\partial R} = 0. \tag{65}$$

The consideration of more complicated questions, for example, the spectroscopy of baryonic states, requires the introduction of other terms like one-gluon exchange ΔE_g or center of mass correction Z/R:

$$M(R) = \frac{3x}{R} + \frac{3\pi}{4}R^3B + \Delta E_g + Z/R\,. \tag{66}$$

However, we shall not consider these more sophisticated developments of the bag model, as they will not be of use for our discussions. The formulae we have just derived will be used in the following chapters, where we shall consider such questions as charge symmetry breaking and the development of the new direction in nuclear physics where the internal structure of a nucleon will play crucial role in the description of finite nuclei.

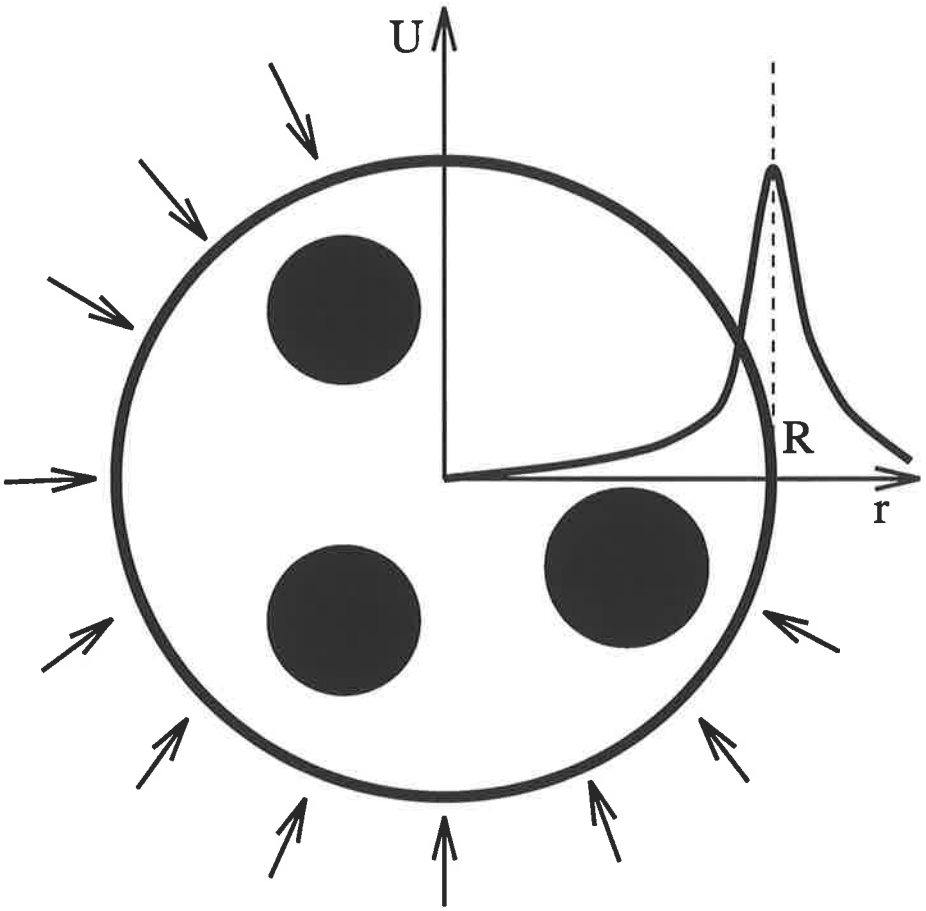

Figure 1: MIT bag model in application to a baryon. Three quarks are confined by external pressure in a cavity of radius R. The motion of the quarks is defined by the form of the scalar potential U.

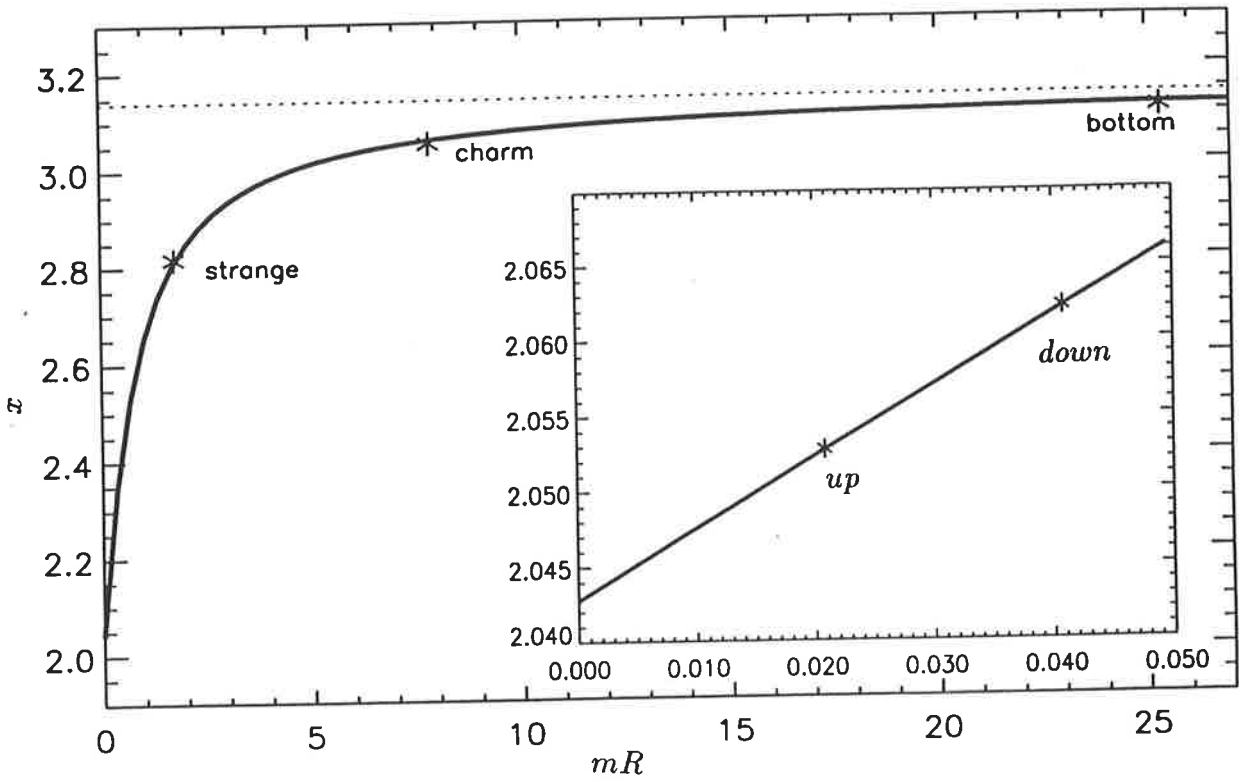

Figure 2: The dependence of the eigenvalue x on the mass of a quark and the size of the bag. (The specific values for up, down etc. correspond to $R = 0.8$ fm.)

3 The bag model in nuclear physics.

3.1 A new direction in nuclear physics.

The existence of strange forces acting between nucleons strongly attracted the attention of scientists from the beginning of our century. They seemed to be strange because they were "invisible" at large distances, independent of the charge of nucleons and also very strong, providing the coexistence of nuclei inspite of the strong repulsion due to Coulomb forces. It was intuitively clear that the clue to this phenomenon was within the nucleons themselves, but nevertheless, the first attempt to solve this question was successfully made about 30 years before the prediction of the existence of quarks by Gell-Mann and N'eman [42] when Yukawa suggested the interaction of baryons through a neutral scalar field [43]. The relevance of this approach was soon noticed and supported by other physicists, and soon Proca extended the model by considering a neutral vector field [44]. After this successful beginning the theory of nuclear physics developed exponentially, and by now there are thousands of works on the subject and even short overviews of the historical progress in this field could constitute a separate work. We direct the reader, interested in the historical process before the advent of the theory of quarks to the review of meson theory of nuclear forces by Green and Sawada [45].

By the beginning of 70's it became clear that even the most sophisticated non-relativistic models [46]-[49] reached their limits and were unable to explain the experimental data. Considering that the mean velocity of nucleons in nucleus is approximately 30-40% of the velocity of light it was obvious that new theories must include relativistic effects. In 1974 Walecka [50] proposed a model which gave quite a reasonable description of the properties of finite nuclei and up to now was considered to be the most realistic one. A prototype of quantum hadrodynamics (QHD) was quantum electrodynamics (QED) from which it derived its name, with the hadro- referring to the interacting particles, hadrons. It is based on nuclear degrees of freedom such as baryon and meson fields. The demand that the theory be renormalizable (as with QED) led to the necessity of fixing coupling constants and masses by experimental data as well as imposing restrictions on the form of the Lagrangian. Actually, there are two QHD models: QHD-I and QHD-II. QHD-I resembles massive QED and allows the calculation of properties of spherical nuclei, $N = Z$. QHD-II is an extension of QHD-I, which incorporates the isovector mesons, π and ρ, to explain the properties of asymmetric nuclear matter and neutron stars with $N \neq Z$.

By now there are a lot of calculations based on these models, and there have been many improvements [51] - [58]. However all have the drawback of being unable to reproduce the properties of finite nuclei without making significant deviations from some of experimental values, e.g. they have too high value of the incompressibility of nuclear matter.

Nevertheless, the simplicity of the model (and the correctness of its main ideas) made it possible to incorporate it in the development of a new theory, we have called it QMC, the Quark Meson Coupling model. The first step in this direction was done by Guichon in 1988 [3]. He proposed a new mechanism for the saturation of nuclear matter based on the internal structure of a nucleon. Nuclear matter is considered as a collection of non-overlapping bags (the radius of a nucleon is about 0.6-0.8 fm. and the distance between two nucleons in the nuclear matter tends to be approximately 1.8 fm) which interact through the exchange of sigma and omega mesons coupled directly to the *quarks* inside these bags. With the use of the bag model it was shown that the internal structure of a nucleon plays a crucial role in the understanding of the phenomenon of saturation. The main point of this model is that the meson fields modify the internal quark motion which

in turn changes the couplings of the mesons to the bound quarks.

The model of Guichon aroused great interest in the possibility of a microscopic description of nuclei and since its creation has been significantly developed. The Fermi motion of the nucleon and center of mass corrections were considered by Fleck et al. [59]; the relationship between this model and QHD was established by K. Saito and A.W. Thomas [61]-[64] who also incorporated the δ meson [63]; we also mention a few other groups which have carried out work related to this model [65].

In part III we shall develop this model, which is based on more fundamental degrees of freedom than those proposed by Walecka, but our calculations are similar in many respects, and so in order to give the reader a clear understanding of the method of calculation, we preview it by a short description of Quantum Hadrodynamics.

3.2 On the method of calculation of the properties of finite nuclei.

We start by giving a mathematical description of the properties of finite nuclei by considering the Lagrangian from QHD:

$$\begin{aligned}\mathcal{L} &= \bar{\psi}(i\gamma_\mu\partial^\mu - M)\psi + \frac{1}{2}(\partial_\mu\sigma\partial^\mu\sigma - m_\sigma^2\sigma^2) + \frac{1}{2}m_\omega^2\omega_\mu\omega^\mu - \\ &\frac{1}{4}F_{\mu\nu}\Omega^{\mu\nu} + \frac{1}{2}m_\rho^2\rho_\mu\rho^\mu - \frac{1}{4}G_{\mu\nu}G^{\mu\nu} + \frac{1}{2}(\partial_\mu\pi\partial^\mu\pi - m_\pi^2) - \\ &\frac{1}{4}H_{\mu\nu}H^{\mu\nu} + g_\sigma\bar{\psi}\sigma\psi - g_\omega\bar{\psi}\gamma_\mu\omega^\mu\psi - g_\rho\bar{\psi}\gamma_\mu\rho^\mu\tau\psi - \\ &\frac{f_\pi}{m_\pi}\bar{\psi}\gamma_5\gamma_\mu\partial^\mu\pi\tau\psi - e\bar{\psi}\gamma_\mu\frac{1}{2}(1+\tau_3)A^\mu\psi \qquad (67)\end{aligned}$$

where

$$\Omega_{\mu\nu} = \partial_\nu\omega_\mu - \partial_\mu\omega_\nu \qquad (68)$$

$$G_{\mu\nu} = \partial_\nu\rho_\mu - \partial_\mu\rho_\nu \qquad (69)$$

$$H_{\mu\nu} = \partial_\nu A_\mu - \partial_\mu A_\nu \qquad (70)$$

and A is the electromagnetic field, M the mass of the nucleon, σ, ω_μ, π and ρ_μ are the meson fields and $m_\sigma, m_\omega, m_\pi$ and m_ρ are their masses respectively. We shall consider the case of a spherical nucleus and work within the mean field approximation where we replace meson field operators in (70) by their expectation values, i.e. classical fields V_σ, V_ω, V_ρ, V_A.

$$\begin{aligned}\mathcal{L} &= \bar{\psi}[i\gamma_\mu\partial^\mu - g_\omega\gamma^0V_\omega - (M - g_\sigma V_\sigma)]\psi \\ &-\frac{1}{2}[(\nabla V_\sigma)^2 + m_\sigma^2V_\sigma^2] + \frac{1}{2}[(\nabla V_\omega)^2 + m_\omega^2V_\omega^2] \\ &+\frac{1}{2}(\nabla V_A)^2 + \frac{1}{2}[(\nabla V_\rho)^2 + m_\omega^2V_\rho^2] \\ &-\bar{\psi}[\frac{1}{2}g_\rho\tau_3\gamma^0V_\rho + \frac{1}{2}e(1+\tau_3)\gamma^0V_A]\psi. \qquad (71)\end{aligned}$$

From the Euler-Lagrange equations

$$\frac{\partial\mathcal{L}}{\partial\phi} - \partial_\mu\left[\frac{\partial\mathcal{L}}{\partial(\partial_\mu\phi)}\right] = 0 \qquad (72)$$

one can easily obtain the equations of motion for the meson fields

$$(\Box + m_\sigma^2)\sigma = g_\sigma \bar{\psi}\psi \equiv g_\sigma \rho_\sigma \tag{73}$$
$$(\Box + m_\omega^2)\omega = g_\omega \bar{\psi}\gamma^0\psi = g_\omega \psi^\dagger \psi \equiv g_\omega \rho_\omega, \tag{74}$$

and the Dirac equation

$$[i\gamma_\mu \partial^\mu - g_\omega \gamma^0 V_\omega - (M - g_\sigma V_\sigma) - \frac{1}{2} g_\rho \tau_3 \gamma^0 V_\rho - \frac{1}{2} e(1+\tau_3)\gamma^0 V_A]\psi = 0. \tag{75}$$

Local source terms, ρ_σ and ρ_ω, can be found with the use of the eq. (14) and finally we write out the complete set of equations which will allow us to calculate the properties of nuclei: wave function

$$\psi_{im} = \begin{pmatrix} G_i(r) \\ i(\vec{\boldsymbol{n}}\vec{\boldsymbol{\sigma}})F_i(r) \end{pmatrix} \Omega_{j_i m} \tag{76}$$

with $\Omega_{j_n m}$ normalized such that

$$\sum_{m=-j_i}^{j_i} \Omega_{j_i m}^\dagger \Omega_{j_i m} = \frac{2j_i + 1}{4\pi}, \tag{77}$$

the equations for the meson fields

$$\begin{cases} \frac{\mathrm{d}^2}{\mathrm{d}r^2} V_\sigma(r) + \frac{2}{r}\frac{\mathrm{d}}{\mathrm{d}r} V_\sigma(r) - m_\sigma^2 V_\sigma(r) & = -g_\sigma \rho_\sigma(r) \\ & \equiv -g_\sigma \sum\limits_{i=n+p} (2j_i+1)\big(G_i^2(r) - F_i^2(r)\big) \\ \frac{\mathrm{d}^2}{\mathrm{d}r^2} V_\omega(r) + \frac{2}{r}\frac{\mathrm{d}}{\mathrm{d}r} V_\omega(r) - m_\omega^2 V_\omega(r) & = -g_\omega \rho_B(r) \\ & \equiv -g_\omega \sum\limits_{i=n+p} (2j_i+1)\big(G_i^2(r) + F_i^2(r)\big) \\ \frac{\mathrm{d}^2}{\mathrm{d}r^2} V_\rho(r) + \frac{2}{r}\frac{\mathrm{d}}{\mathrm{d}r} V_\rho(r) - m_\rho^2 V_\rho(r) & = -\tfrac{1}{2} g_\rho \rho_\rho(r) \\ & \equiv -\tfrac{1}{2} g_\rho \sum\limits_{i=n+p} (2j_i+1)\big(G_i^2(r) + F_i^2(r)\big)(-1)^{t_i - 1/2} \\ \frac{\mathrm{d}^2}{\mathrm{d}r^2} V_A(r) + \frac{2}{r}\frac{\mathrm{d}}{\mathrm{d}r} V_A(r) - m_A^2 V_A(r) & = -e\rho_A(r) \\ & \equiv -e \sum\limits_{i=n+p} (2j_i+1)\big(G_i^2(r) + F_i^2(r)\big)(t_i + \tfrac{1}{2}) \end{cases} \tag{78}$$

and for the baryon wave functions

$$\begin{cases} \frac{\mathrm{d}}{\mathrm{d}r} G_i(r) & + \frac{\varpi}{r} G_i(r) \\ & - [E_i - g_\omega V_\omega(r) - t_i g_b V_b(r) - (t_i + 1/2) e V_A(r) + M - g_\omega V_\omega(r)] F_i(r) = 0 \\ \frac{\mathrm{d}}{\mathrm{d}r} F_i(r) & - \frac{\varpi}{r} F_i(r) \\ & + [E_i - g_\omega V_\omega(r) - t_i g_b V_b(r) - (t_i + 1/2) e V_A(r) - M + g_\omega V_\omega(r)] G_i(r) = 0 \end{cases} \tag{79}$$

where $t_i = 1/2$ for protons, $t_i = -1/2$ for neutrons.

The baryon wave functions satisfy the usual normalization condition reflecting the fact that the probability for finding each particle somewhere in space is equal one:

$$\int_0^\infty \mathrm{d}r\ 4\pi r^2 \big(G_i^2(r) + F_i^2(r)\big) = 1. \tag{80}$$

To define the system of equations completely we also have to impose boundary conditions which, as we shall soon see, can simplify the calculation significantly.

The numerical method for solving this system is described in a few papers [50, 55] without, however, sufficient explanation for some steps. Moreover, we will see that this method can be significantly enchanced.

To begin, from the point of view of boundary conditions, they could be chosen very simply: one arbitrary constant for every derivative, i.e. 2 constants for each of the meson field equations and one for every baryon wavefunction. Thus for a nucleus of oxygen ^{16}O, for example, we would have 14 and for calcium ^{40}Ca - 20 boundary conditions and it is clear that even if we take the simplest method to solve this system it will give us huge calculational time. To come to a reasonable time for the calculation we shall try both - to reduce the number of boundary conditions, by more detailed investigation of the system, and to find the appropriate representation of the equations.

First, we solve the simplest case, where $\varpi = -1$,

$$\begin{cases} \frac{\mathrm{d}^2}{\mathrm{d}r^2}V(r) + \frac{2}{r}\frac{\mathrm{d}}{\mathrm{d}r}V(r) - m^2V(r) = G^2(r) + F^2(r) \\ \frac{\mathrm{d}}{\mathrm{d}r}G(r) - [E + M - V(r)]F(r) = 0 \\ \frac{\mathrm{d}}{\mathrm{d}r}F(r) + \frac{2}{r}F(r) + [E - M + V(r)]G(r) = 0, \end{cases} \tag{81}$$

where the solution gives sufficient information for the set of equations (78-79).

We expand $V(r), G(r)$ and $F(r)$ at $r \to 0$ in a Taylor series like, e.g. $I(r) = C_{i0} + C_{i1}r + C_{i2}r^2$, and substitute into (81). The result is that one of the equations includes a term C_{G1}/r, implying $C_{G1} = 0$ and as a consequence, $C_{F0} = 0$. Finally the solution of the first of equation (81) gives the result which is of particular interest, namely, for the field $V(r)$ to be finite it must have its first derivative equal to zero. It is this constraint that reduces the number of unknown coefficients by one in each of the field equations and by one for every pair of baryon wave functions.

Secondly, as pointed out by Walecka and Serot [2], the contribution from A and ρ is so small that we can neglect them[14]. In this case the system (78-79) simplifies to

$$\begin{cases} \frac{\mathrm{d}^2}{\mathrm{d}r^2}V_\sigma(r) + \frac{2}{r}\frac{\mathrm{d}}{\mathrm{d}r}V_\sigma(r) - m_\sigma^2 V_\sigma(r) = -g_\sigma \sum\limits_{i=n+p} (2j_i+1)\big(G_i^2(r) - F_i^2(r)\big) \\ \frac{\mathrm{d}^2}{\mathrm{d}r^2}V_\omega(r) + \frac{2}{r}\frac{\mathrm{d}}{\mathrm{d}r}V_\omega(r) - m_\omega^2 V_\omega(r) = -g_\omega \sum\limits_{i=n+p} (2j_i+1)\big(G_i^2(r) + F_i^2(r)\big) \\ \frac{\mathrm{d}}{\mathrm{d}r}G_i(r) + \frac{\varpi}{r}G_i(r) - [E_i - g_\omega V_\omega(r) + M - g_\sigma V_\sigma(r)]F_i(r) = 0 \\ \frac{\mathrm{d}}{\mathrm{d}r}F_i(r) - \frac{\varpi}{r}F_i(r) + [E_i - g_\omega V_\omega(r) - M + g_\sigma V_\sigma(r)]G_i(r) = 0 \end{cases} \tag{82}$$

with the boundary conditions for meson fields

$$\begin{cases} V_\omega(0) = C_\omega \\ V'_\omega(0) = 0 \\ V_\sigma(0) = C_\sigma \\ V'_\sigma(0) = 0. \end{cases} \tag{83}$$

The boundary conditions for the baryon wave functions depend on ϖ and, for example, with $\varpi = -1$ are

$$\begin{cases} G(0) = C_G \\ F(0) = 0 \end{cases} \tag{84}$$

The equations above could be solved by applying one of the standard methods for solving systems of differential equations - we shall use the Runge-Kutta method.

[14] We'll investigate the effects of these fields later.

Initially it appeared that it was not possible to get all the functions (sigma and omega fields as well as baryon wave functions) to tend to zero at large distances from the center. We could make only one of the functions behave as we wanted but not all at once. From the mathematical point of view it is not obvious that the system under consideration has to have the solution we expect (when all functions tend to zero at large distances). Nevertheless the existence of such a solution has been shown by several groups (see for example Ref. [60]). The reason for the divergence appears to be very simple: the solution of any of the equations from the system at spatial infinity has two parts - one in the form e^{+r} and another one in the form e^{-r}. At some stage the mistake that accumulates in the calculation allows the development of the solution with positive exponent.

It is at this stage that it was proposed to solve the system from both sides, from $r = 0$ and $r = \infty$, and to match them at some intermediate radius to determine the eigenvalue E. In addition to this Walecka proposed following Green functions

$$D(r, r', m) = -\frac{1}{rr'm} sinh(mr_<)\ e^{-mr_>} \tag{85}$$

to convert the differential equation for meson fields, which were difficult to handle due to them being of the second order, into an integral. Now V_σ and V_ω could be calculated without fear of becoming divergent:

$$V(r) = \int_0^\infty \mathrm{d}r'\ r'^2(-g\rho(r'))D(r, r', m). \tag{86}$$

Using this approach all problems are overcome when we calculate meson fields and wave functions for Helium (Fig. 3, 4)[15].

The time for calculation, however, remains quite large and this presents some difficulties in effective use of the program. We decided to look back and find out whether the method of two-side matching is really necessary even after reformulation of the meson fields.

There is another way of solving the system (81). The idea of the method is simple. Suppose, we have the exact graph of some function, then the deviation from the exact value of energy will send the curve either below the x-axis or it will exponentially grow in the upper plane. If we look at Fig. 4 we see that the two curves, one of which is calculated by matching type method and one by the method just described, and which represent the baryon density, $\rho_B(r) \equiv \sum_{i=n+p} (2j_i + 1)\big(G_i^2(r) + F_i^2(r)\big)$, coincide for both methods.

We have used this new approach for many calculations, some of which will be presented later and have found it to be precise, fast and reliable. While working on it we found that all groups of scientists that make similar calculations use the method developed 20 years ago by Walecka and we now hope that our finding will allow calculations to be carried out more efficiently.

Let us return to the bag model and pose the question of how it actually enters the theory of nuclear physics. In all previous formulae there was no place where we met the quarks or their effects. Mesons were interacting with pointlike nucleons as described by terms of the form $g_i\bar{\psi}V_i\psi$. Couplings g_i are constant and are chosen so as to reproduce the saturation properties of nuclear matter. Using the new approach, however, where mesons couple directly to quarks, the couplings are no longer constants and are determined from the consideration of the meson-nucleon interactions within the bag model[61]-[64]. Strictly speaking, g_σ is now a function of the meson field V_σ. The system (78-79) becomes more complicated, but it can be solved numerically using the method described above. We discuss this new approach to nuclear physics with respect to finite nuclei and nuclear matter in part III as well as providing results of our calculations.

[15]We used the following values of coupling constants and masses: $m_\sigma = 520MeV, m_\omega = 783MeV, M = 939MeV, g_\sigma^2 = 109.6, g_\omega^2 = 190.4$.

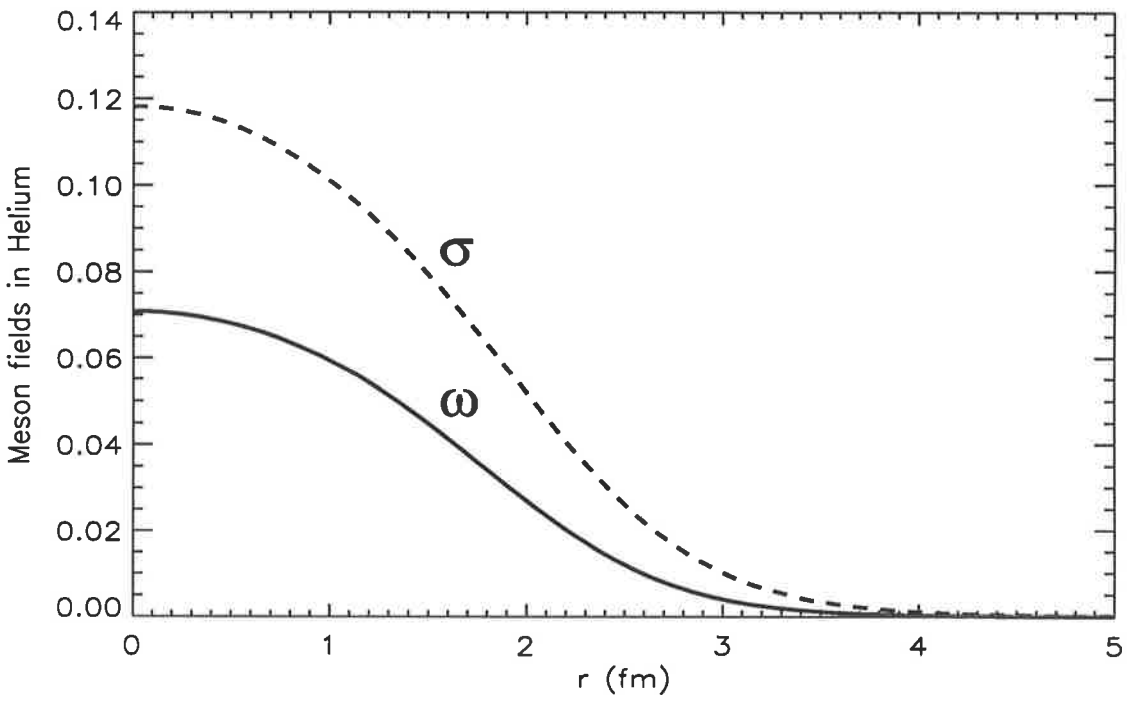

Figure 3: Meson fields σ and ω in Helium.

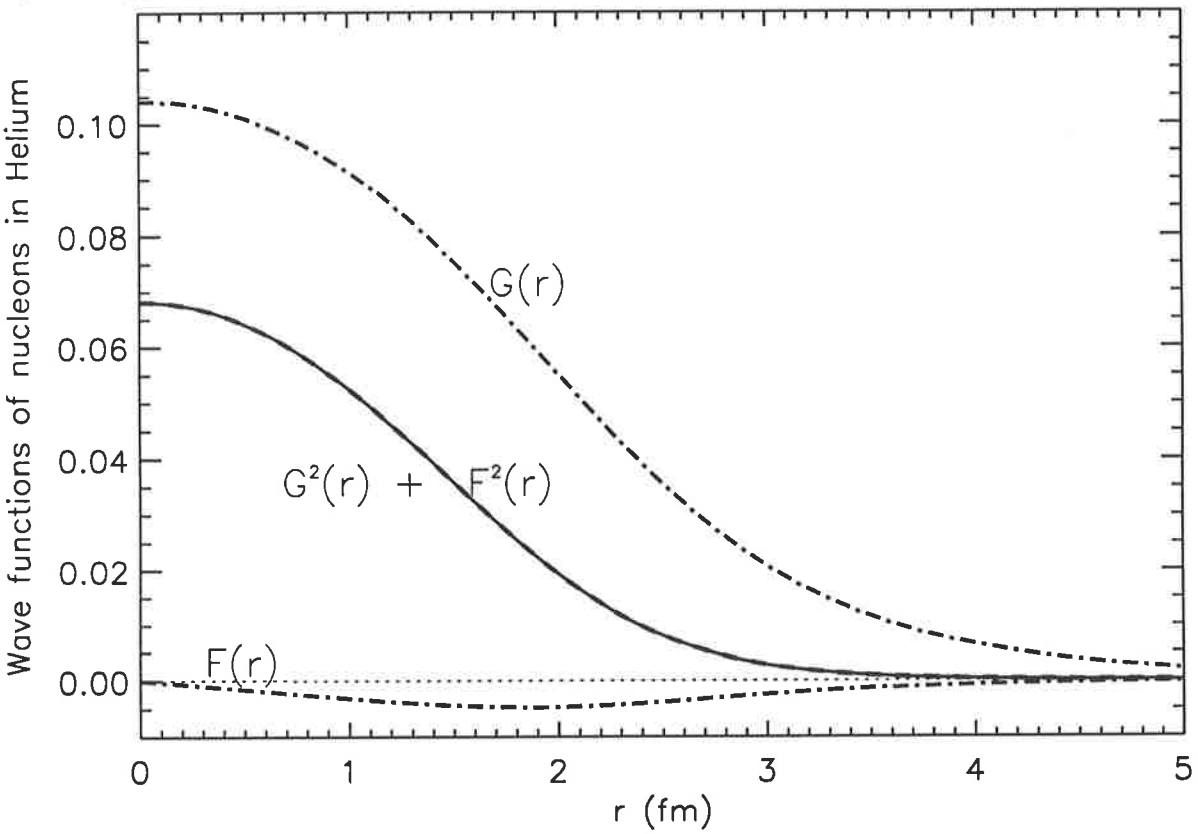

Figure 4: Wave functions $G(r)$, $F(r)$ and baryon density in Helium. There are two curves that represent the baryon density - the solid line is calculated by the method described in Ref. [2] and the dashed line, found by the method described in this work. For the convenience of representation functions $G(r)$ and $F(r)$ are shown on a different scale then the function $G^2(r) + F^2(r)$, which is normalized to $1/4\pi$.

4 Summary

This chapter presented an overview of the origin of the bag model and of the development of QHD. A large part was devoted to the derivation of the formulae describing the bag model and this should be enough to apply them to the questions of particle physics. By now the bag model is so much developed in applications to different directions in physics that the reader can find the answers to almost any of the questions he might have. There are spherical and elliptical bag models, with finite and infinite boundaries; free models and those with external fields; and our discussion above is a convenient starting point for the study of complicated systems or phenomena.

We have also shown how the complicated system of integro-differential equations can be solved in very simple way, and how it can be used to improve the calculations, making them more accurate and efficient.

Addendum:

There have been numerous earlier attempts to model nuclear structure based on the MIT bag, see for example:

1) Shigenori Kagiyama, Akihiro Nakamura, Toshihiro Omodaka (Kagoshima U.), *Z.Phys.* **C53**, 163-168 (1992)
2) M.C. Birse (Manchester U.), J.J. Rehr, L. Wilets (Washington U., Seattle), *Phys.Rev.* **C38**, 359-364 (1988)
3) Chun Wa Wong (UCLA), *Singapore Conf.*, 1197 (1978)
4) C.W. Wong, K.F. Liu (UCLA), *Phys.Rev.Lett.*, **41**, 82 (1978)
5) Brian D. Serot (Indiana U.), John Dirk Walecka (CEBAF), Invited talks given at 7th Int. Conf. on Recent Progress in Many-Body Theories, Minneapolis, MN, Aug 26-31,1991.
6) Qi-Ren Zhang, Bin Li, La-Sheng Yuan, Zhi-Xin Li (Beijing U.), Peking 1987, Proceedings, *Medium energy physics* 522-523.
7) Q. Zhang, C. Derreth, A. Schafer, W. Greiner (Frankfurt U.), *J.Phys.* **G12**, L19-L23 (1986)

Part II
Application of the bag model to particle physics.

5 Introduction

In this section we apply the bag model to studying few body problems in the field of particle physics.

We begin with a short overview of deep inelastic scattering, paying particular attention to the physical meaning of the quantities involved in its description. Then we address the question of charge symmetry violation (CSV) in nucleons by calculating the valence distribution of down quarks in the proton and up quarks in the neutron, taking into consideration the major sources of CSV.

In Chapter 7 we delve into the problem of the numerical evolution of structure functions, introducing two new methods and providing comparisons with calculations based on well-known approaches.

The investigation of CSV described in Section 6.2 is then extended to make similar estimates for the pion. We examine the sensitivity of pion-induced Drell-Yan measurements to such effects and evaluate the background terms in order to study the possibility of providing experimental measurements.

In conclusion, we study the pion sea quark distributions which are presently relatively poorly determined and show how Drell-Yan measurements allow the extraction of the pion sea distribution. We investigate whether the presence of charge symmetry violating contributions still permits the experimental determination of these distributions.

6 Charge symmetry violation in baryons.

6.1 DIS

The process of deep inelastic scattering, which is depicted in Fig 5, is a subject of intensive study and attention [66]-[72]. Usually this is a scattering of a lepton or hadron off another hadron (pion or baryon) and it is the leptonic case we consider here. The parameters needed to describe this process are as follows:

$M-$ mass of the hadron
$m-$ mass of the lepton
$P^\mu = (E, \vec{\boldsymbol{P}})-$ four-momentum of the target (nucleon)
$l^\mu = (e, \vec{\boldsymbol{p}})-$ four-momentum of the lepton
$q^\mu = l^{\mu\prime} - l^\mu-$ four-momentum transfer between lepton and nucleon
$E-$ energy of a hadron
$e-$ energy of a lepton
$\xi = (t, \vec{\boldsymbol{\xi}})-$ time-space coordinates
$f-$ hadronic final state
$\alpha-$ angle between initial and final directions of the motion of a lepton
$x-$ fraction of the target momentum carried by the struck quark $\equiv Q^2/2P \cdot q$.

The prime is kept here for final state particles.

There are three kinematic invariants that can be made out of the four four-momenta defining the initial and final states of the system (i.e. l', l, P and P' with only 3 of them being independent). This is a conseqence of momentum conservation and as such, they are independent of the nature of the particles and their interactions

$q^2 = (l' - l)^2 = (e' - e)^2 - (\vec{\boldsymbol{p}}' - \vec{\boldsymbol{p}})^2$
$s^2 = (l + P)^2 = (e + E)^2 - (\vec{\boldsymbol{p}} + \vec{\boldsymbol{P}})^2$
$P'^2 = M'^2$ - the mass of the hadronic final state.

(In the case of the elastic scattering P' is a known quantity, $P'^2 = P^2$, and so there are just two kinematical invariants needed).

Fig. 5 suggests the following form for the inclusive differential cross section in the laboratory frame:

$$\mathrm{d}\sigma = \frac{\mathrm{d}^3\vec{\boldsymbol{p}}'}{4I(2\pi)^3 2e'} \sum_f (2\pi)^4 \delta^4(P + P' - p - p') \left| -\frac{4\pi e^2}{(p - p')^2} (\bar{u}'\gamma_\mu u) J^\mu_{fi} \right|^2 \tag{87}$$

while for unpolarised lepton scattering it can be represented as

$$\frac{\mathrm{d}^2\sigma}{\mathrm{d}x\mathrm{d}Q^2} = \frac{\pi\alpha^3}{Q^2 e^2 M x^2} L^{\mu\nu}(q^2, s, P^2) W_{\mu\nu}(q^2, P^2). \tag{88}$$

The dependence of the tensor $W_{\mu\nu}$ on two of three invariants is understood from Fig. (5) where only P_i and q_i are relevant to the lower vertex. The tensor $L^{\mu\nu}$ is fully understood, but $W_{\mu\nu}$ contains unknown hadronic currents and we shall concentrate on this.

It is convenient to use the invariant $\nu = \frac{q^\mu P_\mu}{M}$ instead of P'^2 for the structure function $W_{\mu\nu}$ which, as a consequence of energy-momentum conservation, contains

$$\delta\left(1 + \frac{q^2}{2M\nu}\right) \tag{89}$$

in the case of elastic scattering. In the case of the scattering of two particles without annihilation ($q^2 < 0$) it is also convenient to make the change of variable from q^2 to Q^2: $Q^2 = -q^2 > 0$. As for the **physical sense** of q^2 , it is obscured when expressed like $q^2 = (l' - l)^2$ and is easier to understand in the form $-q^2 = 2M\nu - (P'^2 - M^2)$. In the target rest frame ν is the change of the energy of a lepton, $\nu = e' - e$, and so $\sqrt{-q^2/2M}$ is proportional to that part of the energy transferred from the lepton to hadron which goes to the change of the kinetic energy of the latter. It is also useful to note that there are following limits for the ratio $0 \leq \frac{-q^2}{2M\nu} \leq 1$.

After learning more about deep inelastic scattering we can come to another treatment of q^2. In the case when Bjorken limit holds (see below), $-q^2$ can be expressed through

the parameter $x = \frac{-q^2}{2M\nu}$ which is treated as a fractional momentum of the struck quark in the probed nucleon. When $x = 1$ the struck quark uniquely defines the motion of the whole nucleon and all the energy transferred from electron energy goes to the change of the kinetic energy. On the contrary, when $x = 0$ nothing can change the motion of the hadron and all the energy goes to the increase of its mass. In practice, when we deal with a finite range of transferred energies, the Bjorken limit loses its validity for small x, because then the value of q^2 is not large enough.

In the striving for the simplest description of the three- or two-quark system (baryons or mesons) it is tempting to describe deep inelastic scattering from quarks as an incoherent scattering from free particles. It is necessary then to define the conditions under which this description could take place. Namely

1) to consider quarks as free we have to require that the time for the inelastic interaction, which is equal to the lifetime of the virtual photon ($\tau_{dis} \simeq 1/\sqrt{|q^2|}$), is much smaller than the lifetime of the virtual states of quarks. It can be shown [73] that we have to satisfy to the relation

$$\frac{1}{\sqrt{|q^2|}} \ll \frac{1}{\sqrt{(xM)^2 + m_2^2} + \sqrt{((1-x)M)^2 + m_1^2} - \sqrt{2}M} \tag{90}$$

which is clearly valid at sufficiently large q^2.

2) for the scattering from the individual quarks to be incoherent the momentum transfers must be much larger than the mass of the hadron, $-q^2 \gg M$.

It is well known that if we expose a particle to the action of a force, $\vec{F}$, then its average velocity will be closer to the speed of light the larger the force

$$\vec{F} = \frac{\mathrm{d}\vec{p}}{\mathrm{d}t} = \frac{\mathrm{d}}{\mathrm{d}t}\frac{m_0\vec{v}}{\sqrt{1 - \vec{v}^2/c^2}}, \tag{91}$$

but this result plays an important role in deep inelastic scattering and is known as the **light-cone** phenomenon. It is worth noting that the shift in the coordinate of a particle (which, obviously, is the time of the interaction times speed of light) is of the magnitude $\tau c \simeq c/\sqrt{|q^2|}$ and tends to zero as $q^2 \to \infty$. It is also useful to see that spatial distances can be as large as one wishes, $|\Delta\vec{\xi}| \simeq 1/Mx$ and thus it is ξ^2 which is the parameter that should be considered, rather than ξ, in the questions dealing with the expansion over ξ (for example in the expansion of the product of operators $J_\mu(\xi)J^\mu(0)$).

Now, having defined everything necessary for the description of deep inelastic scattering, we write out the explicit form of the tensors $L^{\mu\nu}$ and $W_{\mu\nu}$:

$$L^{\mu\nu} = 4l^\mu l^{\nu\prime} - 2(l^\mu q^\nu + l^\nu q^\mu) + q^2 g^{\mu\nu} \tag{92}$$

$$W_{\mu\nu}(q,P) = \sum_f (2\pi)^4 \delta^4(P' - P - q)\ \langle N|J_\mu(0)|f\rangle\langle f|J_\nu(0)|N\rangle \tag{93}$$

$$= \left(\frac{q_\mu q_\nu}{q^2} - \mathrm{g}_{\mu\nu}\right) W_1(q^2, P^2) + \left(P_\mu - \frac{P\cdot q}{q^2}q_\mu\right)\left(P_\nu - \frac{P\cdot q}{q^2}q_\nu\right) W_2(q^2, P^2) \tag{94}$$

The last equation is constructed from the 5 independent tensors that can be made out of the two four-vectors, q^μ and P^μ, and the tensor $\mathrm{g}_{\mu\nu}$ ($\mathrm{g}_{\mu\nu}, \mathrm{q}_\mu\mathrm{q}_\nu, \mathrm{P}_\mu\mathrm{P}_\nu, \mathrm{q}_\mu\mathrm{P}_\nu, \mathrm{q}_\nu\mathrm{P}_\mu$) under

two conditions:

1. The tensor $W_{\mu\nu}$ should be symmetric in its indices as required by the invariance of the tensor under the operation of time reversal: $W_{\mu\nu} = W_{\nu\mu}$. This condition reduces the number of independent tensors to 4.
2. From the requirement that the Lagrangian be invariant under gauge transformations $W_{\mu\nu}q^{\mu} = 0$ and $W_{\mu\nu}q^{\nu} = 0$.

Tensors W_1 and W_2 can be further calculated for elastic scattering and have the form

$$W_2^{el}(q^2,\nu) = \left(F_1^2(q^2) - \frac{k^2q^2}{4M}F_2^2(q^2)\right)\delta\left(\nu + \frac{q^2}{2M}\right) \tag{95}$$

$$W_1^{el}(q^2,\nu) = -\frac{q^2}{4M}(F_1(q^2) + kF_2(q^2))^2\delta\left(\nu + \frac{q^2}{2M}\right) \tag{96}$$

where form factors $F_1(q^2)$ and $F_2(q^2)$ are defined so that $F_1(0) = 1$ and $F_2(0) = 1$ to ensure the correct electromagnetic and magnetostatic interactions and k is the anomalous magnetic moment in Bohr magnetons, $k = 1.79$.

It is clear that in order to know more about the nuclear substructure we have to provide the electron with energies as large as possible. From the first point of view we can think of the resolving power of the probe of the structure within the nucleon as of the wavelength of the virtual photon $\lambda_q = 1/\sqrt{|q^2|}$. But when $q^2 \to \infty$ the threat arises that the structure functions themselves will become infinite. In an attempt to solve this problem Bjorken made a hypothesis that at high energies the physics of hadrons does not contain characteristic values of mass [74].

Although an infinite q^2 ia a potential source of trouble for of $W(\nu, q^2)$ at fixed ν, Bjorken found that if ν grows such that the ratio q^2/ν is constant then the hadronic tensor will depend on only one, finite, variable $\sim q^2/\nu$. It is convenient to choose that variable in the form $x = \frac{Q^2}{M\nu}$ and then let this Bjorken variable x range from 0 to 1 with $x = 1$ corresponding to elastic scattering.

Now, in the Bjorken limit, the structure functions W_1 and W_2 take the form

$$W_1(q^2,\nu) = \frac{F_1(x)}{M} \tag{97}$$

$$W_2(q^2,\nu) = \frac{F_2(x)}{\nu} \tag{98}$$

and equation (96) simplifies to

$$\begin{aligned} W_{\mu\nu}(x) \;=\; & \left(\frac{q_\mu q_\nu}{q^2} - g_{\mu\nu}\right)\frac{F_1(x)}{M} + \\ & \left(P_\mu - \frac{P\cdot q}{q^2}q_\mu\right)\left(P_\nu - \frac{P\cdot q}{q^2}q_\nu\right)\frac{F_2(x)}{\nu} \end{aligned} \tag{99}$$

There are two more important relations that we show here - between functions $F_1(x)$, $F_2(x)$ (Callan-Gross [75]) and quark distributions, which show the physical sense of structure functions:

$$2xF_1(x) = F_2(x) = \sum_i e_i^2[xq_i(x) + x\bar{q}_i(x)] \tag{100}$$

(q_i can be interpreted here as the probability of finding a quark of type i with fraction x of the proton momentum)

It is possible to calculate these structure functions in the simple, spherical MIT bag model [79][16] and the comparison with the experimental data is good. In the next section we extend that work, using the method of the calculation described there and investigate the question of charge symmetry violation in quark structure functions. We show that the relative difference of the quark distributions for the intermediate values of Bjorken x is significantly bigger than it was previously thought to be.

[16]For related methods of the calculation of parton structure function see, for example, Ref. [77]-[82].

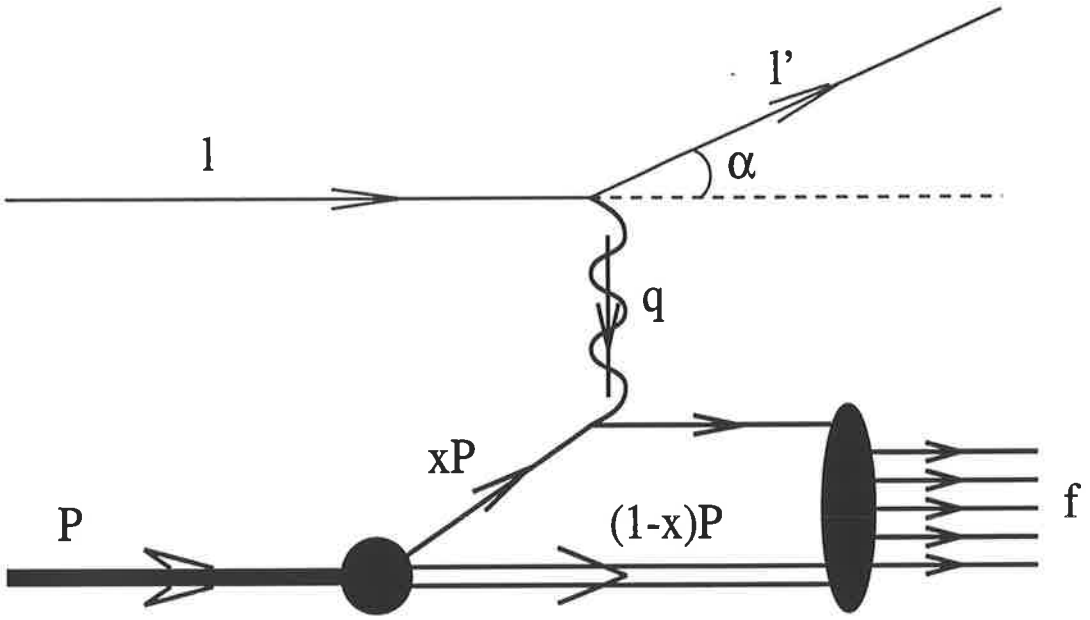

Figure 5: Deep inelastic scattering of a lepton off a nucleon.

6.2 Charge Asymmetry of Parton Distributions

The question of the flavor dependence of parton distributions has been the subject of detailed investigation [79]-[91], particularly since the recent confirmation of the violation of the Gottfried sum-rule [92, 93] by the New Muon Collaboration [94]. Most of this attention has focussed on the rather arbitrary assumption of SU(2) flavor symmetry in the sea, namely that:

$$\overline{d} = \overline{u} = d_{sea} = u_{sea}. \tag{101}$$

This assumption, which is built into almost all phenomenological analyses, is based on the idea that the sea is generated perturbatively through the process $g \rightarrow q\overline{q}$. It is particularly worrying that the violation of the Gottfried sum-rule requires only that:

$$\int \overline{d}(x)dx \neq \int \overline{u}(x)dx, \tag{102}$$

which is much less restrictive than Eq. (101).

Our purpose in this chapter is to investigate an even less restrictive assumption built into *all* analyses of deep-inelastic data. This is charge symmetry, which is part of the notation of the parton model [95]. Although this is, in general, a very good assumption, we will show that for the "minority" quark distributions there is a region of x where **relative** differences between neutron and proton will occur at a level significantly greater than is generally assumed. We will explain the origin of these large relative differences.

Charge symmetry is the invariance of the strong interaction Hamiltonian under a rotation by 180 degrees about the 2-axis in isospace [96]. Such a transformation interchanges protons with neutrons (and up with down quarks). Since these masses are equal to better than 0.2% charge symmetry is expected to be significantly better than isospin in strongly interacting systems. In the context of the parton model, charge symmetry implies $u^n = d^p$, $d^n = u^p$, etc. Indeed the parton distributions $u(x, Q^2)$, $d(x, Q^2)$ and so on are *defined* with respect to the proton, the corresponding quantities in the neutron being determined by charge symmetry.

Within the standard model, $SU(3) \times SU(3)$ chiral symmetry in the light-quark sector is broken by a quark mass term [97, 98]

$$H = \int d^3x(m_u\bar{u}u + m_d\bar{d}d + m_s\bar{s}s). \tag{103}$$

From the observed masses of π, K and η Gasser and Leutwyler [98] found the ratio $m_s/\hat{m} = 25$, where $\hat{m} = \frac{1}{2}(m_u + m_d)$. A connection between m_s and $(m_d - m_u)$ was extracted from the ratio of the strength of SU(3) to SU(2) symmetry breaking obtained from the mass differences $K^+ - K^0, p - n, \Sigma^+ - \Sigma^-, \Xi^0 - \Xi^-$ and from the amplitude for $\rho - \omega$ mixing. The result was $R \equiv (m_s - \hat{m})/(m_d - m_u) \approx 43$ and hence the ratio $m_d/m_u \approx 1.8$ was obtained. The fact that $m_d \neq m_u$ means that both isospin *and* charge symmetry are broken together.

Now to find the absolute values of the light quark masses one has to know $\hat{m}$. An early estimate of Leutwyler [99], based on an SU(6) analysis of meson masses, gave $\hat{m} \approx 5.4$ MeV, while in the framework of QCD sum-rules Vainshtein et al. [100] found $\hat{m} \approx 6.5$ MeV. Another result can be found in the work of S.Narison and E.Rafael [101], who obtained $\hat{m} \approx 4.7$ MeV. We note that to explain the almost perfect isospin symmetry of the strong interactions one should compare the masses of the u and d quarks not to each other but to typical eigenvalues of the strong Hamiltonian – interacting quarks have energies of the order of the strong interaction scale (i.e. of order $m_\rho/2$). Thus one usually expects charge symmetry violation at a level below one percent. As we shall see, at large

x we predict a substantially greater violation of charge symmetry in the minority parton distribution functions.

Our specific aim is to investigate the various effects which break the charge symmetry relation for the valence quarks, $d_V^p(x) = u_V^n(x)$. This requires a method for evaluating quark-parton distributions in a given quark model. Considerable effort has been devoted to this problem over the past twenty years, beginning with the work of Jaffe in the MIT bag model [102] and Le Yaouanc et al. [103] in the non-relativistic quark model [104, 105, 106, 107]. At heart most of these calculations rely on the working hypothesis that the model is an approximate solution to QCD at some low momentum scale, where most of the nucleon's momentum is carried by valence quarks [108]. One evaluates the twist-two distributions at this scale and compares with data after QCD evolution to a scale where the leading twist contribution dominates.

For our calculations we shall use the mathematical apparatus of the MIT bag model, described in Part I, which has the advantage that analytic expressions can be written down for all but the final stages of the calculation. Previous experience suggests that any relativistic confining model should produce similar results. In order to evaluate the bag model parton distributions we employ the method developed by the Adelaide group [109, 110, 111]. This ensures correct support and has been shown to produce quite a respectable description of the valence distribution and the d/u ratio for values of Bjorken x up to $x \simeq 0.7$. In this model the dominant configurations which determine the parton distributions are two-quark and four-quark intermediate states.

Following the approach of Schreiber et al. [111] the spin-averaged, valence parton distribution associated with a two-quark intermediate state is:

$$q_2^{(u,d)}(x) = \frac{M}{2(2\pi)^2} \sum_{m,\mu} < \mu | P_{(u,d),m} | \mu > \int_{|[M^2(1-x)^2 - M_2^2]/2M(1-x)|}^{\infty} p_n dp_n \frac{|\phi_2(\mathbf{p_n})|^2}{|\phi_3(\mathbf{0})|^2} |\Psi_m(\mathbf{p_n})|^2. \tag{104}$$

Here $q_2^{(u,d)}(x)$ is the up or down quark distribution (at the bag scale) for a two-particle intermediate state, $\Psi_m(\mathbf{p_n})$ is the Fourier transform of the struck quark wave function, M is the mass of the neutron or proton and $< \mu | P_{(u,d),m} | \mu >$ is the probability to find a parton of flavor u or d in the proton with spin μ. In addition, M_2 is the mass of the two-quark intermediate state, and $\phi_l(\mathbf{p})$ is the Fourier transform of the Hill-Wheeler overlap function for an l-quark bag. It has the form

$$|\phi_l(\mathbf{p})|^2 = \int d\mathbf{x} e^{-i\mathbf{p}\cdot\mathbf{x}} \Big[\int d\mathbf{y} \Psi^\dagger(\mathbf{y} - \mathbf{x}) \Psi(\mathbf{y}) \Big]^l, \tag{105}$$

and in the specific case considered here it is

$$\frac{|\phi_2(\mathbf{p_n})|^2}{|\phi_3(\mathbf{0})|^2} = \frac{\Omega^2 - \sin^2\Omega}{u} \frac{\int_0^\Omega \frac{dv}{v} \sin\frac{2uv}{\Omega} T^2(v)}{\int_0^\Omega \frac{dv}{v} T^3(v)} \quad , \quad u = |\mathbf{p_n}| R \tag{106}$$

$$\begin{aligned} T(v) &= \frac{1}{2} - (1 - \cos[2\Omega])(1-b)\frac{v^2}{2\Omega^2} - \frac{1}{2}\cos[2v] + \frac{1}{2}b(\cos[2\Omega] - \cos[2(\Omega - v)]) + \\ &+ (\Omega - v)\sin[2v] + \frac{1}{2\Omega}((\sin[2\Omega] - \sin[2v] - \sin[2(\Omega - v)])(1-b)), \end{aligned} \tag{107}$$

where b denotes m/ε and ε is the quark eigenenergy, given by

$$\varepsilon = \frac{1}{R}\Big[\Omega^2 + (mR)^2\Big]^{1/2}. \tag{108}$$

(In order to avoid mixing of Bjorken x with the x defined in (52) we shall temporarily use Ω instead of the x for the latter)

For a quark of mass m (inside the bag) the $1s$ eigensolution of the Dirac equation can be written in the form

$$\Psi_m(x) = N \begin{bmatrix} \sqrt{1+\frac{m}{\varepsilon}}\; j_0\left[\frac{\Omega|x|}{R}\right]\chi_m \\ \sqrt{1-\frac{m}{\varepsilon}}\; i\sigma\cdot\hat{\mathbf{x}} j_1\left[\frac{\Omega|x|}{R}\right]\chi_m \end{bmatrix} \Theta(R-|x|), \tag{109}$$

where we take the bag radius R to be 0.8 fm. The normalisation constant has the form

$$N^{-2}(\Omega) \;=\; 4\pi R^3 {j_1}^2(\Omega)\frac{2\varepsilon(\varepsilon-1/R)+m/R}{\varepsilon(\varepsilon-m)}. \tag{110}$$

The dominant contribution to the valence quark distribution arises from a two-quark intermediate state, while that for antiquarks is associated with four-quark intermediate states. As in Ref. [111] we treat the four-quark term purely phenomenologically, parameterising it as $(1-x)^7$ with the strength chosen to correctly normalise the valence distribution. (After QCD evolution to 10 GeV^2, where the leading twist calculation can be compared directly with data, the minor uncertainty associated with this procedure is restricted to $x \leq 0.1$.) For simplicity we shall concentrate on the difference between the valence d and u distributions in the proton and neutron respectively. If we use an SU(6) spin-flavor wave function for the nucleon[17] the quantum numbers of the spectator pair are uniquely determined in this case to be $S = I = 1$. Taking into account the spin-dependent force needed to split nucleon and delta (one-gluon-exchange in the original bag model, pions or instantons in other versions) we expect this pair to have a mass, M_2, of order 800 MeV. (The splitting between the $S = 0$ and $S = 1$ di-quarks plays a vital role in the spin-flavor dependence of parton distributions [110, 111, 112] – e.g. the d/u ratio mentioned earlier.)

Our aim is to investigate all the possible sources of difference between d_V^p and u_V^n. One can see that there are four such points. We investigate each of them separately to find their relative strength. The most obvious source is the mass difference between the nucleons – the proton mass, $M^{(p)}$, being lighter than that of the neutron, $M^{(n)}$, by 1.3 MeV. These masses enter Eq. (103) both explicitly, and implicitly through the definition of Bjorken x. The contribution to the relative difference in valence quarks, $2(d_V^p - u_V^n)/(d_V^p + u_V^n)$, is shown at $Q^2 = 10$ GeV^2 by the solid curve in Fig. 6, and at the bag scale in Fig. 7. Clearly the relative difference is insensitive to the scale and can be as large as -2% at $x = 0.7$. Incidentally, we do not show the calculated difference beyond $x = 0.7$ because in this region the valence distribution calculated for the bag drops below the experimentally measured distribution. As a result we cannot be sure that the results are reliable there.

Another possible source is the difference of masses of the intermediate states. For the distribution of up quarks in the neutron the two quark intermediate state consists of two down quarks, while for down quarks in the proton we have two up quarks.

Taking into account the greater Coulomb repulsion in the latter case, as well as the u-d mass difference, we expect a mass splitting of approximately 4 MeV between these two

[17]The wavefunctions of a proton and neutron in then SU(6) model are [83]

$$P = \frac{1}{\sqrt{18}}(2u\uparrow d\downarrow u\uparrow + 2u\uparrow u\uparrow d\downarrow + 2d\downarrow u\uparrow u\uparrow - u\uparrow u\downarrow d\uparrow - d\uparrow u\uparrow u\downarrow - u\downarrow d\uparrow u\uparrow - d\uparrow u\downarrow u\uparrow - d\uparrow u\uparrow u\downarrow - u\downarrow u\uparrow d\uparrow) \tag{111}$$

$$N = \frac{1}{\sqrt{18}}(-2d\uparrow u\downarrow d\uparrow + - 2d\uparrow d\uparrow u\downarrow - 2u\downarrow d\uparrow d\uparrow + u\uparrow d\downarrow d\uparrow - d\uparrow u\uparrow d\downarrow - d\downarrow u\uparrow d\uparrow - d\uparrow d\downarrow u\uparrow - u\uparrow d\uparrow d\downarrow - d\downarrow d\uparrow u\uparrow) \tag{112}$$

di-quark states [113]. The effect of this mass splitting between two quark intermediate states rises to +15% at $x = 0.7$, and is shown by the dash-dot curve in Figs. 6 and 7.

The third, and possibly most obvious, place where charge asymmetry may arise in parton distributions is through the dependence of the the bag wave function (Eq. 109) on the quark mass. In fact this correction is the smallest of the three effects considered thus far, being of order 1 % (for quark masses of 4 MeV and 8 MeV [113]). Finally, the non-linear boundary condition leads to a very small change in the bag radius between proton and neutron. This effect also produces a small charge symmetry breaking contribution which can be as large as -2%– as indicated by the dashed curve in Figs. 6 and 7.

In Figs. 6 and 7 we also show the total influence of all the contributions described above using a heavy solid line. Clearly the charge symmetry violation is dominated by the difference in di-quark mass. Note that while we have chosen m_d and m_u to be 8 MeV and 4 MeV respectively our results are not sensitive to the absolute value of the quark mass but to the difference $(m_d - m_u)$. When these calculations were repeated with a bag radius of 0.6 fm very similar results were obtained. Thus the effect reported here is remarkably insensitive to changes in the momentum scale, the bag radius and the absolute values of the quark masses. Finally we note that since the residual di-quark pair for both the distributions u^p and d^n would be a ud pair the difference between these would be much smaller than the case we have studied.

One might ask whether our prediction of such a large charge symmetry violation is an artifact of assuming a fixed diquark mass. In general one might expect a distribution of di-quark masses rather than a single, sharp mass. In Fig. 8 we show the results of using such a distribution. The calculation is identical to that of Fig. 6, except that the diquark mass is averaged over a distribution of masses centered at 800 MeV (d^p) and 804 MeV (u^n) with a width of 200 MeV ($\sim \Lambda_{QCD}$). For $x \sim 0.7$, the predicted charge symmetry violation is reduced somewhat. Nevertheless, the qualitative effect clearly persists and even the quantitative behavior is very similar – except at the largest values of x. This demonstrates that our prediction for significant charge symmetry violation, in the fractional minority quark parton distributions, is dominated by the diquark mass difference of 4 MeV, the fact that the effective average diquark mass is large (roughly 800 MeV), and the fact that $d^p(x) << u^p(x)$ for large x. As all of these assumptions are quite well founded, we believe that our prediction is robust.

Although our interest here is centered on the distributions of valence quarks we would like to present here our estimates for sea quarks as well. The calculation is done by taking into account all of the sources of CSV that were considered for valence quarks. The result is presented in Fig. 9.

Our estimates for charge symmetry breaking in parton distributions are at first sight surprising. One would naively have expected charge symmetry to be obeyed to well within one percent, whereas we find fractional differences between $d_V^p(x)$ and $u_V^n(x)$ up to ten percent. It would clearly be of great interest to test the theoretical ideas presented here experimentally. This is made rather difficult by the absence of a free neutron target. However, it appears that a comparison of deep-inelastic scattering from protons and deuterons, particularly Drell-Yan processes induced by charged pions, could isolate these effects (see Chapter 8). Finally, the significant size of the effect discussed here suggests that one should also review the application of deep-inelastic scattering to extract parameters of the standard model, since the implicit assumption of charge symmetry in the parton distributions may introduce unexpected problems.

To conclude this Section we would like to point out a related paper by E. Sather [116]. Movivated by the work of Refs.[109]-[112] Sather considered the effect of di-quark mass splitting on charge symmetry breaking in parton distributions. Rather than working with a particular model he developed an approximate method for estimating the effect of di-

quark mass splitting. He also found significantly smaller charge symmetry violation for the 'majority' quarks $u^p - d^n$, than for the 'minority' quarks $d^p - u^n$. Because he did not work with a particular model the smaller charge symmetry breaking effects examined in this letter were not considered by Sather. Although the difference $d^p - u^n$ found by Sather was not as large as our result, he showed that even the smaller difference could produce an error in the extraction of $sin^2\theta_W$ as big as 0.002. This large effect makes the need for experimental verification of our result even more pressing.

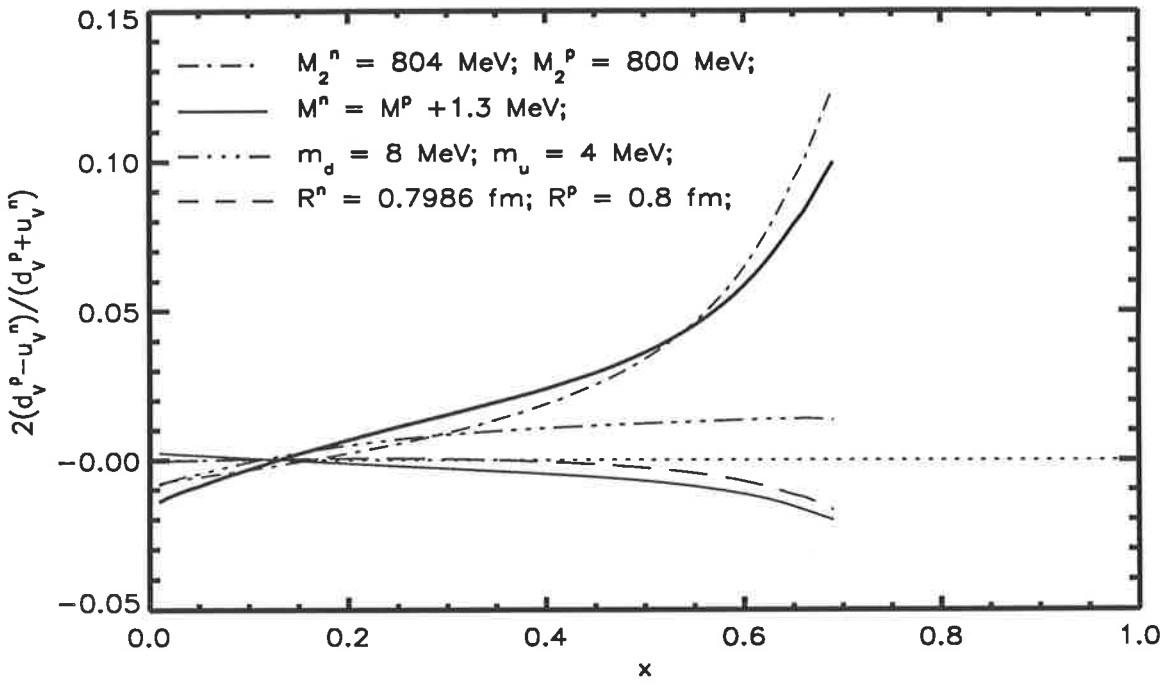

Figure 6: Contributions from various sources to the symmetry breaking for valence quarks at $Q^2 = 10$ GeV^2. Unless otherwise specified, parameters are: $m_d = m_u = 0$ MeV; $M^{(n)} = M^{(p)} = 938.27$ MeV; $M_2^{(n)} = M_2^{(p)} = 800$ MeV; $R^{(n)} = R^{(p)} = 0.8$ fm. The heavy, solid line shows the combined effect of all four contributions.

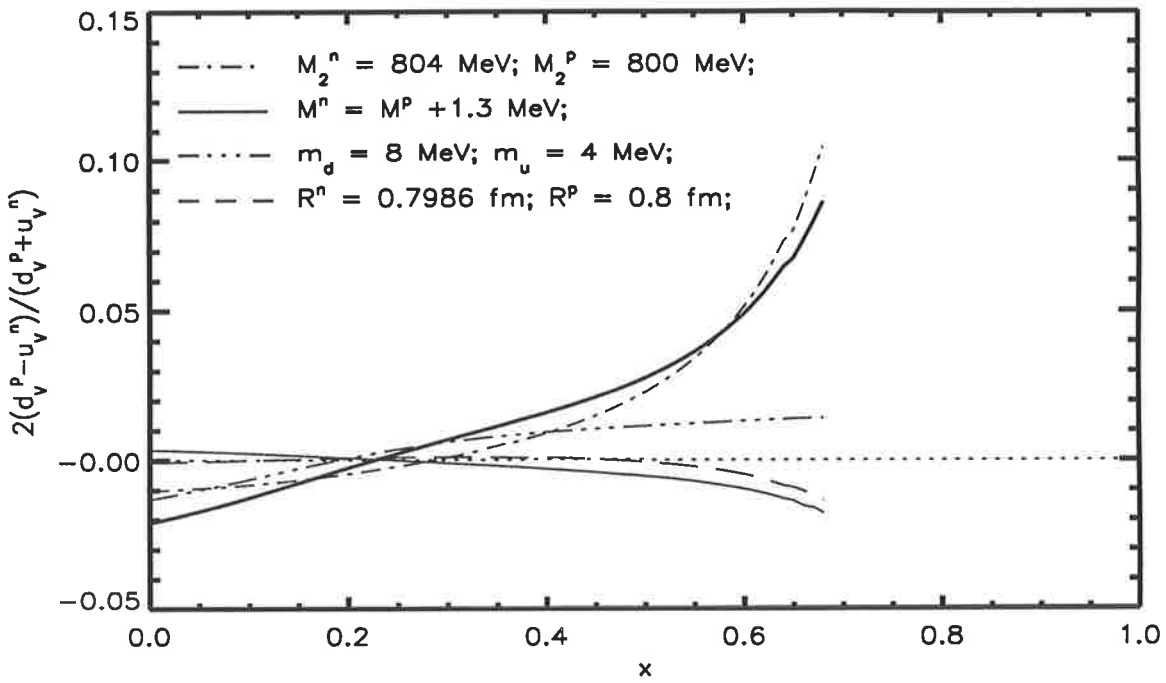

Figure 7: Contributions from various sources to the symmetry breaking for valence quarks at the bag scale. Unless otherwise specified, parameters are: $m_d = m_u = 0$ MeV; $M^{(n)} = M^{(p)} = 938.27$ MeV; $M_2^{(n)} = M_2^{(p)} = 800$ MeV; $R^{(n)} = R^{(p)} = 0.8$ fm. The heavy, solid line shows the combined effect of all four contributions.

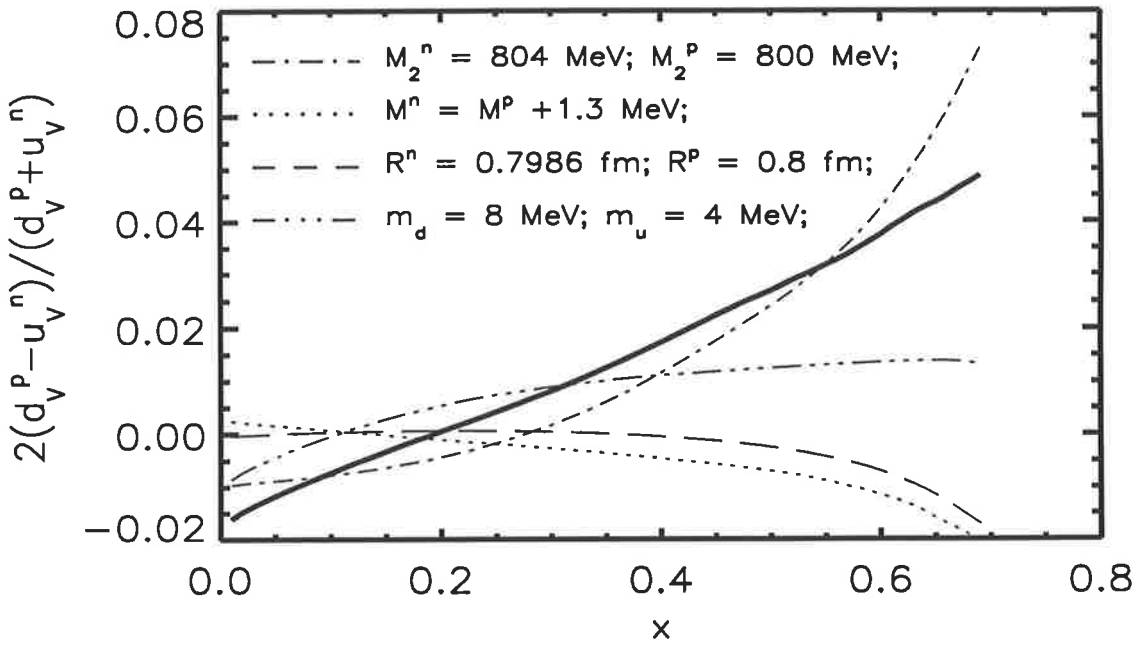

Figure 8: Contributions from various sources to the symmetry breaking for valence quarks at $Q^2 = 10$ GeV^2. Unless otherwise specified, parameters are: $m_d = m_u = 0$ MeV; $M^{(n)} = M^{(p)} = 938.27$ MeV; the average diquark mass is "smeared," with a mean value of 800 MeV and a width of 200 MeV; $R^{(n)} = R^{(p)} = 0.8$ fm. The heavy, solid line shows the combined effect of all four contributions.

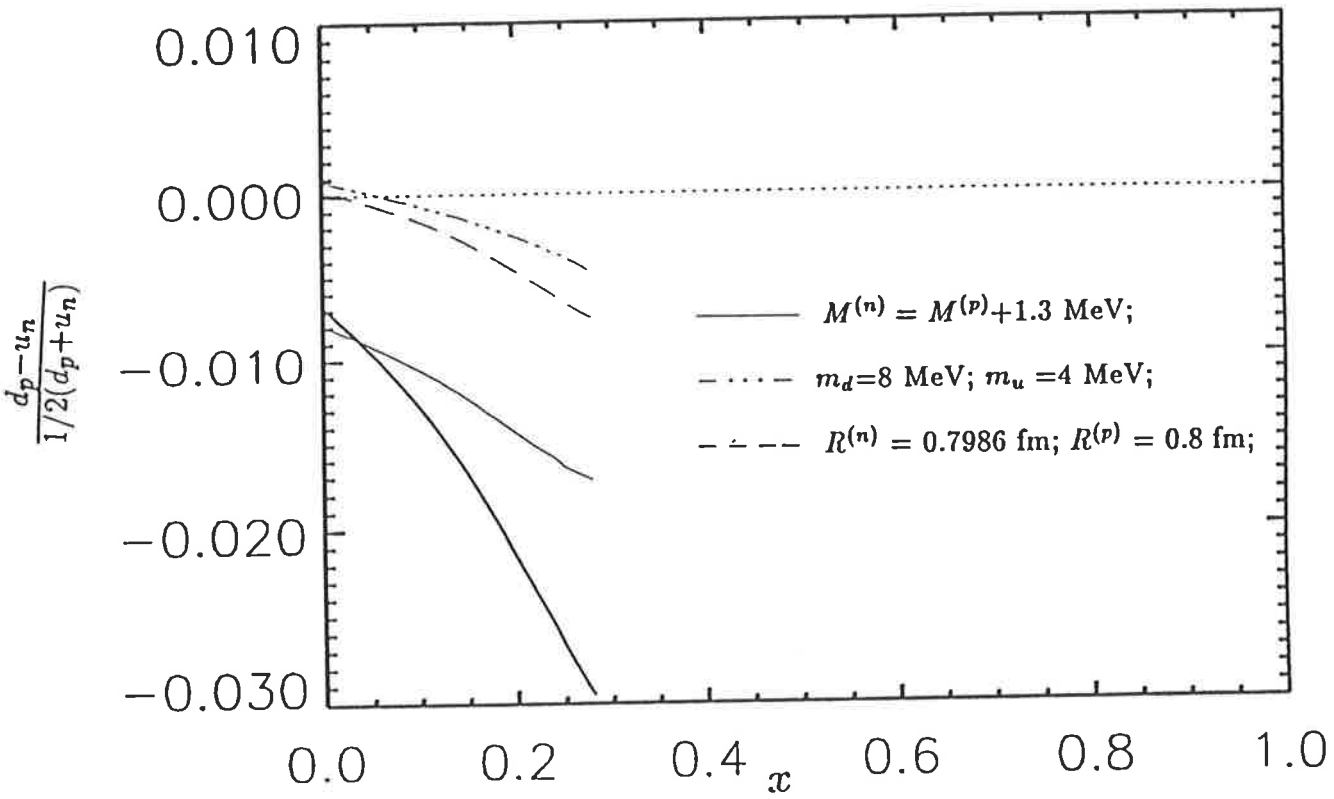

Figure 9: Contributions from various sources to the symmetry breaking for sea quarks at $Q^2 = 10$ GeV^2. Parameters are: $m_d = m_u = 0$ MeV; $M^{(n)} = M^{(p)} = 938.27$ MeV; $M_2^{(n)} = M_2^{(p)} = 800$ MeV; $R^{(n)} = R^{(p)} = 0.8$ fm. The heavy, solid line shows the combined effect of all four contributions.

7 Q^2 dependence of structure functions.

7.1 Phenomenology of Q^2 dependence of structure functions.

The dependence of the quark and gluon content of a hadron on the energy at which the system is probed is qualitatively understood and with the advent of QCD[18] it is possible to describe this phenomenon numerically. However, it is not possible to make a model which would describe the state of quarks at any given value of the energy. As a result, one creates models at the low energy scale where the system made of gluons, all sorts of quarks and other particles appearing at short distances from the quark can be considered as just one complicated particle, the valence quark, with subsequent evolution of the structure functions to the experimental region of values of the momentum transfer Q^2 where they can be compared with the experimental data. We shall discuss the numerical solution of this problem in the next Section, but first let us recall its origin.

An attempt to describe the interaction of particles at short distances led to divergent integrals necessitating a renormalisation procedure which would give the correct physical properties of particles, such as charge, mass and so on. This renormalisation procedure was set up long before the appearance of QCD and applied in QED. As for quarks, ignoring the interaction between quarks at energies greater than 500 MeV is impossible.

Formulae describing the Q^2-dependence of structure functions can be found using the renormalisation group equations. We shall consider the case of non-singlet structure functions only. From one side, it is not complicated by the mixing between gluon and singlet-quark operators and, from the other, provides us with all the information necessary for our further use.

From dimensional arguments it can be shown that the Green function at an arbitrary momentum transfer, μ, can be expressed through its value at some specific momentum transfer, Λ, as

$$G(Q,g,\mu) = Z(g_0,\frac{\Lambda}{\mu})G_0(Q,g_0,\Lambda). \tag{113}$$

The independence of the Green function on the renormalisation scale

$$\mu\frac{\mathrm{d}G}{\mathrm{d}\mu} = 0 \tag{114}$$

leads to the renormalisation group equation for the Wilson coefficients [69]

$$\left(\mu\frac{\partial}{\partial\mu} + \beta(g)\frac{\partial}{\partial g} - \gamma_n\right) C_n(Q^2/\mu^2,g) = 0 \tag{115}$$

where

$$\beta(g) = \mu\frac{\partial g}{\partial\mu} \tag{116}$$

and the anomalous dimension

$$\gamma_n = \mu\frac{\partial}{\partial\mu}(\ln Z_n). \tag{117}$$

[18]Recently there has appeared another model which might be a competitor to QCD [114]. This model, however has not been thoroughly investigated yet and first numerical estimates show that it differs from QCD so little that the present level of experiments can not tell which of the models describes reality better. We shall provide all necessary calculations within QCD, which has proven to be a very powerful tool in the description of DIS.

The solution of equation (115)

$$C_n(Q^2/\mu^2, g^2) = C_n(1, \bar{g}^2)\exp\left[-\int_{g(\mu^2)}^{g(Q^2)} dg' \frac{\gamma_n(g')}{\beta(g')}\right], \tag{118}$$

allows us to find the non-singlet moments through the technique of the operator product expansion, which can be used, finally, for the numerical calculation of the Q^2 dependence of structure functions

$$M_n(Q^2) = \left[\frac{\alpha(Q^2)}{\alpha(\mu^2)}\right]^{\gamma_n/2\beta_0} M_n(\mu^2) \tag{119}$$

with

$$\gamma_n = \frac{8}{3}\left(4\sum_{j=1}^{n}\frac{1}{j} - 3 - \frac{2}{n(n+1)}\right) \tag{120}$$

and the strong coupling

$$\alpha(Q^2) = \frac{4\pi}{\beta_0 \ln(Q^2/\Lambda^2_{QCD})} \tag{121}$$

which is one of the most important quantities in QCD, reflecting the asymptotic behavior of the interaction of quarks at short distances. Λ_{QCD} is an ultra-violet cut-off with the value $\Lambda_{QCD} \sim 200$ MeV.

In all the formulae above, the functions C_n, γ_n and β can be found by the use of perturbation theory and in the first approximation are given by

$$C_n(1, g^2) = C_{0,n} + O(g^2), \tag{122}$$

$$\gamma_n = \gamma_{0,n}\frac{g^2}{16\pi^2} + O(g^2), \tag{123}$$

$$\beta(g) = -\beta_0\frac{g^3}{16\pi^2} + O(g^5). \tag{124}$$

In a few places in the previous chapters there were calculations of structure functions evolved from one energy value to another, which were done using the method developed in [115] and based on Bernstein polynomials. In the next section we offer two other numerical methods and compare them with calculations based on the Laguerre and Bernstein polynomials.

7.2 Numerical description of Q^2 dependence of structure functions.

After the appearance of the first paper on the method of the evolution of structure functions, by Altarelli and Parisi [117], a number of both analytic and numerical methods have been developed. We can highlight the following three approaches:

1. Altarelli-Parisi equation based methods [118, 122].
The Altarelli-Parisi equation is

$$\frac{\mathrm{d}q(x,t)}{\mathrm{d}t} = \int_x^1 \frac{dy}{y} q(y,t) P(\frac{x}{y}) \tag{125}$$

where

$$P(z) = C_2(R)\left(\frac{1+z^2}{(1-z)_+} + \frac{3}{2}\delta(1-z)\right) \tag{126}$$

$$t = -\frac{2}{\beta_0}\ln\left(\frac{\alpha(Q^2)}{\alpha(\mu^2)}\right) \tag{127}$$

and

$$\int_x^1 \frac{f(z)}{(1-z)_+}\mathrm{d}z \equiv \int_x^1 \frac{f(z)-f(1)}{1-z}\mathrm{d}z. \tag{128}$$

Eq. (125) can be represented in another, more convenient form [86]:

$$q(x,t) = \int_x^1 \frac{dy}{y} q(y,t) F(\frac{x}{y},t). \tag{129}$$

2. Mellin transform based methods [123]-[128]:

$$q(x,t) = \int_{c-i\infty}^{c+i\infty} \frac{\mathrm{d}n}{2\pi i} x^n M(n,t_0) e^{-A(n)(t-t_0)} \tag{130}$$

where

$$M(n,t_0) = \int_0^1 \mathrm{d}n\, x^{n-1} q(x,t_0) \tag{131}$$

$$A(n) = \frac{4}{25}\left(1 - \frac{2}{n(n+1)} + 4(\psi(n+1) - \psi(2))\right). \tag{132}$$

3. Bernstein polynomials based methods [129]-[131],[115].

$$q(x,Q^2) = \int_0^1 \Delta(y-x)q(y,Q^2)\mathrm{d}y \tag{133}$$

with $\Delta(y-x)$ represented by Bernstein polynomials

$$\Delta(y-x) = \lim_{N,k\to\infty;k/N\to x}\frac{(N+1)!}{(N-k)!k!}y^k(1-y)^{N-k} \tag{134}$$

$$= \lim_{N,k\to\infty;k/N\to x}\frac{(N+1)!}{k!}\sum_{l=0}^{N-k}\frac{(-1)^l}{l!(N-k-l)!} \tag{135}$$

A few other methods can be found in the literature [132, 133], with various advantages and disadvantages, but they are not widely used. For example, one can use the expansion of the structure function in a series $a_0 + a_1x + a_2x^2 + \cdots + a_nx^n$ which is unfortunately very restricted in its accuracy - and if used with more than 10 components gives incorrect results.

Calculational methods frequently use some approximate form for the structure functions (usually in the form $x^a(1-x)^b$). We note, however, that although this approach gives good results it is less usefull for distributions found in low-energy models, such as the bag model.

We present here new method of numerical evolution which is based on the approximation of the quark distributions as $q(x) = c(d+x)^a(1-x)^b$.

As we have mentioned above, it is often accepted that structure functions can be approximated by the form $cx^a(1-x)^b$. Here we investigate the validity of this approximation numerically.

First of all we note that it is more correct to consider not the approximations to the structure functions (although it is structure functions that are measured in an experiment) but to the quark distributions themselves. In this case we prefer an approximation of the form $c(d+x)^a(1-x)^b$ rather than $cx^a(1-x)^b$, for that better describes the real distributions of quarks. As it is clear we need any 4 moments to find the coefficients a, b, c and d. It would be possible to take *any* four moments only in the case when structure functions exactly obey the form $c(d+x)^a(1-x)^b$. In practice, however, the matter is not so perfect and now we shall see what is happening.

As the sources of inaccuracy will enter the singlet case in the same way as in the non-singlet one, it is enough to consider either the singlet or non-singlet region. To avoid unnecessary problems we restrict ourselves to the latter case.

Let us consider first the evolution which we shall refer to as "mild". For the initial distribution we shall take $q(x) = x(1-x)$ and evolve it from 0.1 to 1 GeV^2.

As one can see from Fig. 10 all three methods give results so close for $x > 0.1$ that it is impossible to distinguish between them. The difference, however, exists and can be seen if we plot the relative (to exact) moments of distributions against the number of the moment (Fig. 11). The result is striking - the line corresponding to the Laguerre polynomial method rushes out of sight just after the 25th moment. Nevertheless, its quark distribution in Fig. 10 looks quite good.

We can quickly solve this puzzle if we recall that by definition the moments are $M(n) = \int_0^1 \mathrm{d}x\, x^{n-1}q(x)$ and this shows us that the large-n moments are responsible for the large x behaviour. Now we see that quark distributions in the region $x < 0.95$ are almost insensitive to the moments with n greater than 20.

It is interesting to understand the role of the first 20 moments and we take a closer look at the region of small x and n (Figs. 12 and 13). Making a tight string at large x three lines start diverging at $x \approx 0.1$. Certainly, a too rapid change in the behavior of these curves cannot correspond to any real quark distribution, and so the best curve is the one corresponding to using just 4-moments. From Fig. 13 we can see what makes the curves so different. Apparently the reason lies in the accuracy of the first moments. Although the accuracy of the moments 1..20 in the calculation based on the Bernstein polynomials is surprising, there is a problem with the very first moment and this is what spoils the small x region of the solid line. As for the Laguerre polynomial method, it only has the first (and 13th) moment exact and this appears to be not enough for an accurate result.

Using these three programs we can now consider more realistic distributions of the form $cx^a(1-x)^b$, for example $x^3(1-x)$, and evolve it from the same 0.1 to 10 GeV^2 (Fig. 14). This kind of distribution, when a is greater then b is related to the system considered on the bag scale ($\sim$ 200-500 MeV). The results of the evolution are presented in Fig. 14. Now the discrepancy between the curves in the region of $x < 0.1$ becomes significant. It is easy to find out which method gives a better result by looking at their moments on Fig. 15.

Apart from the practical use, the evolution based on the approximation $q(x) = c(d + x)^a(1-x)^b$ allows us to investigate the role that different moments play with respect to the accuracy.

There are four series of moments depicted in Fig. 16: (1,2,3), (2,3,4), (1,5,10) and (1,10,25). The comparison of the curves shows that quark distributions are essentially different for the moments (1,2,3) and the rest (Fig. 16). It appears to be very important to keep the first moments accurate for the distributions in the region of $x < 0.2$ be correct. When one leaves these moments unfixed it is not important whether it is 2nd, 5th or the 15th moment that is exact.

The issue from this investigation is that one can successfully use any of the three approximations described above in the region $0.1 < x < 0.95$. Which method one should chose depends on the circumstances.

The method based on Bernstein polynomials is very valuable when evolving distributions of quarks found from low energy models. These sorts of distributions are often very different from those which could be described by the approximation $q(x) = x^a(1-x)^b$.

The main advantage of the method based on the Laguerre polynomials is that in addition to good accuracy it is also the fastest of these three methods.

The last of the methods that we have considered is useful when one wants to get a smooth distribution at small values of Bjorken x without invoking additional parametrisations (as we did, for example, in Chapter 6).

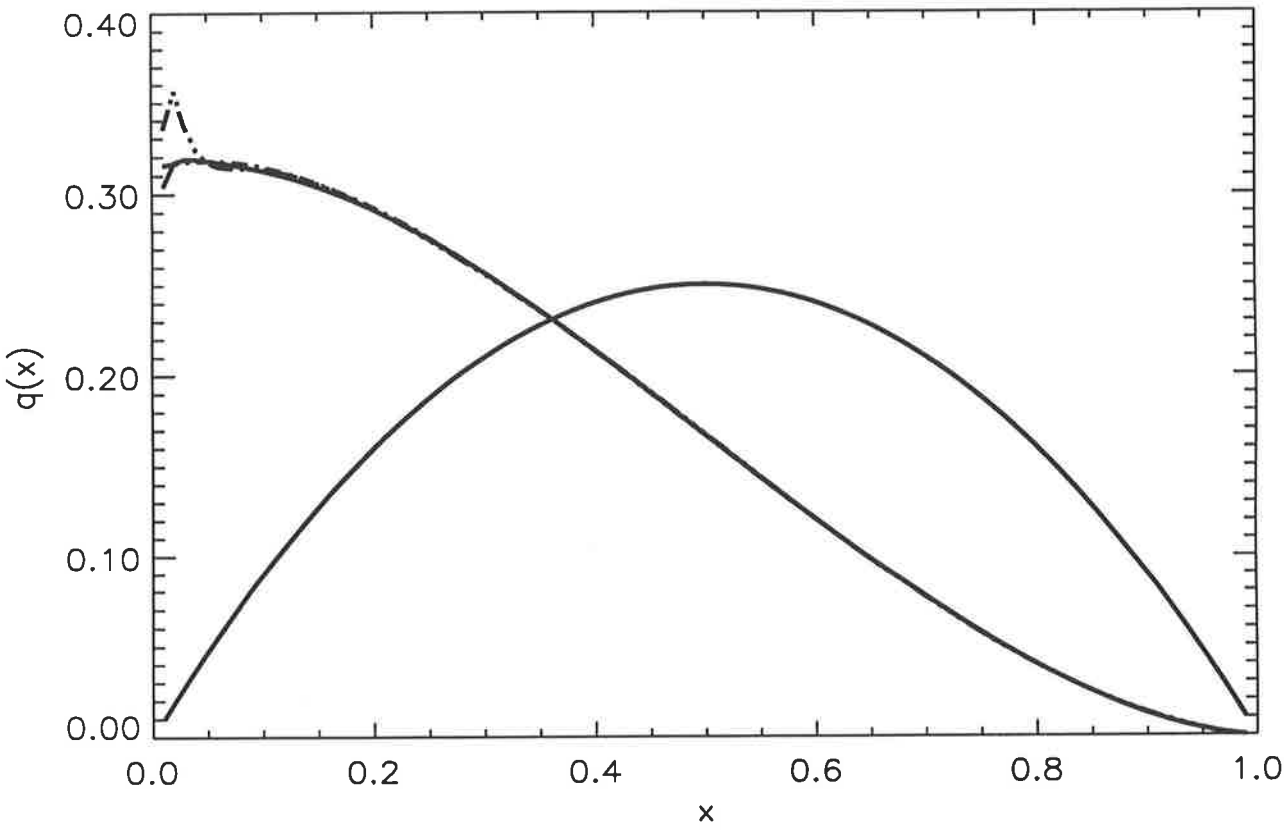

Figure 10: The distribution $x(1-x)$ is evolved from 0.1 to 10 GeV^2 using 3 methods: a) solid line – Bernstein polynomials, b) dash-triple-dot – Laguerre polynomials, c) dash-dot – $q(x) = c(d+x)^a(1-x)^b$.

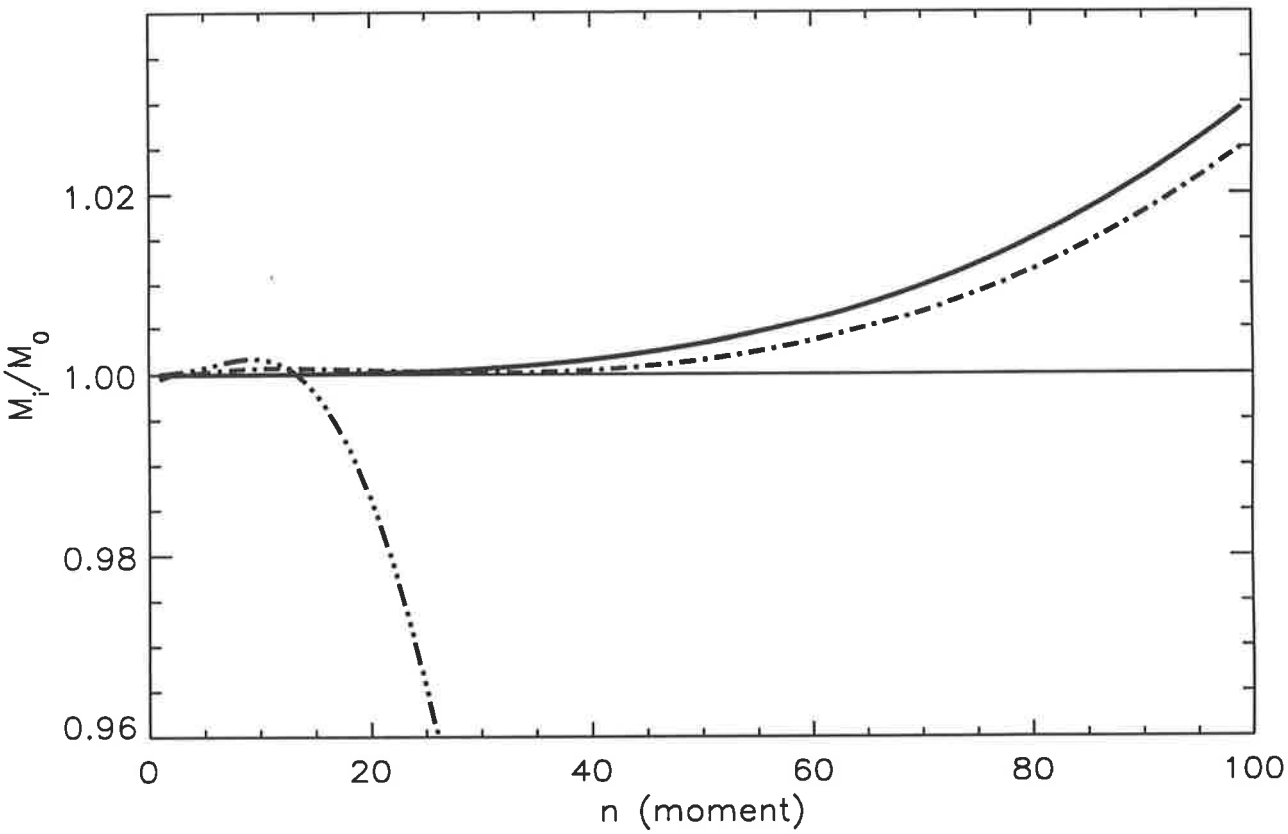

Figure 11: The dependence of the relative moments on the number of the moment for the distribution $x(1-x)$ evolved from 0.1 to 10 GeV^2 using 3 methods: a) solid line – Bernstein polynomials, b) dash-triple-dot – Laguerre polynomials, c) dash-dot – $q(x) = c(d+x)^a(1-x)^b$.

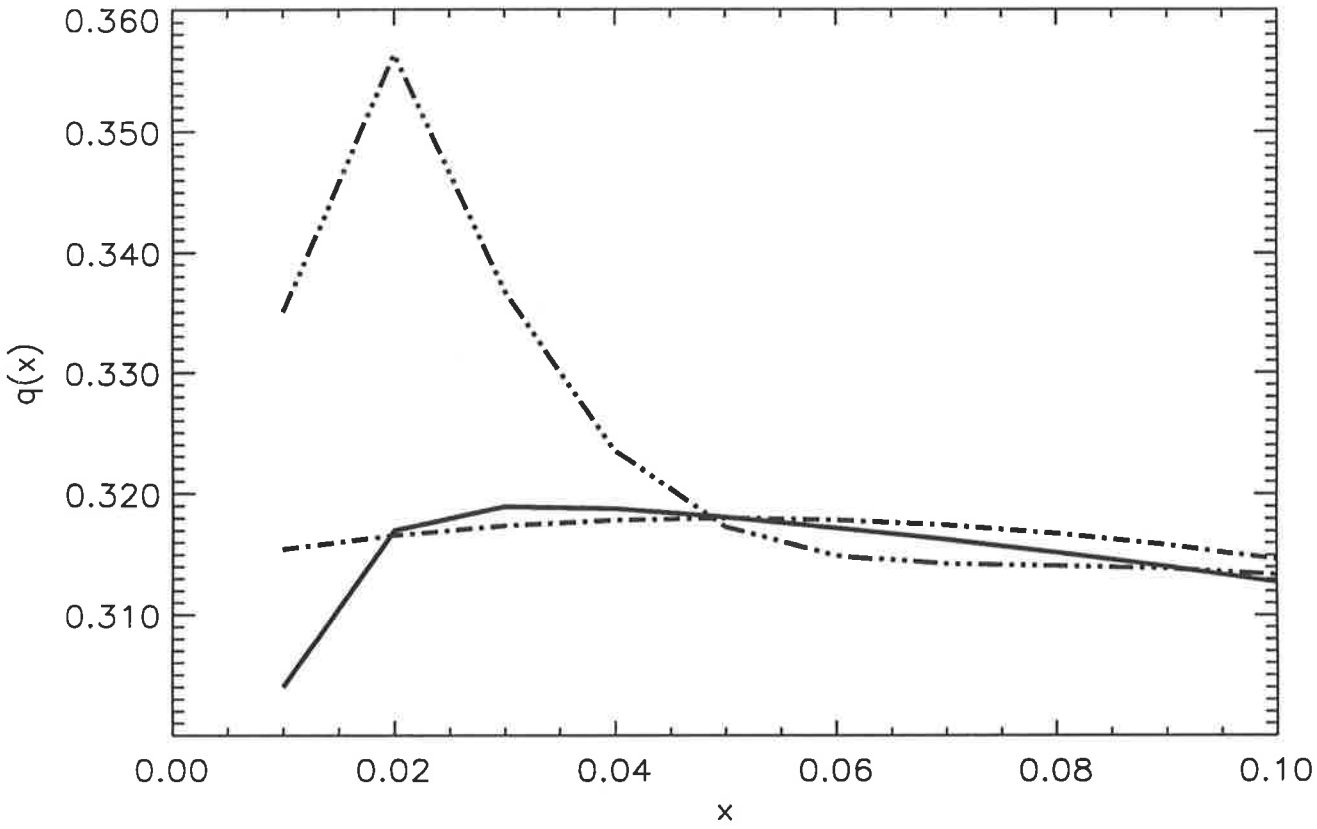

Figure 12: The region of small Bjorken x for the distribution $x(1-x)$ evolved from 0.1 to 10 GeV^2 using 3 methods: a) solid line – Bernstein polynomials, b) dash-triple-dot – Laguerre polynomials, c) dash-dot – $q(x) = c(d+x)^a(1-x)^b$.

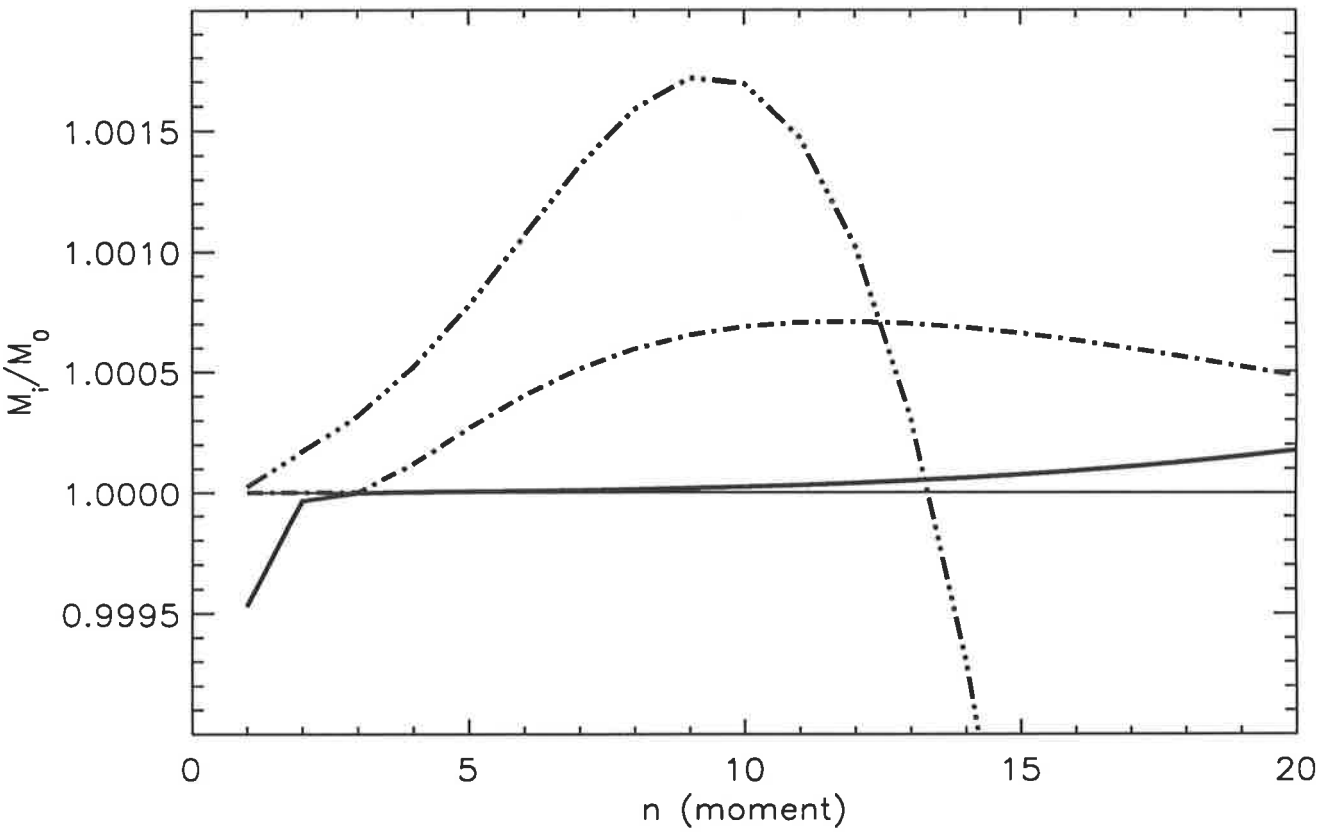

Figure 13: The region of small moments for the distribution $x(1-x)$ evolved from 0.1 to 10 GeV^2 using 3 methods: a) solid line – Bernstein polynomials, b) dash-triple-dot – Laguerre polynomials, c) dash-dot – $q(x) = c(d+x)^a(1-x)^b$.

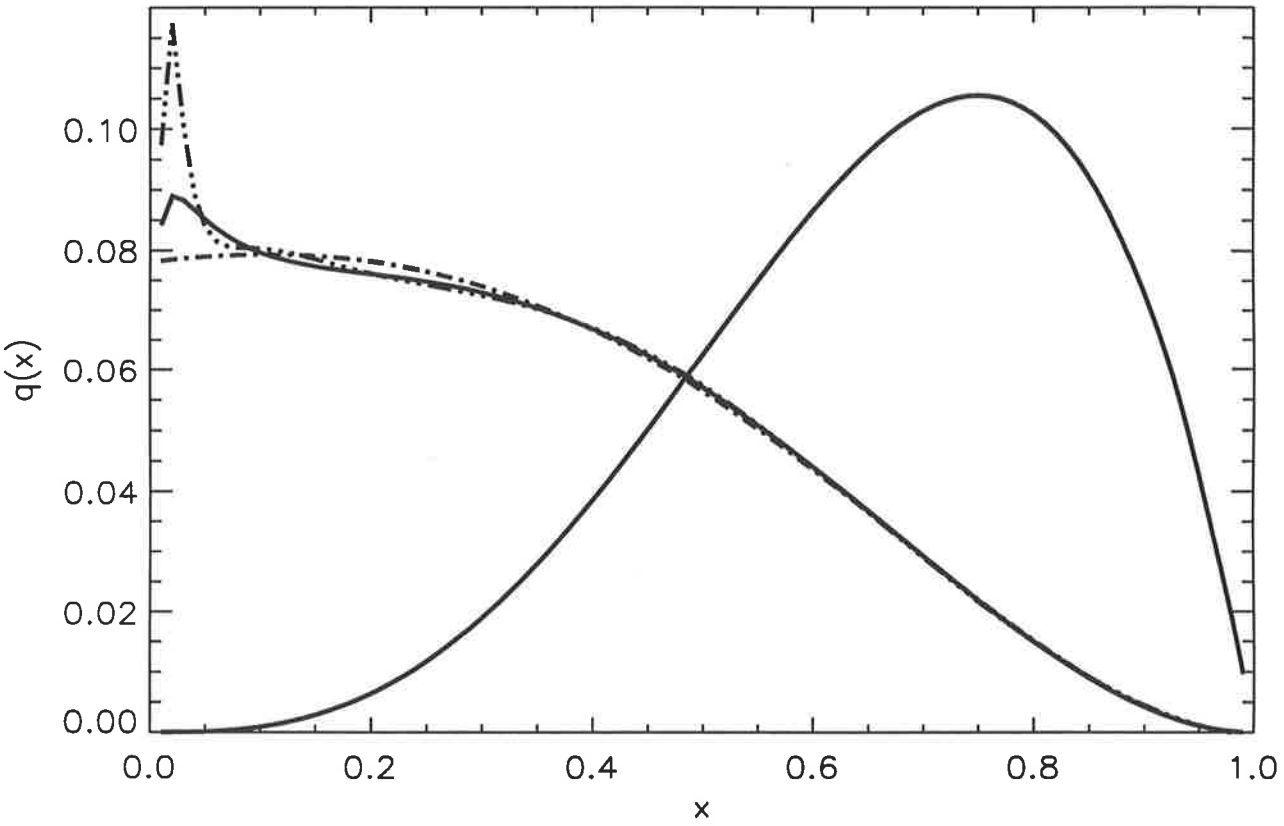

Figure 14: The distribution $x^3(1-x)$ is evolved from 0.1 to 10 GeV^2 using 3 methods: a) solid line – Bernstein polynomials, b) dash-triple-dot – Laguerre polynomials, c) dash-dot – $q(x) = c(d+x)^a(1-x)^b$.

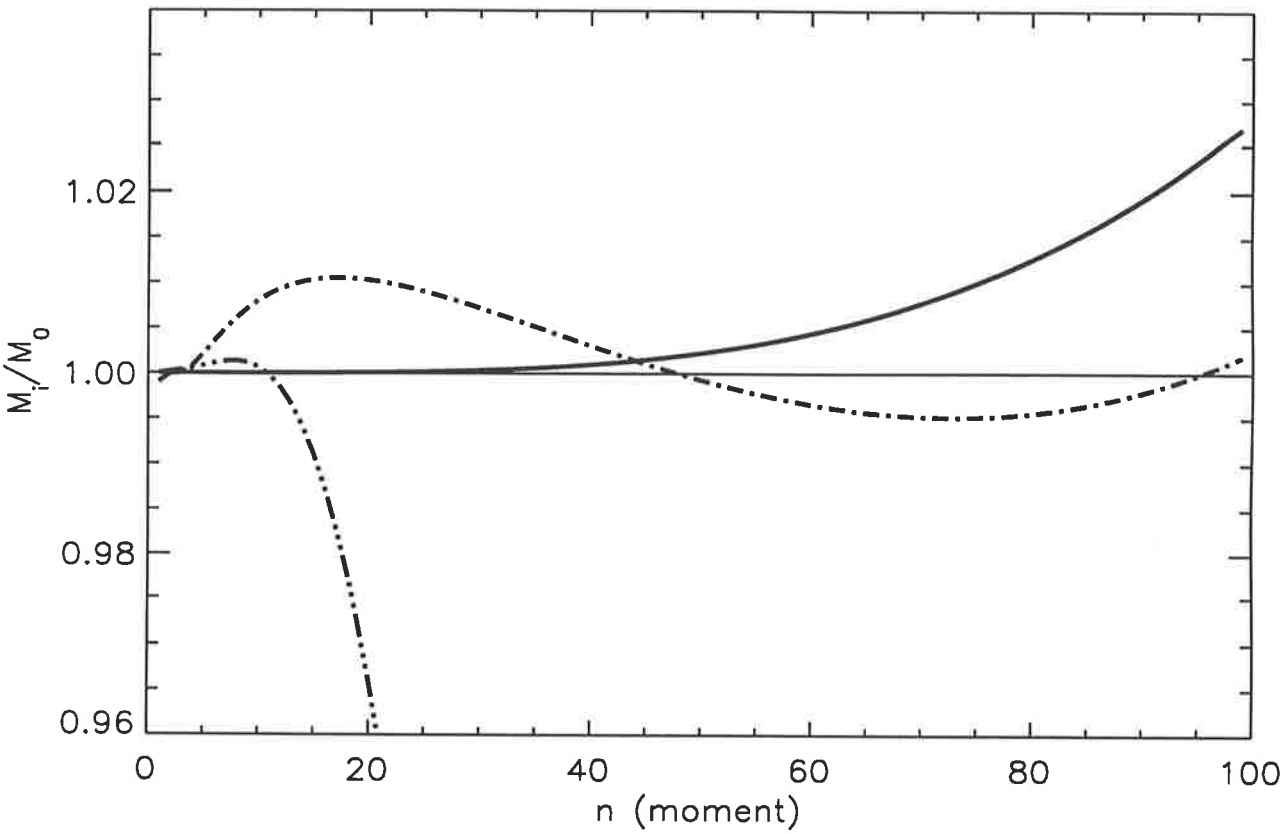

Figure 15: The dependence of the relative moments on the number of the moment for the distribution $x^3(1-x)$ evolved from 0.1 to 10 GeV^2 using 3 methods: a) solid line – Bernstein polynomials, b) dash-triple-dot – Laguerre polynomials, c) dash-dot – $q(x) = c(d+x)^a(1-x)^b$.

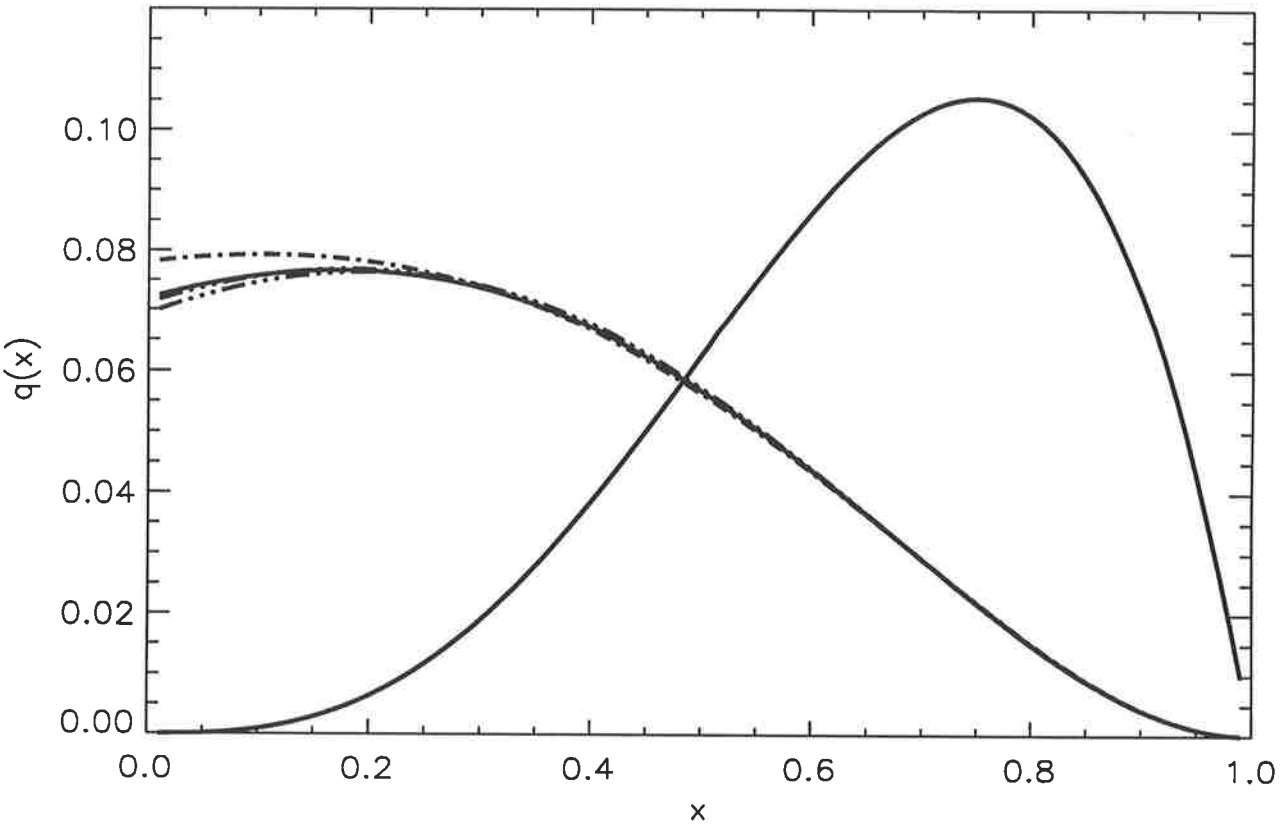

Figure 16: The distribution $x^3(1-x)$ is evolved from 0.1 to 10 GeV^2 using the methods $q(x) = c(d+x)^a(1-x)^b$. Different moments are taken as exact: a) solid line – (2,3,4), b) dash-triple-dot – (1,5,10), c) dash-dot – (1,2,3), d) dash – (1,10,25).

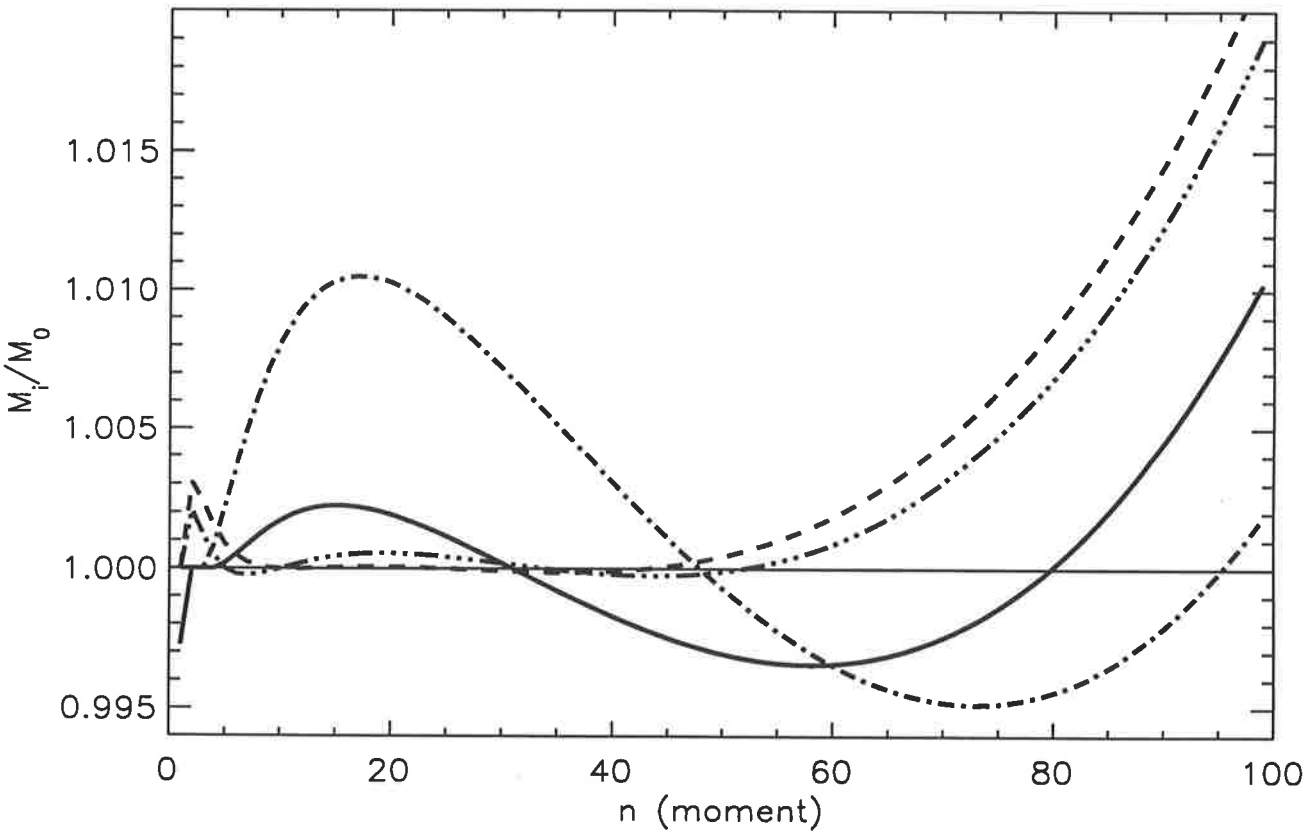

Figure 17: The dependence of the relative moments on the number of the moment for the distribution $x^3(1-x)$ evolved from 0.1 to 10 GeV^2 using the methods $q(x) = c(d+x)^a(1-x)^b$. Different moments are taken as exact: a) solid line – (2,3,4), b) dash-triple-dot – (1,5,10), c) dash-dot – (1,2,3), d) dash – (1,10,25).

8 Drell-Yan process as a probe of CSV in hadrons and the method of measuring sea quarks distributions in pions.

8.1 Drell-Yan process.

Although deep inelastic scattering is a very useful tool for studying hadronic substructure there is another way of extracting valuable information on the distributions of quarks inside nucleons and pions - the Drell-Yan process.

The Drell-Yan process [170] is a hadron-hadron collision in which a lepton-lepton pair is produced along with unobserved hadrons

$$p + p \rightarrow \gamma + X \rightarrow l^+ l^- + X \tag{136}$$

It was hypothesised (on the basis of the parton model) that in the limit

$$s \equiv (p_1 + p_2)^2 \rightarrow \infty \tag{137}$$

but

$$\tau = q^2/s \tag{138}$$

finite (where q^2 is the invariant mass of the virtual particle), the main process is the annihilation of the quark from one hadron with an antiquark from another to form a vector boson. In this case the mass of the boson is

$$q^2 = (x_1 p_1 + x_2 p_2)^2 \tag{139}$$

with x_1 and x_2 being the fractions of the hadron momenta carried by the quarks. Subsequently this virtual boson decays to a e^+e^-, $\mu^+\mu^-$ or $\tau^+\tau^-$ pair in the case of the photon and Z bozon and to $e\nu$, $\mu\nu$ or $\tau\nu$ pairs in the case of the W boson. Here we shall confine ourselves to the case of a photon which is depicted in Fig. 18.

In the centre of mass system the momenta of hadrons are

$$p_1^\mu = (P,\ 0,\ 0,\ P) \tag{140}$$
$$p_2^\mu = (P,\ 0,\ 0, -P) \tag{141}$$

and so

$$s = 4P^2. \tag{142}$$

Considering also that the momenta of quarks 1 and 2 are

$$x_i p_i\ ,\quad i = 1, 2 \tag{143}$$

we find the momentum of the boson and its square to be

$$q^\mu = ((x_1 + x_2)P,\ 0,\ 0,\ (x_1 - x_2)P) \tag{144}$$
$$q^2 = 4x_1 x_2 P^2 \tag{145}$$

and

$$\tau = 4x_1 x_2 P^2/s = x_1 x_2. \tag{146}$$

To calculate the differential cross section of the hadron-hadron collision we have first to consider the subprocess,

$$q + \bar{q} \to l^+ + l^- \tag{147}$$

the cross section for which can be found from the similar process in QED [134]

$$e^+ + e^- \to \mu^+ + \mu^- \tag{148}$$

with

$$\sigma_{e^+e^- \to \mu^+\mu^-} = \frac{4\pi\alpha^2}{3q^2}. \tag{149}$$

Thus, denoting e_i the charge of the quark q_i we find

$$\sigma_{q_i\bar{q}_i \to e^+e^-} = \frac{4\pi\alpha^2 e_i^2}{3n_c q^2}, \tag{150}$$

which is the cross section to be used with parton distributions which are summed over colour.

Now it is simple to reach our goal and the only thing left is to multiply $\sigma_{q\bar{q}\to l^+l^-}$ by the probabilities for finding a quark of type i with momentum fraction x_1 and an antiquark of the same type with fraction x_2

$$q_i(x_1)\mathrm{d}x_1\bar{q}_i(x_2)\mathrm{d}x_2 \tag{151}$$

summed with the similar probabilities, but now for quark carrying momentum x_2 and antiquark - x_1

$$q_i(x_2)\mathrm{d}x_2\bar{q}_i(x_1)\mathrm{d}x_1. \tag{152}$$

Finally we write down the cross-section of the Drell-Yan process as

$$\sigma_{pp\to l^+l^-} = \frac{4\pi\alpha^2}{3n_c q^2}\sum_i e_i^2 \int_0^1 [q_i(x_1)\bar{q}_i(x_2)) + \bar{q}_i(x_1)q_i(x_2)]\frac{\mathrm{d}x_1\mathrm{d}x_2}{x_1x_2}\delta(\frac{1}{x_1x_2} - \frac{s}{q^2}) \tag{153}$$

This formula can be improved by considering QCD corrections which come from a few sources - for example, from the dependence of the quark number densities, $q_i(x)$ on q^2. The reader interested in this topic can find discussions on this subject in Ref. [135]-[141]. We, however, turn our attention to the advantages provided by the Drell-Yan annihilation of meson beams for studying the effect of charge symmetry violation. Before that we would like to mention that the experiments with muons were introduced to directly investigate the question of whether the generation of the massive muon pairs is due to the quark-antiquark annihilation or not. For the isoscalar target one finds the relation[19]

$$\frac{4\pi^+C \to \mu^+\mu^-}{4\pi^-C \to \mu^+\mu^-} = \frac{1}{4} \tag{155}$$

for valence quarks (i.e for $x > 0.2$) and this is found to be in good agreement with experiment [142].

[19]For the target with a protons and b neutrons in the nucleus one can find

$$R = \frac{\pi^+(aP + bN) \to \mu^+\mu^-}{\pi^-(aP + bN) \to \mu^+\mu^-} = \frac{ad^p + bd^n}{4(au^p + bu^n)} \tag{154}$$

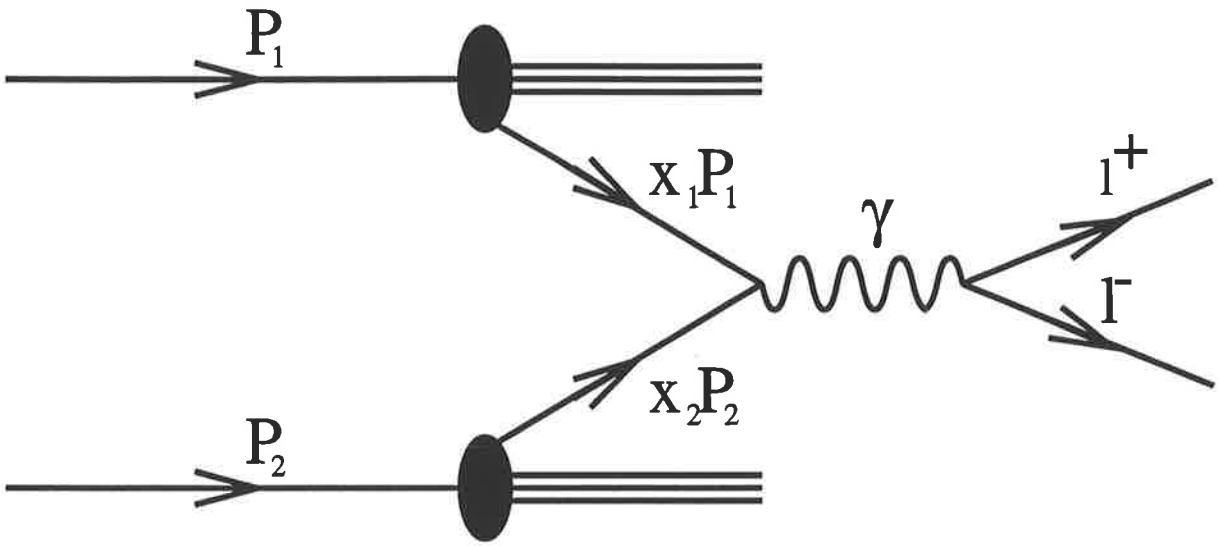

Figure 18: Drell-Yan process.

8.2 Drell-Yan processes as a probe of charge symmetry violation in the pion and nucleon

At present the flavour structure of the nucleon is a topic of intense interest [79]-[88],[144]. This is largely a consequence of unexpected experimental results, such as the discovery by the New Muon Collaboration (NMC) of a violation of the Gottfried sum-rule [145] and the so-called "proton spin crisis" [146, 147, 148] of EMC. There have also been recent theoretical calculations of the violation of charge symmetry in the **valence** quark distributions of the nucleon [149].

In most nuclear systems, charge symmetry is obeyed to within about one percent [150], so one would expect small charge symmetry violation [CSV] in parton distributions. Theoretical calculations suggest that there is a CSV part of the "minority" valence quark distributions (d^p or u^n), with a slightly smaller violation in the "majority" valence distributions (u^p or d^n). Although both CSV contributions are rather small in absolute magnitude, the **fractional** charge symmetry violation in the minority valence quark distributions $r_{min}(x) \equiv 2(d^p(x) - u^n(x))/(d^p(x) + u^n(x))$ can be large, because at large momentum fraction x, $d^p(x)/u^p(x) << 1$. In Chapter 6 we predicted CSV as large as $5 - 10\%$ for the ratio $r_{min}(x)$, in the region $x > 0.5$. The relative size of these CSV effects might require a change in the standard notation for parton distributions [95] in this region. In addition, Sather [149] showed that CSV effects of this magnitude could significantly alter the value of the Weinberg angle extracted from neutral and charged current neutrino interactions.

Since (in this particular region of Bjorken x) we predict fractional charge symmetry violations as large as $5 - 10\%$, it is important to explore experiments which would be sensitive to the relative minority quark distributions in the neutron and proton. Observation of a CSV effect at this level would reinforce confidence in our ability to relate quark models to measured quark-parton distributions – and hence to use deep inelastic scattering as a real probe of non-perturbative aspects of hadron structure [151]. Drell-Yan processes have proven to be a particularly useful source of information on the anti-quark distributions in nuclei [152]. If one uses beams of pions, and concentrates on the region where Bjorken x of the target quarks is reasonably large, then the annihilated quarks will predominantly come from the nucleon and the antiquarks from the pion. Furthermore, for $x \geq 0.4$ to good approximation the nucleon consists of three valence quarks, and the pion is a quark-antiquark valence pair – in particular, π^+ contains a valence $\bar{d}$ and π^- a valence $\bar{u}$. Comparison of Drell-Yan processes induced by π^+ and π^- in this kinematic region will provide a good method of separately measuring d and u quark distributions in the nucleon.

Consider the Drell-Yan process in which a quark with momentum fraction x_1 in a deuteron annihilates with an anti-quark of momentum fraction x_2 in a π^+. Provided that $x_1, x_2 \geq 0.4$, to minimise the contribution from sea quarks, this will be the dominant process. Neglecting sea quark effects, the Drell-Yan cross section will be proportional to:

$$\sigma^{DY}_{\pi^+ D} \sim \frac{1}{9}\left(d^p(x_1) + d^n(x_1)\right)\overline{d}^{\pi^+}(x_2). \tag{156}$$

The corresponding cross section for π^-D is :

$$\sigma^{DY}_{\pi^- D} \sim \frac{4}{9}\left(u^p(x_1) + u^n(x_1)\right)\overline{u}^{\pi^-}(x_2), \tag{157}$$

so that if we construct the ratio, $R^{DY}_{\pi D}$:

$$R^{DY}_{\pi D}(x_1, x_2) = \frac{4\sigma^{DY}_{\pi^+ D} - \sigma^{DY}_{\pi^- D}}{\left(4\sigma^{DY}_{\pi^+ D} + \sigma^{DY}_{\pi^- D}\right)/2}, \tag{158}$$

only charge symmetry violating (CSV) terms contribute. In fact, defining

$$\delta d = d^p - u^n, \quad \delta u = u^p - d^n, \quad \delta\overline{d}^\pi = \overline{d}^{\pi^+} - \overline{u}^{\pi^-}, \tag{159}$$

(and recalling that charge conjugation implies $\overline{d}^{\pi^+} = d^{\pi^-}$ etc.) we find that, to first order in the small CSV terms, the Drell-Yan ratio becomes:

$$\begin{aligned} R^{DY}_{\pi D}(x_1, x_2) &= \left(\frac{\delta d - \delta u}{u^p + d^p}\right)(x_1) + \left(\frac{\delta\overline{d}^\pi}{\overline{d}^{\pi^+}}\right)(x_2), \\ &= R^N_{\pi D}(x_1) + R^\pi(x_2), \end{aligned} \tag{160}$$

Equation (160) is quite remarkable in that only CSV quantities enter, and there is a separation of the effects associated with the nucleon and the pion. Because $R^{DY}_{\pi D}$ is a ratio of cross sections one expects a number of systematic errors to disappear – although the fact that different beams (π^+ and π^-) are involved means that not all such errors will cancel. This certainly needs further investigation, since R^{DY} is obtained by almost complete cancellation between terms in the numerator. The largest "background" term, contributions from nucleon or pion sea, will be estimated later. However we note that Eq. (160) is not sensitive to differences between the parton distributions in the free nucleon and those in the deuteron [153, 154, 155, 156]. For example, if the parton distributions in the deuteron are related to those in the neutron and proton by

$$q_i^D(x) = (1 + \epsilon(x))\,(q_i^p(x) + q_i^n(x)) \quad , \tag{161}$$

then by inspection Eq. (160) will be unchanged. Any correction to the deuteron structure functions which affects the proton and neutron terms identically will cancel in R^{DY}.

It should not be necessary to know absolute fluxes of charged pions to obtain an accurate value for R^{DY}. The yield of J/ψ's from $\pi^+ - D$ and $\pi^- - D$ can be used to normalise the relative fluxes, since the J/ψ's are predominantly produced via gluon fusion processes. The gluon structure functions of the π^+ and π^- are identical, so the relative yield should be unity to within 1%.

Next we turn to the predictions for the charge symmetry violating terms, $\delta d, \delta u$ and $\delta\bar{d}^\pi$ which appear in Eq. (160). As we have seen before, there is at least a theoretical consensus that the magnitude of δd is somewhat larger than δu. This is easy to understand because the dominant source of CSV is the mass difference of the residual di-quark pair when one quark is hit in the deep-inelastic process. For the minority quark distribution the residual di-quark is uu in the proton, and dd in the neutron. Thus, in the difference, $d^p - u^n$, the up-down mass difference enters twice. Conversely, for the majority quark distributions the residual di-quark is a ud-pair in both proton and neutron, so there is no contribution to CSV.

In Fig. 19 we show the predicted CSV terms for the majority and minority quark distributions in the nucleon, as a function of x, calculated for the simple MIT bag model [23, 109]. There are, of course, more sophisticated quark models available but the similarity of the results obtained by Naar and Birse [157] using the color dielectric model suggests that similar results would be obtained in any relativistic model based on confined current quarks. The bag model parameters are listed in this Figure. We choose for the mean di-quark masses 600 MeV for the $S = 0$ case, and 800 MeV for the $S = 1$ case (note that for the minority quark distributions the di-quark is always in an $S = 1$ state). The di-quark mass difference, $m_{dd} - m_{uu}$, is taken to be 4 MeV, a rather well determined difference in the bag model. We note that δu is opposite in sign to δd and, therefore, these two terms add constructively in the Drell-Yan ratio R^{DY} of Eq. (160).

In Fig. 20 we show the fractional change in the minority quark CSV term, $2(d^p - u^n)/(d^p + u^n)$ vs. x for several values of the intermediate mean di-quark mass. Although the precise value of the minority quark CSV changes with mean di-quark mass, the size is always roughly the same and the sign is unchanged. This shows that "smearing" the mean di-quark mass will not dramatically diminish the magnitude of the minority quark CSV term (the mean di-quark mass must be roughly 800 MeV in the $S = 1$ state to give the correct $N - \Delta$ mass splitting).

In Fig. 21 we show the nucleon CSV contribution, $R^N_{\pi D}(x_1)$, calculated using the same bag model. As is customary in these bag model calculations, this term is calculated at the bag model scale (0.5 GeV for $R = 0.8$ fm) and then evolved to higher Q^2 using the QCD evolution equations discussed earlier. As the main uncertainty in our calculation is the mean di-quark mass (the splitting between $S = 0$ and $S = 1$ is kept at 200 MeV [112]), the results are shown for several values of this parameter. In the region $0.4 \leq x \leq 0.7$, we predict R^N will be always positive, with a maximum value of about 0.015. For $x > 0.7$ the struck quark has a momentum greater than 1 GeV which is very unlikely in a mean-field model like the bag. As a consequence the calculated valence distributions for the bag model tends to be significantly smaller than the measured distributions in this region. In these circumstances one cannot regard the large, relative charge symmetry violation found in this region as being reliable and we prefer not to show it. It would be of particular interest to add $q - q$ correlations which are known to play an important role as $x \rightarrow 1$ [158].

For the pion, calculations based on the MIT bag model are really not appropriate. In particular, the light pion mass means that centre of mass corrections are very large, and of course bag model calculations do not recognise the pion's Goldstone nature. On the other hand the model of Nambu and Jona-Lasinio (NJL) [159] is ideally suited to treating the structure of the pion, and there has been recent work, notably by Toki and collaborators, in calculating the structure function of the pion (and other mesons) in this model [160, 161]. The essential element of their calculation was the evaluation of the so-called handbag diagram for which the forward Compton amplitude is:

$$T_{\mu\nu} = i \int \frac{d^4k}{(2\pi)^4} Tr[\gamma_\mu Q \frac{1}{\not k} \gamma_\nu Q T_-] + (T_+ term), \tag{162}$$

where

$$T_- = S_F(k - q, M_1) g_{\pi qq} \tau_+ i\gamma_5 S_F(k - p - q, M_2) g_{\pi qq} \tau_- i\gamma_5 S_F(k - q, M_1), \tag{163}$$

represents the contribution with an anti-quark of mass M_2 as spectator to the absorption of the photon (of momentum q) by a quark. In Eq. (163) $g_{\pi qq}$ is the pion-quark coupling constant, Q the charge of the struck quark, p the momentum of the target meson, and S_F the quark propagator. T_+ is the corresponding term where the quark is a spectator and the anti-quark undergoes a hard collision. As in our bag model studies this model was used to determine the leading twist structure function at some low scale (0.25 GeV in this case), and then evolved to high-Q^2 using the Altarelli-Parisi equations [117]. The agreement between the existing data and the calculations for the pion and kaon obtained in Ref. [160] is quite impressive.

In the light of the successful application of the NJL model to the structure functions of the pion and the kaon, where the dominant parameter is the mass difference between the constituent strange and non-strange quarks (assumed to be about 180 MeV), it seems natural to use the same model to describe the small difference $\delta\bar{d}^\pi$ (c.f. Eq. (159)) arising from the 3 MeV constituent mass difference of the u and d [150]. We have carried out such a calculation. Fig. 22 shows the pionic contribution to the CSV Drell-Yan ratio,

$R^\pi(x_2)$, corresponding to this mass difference and an average non-strange quark mass of 350 MeV – as used in Ref.[160, 161]. The dashed curve is the result at the bag scale, and the solid curve shows the result evolved to $Q^2 = 10$ GeV^2. For $x_2 > 0.3$, we predict that R^π will be positive and increase monotonically, reaching a value of about 0.01 at $x_2 = 0.8$ and increasing to about 0.02 as $x_2 \to 1$. (We note that there is some ambiguity in translating the usual Euclidean cut-off in the NJL model into the cutoff needed for deep inelastic scattering. In order to study charge symmetry violation we particularly need to start with a model that gives a good description of the normal pion structure function. For this reason we have chosen to follow the method used in Ref.[160] rather than Ref.[161].)

Up to this point we have neglected the nucleon and pion sea quark contributions. Since the Drell-Yan ratios arising from CSV are very small (viz. Fig. 21 and 22), even small contributions from sea quarks could have a substantial effect. The dominant contribution will arise from interference between one sea quark and one valence quark. Assuming charge symmetry for the quark distributions, and using the same form for the quark and antiquark distributions in the pion, the sea-valence contribution to the Drell-Yan ratio of Eq. (160) has the form

$$\begin{aligned} R^{SV}_{\pi D}(x_1,x_2) &= \frac{3\sigma^{SV}_{\pi D}(x_1,x_2)}{\left(\frac{4}{9}\overline{d}^\pi_v(x_2)\left(u^p_v(x_1)+d^p_v(x_1)\right)+\frac{5}{2}\sigma^{SV}_{\pi D}(x_1,x_2)\right)}; \\ \sigma^{SV}_{\pi D}(x_1,x_2) &\equiv \frac{5}{9}\left[2\pi_v(x_2)u^p_s(x_1)+\pi_s(x_2)\left(u^p_v(x_1)+d^p_v(x_1)\right)\right]. \end{aligned} \tag{164}$$

Unlike the CSV contributions of Eq. (160), the sea-valence term does not separate. In Fig. 23 we show the sea-valence term as a function of x_1 and x_2 using recent phenomenological nucleon and pion parton distributions [162]. The sea-valence contribution, although extremely large at small x, decreases rapidly as x increases. For $x \geq 0.5$, the sea-valence term is no larger than the CSV "signal". With accurate phenomenological nucleon and pion quark distributions, it should be possible to calculate this contribution reasonably accurately (the main uncertainty being the magnitude of the pion sea). For smaller values ($x_1 \approx x_2 \approx 0.4$, where the background dominates, we could use the data to normalise the pion sea contribution; we should then be able to predict the sea-valence term rather accurately for larger x values, where the CSV contributions become progressively more important. We could also exploit the very different dependence on x_1 and x_2 of the background and CSV terms. We conclude that the CSV terms could be extracted even in the presence of a sea-valence "background". We emphasise that our proposed Drell-Yan measurement would constitute the first direct observation of charge symmetry violation for these quark distributions.

The Drell-Yan CSV ratio $R^{DY}_{\pi D}$ of Eq. (160) is the sum of the nucleon CSV term of Fig. 21 and the pion term of Fig. 22, at the respective values of Bjorken x. Since both quantities are positive, they will add to give the experimental ratio. Despite the fact that the fractional minority quark CSV term is as large as 10% (c.f. Fig. 20), the nucleonic CSV ratio $R^N_{\pi D}$ is more like 1-2%. This is because δd in Eq. (160) is divided by $u^p + d^p$ and since $d^p(x) << u^p(x)$ at large x the nucleon CSV term is significantly diminished. A much larger ratio could be obtained by comparing the $\pi^+ - p$ and "$\pi^- - n$" Drell-Yan processes through the ratio:

$$R^{DY}_{\pi N}(x_1,x_2) = \frac{4\sigma^{DY}_{\pi^+ p}+\sigma^{DY}_{\pi^- p}-\sigma^{DY}_{\pi^- D}}{\left(4\sigma^{DY}_{\pi^+ p}-\sigma^{DY}_{\pi^- p}+\sigma^{DY}_{\pi^- D}\right)/2}. \tag{165}$$

To first order in the small CSV quantities, this ratio can be written:

$$\begin{aligned} R_{\pi N}^{DY}(x_1, x_2) &= \frac{\delta d}{d^p}(x_1) + \left(\frac{\delta \overline{d}^{\pi}}{\overline{d}^{\pi^+}}\right)(x_2), \\ &= R_{\pi N}^{N}(x_1) + R^{\pi}(x_2). \end{aligned} \tag{166}$$

Once again, the ratio separates completely in x_1 and x_2, and the pion CSV term is identical with Eq. (160). However, the nucleon CSV term is much larger – in fact, it is precisely the ratio given in Fig. 20, so we expect CSV effects at the 5-10 % level for this quantity.

Some care will need to be taken to normalise cross sections since one is comparing Drell-Yan processes on protons and deuterons. This should be feasible by bombarding both hydrogen and deuterium targets simultaneously with charged pion beams. Eq. (166) assumes that deuteron structure functions are just the sum of the free nucleon terms; if we include corrections in the form of Eq. (161), we obtain an additional first-order correction

$$\delta R_{\pi N}^{DY}(x_1) = -\epsilon(x_1)\left(\frac{u^p + d^p}{d^p}\right)(x_1) \tag{167}$$

This preserves the separation into nucleonic and pionic CSV terms, but depends on 'EMC' changes in the deuteron structure functions relative to free proton and neutron distributions, and on the u/d ratio of proton distributions. For large x, $u(x)/d(x) >> 1$, so the EMC term could be significant even for small values of $\epsilon(x)$. For $x \sim 0.5$, where $u^p/d^p \approx 4$, if $\epsilon(x)$ is as large as -0.02 then $\delta R_{\pi N}^{DY}(x = 0.5) \approx 0.10$. At larger x the EMC contribution could be even bigger, and might conceivably dominate the CSV terms. Since all terms (pion and nucleon CSV, and EMC) are predicted to have the same sign in the region $0.3 < x < 0.8$ (we expect $\epsilon(x) < 0$ in this region), the ratio $R_{\pi N}^{DY}$ could be as large as 0.3. In view of this sensitivity to the EMC term, it is important that accurate calculations be carried out of Fermi motion and binding corrections for the deuteron, including possible flavour dependence of such corrections. Melnitchouk, Schreiber and Thomas [156, 163] have recently studied the contributions to $\epsilon(x)$ in the deuteron.

We have also calculated the sea-valence contribution to the Drell-Yan ratio $R_{\pi N}^{DY}$. Relative to the deuteron measurement, we predict a CSV contribution which increases by about a factor 5. The sea-valence background also increases by about the same factor. So our remarks about the sea-valence background and the CSV "signal" are equally valid for these Drell-Yan processes.

In conclusion, we have shown that by comparing the Drell-Yan yield for π^+ and π^- on nucleons or deuterons, one might be able to extract the charge symmetry violating [CSV] parts of **both** pion and nucleon. We discussed two different linear combinations of π^+ and π^- induced Drell-Yan cross sections, which produce a result directly proportional to the CSV terms. Furthermore, we found that the ratio of Drell-Yan cross sections **separates** completely into two terms, one of which ($R^N(x_N)$) depends only on the nucleon CSV, and the other ($R^{\pi}(x_{\pi})$) depends on the pion CSV contribution. Thus if this ratio can be accurately measured as a function of x_N and x_{π}, both the nucleon and pion CSV terms might be extracted. The largest background should arise from terms involving one sea quark and one valence quark. Such contributions, although relatively large, should be able to be predicted quite accurately, and may be subtracted off through their very different behavior as a function of nucleon and pion x. As the x_1 and x_2 values of interest for the proposed measurements are large ($x > 0.5$), a beam of 40-50 GeV pions will produce sufficiently massive dilepton pairs that the Drell-Yan mechanism is applicable. A flux of more than 10^9 pions/sec. is desirable, which may mean that the experiment is not feasible until the new FNAL Main Ring Injector becomes operable.

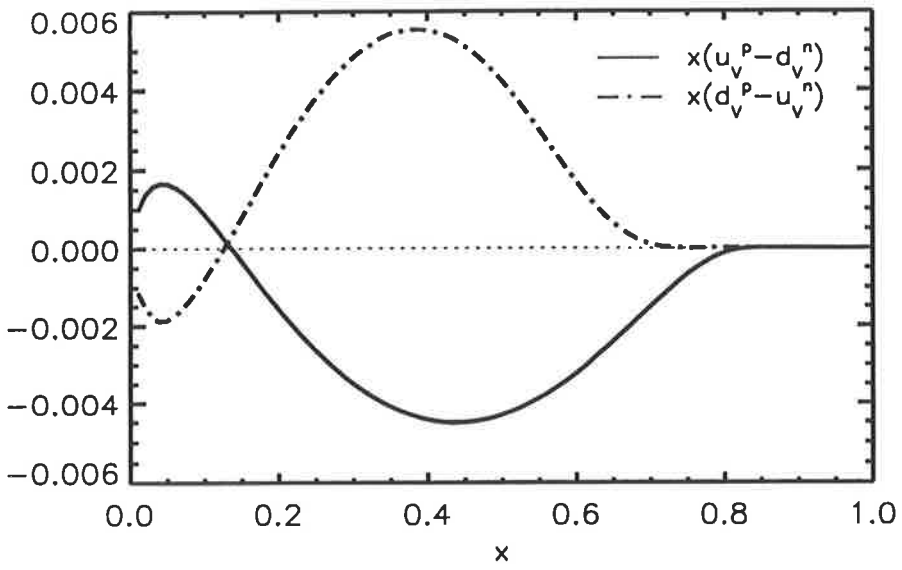

Figure 19: Predicted charge symmetry violation (CSV), calculated using the MIT bag model. Dashed curve: "minority" quark CSV term, $x\delta d(x) = x\,(d^p(x) - u^n(x))$; solid curve: "majority" quark CSV term, $x\delta u(x) = x\,(u^p(x) - d^n(x))$.

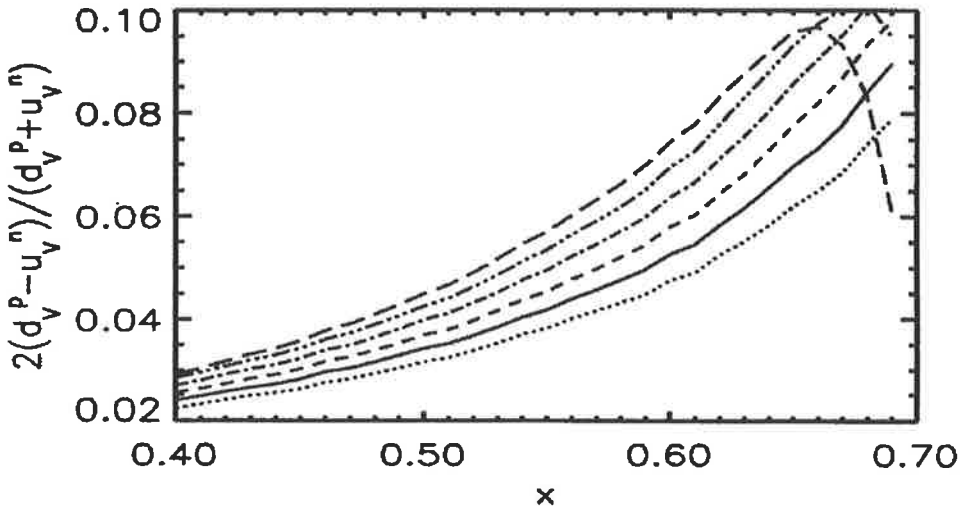

Figure 20: Fractional minority quark CSV term, $\delta d(x)/d^p(x)$, vs. x, as a function of the average di-quark mass $\overline{m}_d = (m_{uu} + m_{dd})/2$. The di-quark mass difference is fixed at $\delta m_d = m_{dd} - m_{uu} = 4$ MeV. From top to bottom, the curves correspond to average di-quark mass $\overline{m}_d = 850$, 830, 810, 790, 770, and 750 MeV. The curves have been evolved to $Q^2 = 10$ GeV^2. This quantity is the nucleonic CSV term for the Drell-Yan ratio $R^{DY}_{\pi N}$.

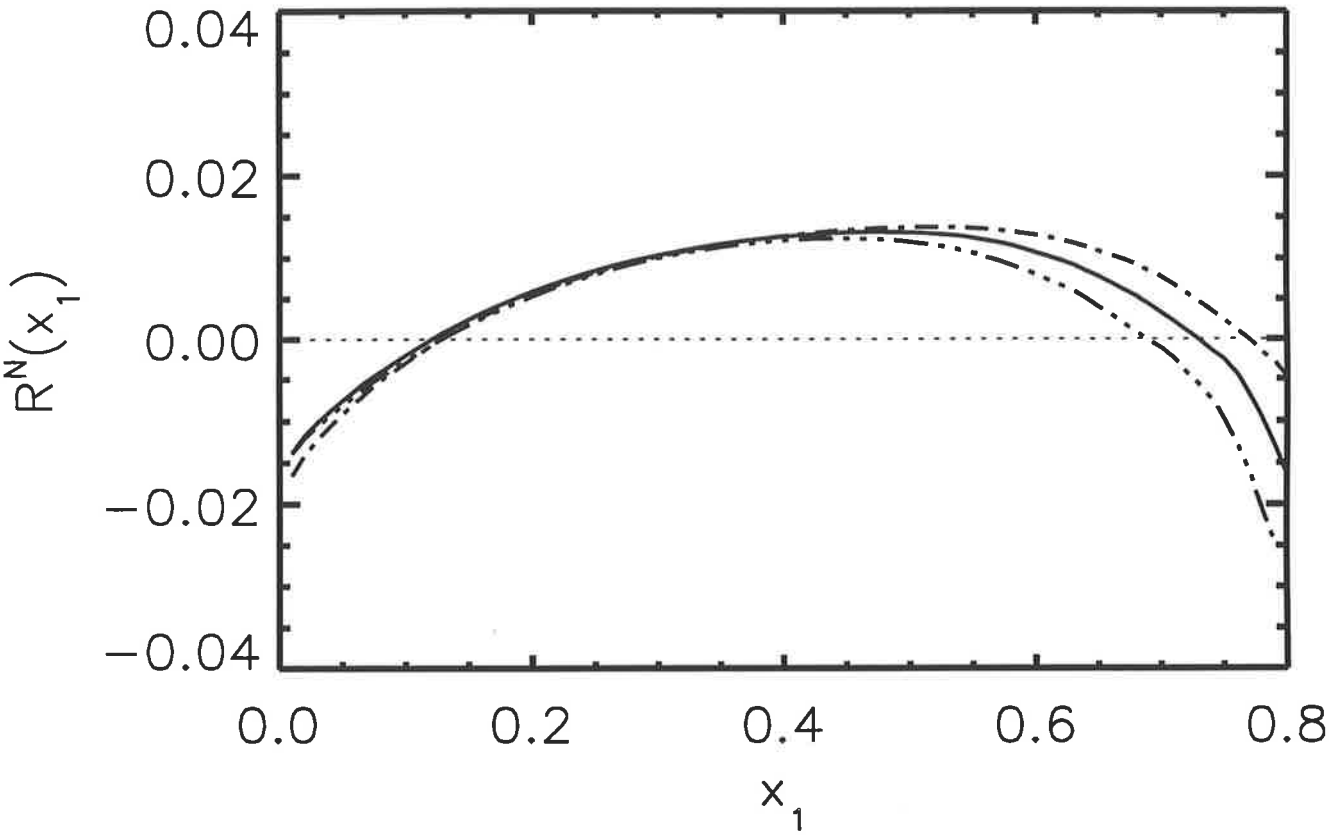

Figure 21: Contributions from various sources to the nucleonic charge symmetry breaking term $R_{\pi D}^{DY}$, evolved to $Q^2 = 10$ GeV^2, for pion-induced Drell-Yan ratios on deuterons. Unless otherwise specified, parameters are: $m_d = m_u = 0$ MeV; $M^{(n)} = M^{(p)} = 938.27$ MeV; $R^{(n)} = R^{(p)} = 0.8$ fm; $\delta m_d = m_{dd} - m_{uu} = 4$ MeV. Curves represent different values of average di-quark mass. Dash-dot: $\overline{m}_{qq} = 750$ MeV; solid: 800 MeV; dash-triple-dot: 850 MeV.

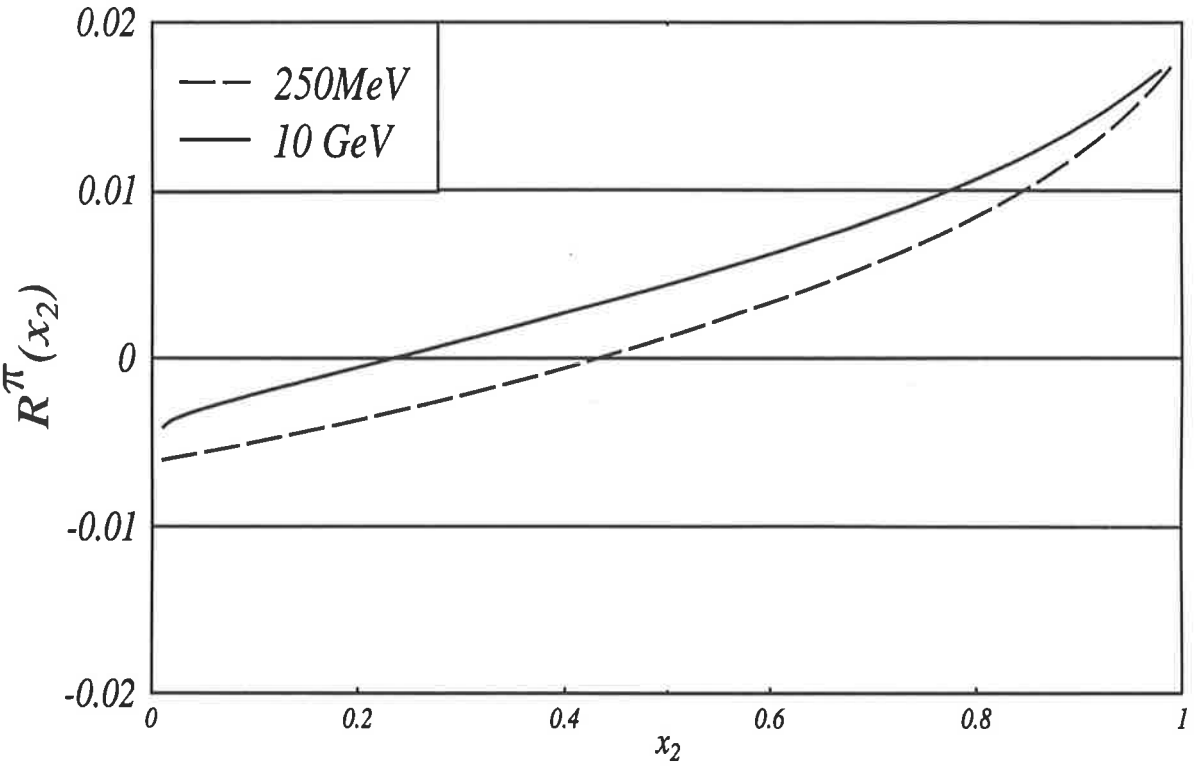

Figure 22: Calculation of the pion CSV contribution R^π for average nonstrange quark mass 350 MeV, and mass difference $m_d - m_u = 3$ MeV. Dashed curve: R^π evaluated at the bag scale, $\mu = 250$ MeV; solid curve: the same quantity evolved to $Q^2 = 10$ GeV^2.

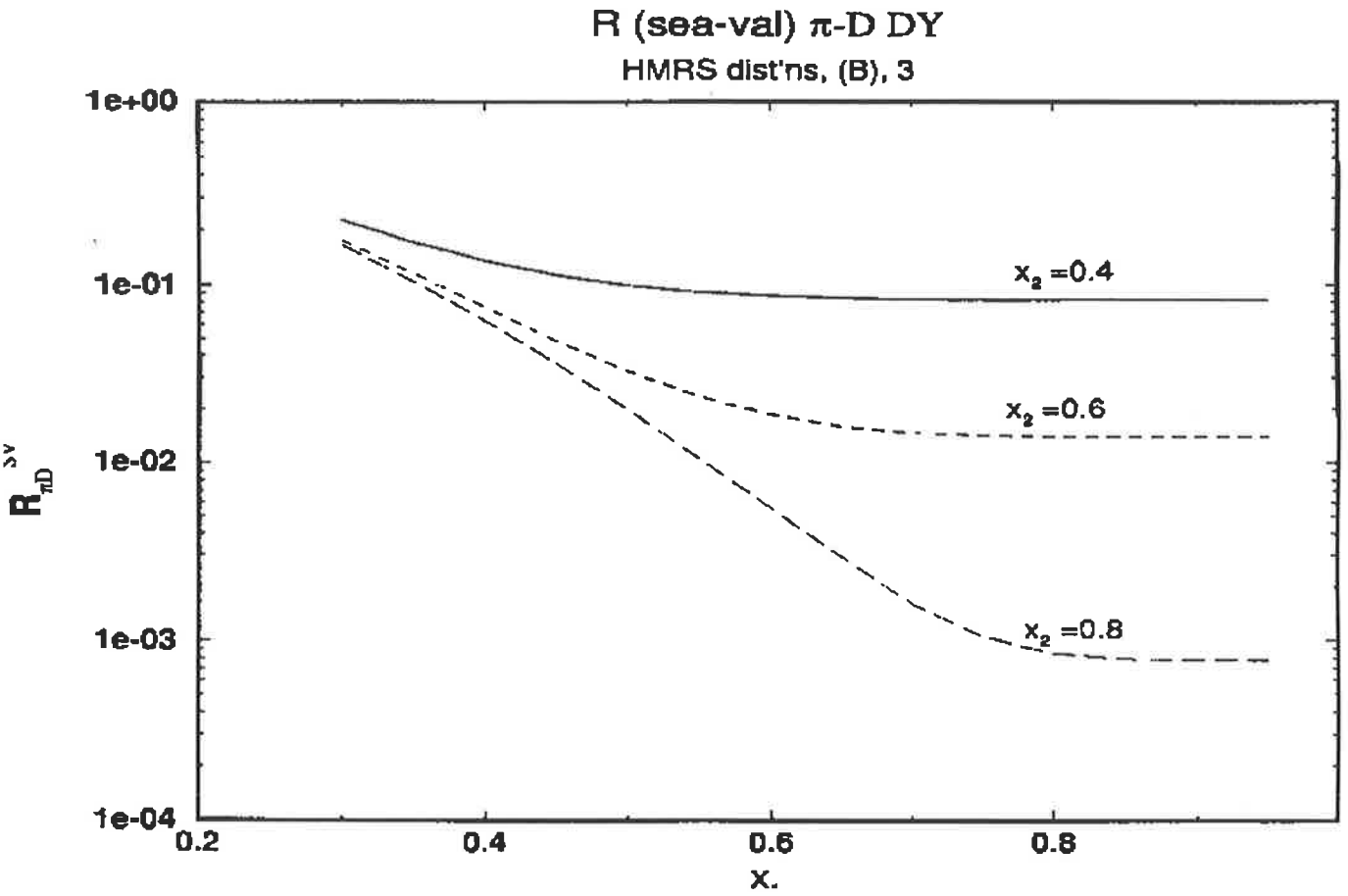

Figure 23: The sea-valence contribution $R_{\pi D}^{SV}$ to pion-induced Drell-Yan ratios on deuterons, as a function of nucleon x_1. Solid curve: pion $x_2 = 0.4$; dashed curve: $x_2 = 0.6$; long-dashed curve: $x_2 = 0.8$.

8.3 Probing the pion sea with π-D Drell-Yan processes

Deep inelastic lepton-nucleon scattering measurements, together with Drell-Yan and prompt photon data, enable us to establish the valence and sea quark distributions for nucleons. Recently Sutton et al. [164] have used Drell-Yan and prompt photon data to extract pion structure functions. They used Drell-Yan pion-nucleus data from the CERN NA10 [165, 166] and FNAL E615 [167] experiments, and prompt photon data from the WA70 [168] and NA3 [169] Collaborations. Although the pion valence quark distributions can be constrained reasonably well by existing data, there are relatively few constraints on the pion sea distribution. Presently there is insufficient, experimental Drell-Yan data for the process $\pi^{\pm}N \to \mu^+\mu^- X$, for $x_\pi \leq 0.2$ to determine the pion sea quark distribution unambiguously.

Here we point out that the pion sea can be extracted rather directly from a comparison between Drell-Yan processes induced by charged pions on an isoscalar target such as deuterium.

As we have discussed, in Drell-Yan processes [170], a quark (antiquark) of a certain flavor in the projectile annihilates an antiquark (quark) of the same flavor in the target, producing an intermediate photon which later decays into a $\mu^+ - \mu^-$ pair. For nucleon-nucleus events, the antiquark is necessarily part of the sea, so all Drell-Yan events involve at least one sea quark. Since a pion has one valence quark and one valence antiquark, various combinations of valence and sea quarks are possible for pion-nucleus Drell-Yan processes. However, combinations of positive and negative charged pions (on isoscalar targets) allow the valence-valence interactions to be separated in a straightforward way.

Assuming a deuteron target, Drell-Yan cross sections for positive and negative pions have the form

$$\begin{aligned}
\sigma_{DY}^{\pi^+ D}(x, x_\pi) &= \left[\frac{1}{9} q_v^\pi(x_\pi) + \frac{5}{9} q_s^\pi(x_\pi)\right] [u_v^p(x) + d_v^p(x)] \\
&+ \left[\frac{10}{9} q_v^\pi(x_\pi) + \frac{20 + 4\kappa}{9} q_s^\pi(x_\pi)\right] q_s^N(x), \\
\sigma_{DY}^{\pi^- D}(x, x_\pi) &= \left[\frac{4}{9} q_v^\pi(x_\pi) + \frac{5}{9} q_s^\pi(x_\pi)\right] [u_v^p(x) + d_v^p(x)] \\
&+ \left[\frac{10}{9} q_v^\pi(x_\pi) + \frac{20 + 4\kappa}{9} q_s^\pi(x_\pi)\right] q_s^N(x). \qquad (168)
\end{aligned}$$

In Eq. 168 we assumed the validity of charge symmetry $d^n(x) = u^p(x)$, $u^n(x) = d^p(x)$ and etc. In addition, for the pion sea we assumed SU(3) symmetry, i.e. the up, down and strange quark sea distributions in the pion are equal, $u_\pi = d_\pi = s_\pi$. Finally, for the nucleon we assumed $q_s^N(x) \equiv (u_s(x) + d_s(x))/2 = s(x)/\kappa$, where the fraction of the strange sea is chosen to reproduce the experimental ratio of dimuon events to single-muon events in neutrino-induced reactions [171]-[173] at the scale $Q^2 = Q_0^2 = 4$ GeV^2.

Under these assumptions, the valence-valence contribution for $\pi^- - D$ Drell-Yan processes is four times that for $\pi^+ - D$, while the sea-valence and sea-sea contributions are equal. Consequently, if we form the linear combinations

$$\begin{aligned}
\Sigma_s^{\pi D} &= 4\sigma_{DY}^{\pi^+ D} - \sigma_{DY}^{\pi^- D} \\
\Sigma_v^{\pi D} &= -\sigma_{DY}^{\pi^+ D} + \sigma_{DY}^{\pi^- D} \qquad (169)
\end{aligned}$$

Σ_s contains no valence-valence contribution (it contains only sea-valence and sea-sea terms), while Σ_v contains only a valence-valence term. In terms of sea and valence distributions (for pion and proton), these quantities have the form:

$$\Sigma_s^{\pi D} = \frac{10}{3} q_v^\pi(x_\pi) q_s^N(x) + \frac{5}{3} q_s^\pi(x_\pi)[u_v^p(x) + d_v^p(x)] + \frac{20 + 4\kappa}{3} q_s^\pi(x_\pi) q_s^N(x)$$

$$\Sigma_{\rm v}^{\pi D} = \frac{1}{3} q_v^\pi(x_\pi)[u_v^p(x) + d_v^p(x)]. \tag{170}$$

This means that if one measures π^+ and π^- Drell-Yan cross sections on the deuteron, and constructs the quantities Σ_s and $\Sigma_{\rm v}$, then the valence-valence pion-nucleon parton distributions can be extracted from $\Sigma_{\rm v}$, and the pion and/or nucleon sea can be obtained from Σ_s. Since the nucleon and pion valence distributions are reasonably well known, one should be able to determine the quantity $\Sigma_{\rm v}$ rather accurately.

If one defines the sea-to-valence ratios for pion and nucleon,

$$\begin{aligned} r_{sv}^N(x) &\equiv [u_s^p(x) + d_s^p(x)]/[u_v^p(x) + d_v^p(x)] \\ r_{sv}^\pi(x) &\equiv q_s^\pi(x)/q_v^\pi(x), \end{aligned} \tag{171}$$

then we have

$$\begin{aligned} R_{\rm s/v}(x, x_\pi) &\equiv \Sigma_s^{\pi D}/\Sigma_{\rm v}^{\pi D} \\ &= 5\, r_{sv}^N(x) + 5\, r_{sv}^\pi(x_\pi) + (10 + 2\kappa)\, r_{sv}^\pi(x_\pi)\, r_{sv}^N(x) \qquad (172) \\ &= \frac{10 q_s^N d_v^{\pi^-} + 5(d_v^p + u_v^p) q_s^\pi + 22 q_s^N q_s^\pi}{(d_v^p + u_v^p) d_v^{\pi^-}} \qquad (173) \end{aligned}$$

Although this does not "separate" entirely into pieces depending only on x or x_π it is relatively easy to isolate the piece depending on the pion sea by measuring $R_{\rm s/v}$ at reasonably large x, where r_{sv}^N becomes quite small. Furthermore, if one assumes that the nucleon valence and sea are known, together with the pion valence distributions, then $R_{\rm s/v}$ will be quite sensitive to the relative magnitude of the pion sea.

In Fig. 24 we show the predicted ratios $r_{sv}^\pi(x)$ and $r_{sv}^N(x)$. The sea-to-valence ratio drops off rapidly with increasing x. In Fig. 24 we have used the HMRS(B) solution for the nucleon quark distributions [174] together with pion fit 3 [164], in which the sea carries 10% of the pion's momentum at $Q^2 = 4$ GeV^2. At large x, $r_{sv}^N(x)$ is considerably smaller than the pion sea/valence ratio. This is because the nucleon sea of Harriman et al. [174] falls off very rapidly with increasing x [like $(1-x)^{9.75}$, relative to u_v^p which falls off like $(1-x)^{4.07}$]. Therefore as x increases, $r_{sv}^N(x)$ falls off very rapidly, and much faster than the pion sea/valence ratio. One can check this by measuring $\Sigma_{\rm v}$. Assuming that one knows both the pion and nucleon valence distributions, one should be able to predict this, and to predict the dependence of $\Sigma_{\rm v}$ on both x and x_π. Once this has been verified, one can use $R_{\rm s/v}$ to determine the pion sea quark distribution.

In Figs. 25, 29 and 27 we show predictions for $R_{\rm s/v}$ vs. x_π, for three values of nucleon momentum fraction x (0.4, 0.5 and 0.6). For each value of x, we plot four different curves corresponding to different phenomenological fits of Sutton et al. [164]. These correspond to different fits to the NA10 Drell-Yan data [165, 166], in which the pion sea carries from 5% to 20% of the pion's momentum at $Q^2 = Q_0^2 = 4$ GeV^2 (i.e., these are fits $2-5$ of Ref. [164]). First, the predicted ratio $R_{\rm s/v}$ is relatively large: for $x = 0.4$ and $x_\pi = 0.3$, $R_{s/v}$ varies from around 0.2 to 0.7 depending on the momentum fraction carried by the sea. Second, $R_{\rm s/v}$ is extremely sensitive to the momentum fraction carried by the pion sea. The quantity $R_{\rm s/v}$ is roughly linear in this momentum fraction; the difference between those values where 5% of the pion's momentum is carried by the sea, and that for distributions where 20% is carried by the sea quarks, is roughly a factor of 4 in $R_{\rm s/v}$.

Thus even qualitative measurements of $R_{\rm s/v}$ should be able to differentiate between pion parton distributions in which the sea carries different fractions of the pion's momentum. Even for values of x_π as large as 0.5, where the pion sea/valence ratio is about 0.01, the quantity $R_{s/v}$ is still relatively large (about $0.1 \to 0.15$), and varies significantly depending on which pion sea one chooses.

In Figs. 28, 29 and 30 we show the quantity $R_{s/v}$ vs. x_π, for three values of nucleon momentum fraction x (0.3, 0.4 and 0.6). As in Figs. 25-27, the four different curves correspond to pion structure functions where the sea carries different fractions of the pion's momentum. Figs. 28-30 differ from Figs. 25-27 in that we use the CTEQ(3M) [176] nucleon structure functions, rather than the HMRS(B) structure functions of Figs. 25-27 [20]. Although there are some minor quantitative differences between Figs. 28-30 and Figs. 25-27, qualitatively it is still straightforward to differentiate experimentally between the various pion sea distributions. In both Figs. 28-30 and Figs. 25-27, the quantity $R_{s/v}$ allows one to extract the pion sea distribution, and $R_{s/v}$ is extremely sensitive to the fraction of the pion momentum carried by the sea.

The Drell-Yan ratio given in Eq. (173) was derived assuming charge symmetry for the nucleon and pion structure functions. When calculating the relation Σ_s/Σ_v one should be careful with the corrections to the distributions of quarks, coming from two main reasons: a) masses of *up* and *down* quarks are not equal to each other, which leads to charge symmetry breaking (CSB) and b) there is an interaction between nucleons leading to the deviation of distributions of quarks from those in a single nucleon. Although these corrections are small ($\sim 5\%$) they may become significant on the background of pieces left after cancellations in Σ_s/Σ_v. In a Chapter 6 we estimated charge symmetry violation [CSV] for both nucleon and pion (see also Ref. [177]) and found that the "minority" CSV term, δd, was surprisingly large. If we include CSV terms, then to lowest order in charge symmetry violation the sea/valence ratio $R_{s/v}$ will acquire an additional term

$$R_{vs}^{(1)} = -\frac{(4d_v^{\pi^-}+3q_s^\pi)}{3d_v^{\pi^-}}\frac{\delta u_v}{(d_v^p+u_v^p)} + \frac{4(d_v^{\pi^-}-q_s^\pi)}{3d_v^{\pi^-}}\frac{\delta d_v}{(d_v^p+u_v^p)} - (\frac{8q_s^N}{(d_v^p+u_v^p)} - \frac{4}{3})\frac{\delta d_v^\pi}{d_v^{\pi^-}} \quad (178)$$

where we have the charge symmetry violations

$$\begin{aligned} \delta d_v(x) &\equiv d_v^p(x) - u_v^n(x) \\ \delta u_v(x) &\equiv u_v^p(x) - d_v^n(x) \\ \delta \bar{d}_v^\pi(x) &\equiv \bar{d}_v^{\pi^+}(x) - \bar{u}_v^{\pi^-}(x) \end{aligned} \quad (179)$$

In Figs. 25-27, we have already included the CSV contributions in $R_{s/v}$. In Fig. 31, we show the CSV contributions $\delta R_{s/v}$ for $\pi - D$ Drell-Yan processes, assuming various values

[20] The most recent parametrizations of distributions of quarks in a nucleon of the group of A.D. Martin et. al. are [175]

$$\begin{aligned} xu_v &= 2.0x^{0.538}(1-x)^{3.96}(1-0.39\sqrt{x}+5.13x) \\ xd_v &= 0.3x^{0.330}(1-x)^{4.71}(1+5.03\sqrt{x}+5.56x) \\ xq_s &= 0.051x^{0.3}(1-x)^{9.27}(1-1.15\sqrt{x}+15.6x) \end{aligned} \quad (174)$$

normalised such that $\int_0^1 d_v(x)dx = 1$ and $\int_0^1 u_v(x)dx = 2$ at $Q^2 = 4$ GeV^2.

H.L. Lai et.al. present another form of distributions [176]:

$$\begin{aligned} xd_v &= 0.269x^{0.278}(1-x)^{3.67}(1+29.6x^{0.807}) \\ xu_v &= 1.239x^{0.521}(1-x)^{3.18}(1-0.85x^{1.82}) \\ xq_s &= 0.061x^{-0.258}(1-x)^{8.45}(1+12.7x^{1.1}) \end{aligned} \quad (175)$$

As for the quarks in a pion we took their distributions from Ref. [164]

$$xq_s^\pi = \frac{1}{6}0.6(1-x)^5 \quad (176)$$

$$xd_v^{\pi^-} = x^{0.61}(1-x)^{1.08} \quad (177)$$

also measured at $Q^2 = 4$ GeV^2.

for the momentum fraction carried by the pion sea. Comparing Fig. 31 with Figs. 25-27 shows that, for reasonably small values of x_π, charge symmetry violation makes a quite a small contribution – of the order of $1-2$ percent of $R_{s/v}$. This relative contribution grows with increasing x_π, so that for $x_\pi \approx 0.5$ the contribution is of the order of 10%. Clearly, it should be possible to extract the pion sea from such measurements even in the presence of charge symmetry violating amplitudes for both nucleon and pion. Finally, the magnitude of the CSV contributions depends very weakly on the fraction of the pion momentum carried by the sea.

These results should hold for Drell-Yan processes induced by π^+ and π^- on any isoscalar target, such as ^{12}C or ^{16}O. Furthermore, EMC effects (shifts in the quark distributions between free nucleons and nuclei) [178]-[179] will not affect the quantity $R_{s/v}$, provided these effects are the same for up and down quarks (and protons and neutrons). Such corrections would be the same for both numerator and denominator of $R_{s/v}$, and would cancel.

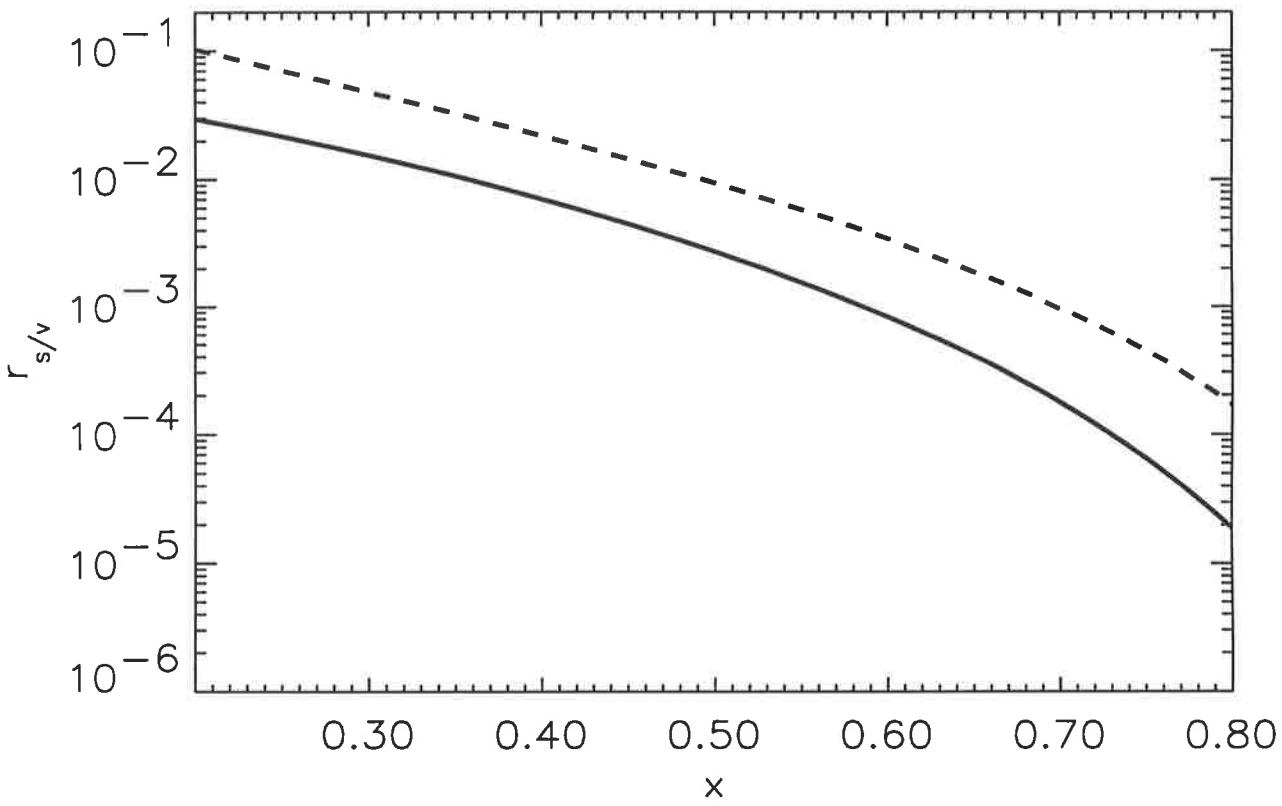

Figure 24: Predicted sea/valence ratio for pion and nucleon. Dashed curve: $r^{\pi}_{sv}(x)$; solid curve: $r^{N}_{sv}(x)$ vs. momentum fraction x.

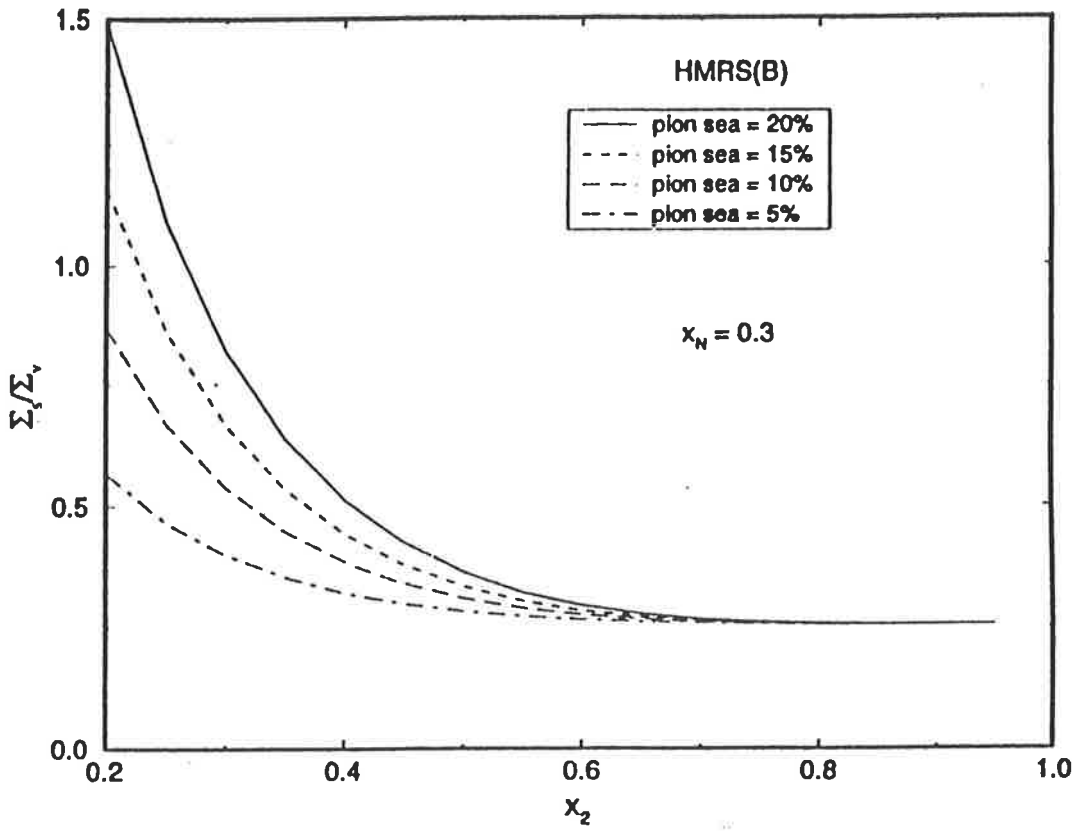

Figure 25: Predicted sea/valence term $R_{s/v}$ vs. the pion momentum fraction $x_2 \sim x_\pi$, for various pion sea quark distributions, which vary according to the fraction of the pion's momentum carried by the pion sea. Solid curve: pion sea carries 20% of the pion's momentum; dashed curve: pion sea of 15%; long-dashed curve: pion sea of 10%; dot-dashed curve: pion sea of 5%. Nucleon distributions are the HMRS(B) distributions. Nucleon momentum fraction $x_N = 0.3$.

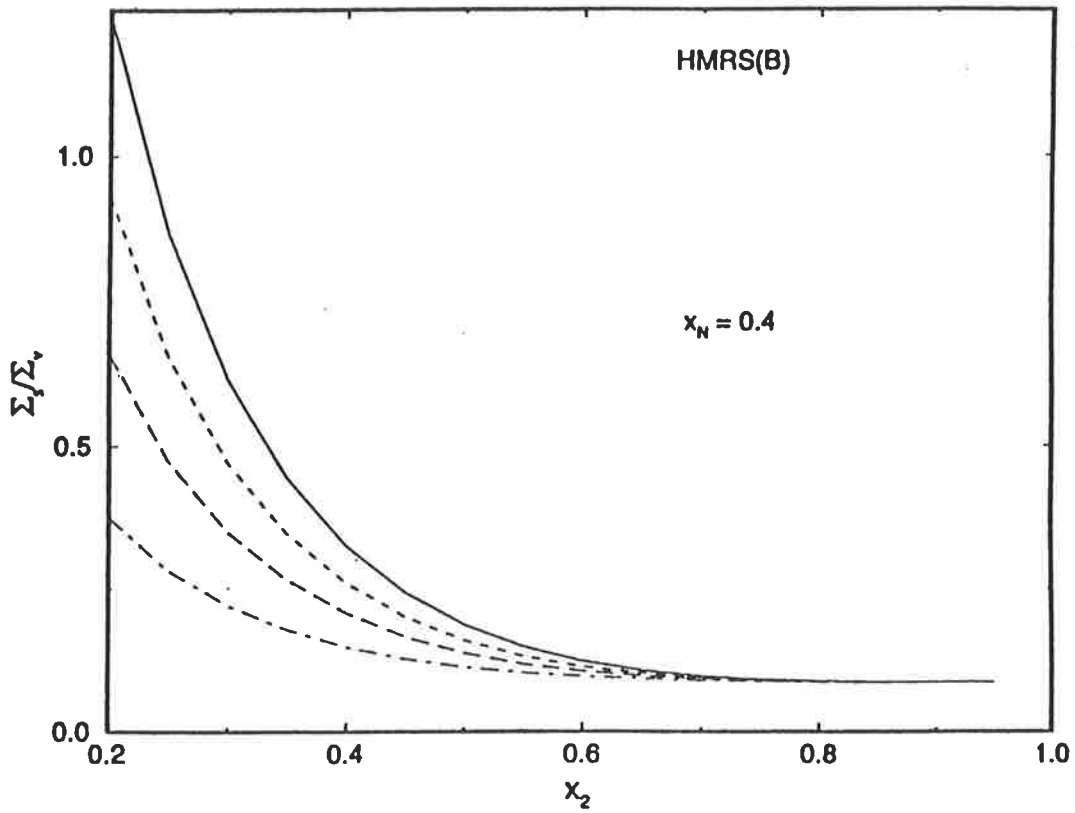

Figure 26: Predicted sea/valence term $R_{s/v}$ vs. the pion momentum fraction $x_2 \sim x_\pi$, for various pion sea quark distributions, which vary according to the fraction of the pion's momentum carried by the pion sea. Solid curve: pion sea carries 20% of the pion's momentum; dashed curve: pion sea of 15%; long-dashed curve: pion sea of 10%; dot-dashed curve: pion sea of 5%. Nucleon distributions are the HMRS(B) distributions. Nucleon momentum fraction $x_N = 0.4$.

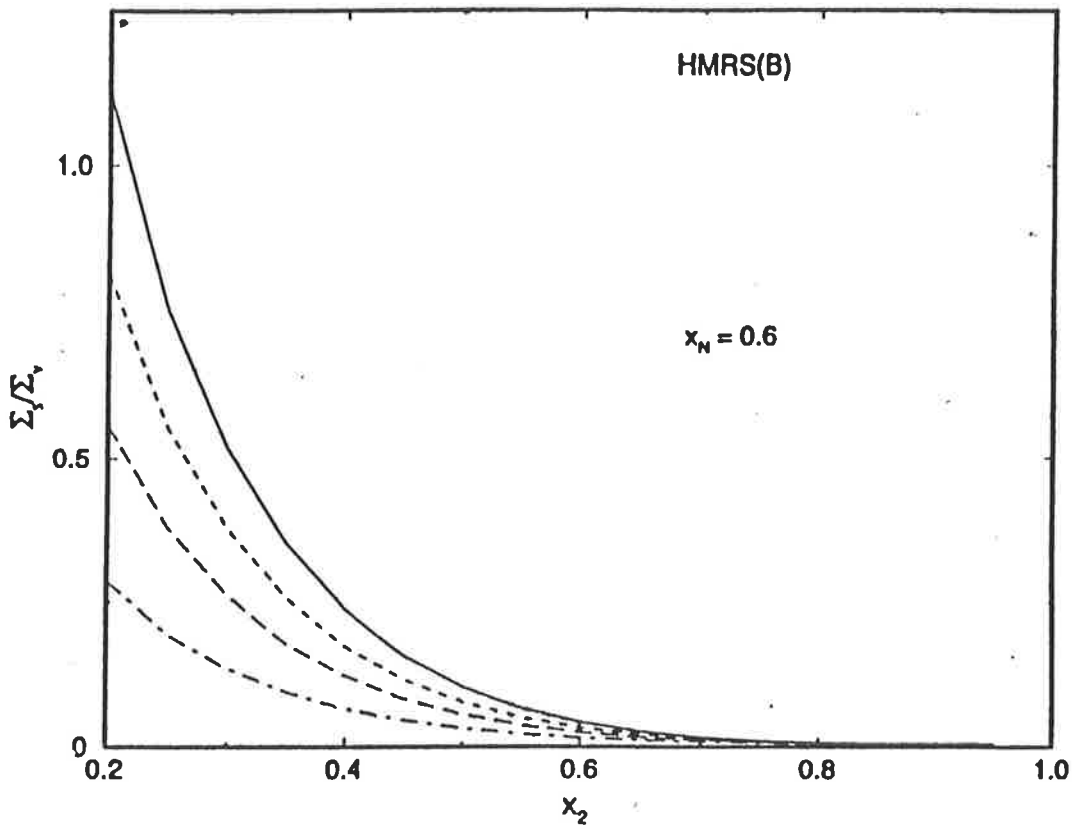

Figure 27: Predicted sea/valence term $R_{s/v}$ vs. the pion momentum fraction $x_2 \sim x_\pi$, for various pion sea quark distributions, which vary according to the fraction of the pion's momentum carried by the pion sea. Solid curve: pion sea carries 20% of the pion's momentum; dashed curve: pion sea of 15%; long-dashed curve: pion sea of 10%; dot-dashed curve: pion sea of 5%. Nucleon distributions are the HMRS(B) distributions. Nucleon momentum fraction $x_N = 0.6$.

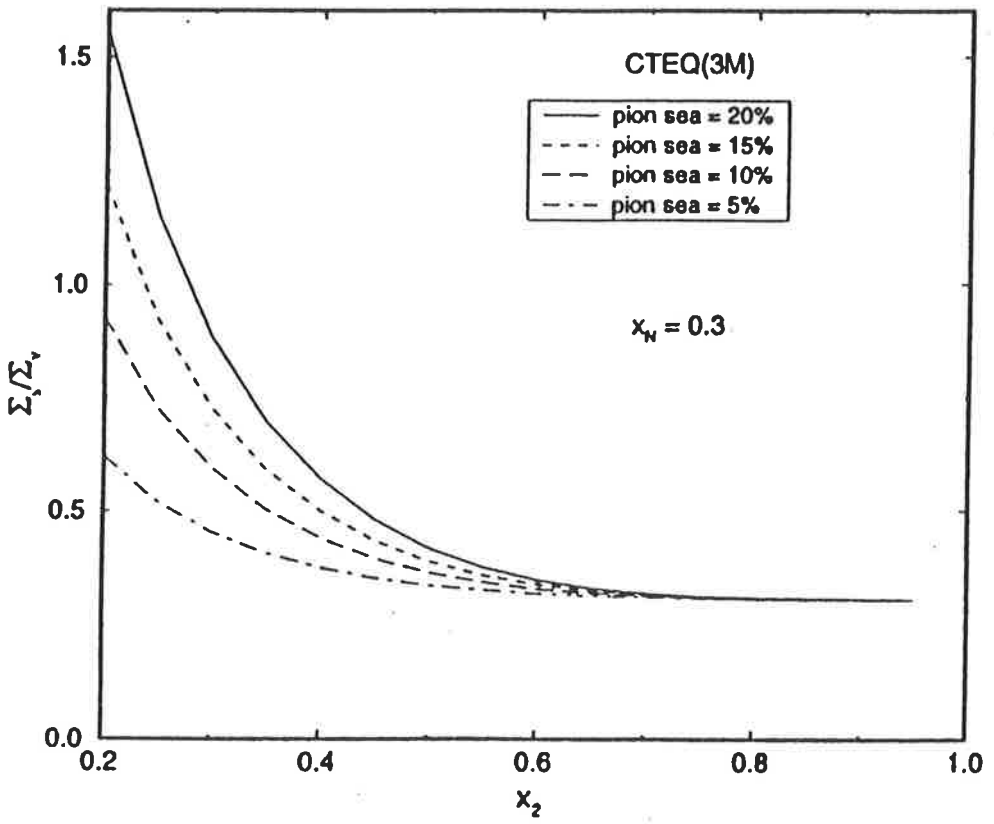

Figure 28: Predicted sea/valence term $R_{s/v}$ vs. the pion momentum fraction $x_2 \sim x_\pi$, for various pion sea quark distributions, which vary according to the fraction of the pion's momentum carried by the pion sea. Solid curve: pion sea carries 20% of the pion's momentum; dashed curve: pion sea of 15%; long-dashed curve: pion sea of 10%; dot-dashed curve: pion sea of 5%. Nucleon distributions are the CTEQ(3M) distributions. Nucleon momentum fraction $x_N = 0.3$.

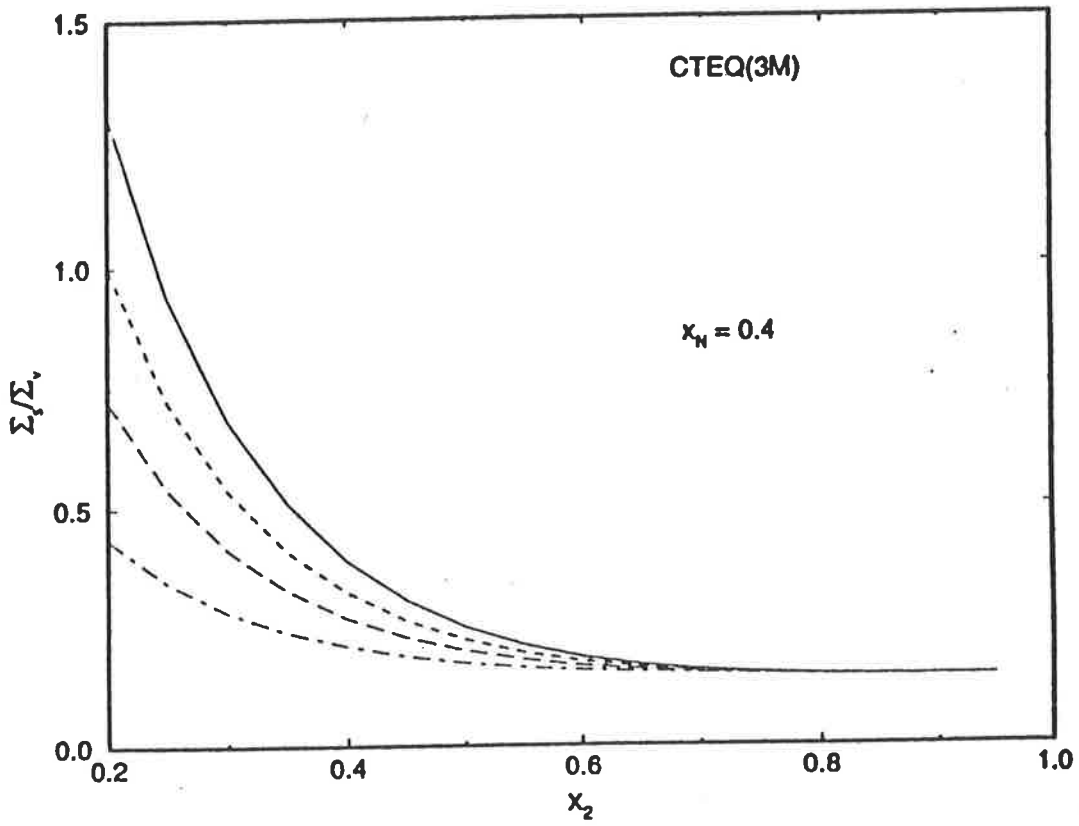

Figure 29: Predicted sea/valence term $R_{s/v}$ vs. the pion momentum fraction $x_2 \sim x_\pi$, for various pion sea quark distributions, which vary according to the fraction of the pion's momentum carried by the pion sea. Solid curve: pion sea carries 20% of the pion's momentum; dashed curve: pion sea of 15%; long-dashed curve: pion sea of 10%; dot-dashed curve: pion sea of 5%. Nucleon distributions are the CTEQ(3M) distributions. Nucleon momentum fraction $x_N = 0.4$.

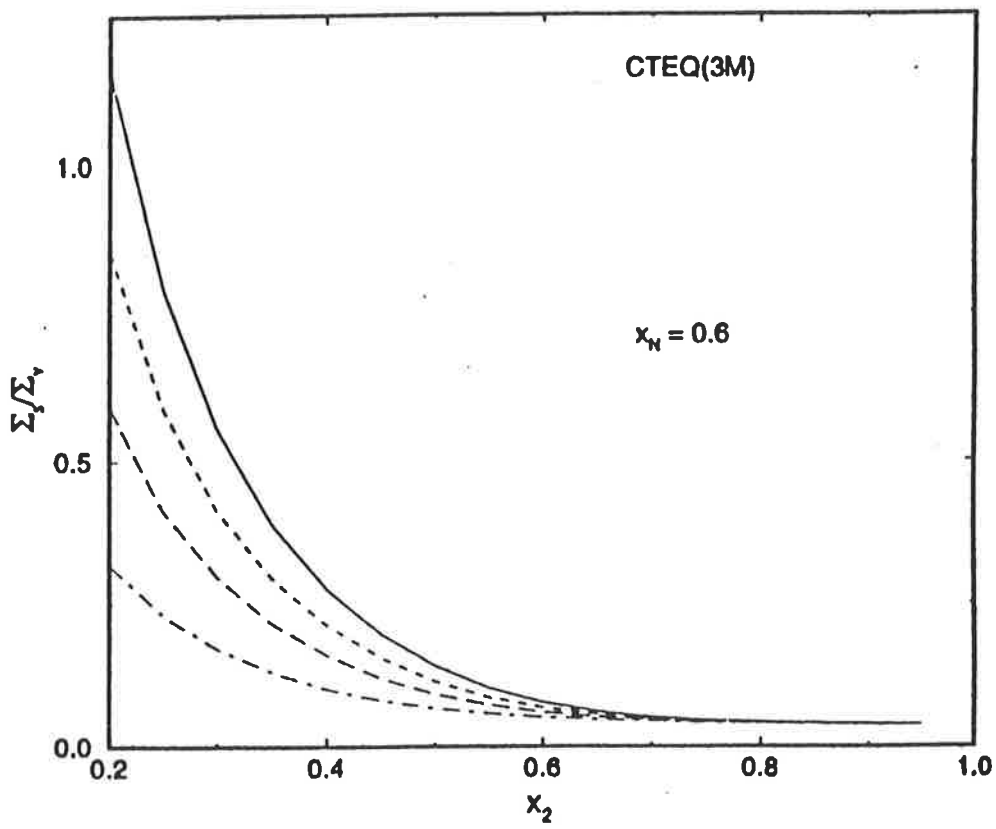

Figure 30: Predicted sea/valence term $R_{s/v}$ vs. the pion momentum fraction $x_2 \sim x_\pi$, for various pion sea quark distributions, which vary according to the fraction of the pion's momentum carried by the pion sea. Solid curve: pion sea carries 20% of the pion's momentum; dashed curve: pion sea of 15%; long-dashed curve: pion sea of 10%; dot-dashed curve: pion sea of 5%. Nucleon distributions are the CTEQ(3M) distributions. Nucleon momentum fraction $x_N = 0.6$.

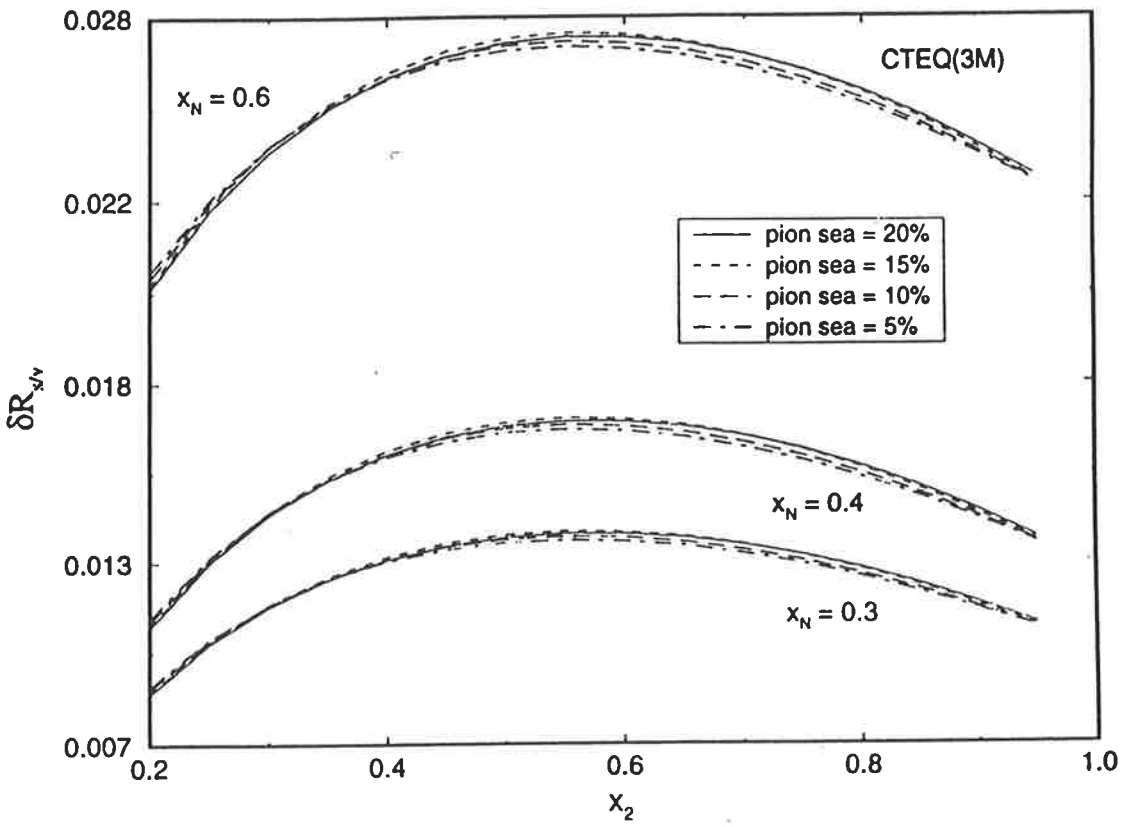

Figure 31: Charge-symmetry violating contributions $\delta R_{s/v}$ to the sea/valence ratio $R_{s/v}$.

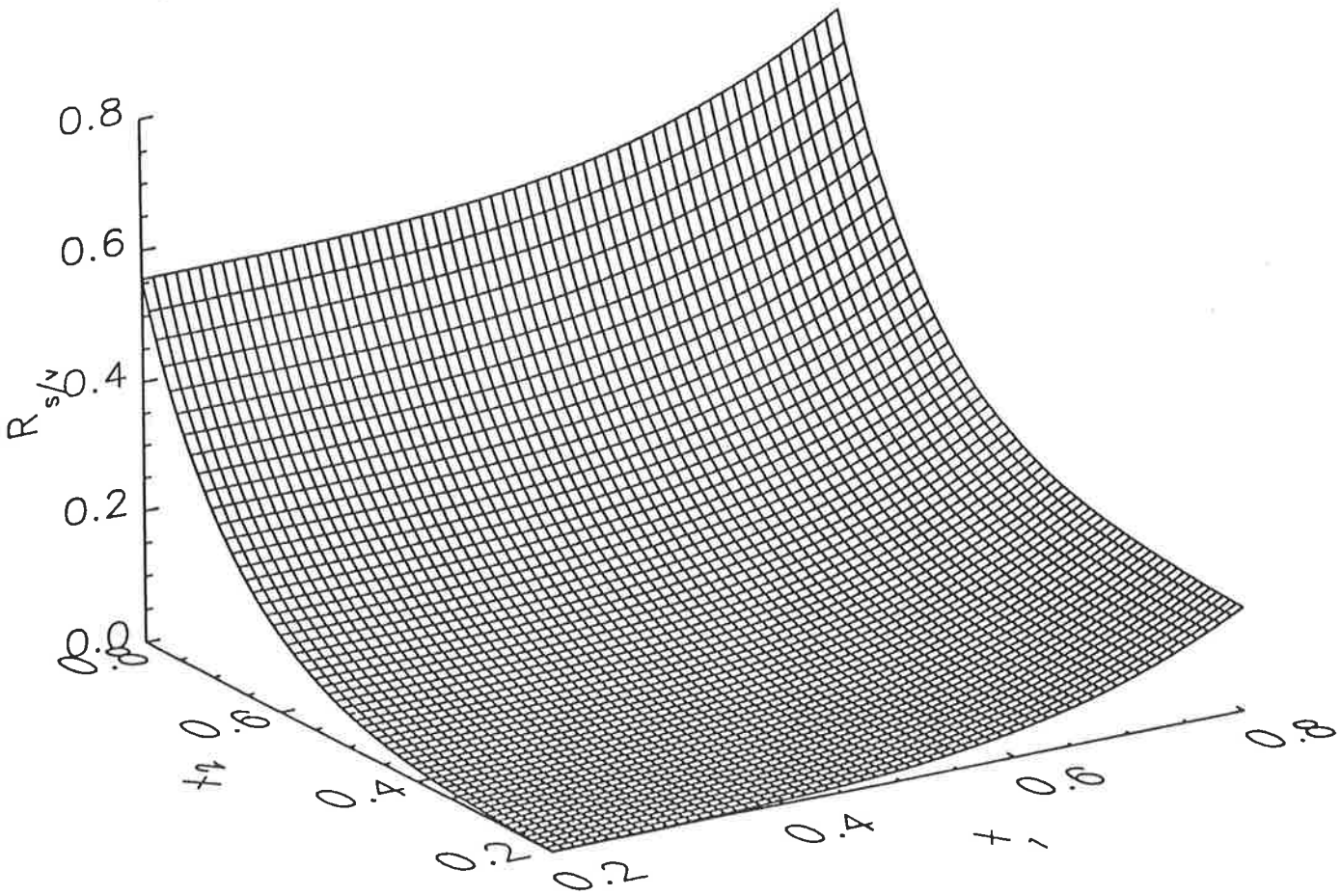

Figure 32: Predicted sea/valence term $R_{s/v}$ vs. the pion momentum fraction $x_2 \sim x_\pi$ and nucleon momentum fraction $x_1 \sim x_N$ for pion sea quark distribution carrying 5% of the pion's momentum.

9 Summary.

This chapter was devoted to the application of the bag model to the study of charge symmetry violation in parton distributions. We have estimated the value of charge symmetry breaking in parton distributions and found surprising results, namely, that the fractional differences between $d_V^p(x)$ and $u_V^n(x)$ can be as large as 10% for intermediate values of Bjorken x.

As a natural extension we also estimated charge symmetry violation for the pion and examined the sensitivity of pion-induced Drell-Yan measurements to such effects. We showed that combinations of π^+ and π^- data on deuterium and hydrogen are sensitive to them, and further that the pion and nucleon charge symmetry violating terms separate as a function of x_π and x_N respectively. We also estimated the background terms which must be evaluated to extract charge symmetry violation.

Another question that we have studied was the evolution of quark distributions. We compared various calculations based on such well-known approaches as the Bernstein polynomial and Altarelli-Parisi methods with two *new* methods and investigated the problems of numerical evolution.

Finally, we have highlighted the advantages of using the Drell-Yan process to study the pion sea-quark distributions which are relatively poorly determined at the moment. We have shown that combinations of π^+ and π^- Drell-Yan measurements on deuterium allow the pion sea distribution to be extracted. The contribution from the pion sea was found to be comparable with that from its valence quarks and hence the experiment should be quite sensitive to the fraction of the pion momentum carried by the sea. We estimated the charge symmetry violating contributions to these processes, and showed that they should not prevent us from extracting the pion sea distributions.

Part III
Application of the bag model to nuclear physics.

10 Introduction

The nuclear many-body problem has been the object of enormous theoretical attention for decades. Apart from the non-relativistic treatments based upon realistic two-body forces [181], there are also studies of three-body effects and higher [182]. The importance of relativity has been recognised in a host of treatments under the general heading of Dirac-Brueckner [183, 184]. This approach has also had considerable success in the treatment of scattering processes [185]. At the same time, the simplicity of Quantum Hadrodynamics (QHD) [50, 2] has to led to its widespread application, and to attempts to extend it to incorporate the density dependence of the couplings [186] that seems to be required empirically.

One of the fundamental, unanswered questions in this field concerns the role of sub-nucleon degrees of freedom (quarks and gluons) in determining the equation of state. There is little doubt that, at sufficiently high density (perhaps $5 - 10\rho_0$, with ρ_0 the saturation density of symmetric nuclear matter), quarks and gluons must be the correct degrees of freedom and major experimental programs in relativistic heavy ion physics are either planned or underway [187, 188] to look for this transition. In order to calculate the properties of neutron stars [189] one needs an equation of state from very low density to many times ρ_0 at the centre. A truly consistent theory describing the transition from meson and baryon degrees of freedom to quarks and gluons might be expected to incorporate the internal quark and gluon degrees of freedom of the particles themselves. Our investigation may be viewed as a first step in this direction. We shall work with the quark-meson coupling (QMC) model originally proposed by Guichon [3] and since developed extensively [190, 191].

Within the QMC model [3] the properties of nuclear matter are determined by the self-consistent coupling of scalar (σ) and vector (ω) fields to the *quarks within the nucleons*, rather than to the nucleons themselves. As a result of the scalar coupling the internal structure of the nucleon is modified with respect to the free case. In particular, the small mass of the quark means that the lower component of its wave function responds rapidly to the σ field, with a consequent decrease in the scalar density. As the scalar density is itself the source of the σ field this provides a mechanism for the saturation of nuclear matter where the quark structure plays a vital role.

In a simple model where nuclear matter was considered as a collection of static, non-overlapping bags it was shown that a satisfactory description of the bulk properties of nuclear matter can be obtained [3, 190]. Of particular interest is the fact that the extra degrees of freedom, corresponding to the internal structure of the nucleon, result in a lower value of the incompressibility of nuclear matter than obtained in approaches based on point-like nucleons – such as QHD [2]. In fact, the prediction is in agreement with the experimental value once the binding energy and saturation density are fixed. Improvements to the model, including the addition of Fermi motion, have not altered the dominant saturation mechanism. Furthermore, it is possible to give a clear understanding of the relationship between this model and QHD [190] and to study variations of hadron properties in nuclear matter [191]. Surprisingly the model seems to provide a semi-quantitative explanation of the Okamoto-Nolen-Schiffer anomaly [193] when quark mass differences

are included [62]. A further application of the model, including quark mass differences, has suggested a previously unknown correction to the extraction of the matrix element, V_{ud}, from super-allowed Fermi beta-decay [194]. Finally the model has been applied to the case where quark degrees of freedom are undisputedly involved – namely the nuclear EMC effect [195].

Because the model has so far been constructed for infinite nuclear matter its application has been limited to situations which either involve bulk properties or where the local density approximation has some validity. Our aim here is to overcome this limitation by extending the model to finite nuclei. In general this is a very complicated problem and our approach will be essentially classical. Our starting point will be exactly as for nuclear matter. That is, we assume that on average the quark bags do not overlap and that the quarks are coupled locally to average σ and ω fields. The latter will now vary with position, while remaining time independent – as they are mean fields. For deformed or polarised nuclei one should also consider the space components of the vector field. In order to simplify the present discussion we restrict ourselves to spherical, spin-saturated nuclei.

Our approach to the problem will be within the framework of the Born-Oppenheimer approximation. Since the quarks typically move much faster than the nucleons we assume that they always have time to adjust their motion so that they are in the lowest energy state. In order to account for minimal relativistic effects it is convenient to work in the instantaneous rest frame (IRF) of the nucleon. Implicitly one then knows both the position and the momentum of the nucleon, so that the treatment of the motion of the nucleon is classical – at least, as long as the quarks are being considered explicitly. The quantisation of the motion of the nucleon is carried out after the quark degrees of freedom have been eliminated.

In Sect. 11 we show how the Born-Oppenheimer approximation can be used to treat the quark degrees of freedom in a finite nucleus. In Sect. 12 we derive the classical equation of motion for a bag in the meson fields, including the spin-orbit interaction which is treated in first order in the velocity. We then quantize the nucleon motion in a non relativistic way. The self consistent equations for the meson fields are derived in Sect. 13. In Sect. 14 we summarize the model in the form of a self-consistent procedure. The use of this non relativistic formulation is postponed to future work. To allow a clear comparison with QHD we propose a relativistic formulation which is then applied, in Sect. 16, to nuclear matter. Some initial results for finite nuclei are also presented.

11 The Born-Oppenheimer approximation.

In what follows the coordinates in the rest frame of the nucleus (NRF) will be denoted without primes: $(t, \vec{r})$. In this frame the nucleon follows a classical trajectory, $\vec{R}(t)$. Denoting the instantaneous velocity of the nucleon as $\vec{v} = d\vec{R}/dt$, we can define an instantaneous rest frame for the nucleon at each time t. The coordinates in this IRF are $(t', \vec{r}')$:

$$\begin{aligned} r_L &= r'_L \cosh\xi + t' \sinh\xi, \\ \vec{r}_\perp &= \vec{r}_\perp{}', \\ t &= t' \cosh\xi + r'_L \sinh\xi, \end{aligned} \tag{180}$$

where r_L and $\vec{r}_\perp$ are the components respectively parallel and transverse to the velocity and ξ is the rapidity defined by $\tanh\xi = |\vec{v}(t)|$.

Our assumption that the quarks have time to adjust to the local fields in which the nucleon is moving is exact if the fields are constant – i.e. if the motion of the nucleon has no

acceleration. It is, of course, very important to examine the validity of the approximation for a typical nuclear environment. For this purpose we take the nucleon motion to be non-relativistic. Assume that at time 0 the nucleon is at $\vec{R}_0$. After time t, assuming t small enough, we have

$$\vec{R}(t) = \vec{R}_0 + \vec{v}_0 t + \frac{1}{2}t^2\vec{\alpha}_0, \tag{181}$$

where $\vec{\alpha}_0$ $(= \vec{F}/M_N = -\vec{\nabla}V/M_N)$ is the acceleration and M_N is the free nucleon mass. We shall take the potential to be a typical Woods-Saxon form with depth $V_0 \sim -50$ MeV, surface thickness $a \sim 2$ fm and radius $R_A \sim 1.2A^{1/3}$ fm. The maximum acceleration occurs at $R = R_A$ and takes the value

$$\vec{\alpha}_{max} = V_0\frac{\hat{R}}{aM_N}. \tag{182}$$

Therefore, in the IRF we have

$$\vec{R}'(t) \sim \vec{R}'_0 + \frac{1}{2}t^2\frac{V_0}{aM_N}\hat{R}_0, \tag{183}$$

and, in the worst case, relative to the size of the nucleon itself (R_B), the departure from a fixed position, is

$$\left|\frac{R'(t) - R'_0}{R_B}\right| \sim \frac{1}{2}t^2\frac{|V_0|}{aM_N R_B} \sim \frac{t^2}{80}, \tag{184}$$

with t in fm. Thus, as long as the time taken for the quark motion to change is less than ~ 9 fm, the nucleon position in the IRF can be considered as unchanged. Since the typical time for an adjustment in the motion of the quarks is given by the inverse of the typical excitation energy, which is of order 0.5 fm, this seems quite safe.

As we have just seen, it is reasonable to describe the internal structure of the nucleon in the IRF. In this frame we shall adopt the static spherical cavity approximation to the MIT bag for which the Lagrangian density is

$$\mathcal{L}_0 = \bar{q}'(i\gamma^\mu\partial_\mu - m_q)q' - BV, \qquad \text{for } |\vec{u}'| \leq R_B, \tag{185}$$

with B the bag constant, R_B the radius of the bag, m_q the quark mass and $\vec{u}'$ the position of the quark from the center of the bag (in the IRF): $\vec{u}' = \vec{r}' - \vec{R}'$. We shall denote as u' the 4-vector $(t', \vec{u}')$. The field $q'(u'_0, \vec{u}')$ is the quark field in the IRF, which must satisfy the boundary condition

$$(1 + i\vec{\gamma}\cdot\hat{u}')q' = 0, \qquad \text{at } |\vec{u}'| = R_B. \tag{186}$$

Next we must incorporate the interaction of the quarks with the scalar (σ) and vector (ω) mean fields generated by the other nucleons. In the nuclear rest frame they are self-consistently generated functions of position – $\sigma(\vec{r})$ and $\omega(\vec{r})$. Using the scalar and vector character of these fields, we know that in the IRF their values are

$$\begin{aligned} \sigma_{IRF}(t', \vec{u}') &= \sigma(\vec{r}), \\ \omega_{IRF}(t', \vec{u}') &= \omega(\vec{r})\cosh\xi, \\ \vec{\omega}_{IRF}(t', \vec{u}') &= -\omega(\vec{r})\hat{v}\sinh\xi, \end{aligned} \tag{187}$$

and the interaction term is

$$\mathcal{L}_I = g^q_\sigma\bar{q}'q'(u')\sigma_{IRF}(u') - g^q_\omega\bar{q}'\gamma_\mu q'(u')\omega^\mu_{IRF}(u'), \tag{188}$$

where g_σ^q and g_ω^q are the quark-meson coupling constants for σ and ω, respectively. Apart from isospin considerations, the effect of the ρ meson can be deduced from the effect of the ω. Thus we postpone its introduction to the end of this section.

Since we wish to solve for the structure of the nucleon in the IRF we need the Hamiltonian and its degrees of freedom in this frame. This means that the interaction term should be evaluated *at equal time* t' for all points $\vec{u}\,'$ in the bag. Suppose that at time t' the bag is located at $\vec{R}'$ in the IRF. Then, in the NRF it will be located at $\vec{R}$ at time T defined by

$$\begin{aligned} R_L &= R'_L \cosh\xi + t' \sinh\xi, \\ \vec{R}_\perp &= \vec{R}'_\perp, \\ T &= t' \cosh\xi + R'_L \sinh\xi. \end{aligned} \tag{189}$$

For an arbitrary point $\vec{r}\,'$ $(= \vec{u}\,' + \vec{R}')$ in the bag, at the same time t', we have an analogous relation

$$\begin{aligned} r_L &= r'_L \cosh\xi + t' \sinh\xi, \\ \vec{r}_\perp &= \vec{r}_\perp\,', \\ t &= t' \cosh\xi + r'_L \sinh\xi, \end{aligned} \tag{190}$$

from which we deduce

$$\begin{aligned} r_L &= R'_L \cosh\xi + t' \sinh\xi + u'_L \cosh\xi, \\ &= R_L + u'_L \cosh\xi, \\ \vec{r}_\perp &= \vec{R}_\perp + \vec{u}_\perp\,'. \end{aligned} \tag{191}$$

This leads to the following expression for the σ field

$$\sigma_{IRF}(t', \vec{u}\,') = \sigma(R_L(T) + u'_L \cosh\xi, \vec{R}_\perp(T) + \vec{u}_\perp\,'), \tag{192}$$

with a corresponding equation for the ω field.

The spirit of the Born-Oppenheimer approximation is to solve the equation of motion for the quarks with the position $\vec{R}(T)$ regarded as a fixed parameter. In order to test the reliability of this approximation we consider a non-relativistic system and neglect finite-size effects. That is, we take

$$\sigma_{IRF}(t', \vec{u}\,') \sim \sigma(\vec{R}(T)). \tag{193}$$

As we noted earlier, the typical time scale for a change in the motion of the quark is $\tau \sim 0.5$ fm. During this time the relative change of σ due to the motion of the bag is

$$\frac{\Delta\sigma}{\sigma} = \vec{v} \cdot \hat{R} \frac{\sigma'}{\sigma} \tau. \tag{194}$$

It is reasonable to assume that σ roughly follows the nuclear density, and as long as this is constant, $\Delta\sigma$ vanishes and the approximation should be good. The variation of the density occurs mainly in the surface where it drops to zero from ρ_0 (the normal nuclear density) over a distance d of about 2 fm. Therefore we can estimate $|\sigma'/\sigma|$ as approximately $1/d$ in the region where ρ varies. The factor $\vec{v} \cdot \hat{R}$ depends on the actual trajectory, but as a rough estimate we take $\hat{v} \cdot \hat{R} \sim 1/3$. That is, we suppose that the probability for $\hat{v}$ is isotropic. For the magnitude of the velocity we take k_F/M_N with $k_F = 1.7$ fm^{-1} the Fermi momentum. With these estimates we find

$$\frac{\Delta\sigma}{\sigma} \sim \frac{0.36 \cdot 0.5}{3 \cdot 2} \sim 3\%, \tag{195}$$

which is certainly small enough to justify the use of the Born-Oppenheimer approximation. Clearly this amounts to neglecting terms of order v in the argument of σ and ω. In order to be consistent we therefore also neglect terms of order v^2 – that is, we replace $u'_L \cosh\xi$ by u'_L.

12 Equation of motion for a bag in the nuclear field

12.1 Leading term in the Hamiltonian

Following the considerations of the previous section, in the IRF the interaction Lagrangian density takes the simple, approximate form:

$$\mathcal{L}_I = g^q_\sigma \bar{q}' q'(t', \vec{u}')\sigma(\vec{R}+\vec{u}') - g^q_\omega \bar{q}'[\gamma_0 \cosh\xi + \vec{\gamma}\cdot\hat{v}\sinh\xi]q'(t',\vec{u}')\omega(\vec{R}+\vec{u}'). \quad (196)$$

The corresponding Hamiltonian is [1]

$$\begin{aligned} H &= \int_0^{R_B} d\vec{u}'\, \bar{q}'[-i\vec{\gamma}\cdot\vec{\nabla} + m_q - g^q_\sigma\sigma(\vec{R}+\vec{u}') \\ &\quad + g^q_\omega\omega(\vec{R}+\vec{u}')(\gamma^0\cosh\xi + \vec{\gamma}\cdot\hat{v}\sinh\xi)]q'(t',\vec{u}') + BV, \end{aligned} \quad (197)$$

while the momentum is simply

$$\vec{P} = \int_0^{R_B} d\vec{u}'\, q'^\dagger[-i\vec{\nabla}]q'. \quad (198)$$

As the σ and ω fields only vary appreciably near the nuclear surface, where $R \gg |\vec{u}'|$ (since $|\vec{u}'|$ is bounded by the bag radius), it makes sense to split H into two parts:

$$H = H_0 + H_1, \quad (199)$$

$$\begin{aligned} H_0 &= \int_0^{R_B} d\vec{u}'\, \bar{q}'[-i\vec{\gamma}\cdot\vec{\nabla} + m_q - g^q_\sigma\sigma(\vec{R}) \\ &\quad + g^q_\omega\omega(\vec{R})(\gamma^0\cosh\xi + \vec{\gamma}\cdot\hat{v}\sinh\xi)]q'(t',\vec{u}') + BV, \end{aligned} \quad (200)$$

$$\begin{aligned} H_1 &= \int_0^{R_B} d\vec{u}'\, \bar{q}'[-g^q_\sigma(\sigma(\vec{R}+\vec{u}') - \sigma(\vec{R})) \\ &\quad + g^q_\omega(\omega(\vec{R}+\vec{u}') - \omega(\vec{R}))(\gamma^0\cosh\xi + \vec{\gamma}\cdot\hat{v}\sinh\xi)]q'(t',\vec{u}'), \end{aligned} \quad (201)$$

and to consider H_1 as a perturbation.

Suppose we denote as ϕ^α the complete and orthogonal set of eigenfunctions defined by

$$\begin{aligned} h\phi^\alpha(\vec{u}') &\equiv (-i\gamma^0\vec{\gamma}\cdot\vec{\nabla} + m^*_q\gamma^0)\phi^\alpha(\vec{u}'), \\ &= \frac{\Omega_\alpha}{R_B}\phi^\alpha(\vec{u}'), \end{aligned} \quad (202)$$

$$(1 + i\vec{\gamma}\cdot\hat{u}')\phi^\alpha(\vec{u}') = 0, \quad \text{at } |\vec{u}'| = R_B, \quad (203)$$

$$\int_0^{R_B} d\vec{u}'\, \phi^{\alpha\dagger}\phi^\beta = \delta^{\alpha\beta}, \quad (204)$$

with $\{\alpha\}$ a collective symbol for the quantum numbers and m^*_q a parameter. Here we recall the expression for the lowest positive energy mode, ϕ^{0m}, with m the spin label:

$$\phi^{0m}(t',\vec{u}') = \mathcal{N}\begin{pmatrix} j_0(xu'/R_B) \\ i\beta_q\vec{\sigma}\cdot\hat{u}' j_1(xu'/R_B)\end{pmatrix}\frac{\chi_m}{\sqrt{4\pi}}, \quad (205)$$

[1] Only the quark degrees of freedom are active. The nucleon position and velocity are parameters as discussed earlier.

where

$$\Omega_0 = \sqrt{x^2 + (m_q^\star R_B)^2}, \quad \beta_q = \sqrt{\frac{\Omega_0 - m_q^\star R_B}{\Omega_0 + m_q^\star R_B}}, \tag{206}$$

$$\mathcal{N}^{-2} = 2R_B^3 j_0^2(x)[\Omega_0(\Omega_0 - 1) + m_q^\star R_B/2]/x^2. \tag{207}$$

For this mode, the boundary condition at the surface amounts to

$$j_0(x) = \beta_q j_1(x). \tag{208}$$

We expand the quark field in the following way

$$q'(t', \vec{u}') = \sum_\alpha e^{-i\vec{k}\cdot\vec{u}'} \phi^\alpha(\vec{u}') b_\alpha(t'), \tag{209}$$

with $\vec{k}$ chosen as

$$\vec{k} = g_q^\omega \omega(\vec{R}) \hat{v} \sinh\xi, \tag{210}$$

in order to guarantee the correct rest frame momentum for a particle in a vector field. Substituting into the equation for H_0 we find

$$\begin{aligned} H_0 &= \sum_\alpha \frac{\Omega_\alpha}{R_B} b_\alpha^\dagger b_\alpha - \sum_{\alpha\beta} \langle\alpha|(g_\sigma^q \sigma(\vec{R}) - m_q + m_q^\star)\gamma_0|\beta\rangle b_\alpha^\dagger b_\beta \\ &\quad + \hat{N}_q g_\omega^q \omega(\vec{R}) \cosh\xi + BV \qquad (211) \\ \vec{P} &= \sum_{\alpha\beta} \langle\alpha| - i\vec{\nabla}|\beta\rangle b_\alpha^\dagger b_\beta - \hat{N}_q \vec{k}, \qquad (212) \end{aligned}$$

with the notation

$$\langle\alpha|A|\beta\rangle = \int_0^{R_B} d\vec{u}'\, \phi^{\alpha\dagger}(\vec{u}') A \phi^\beta(\vec{u}') \quad \text{and} \quad \hat{N}_q = \sum_\alpha b_\alpha^\dagger b_\alpha. \tag{213}$$

Choosing $m_q^\star = m_q - g_\sigma^q \sigma(\vec{R})$ (in which case the frequency Ω_α and the wave function ϕ^α become dependent on $\vec{R}$ through σ) we get for the leading part of the energy and momentum operator

$$H_0^{IRF} = \sum_\alpha \frac{\Omega_\alpha(\vec{R})}{R_B} b_\alpha^\dagger b_\alpha + BV + \hat{N}_q g_\omega^q \omega(\vec{R}) \cosh\xi, \tag{214}$$

$$\vec{P}^{IRF} = \sum_{\alpha\beta} \langle\alpha| - i\vec{\nabla}|\beta\rangle b_\alpha^\dagger b_\beta - \hat{N}_q g_\omega^q \omega(\vec{R}) \hat{v} \sinh\xi. \tag{215}$$

If we quantize the b_α in the usual way, we find that the unperturbed part of H is diagonalised by states of the form $|N_\alpha, N_\beta, \cdots\rangle$ with N_α the eigenvalues of the number operator $b_\alpha^\dagger b_\alpha$ for the mode $\{\alpha\}$. According our working hypothesis, the nucleon should be described by three quarks in the lowest mode ($\alpha = 0$) and should remain in that configuration as $\vec{R}$ changes. As a consequence, in the expression for the momentum, the contribution of the gradient acting on ϕ averages to zero by parity and we find that the leading terms in the expression for the energy and momentum of the nucleon in the IRF are:

$$E_0^{IRF} = M_N^\star(\vec{R}) + 3g_\omega^q \omega(\vec{R}) \cosh\xi, \tag{216}$$

$$\vec{P}^{IRF} = -3g_\omega^q \omega(\vec{R}) \hat{v} \sinh\xi, \tag{217}$$

with

$$M_N^\star(\vec{R}) = \frac{3\Omega_0(\vec{R})}{R_B} + BV. \tag{218}$$

Since we are going to treat the corrections to leading order in the velocity, they will not be affected by the boost back to the NRF. Therefore we can apply the Lorentz transformation to Eqs.(216) and (217) to get the leading terms in the energy and momentum in the NRF. Since there is no possibility of confusion now, we write the NRF variables without the NRF index. The result is

$$E_0 = M_N^\star(\vec{R})\cosh\xi + 3g_\omega^q\omega(\vec{R}), \tag{219}$$

$$\vec{P} = M_N^\star(\vec{R})\hat{v}\sinh\xi, \tag{220}$$

which implies

$$E_0 = \sqrt{M_N^{\star 2}(\vec{R}) + \vec{P}^2} + 3g_\omega^q\omega(\vec{R}). \tag{221}$$

At this point we recall that the effective mass of the nucleon, $M_N^\star(\vec{R})$, defined by Eq.(218) does not take into account the fact that the center of mass of the quarks does not coincide with the center of the bag. By requiring that all of the quarks remain in the same orbit one forces this to be realized in expectation value. However, one knows that the virtual fluctuations to higher orbits would decrease the energy. This c.m. correction is studied in detail in the Appendix, where it is shown that it is only very weakly dependent on the external field strength for the densities of interest. For the zero point energy due to the fluctuations of the gluon field, we assume that it is the same as in free space. Thus we parametrize the sum of the c.m. and gluon fluctuation corrections in the familiar form, $-z_0/R_B$, where z_0 is *independent* of the density. Then the effective mass of the nucleon in the nucleus takes the form

$$M_N^\star(\vec{R}) = \frac{3\Omega_0(\vec{R}) - z_0}{R_B} + BV, \tag{222}$$

and we assume that the equilibrium condition is

$$\frac{dM_N^\star(\vec{R})}{dR_B} = 0, \tag{223}$$

which is the usual non-linear boundary condition. This is again justified by the Born-Oppenheimer approximation, according to which the internal structure of the nucleon has enough time to adjust to the varying external field so as to stay in its ground state.

The parameters B and z_0 are fixed by the free nucleon mass ($M_N = 939$ MeV) using Eqs.(222) and (223) applied to the free case. In the following we keep the free bag radius, R_B^0, as a free parameter. The results are shown in Table 1.

Table 1: $B^{1/4}$(MeV) and z_0 for some bag radii using $m_q = 5$ MeV.

R_B^0(fm)	0.6	0.8	1.0
$B^{1/4}$	210.9	170.0	143.8
z_0	4.003	3.295	2.587

12.2 Corrections due to H_1 and Thomas precession

We estimate the effect of H_1 in perturbation theory by expanding $\sigma(\vec{R}+\vec{u}')$ and $\omega(\vec{R}+\vec{u}')$ in powers of $\vec{u}'$ and computing the effect to first order. To this order several terms give zero because of parity and one is left with

$$\langle(0)^3|H_1|(0)^3\rangle = g_\omega^q \sum_{\alpha\beta}\langle(0)^3|b_\alpha^\dagger b_\beta|(0)^3\rangle\langle\alpha|\gamma^0\vec{\gamma}\cdot\hat{v}\vec{u}'\sinh\xi|\beta\rangle\cdot\vec{\nabla}_R\omega(\vec{R}). \tag{224}$$

Here we need to be more precise about the meaning of the labels α,β. Suppose we set $\{\alpha\}=\{0,m_\alpha\}$ with m_α the spin projection of the quark in mode $\{0\}$, then we find

$$\langle(0)m_\alpha|\gamma^0\vec{\gamma}\cdot\hat{v}\vec{u}'\sinh\xi|(0)m_\beta\rangle = -I(\vec{R})\langle m_\alpha|\frac{\vec{\sigma}}{2}|m_\beta\rangle\times\hat{v}\sinh\xi, \tag{225}$$

with

$$\begin{aligned} I(\vec{R}) &= \frac{4}{3}\mathcal{N}^2\int_0^{R_B} du'\,u'^3 j_0(xu'/R_B)\beta_q j_1(xu'/R_B), &(226)\\ &= \frac{R_B}{3}\left(\frac{4\Omega_0+2m_q^\star R_B-3}{2\Omega_0(\Omega_0-1)+m_q^\star R_B}\right). &(227)\end{aligned}$$

The integral, $I(\vec{R})$, depends on $\vec{R}$ through the implicit dependence of R_B and x on the local scalar field. Its value in the free case, I_0, can be related to the nucleon isoscalar magnetic moment: $I_0 = 3\mu_s/M_N$ with $\mu_s = \mu_p+\mu_n$ and $\mu_p = 2.79$, $\mu_n = -1.91$ the experimental values. By combining Eqs.(224), (225) and (220) we then find

$$\begin{aligned}\langle(0)^3|H_1|(0)^3\rangle &= \mu_s\frac{I(\vec{R})}{I_0}\frac{1}{M_N R}\left(\frac{d}{dR}3g_\omega^q\omega(\vec{R})\right)\vec{S}\cdot\vec{R}\times\hat{v}\sinh\xi &(228)\\ &= \mu_s\frac{I(\vec{R})M_N^\star(\vec{R})}{I_0 M_N}\frac{1}{M_N^{\star 2}(\vec{R})R}\left(\frac{d}{dR}3g_\omega^q\omega(\vec{R})\right)\vec{S}\cdot\vec{L}, &(229)\end{aligned}$$

with $\vec{S}$ the nucleon spin operator and $\vec{L}$ its angular momentum.

This spin-orbit interaction is nothing but the interaction between the magnetic moment of the nucleon with the "magnetic" field of the ω seen from the rest frame of the nucleon. This induces a rotation of the spin as a function of time. However, even if μ_s were equal to zero, the spin would nevertheless rotate because of Thomas precession, which is a relativistic effect *independent* of the structure. It can be understood as follows.

Let us assume that at time t, the spin vector is $\vec{S}(t)$ in the IRF(t). Then we expect that, at time $t+dt$ the spin has the same direction if it is viewed from the frame obtained by boosting the IRF(t) by $d\vec{v}$ so as to get the right velocity $\vec{v}(t+dt)$. That is, the spin looks at rest in the frame obtained by first boosting the NRF to $\vec{v}(t)$ and then boosting by $d\vec{v}$. This product of Lorentz transformation amounts to a boost to $\vec{v}(t+dt)$ times a rotation. So, viewed from the IRF$(t+dt)$, the spin appears to rotate. In order that our Hamiltonian be correct it should contain a piece H_{prec} which produces this rotation through the Hamilton equations of motion. A detailed derivation can be found in Refs.[204, 202] and the result is

$$H_{prec} = -\frac{1}{2}\vec{v}\times\frac{d\vec{v}}{dt}\cdot\vec{S}. \tag{230}$$

The acceleration is obtained from the Hamilton equations of motion applied to the leading order Hamiltonian, Eq.(221). To lowest order in the velocity one finds

$$\frac{d\vec{v}}{dt} = -\frac{1}{M_N^\star(\vec{R})}\vec{\nabla}[M_N^\star(\vec{R})+3g_\omega^q\omega(\vec{R})]. \tag{231}$$

If we put this result into Eq.(230) and add the result to Eq.(229), we get the total spin orbit interaction (to first order in the velocity)

$$H_{prec.} + H_1 = V_{s.o}(\vec{R})\vec{S}\cdot\vec{L}, \tag{232}$$

where

$$V_{s.o}(\vec{R}) = -\frac{1}{2M_N^{\star 2}(\vec{R})R}\left[\left(\frac{d}{dR}M_N^{\star}(\vec{R})\right) + (1-2\mu_s\eta(\vec{R}))\left(\frac{d}{dR}3g_\omega^q\omega(\vec{R})\right)\right], \tag{233}$$

and

$$\eta(\vec{R}) = \frac{I(\vec{R})M_N^{\star}(\vec{R})}{I_0 M_N}. \tag{234}$$

12.3 Total Hamiltonian for a bag in the meson mean fields

To complete the derivation we now introduce the effect of the neutral ρ meson. The interaction term that we must add to $\mathcal{L}_I$ (see Eq.(188)) is

$$\mathcal{L}_I^\rho = -g_\rho^q\bar{q}'\gamma_\mu\frac{\tau_\alpha}{2}q'(u')\rho_{\alpha,IRF}^\mu(u'), \tag{235}$$

where $\rho_{\alpha,IRF}^\mu$ is the ρ meson field with isospin component α and τ^α are the Pauli matrices acting on the quarks. In the mean field approximation only $\alpha = 3$ contributes. If we denote by $b(\vec{R})$ the mean value of the time component of the field in the NRF, we can transpose our results for the ω field. The only difference comes from trivial isospin factors which amount to the substitutions

$$3g_\omega^q \to g_\rho^q\frac{\tau_3^N}{2}, \quad \mu_s \to \mu_v = \mu_p - \mu_n, \tag{236}$$

where $\tau_3^N/2$ (with eigenvalues $\pm 1/2$) is the nucleon isospin operator.

This leads to our final result for the NRF energy-momentum of the nucleon moving in the mean fields, $\sigma(\vec{R}), \omega(\vec{R})$ and $b(\vec{R})$:

$$E = M_N^{\star}(\vec{R})\cosh\xi + V(\vec{R}), \tag{237}$$

$$\vec{P} = M_N^{\star}(\vec{R})\hat{v}\sinh\xi, \tag{238}$$

with

$$V(\vec{R}) = V_c(\vec{R}) + V_{s.o.}(\vec{R})\vec{S}\cdot\vec{L}, \tag{239}$$

$$V_c(\vec{R}) = 3g_\omega^q\omega(\vec{R}) + g_\rho^q\frac{\tau_3^N}{2}b(\vec{R}), \tag{240}$$

$$V_{s.o}(\vec{R}) = -\frac{1}{2M_N^{\star 2}(\vec{R})R}[\Delta_\sigma + (1-2\mu_s\eta(\vec{R}))\Delta_\omega + (1-2\mu_v\eta(\vec{R}))\frac{\tau_3^N}{2}\Delta_\rho] \tag{241}$$

$$\Delta_\sigma = \frac{d}{dR}M_N^{\star}(\vec{R}),\ \Delta_\omega = \frac{d}{dR}3g_\omega^q\omega(\vec{R}),\ \Delta_\rho = \frac{d}{dR}g_\rho^q b(\vec{R}). \tag{242}$$

Up to terms of higher order in the velocity, this result for the spin-orbit interaction agrees with that of Achtzehnter and Wilets [203] who used an approach based on the non-topological soliton model. As pointed out in [203], for a point-like Dirac particle one has $\mu_s = 1$ while the physical value is $\mu_s = 0.88$. Thus, in so far as the omega contribution to the spin-orbit force is concerned, the point-like result is almost correct. This is clearly not the case for the rho contribution since we still have $\mu_v = 1$ for the point-like particle while experimentally $\mu_v = 4.7$.

12.4 Quantization of the nuclear Hamiltonian

Until now the motion of the nucleon has been considered as classical, but we must now quantize the model. We do that here in the non-relativistic framework. That is, we consider a theory where the particle number is conserved and we keep only terms up to those quadratic in the velocity. (Here we drop the spin dependent correction since it already involves the velocity. It is reinserted at the end.)

The simplest way to proceed is to realize that the equations of motion

$$E = M_N^\star(\vec{R})\cosh\xi + V_c(\vec{R}), \tag{243}$$

$$\vec{P} = M_N^\star(\vec{R})\hat{v}\sinh\xi, \tag{244}$$

can be derived from the following Lagrangian

$$L(\vec{R},\vec{v}) = -M_N^\star(\vec{R})\sqrt{1-v^2} - V_c(\vec{R}). \tag{245}$$

Thus the expansion is simply

$$L_{nr}(\vec{R},\vec{v}) = \frac{1}{2}M_N^\star(\vec{R})v^2 - M_N^\star(\vec{R}) - V_c(\vec{R}) + \mathcal{O}(v^4) \tag{246}$$

Neglecting the $\mathcal{O}(v^4)$ terms we then go back to the (still classical) Hamilton variables and find (note that the momentum is not the same as before the expansion)

$$H_{nr}(\vec{R},\vec{P}) = \frac{\vec{P}^2}{2M_N^\star(\vec{R})} + M_N^\star(\vec{R}) + V_c(\vec{R}). \tag{247}$$

If we quantize by the substitution $\vec{P} \to -i\vec{\nabla}_R$ we meet the problem of ordering ambiguities since now $M_N^\star(\vec{R})$ and $\vec{P}$ no longer commute. The classical kinetic energy term $\vec{P}^2/2M_N^\star(\vec{R})$ allows 3 quantum orderings

$$T_1 = \vec{P}\cdot\hat{A}\vec{P},\quad T_2 = \hat{A}\vec{P}^2,\quad T_3 = \vec{P}^2\hat{A}, \tag{248}$$

where $\hat{A} = 1/(2M_N^\star(\vec{R}))$. However, since we want the Hamiltonian to be hermitian the only possible combination is

$$T = zT_1 + \frac{1-z}{2}(T_2+T_3), \tag{249}$$

with z an arbitrary real number. Using the commutation relations one can write

$$T_2 + T_3 = 2T_1 - \frac{1-z}{2}(\nabla_R^2\hat{A}), \tag{250}$$

so that the kinetic energy operator

$$T = T_1 - \frac{1-z}{2}(\nabla_R^2\hat{A}), \tag{251}$$

is only ambiguous through the term containing the second derivative of $\hat{A} = 1/(2M_N^\star(\vec{R}))$. Since we have expanded the meson fields only to first order in the derivative to get the classical Hamiltonian it is consistent to neglect such terms. So our quantum Hamiltonian takes the form

$$H_{nr}(\vec{R},\vec{P}) = \vec{P}\cdot\frac{1}{2M_N^\star(\vec{R})}\vec{P} + M_N^\star(\vec{R}) + V(\vec{R}), \tag{252}$$

where we have reintroduced the spin-orbit interaction. The nuclear quantum Hamiltonian appropriate to a mean field calculation is then

$$H_{nr} = \sum_{i=1,A} H_{nr}(\vec{R}_i,\vec{P}_i),\quad \vec{P}_i = -i\vec{\nabla}_i. \tag{253}$$

The problem is manifestly self consistent because the meson mean fields, upon which H_{nr} depends through $M_N^\star$ and V, themselves depend on the eigenstates of H_{nr}.

13 Equations for the meson fields

The equation of motion for the meson-field operators ($\hat{\sigma}$, $\hat{\omega}^\nu$, $\hat{\rho}^{\nu,\alpha}$) are

$$\partial_\mu\partial^\mu\hat{\sigma} + m_\sigma^2\hat{\sigma} = g_\sigma^q\overline{q}q, \tag{254}$$
$$\partial_\mu\partial^\mu\hat{\omega}^\nu + m_\omega^2\hat{\omega}^\nu = g_\omega^q\overline{q}\gamma^\nu q, \tag{255}$$
$$\partial_\mu\partial^\mu\hat{\rho}^{\nu,\alpha} + m_\rho^2\hat{\rho}^{\nu,\alpha} = g_\rho^q\overline{q}\gamma^\nu\frac{\tau^\alpha}{2}q. \tag{256}$$

The mean fields are defined as the expectation values in the ground state of the nucleus, $|A\rangle$:

$$\langle A|\hat{\sigma}(t,\vec{r})|A\rangle = \sigma(\vec{r}), \tag{257}$$
$$\langle A|\hat{\omega}^\nu(t,\vec{r})|A\rangle = \delta(\nu,0)\omega(\vec{r}), \tag{258}$$
$$\langle A|\hat{\rho}^{\nu,\alpha}(t,\vec{r})|A\rangle = \delta(\nu,0)\delta(\alpha,3)b(\vec{r}). \tag{259}$$

The equations which determine them are the expectation values of Eqs.(254), (255) and (256). First we need the expectation values of the sources

$$\langle A|\overline{q}q(t,\vec{r})|A\rangle, \langle A|\overline{q}\gamma^\nu q(t,\vec{r})|A\rangle \text{ and } \langle A|\overline{q}\gamma^\nu\frac{\tau^\alpha}{2}q(t,\vec{r})|A\rangle. \tag{260}$$

As before, we shall simplify the presentation by not treating the ρ meson explicitly until the end. In the mean field approximation the sources are the sums of the sources created by each nucleon – the latter interacting with the meson fields. Thus we write

$$\overline{q}q(t,\vec{r}) = \sum_{i=1,A}\langle\overline{q}q(t,\vec{r})\rangle_i, \tag{261}$$
$$\overline{q}\gamma^\nu q(t,\vec{r}) = \sum_{i=1,A}\langle\overline{q}\gamma^\nu q(t,\vec{r})\rangle_i, \tag{262}$$

where $\langle\cdots\rangle_i$ denotes the matrix element in the nucleon i located at $\vec{R}_i$ at time t. According to the Born-Oppenheimer approximation, the nucleon structure is described, in its own IRF, by 3 quarks in the lowest mode. Therefore, in the IRF of the nucleon i, we have

$$\langle\overline{q}'q'(t',\vec{r}')\rangle_i = 3\sum_m\overline{\phi}_i^{0,m}(\vec{u}')\phi_i^{0,m}(\vec{u}') = 3s_i(\vec{u}'), \tag{263}$$
$$\langle\overline{q}'\gamma^\nu q'(t',\vec{r}')\rangle_i = 3\delta(\nu,0)\sum_m\phi_i^{\dagger 0,m}(\vec{u}')\phi_i^{0,m}(\vec{u}') = 3\delta(\nu,0)w_i(\vec{u}'), \tag{264}$$

where the space components of the vector current gives zero because of parity. At the common time t in the NRF we thus have

$$R'_{i,L} = R_{i,L}\cosh\xi_i - t\sinh\xi_i, \quad \vec{R}'_{i,\perp} = \vec{R}_{i,\perp}, \tag{265}$$
$$r'_L = r_L\cosh\xi_i - t\sinh\xi_i, \quad \vec{r}_\perp{}' = \vec{r}_\perp. \tag{266}$$

Therefore

$$u'_{i,L} = (r_L - R_{i,L})\cosh\xi_i, \qquad \vec{u}_{i,\perp}{}' = \vec{r}_\perp - \vec{R}_{i,\perp}, \tag{267}$$

and from the Lorentz transformation properties of the fields we get

$$\langle\overline{q}q(t,\vec{r})\rangle_i = 3s_i((r_L - R_{i,L})\cosh\xi_i, \vec{r}_\perp - \vec{R}_{i,\perp}), \tag{268}$$
$$\langle\overline{q}\gamma^0 q(t,\vec{r})\rangle_i = 3w_i((r_L - R_{i,L})\cosh\xi_i, \vec{r}_\perp - \vec{R}_{i,\perp})\cosh\xi_i, \tag{269}$$
$$\langle\overline{q}\vec{\gamma}q(t,\vec{r})\rangle_i = 3w_i((r_L - R_{i,L})\cosh\xi_i, \vec{r}_\perp - \vec{R}_{i,\perp})\hat{v}_i\sinh\xi_i. \tag{270}$$

These equations can be re-written in the form

$$\langle \overline{q}q(t,\vec{r})\rangle_i = \frac{3}{(2\pi)^3}(\cosh\xi_i)^{-1}\int d\vec{k}\, e^{i\vec{k}\cdot(\vec{r}-\vec{R}_i)}\, S(\vec{k},\vec{R}_i), \tag{271}$$

$$\langle \overline{q}\gamma^0 q(t,\vec{r})\rangle_i = \frac{3}{(2\pi)^3}\int d\vec{k}\, e^{i\vec{k}\cdot(\vec{r}-\vec{R}_i)}\, W(\vec{k},\vec{R}_i), \tag{272}$$

$$\langle \overline{q}\vec{\gamma}q(t,\vec{r})\rangle_i = \frac{3}{(2\pi)^3}\vec{v}_i\int d\vec{k}\, e^{i\vec{k}\cdot(\vec{r}-\vec{R}_i)}\, W(\vec{k},\vec{R}_i), \tag{273}$$

with

$$S(\vec{k},\vec{R}_i) = \int d\vec{u}\, e^{-i(\vec{k}_\perp\cdot\vec{u}_\perp + k_L u_L/\cosh\xi_i)}\, s_i(\vec{u}), \tag{274}$$

$$W(\vec{k},\vec{R}_i) = \int d\vec{u}\, e^{-i(\vec{k}_\perp\cdot\vec{u}_\perp + k_L u_L/\cosh\xi_i)}\, w_i(\vec{u}). \tag{275}$$

Finally, the mean field expressions for the meson sources take the form

$$\langle A|\overline{q}q(t,\vec{r})|A\rangle = \frac{3}{(2\pi)^3}\int d\vec{k}\, e^{i\vec{k}\cdot\vec{r}}\langle A|\sum_i(\cosh\xi_i)^{-1}e^{-i\vec{k}\cdot\vec{R}_i}\, S(\vec{k},\vec{R}_i)|A\rangle, \tag{276}$$

$$\langle A|\overline{q}\gamma^0 q(t,\vec{r})|A\rangle = \frac{3}{(2\pi)^3}\int d\vec{k}\, e^{i\vec{k}\cdot\vec{r}}\langle A|\sum_i e^{-i\vec{k}\cdot\vec{R}_i}\, W(\vec{k},\vec{R}_i)|A\rangle, \tag{277}$$

$$\langle A|\overline{q}\vec{\gamma}q(t,\vec{r})|A\rangle = 0, \tag{278}$$

where the last equation follows from the fact that the velocity vector averages to zero.

To simplify further, we remark that a matrix element of the form

$$\langle A|\sum_i e^{-i\vec{k}\cdot\vec{R}_i}\ldots|A\rangle \tag{279}$$

is negligible unless k is less than, or of the order of, the reciprocal of the *nuclear* radius. But in Eqs.(274) and (275) $\vec{k}$ is multiplied by $\vec{u}$ which is bounded by the *nucleon* radius. Hence, if we restrict the application of the model to large enough nuclei, we can neglect the argument of the exponential in Eqs.(274) and (275). The evaluation of the correction to this approximation will be postponed to a future work.

We now define the scalar, baryonic and isospin densities of the nucleons in the nucleus by

$$\rho_s(\vec{r}) = \langle A|\sum_i \frac{M_N^\star(\vec{R}_i)}{E_i - V(\vec{R}_i)}\delta(\vec{r}-\vec{R}_i)|A\rangle, \tag{280}$$

$$\rho_B(\vec{r}) = \langle A|\sum_i \delta(\vec{r}-\vec{R}_i)|A\rangle, \tag{281}$$

$$\rho_3(\vec{r}) = \langle A|\sum_i \frac{\tau_3^N}{2}\delta(\vec{r}-\vec{R}_i)|A\rangle, \tag{282}$$

where we have used Eq.(237) to eliminate the factor $(\cosh\xi_i)^{-1}$. Note that the definition of the scalar density makes sense because, in mean field approximation, each nucleon is moving in an orbital with a given energy. The meson sources then take the simple form

$$\langle A|\overline{q}q(t,\vec{r})|A\rangle = 3S(\vec{r})\rho_s(\vec{r}), \tag{283}$$

$$\langle \Lambda|\overline{q}\gamma^\nu q(t,\vec{r})|A\rangle = 3\delta(\nu,0)\rho_B(\vec{r}), \tag{284}$$

$$\langle A|\overline{q}\gamma^\nu\frac{\tau^\alpha}{2}q(t,\vec{r})|A\rangle = \delta(\nu,0)\delta(\alpha,3)\rho_3(\vec{r}), \tag{285}$$

where we have deduced the source of the ρ from that for the ω. We have used the notation

$$S(\vec{r}) = S(\vec{0},\vec{r}) = \int d\vec{u}\; s_{\vec{r}}(\vec{u}), \tag{286}$$

$$= \frac{\Omega_0/2 + m_q^* R_B(\Omega_0 - 1)}{\Omega_0(\Omega_0 - 1) + m_q^* R_B/2}, \tag{287}$$

where the subscript $\vec{r}$ reminds us that the function $s_{\vec{r}}(\vec{u})$ must be evaluated in the scalar field existing at $\vec{r}$.

Since their sources are time independent and since they do not propagate, the mean meson fields are also time independent. So by combining Eqs.(254) to (259) and Eqs.(283), (284) and (285), we get the desired equations for $\sigma(\vec{r}), \omega(\vec{r})$ and $b(\vec{r})$:

$$(-\nabla_r^2 + m_\sigma^2)\sigma(\vec{r}) = g_\sigma C(\vec{r})\rho_s(\vec{r}), \tag{288}$$

$$(-\nabla_r^2 + m_\omega^2)\omega(\vec{r}) = g_\omega \rho_B(\vec{r}), \tag{289}$$

$$(-\nabla_r^2 + m_\rho^2)b(\vec{r}) = g_\rho \rho_3(\vec{r}). \tag{290}$$

where the nucleon coupling constants and C are defined by

$$g_\sigma = 3g_\sigma^q S(\sigma = 0),\quad g_\omega = 3g_\omega^q,\quad g_\rho = g_\rho^q,\quad C(\vec{r}) = S(\vec{r})/S(\sigma = 0). \tag{291}$$

For completeness we recall that the mean fields carry the following energy

$$E^{meson} = \frac{1}{2}\int d\vec{r}\,[(\vec{\nabla}\sigma)^2 + m_\sigma^2\sigma^2 - (\vec{\nabla}\omega)^2 - m_\omega^2\omega^2 - (\vec{\nabla}b)^2 - m_\rho^2 b^2]. \tag{292}$$

14 The problem of self-consistency

Our quark model for finite nuclei is now complete. As the main equations are scattered through the text, it is useful to summarize the procedure which we have developed as follows:

1. Choose the bare quark mass, m_q, and adjust the bag parameters, B and z_0, to fit the free nucleon mass and its bag radius (see Eq.(222) and Table 1).

2. Assume that the coupling constants and the masses of the mesons are known (see Table 2 in Sec.16.1).

3. Evaluate the nucleon properties, $I(\sigma)$ (Eq.(227)) and $S(\sigma)$ (Eq.(287)), for a range of values of σ (see also Eqs.(313) and (314) in Sec.16.1).

4. Guess an initial form for the densities, $\rho_s(\vec{r}), \rho_B(\vec{r})$ and $\rho_3(\vec{r})$, in Eqs.(280), (281) and (282).

5. For $\rho_s(\vec{r})$ fixed, solve Eq.(288) for the σ field.

6. For $\rho_B(\vec{r})$ and $\rho_3(\vec{r})$ fixed, solve Eqs.(289) and (290) for the ω and ρ fields.

7. Evaluate the effective mass $M_N^*(\vec{r})$ and the potential $V(\vec{r})$ according to Eqs.(222) and (239). The bag radius at each point in the nucleus is fixed by Eq.(223). We note that for practical purposes it is possible to separate the solution of the bag equations and the finite nucleus. Because of the Born-Oppenheimer approximation, and the fact that H_1 (in Eq.(201)) can be treated perturbatively, $M_N^*(\vec{r})$ and $C(\vec{r})$ can be expressed entirely as functions of the local σ field at $\vec{r}$. Indeed, we shall see that a simple form, linear in $g_\sigma\sigma$, works extremely well.

8. Solve the eigenvalue problem defined by the nuclear Hamiltonian Eq.(253) and generate the shell model from which the densities $\rho_s(\vec{r}), \rho_B(\vec{r})$ and $\rho_3(\vec{r})$ can be computed according to Eqs.(280), (281) and (282).

9. Go to 5 and iterate until self-consistency is achieved.

This procedure has to be repeated for each nucleus, which certainly implies considerable numerical work. We plan to study the implications of this non-relativistic formulation in a future work.

15 Relativistic formulation

Here we attempt to formulate the model as a relativistic field theory for the nucleon in order to have a direct comparison with the widely used QHD. We make no attempt to justify the formulation of local relativistic field theory at a fundamental level because this is not possible for a composite nucleon. Our point is that, in the mean field approximation, QHD has had considerable phenomenological success. We therefore try to express our results in this framework. The idea is to write a relativistic Lagrangian and to check that, in some approximation, it is equivalent to our non-relativistic formulation.

As shown earlier, our basic result is that essentially the nucleon in the meson fields behaves as a point like particle of effective mass $M_N^\star(\sigma(\vec{r}))$ moving in a potential $g_\omega\omega(\vec{r})$. From now on we do not consider the ρ coupling as we shall only apply the model to $N = Z$ nuclei. We shall also forget about the small correction to the spin orbit force of the ω because, as we already pointed out, for symmetric nuclei it is almost entirely generated by the Dirac equation. A possible Lagrangian density for this system is

$$\mathcal{L} = i\overline{\psi}\gamma \cdot \partial\psi - M_N^\star(\hat{\sigma})\overline{\psi}\psi - g_\omega\hat{\omega}^\mu\overline{\psi}\gamma_\mu\psi + \mathcal{L}_{mesons}, \tag{293}$$

where ψ, $\hat{\sigma}$ and $\hat{\omega}^\mu$ are respectively the nucleon, σ and ω field operators. The free meson Lagrangian density is

$$\mathcal{L}_{mesons} = \frac{1}{2}(\partial_\mu\hat{\sigma}\partial^\mu\hat{\sigma} - m_\sigma^2\hat{\sigma}^2) - \frac{1}{2}\partial_\mu\hat{\omega}_\nu(\partial^\mu\hat{\omega}^\nu - \partial^\nu\hat{\omega}^\mu) + \frac{1}{2}m_\omega^2\hat{\omega}^\mu\hat{\omega}_\mu. \tag{294}$$

The comparison with QHD is straightforward. If we define the field dependent coupling constant $g_\sigma(\hat{\sigma})$ by

$$M_N^\star(\hat{\sigma}) = M_N - g_\sigma(\hat{\sigma})\hat{\sigma}, \tag{295}$$

it is easy to check that $g_\sigma(\sigma = 0)$ is equal to the coupling constant g_σ defined in Eq.(291). Then we write the Lagrangian density as

$$\mathcal{L} = i\overline{\psi}\gamma \cdot \partial\psi - M_N\overline{\psi}\psi + g_\sigma(\hat{\sigma})\hat{\sigma}\overline{\psi}\psi - g_\omega\hat{\omega}^\mu\overline{\psi}\gamma_\mu\psi + \mathcal{L}_{mesons}, \tag{296}$$

and clearly the only difference from QHD lies in the fact that the internal structure of the nucleon has forced a (known) dependence of the scalar meson-nucleon coupling constant on the scalar field itself.

In the mean field approximation, the meson field operators are replaced by their time independent expectation values in the ground state of the nucleus:

$$\hat{\sigma}(t,\vec{r}) \rightarrow \sigma(\vec{r}), \quad \hat{\omega}^\mu(t,\vec{r}) \rightarrow \ delta(\mu,0)\omega(\vec{r}), \tag{297}$$

and variation of the Lagrangian yields the Dirac equation

$$i\gamma \cdot \partial\psi - M_N^\star(\sigma) - g_\omega\omega\gamma_0\psi = 0, \tag{298}$$

as well as the equations for the meson mean fields

$$(-\nabla_r^2 + m_\sigma^2)\sigma(\vec{r}) = \left(\frac{\partial}{\partial\sigma}M_N^\star(\sigma)\right)\langle A|\overline{\psi}\psi(\vec{r})|A\rangle, \quad (299)$$

$$(-\nabla_r^2 + m_\omega^2)\omega(\vec{r}) = g_\omega\langle A|\psi^\dagger\psi(\vec{r})|A\rangle. \quad (300)$$

Using the Foldy-Wouthuysen transformation (see Ref.[203] for the details), one can show that the Dirac equation (298) gives back our non-relativistic, quantum Hamiltonian (without the ρ coupling) under the following conditions:

- only terms of second order in the velocity are kept,
- second derivatives of the meson fields are ignored,
- the fields are small with respect to the nucleon mass,
- the difference between $\mu_s = .88$ and $\mu_s(point) = 1$ can be neglected.

The fact that $\mu_v = 4.7$ is very different from $\mu_v(point) = 1$ prevents one from using this simple scheme for the ρ coupling. The spin-orbit potential would be completely different from the one obtained in Eq.(241). Since the ρ is not required in the treatment of symmetric nuclei we postpone to future work its introduction in the relativistic framework.

In the same approximations one finds that $\langle A|\overline{\psi}\psi(\vec{r})|A\rangle$ and $\langle A|\psi^\dagger\psi(\vec{r})|A\rangle$ are respectively equal to the previously defined scalar source, ρ_s (Eq.(280)), and vector source, ρ_B (Eq.(281)). (In nuclear matter the approximation is in fact exact). Therefore the equations (299) and (300) for the meson fields reproduce our previous results given in Eqs.(288) and (289) provided the relation

$$C(\sigma)g_\sigma(\sigma = 0) = -\frac{\partial}{\partial\sigma}M_N^\star(\sigma), \quad (301)$$

$$= \frac{\partial}{\partial\sigma}(g_\sigma(\sigma)\sigma), \quad (302)$$

is satisfied, which can be checked explicitly from the definition of $M_N^\star(\sigma)$ and $C(\sigma)$.

Within the limits specified above, the Lagrangian density given in Eq.(293) looks acceptable and we shall proceed to study its numerical consequences.

16 Applications

Before turning to finite nuclei, we first explain briefly how the general formalism applies in the case of nuclear matter.

16.1 Infinite Nuclear Matter

In symmetric, infinite nuclear matter the sources of the fields are constant and can be related to the nucleon Fermi momentum k_F according to [2]

$$\langle A|\psi^\dagger\psi(\vec{r})|A\rangle = \frac{4}{(2\pi)^3}\int^{k_F} d\vec{k} = \frac{2k_F^3}{3\pi^2}, \quad (303)$$

$$\langle A|\overline{\psi}\psi(\vec{r})|A\rangle = \frac{4}{(2\pi)^3}\int^{k_F} d\vec{k}\frac{M_N^\star}{\sqrt{M_N^{\star 2} + \vec{k}^2}}, \quad (304)$$

where $M_N^\star$ denotes the constant value of the effective nucleon mass defined by Eq.(222), or equivalently, Eq.(295). Obviously these equations can also be deduced from the definitions (Eqs.(280) and (281)) of the scalar and vector densities provided that, for ρ_s, one uses Eqs.(237) and (238) to write

$$\frac{M_N^\star}{E-V} = \frac{1}{\cosh\xi} = \frac{M_N^\star}{\sqrt{M_N^{\star 2}+\vec{k}^2}}. \tag{305}$$

Let $(\overline{\sigma},\overline{\omega})$ be the constant mean-values of the meson fields. From Eqs.(288) and (289) we find

$$\overline{\omega} = \frac{g_\omega \rho_B}{m_\omega^2}, \tag{306}$$

$$\overline{\sigma} = \frac{g_\sigma}{m_\sigma^2} C(\overline{\sigma}) \frac{4}{(2\pi)^3} \int^{k_F} d\vec{k} \frac{M_N^\star}{\sqrt{M_N^{\star 2}+\vec{k}^2}}, \tag{307}$$

where $C(\overline{\sigma})$ is now the constant value of C in the scalar field.[2] As emphasised by Saito and Thomas [190], the self-consistency equation for $\overline{\sigma}$, Eq.(307), is the same as that in QHD *except* that in the latter model one has $C(\overline{\sigma}) = 1$ (i.e. the quark mass is infinitely heavy).

Once the self-consistency equation for $\overline{\sigma}$ has been solved, one can evaluate the energy per nucleon. ¿From the Dirac equation (298), or simply using Eq.(237), the energy of a nucleon with momentum $\vec{k}$ is

$$E(\vec{k}) = V + M_N^\star \cosh\xi = g_\omega \overline{\omega} + \sqrt{M_N^{\star 2}+\vec{k}^2}, \tag{308}$$

which contributes to the energy per nucleon by the amount

$$E^{nucl.}/A = \frac{4}{\rho_B (2\pi)^3} \int^{k_F} d\vec{k} E(\vec{k}), \tag{309}$$

$$= \frac{1}{\rho_B}\left[g_\omega \overline{\omega}\rho_B + \frac{4}{(2\pi)^3}\int^{k_F} d\vec{k}\sqrt{M_N^{\star 2}+\vec{k}^2}\right]. \tag{310}$$

The contribution of the energy stored in the meson fields is, from Eq.(292),

$$E^{meson}/A = \frac{1}{2\rho_B}(m_\sigma^2\overline{\sigma}^2 - m_\omega^2\overline{\omega}^2), \tag{311}$$

and using the expression for $\overline{\omega}$ we finally obtain the following expression for the energy per nucleon

$$E^{total}/A = \frac{1}{\rho_B}\left[\frac{4}{(2\pi)^3}\int^{k_F} d\vec{k}\sqrt{M_N^{\star 2}+\vec{k}^2} + \frac{m_\sigma^2\overline{\sigma}^2}{2} + \frac{g_\omega^2\rho_B^2}{2m_\omega^2}\right]. \tag{312}$$

We determine the coupling constants, g_σ and g_ω, so as to fit the binding energy (-15.7 MeV) per nucleon and the saturation density ($\rho_0 = 0.15$ fm^{-3}) for symmetric nuclear matter at equilibrium. The coupling constants and some calculated properties of nuclear matter (with $m_q = 5$ MeV, $m_\sigma = 550$ MeV and $m_\omega = 783$ MeV) at the saturation density are listed in Table 2. The most notable fact is that the calculated incompressibility, K, is well within the experimental range: $K \approx 200 - 300$ MeV [197]. Also our effective nucleon mass is much larger than in the case of QHD. In the last two columns of Table 2 we show the relative modifications (with respect to their values at zero density) of the bag radius and the lowest eigenvalue, x, at saturation density. The changes are not large. In order

Table 2: Coupling constants and calculated nucleon properties in symmetric nuclear matter at normal nuclear matter density. The effective nucleon mass, $M_N^\star$, and the nuclear incompressibility, K, are quoted in MeV. The bottom row is for QHD-II.

R_B^0(fm)	$g_\sigma^2/4\pi$	$g_\omega^2/4\pi$	$M_N^\star$	K	$\frac{\delta R_B}{R_B^0}$	$\frac{\delta x}{x_0}$
0.6	5.86	6.34	729	295	-0.02	-0.13
0.8	5.40	5.31	754	280	-0.02	-0.16
1.0	5.07	4.56	773	267	-0.02	-0.21
QHD	7.29	10.8	522	540	–	–

to show the relative insensitivity to the quark mass (as long as it is small) we note that $M_N^\star$ = (756, 753) MeV at saturation density and K = (278, 281) MeV for R_B^0 = 0.8 fm and m_q = (0, 10) MeV, respectively.

In Figs.33 and 34, we show the mean-field values of the σ meson and the effective nucleon mass in medium, respectively. In both cases their dependence on the bag radius is rather weak. The scalar density ratio, $C(\overline{\sigma})$, and the ratio of the integral $I(\overline{\sigma})$ to I_0 are plotted as a function of $g_\sigma\overline{\sigma}$ in Figs.35 and 36, respectively. As $\overline{\sigma}$ increases, the scalar density ratio decreases linearly, while the ratio, I/I_0, gradually increases. Here we note that $S(0)$ = (0.4819, 0.4827, 0.4834) and I_0 = (0.2421, 0.3226, 0.4028) fm for R_B^0 = (0.6, 0.8, 1.0) fm, respectively.

It would be very useful to give a simple parametrization for C and I/I_0 because they are completely controlled by only the strength of the local σ field. We can easily see that C is well approximated by the linear form:

$$C(\overline{\sigma}) = 1 - a \times (g_\sigma\overline{\sigma}), \tag{313}$$

with $g_\sigma\overline{\sigma}$ in MeV and a = (6.6, 8.8, 11) $\times 10^{-4}$, for R_B^0 = (0.6, 0.8, 1.0) fm, respectively. For I/I_0 we find a quadratic form:

$$\frac{I(\overline{\sigma})}{I_0} = 1 + b_1 \times (g_\sigma\overline{\sigma}) - b_2 \times (g_\sigma\overline{\sigma})^2, \tag{314}$$

with b_1 = (3.7, 4.9, 6.1) $\times 10^{-4}$ and b_2 = (3.9, 5.2, 6.5) $\times 10^{-7}$. More comments and discussion of the results for nuclear matter can be found in the previous publications [3, 190].

As a practical matter, we note that Eq.(302) is easily solved for $g_\sigma(\sigma)$ in the case where $C(\sigma)$ is linear in $g_\sigma\bar{\sigma}$ – as we found in Eq.(313). In fact, it is easy to show that

$$M_N^\star = M_N - (1 - \frac{a}{2} g_\sigma\bar{\sigma}) g_\sigma\bar{\sigma}, \tag{315}$$

(recall $g_\sigma \equiv g_\sigma(\sigma = 0)$, Eq.(291)) so that the effective σN coupling constant decreases at half the rate of $C(\sigma)$. (Equation (315) is quite accurate up to twice nuclear matter density.) Having explicitly solved the nuclear matter problem by self-consistently solving for the quark wave functions in the bag in the mean scalar field *one can solve for the properties of finite nuclei without explicit reference* to the internal structure of the nucleon. All one needs is Eqs.(313) and (315) for $C(\sigma)$ and $M_N^\star$ as a function of $g_\sigma\bar{\sigma}$.

[2]Note the change in notation from the earlier papers of Saito and Thomas where C was used for what we now call S.

16.2 Initial results for finite nuclei

To illustrate that the approach has some promise, we have performed some preliminary calculations for such nuclei as ^{16}O, ^{40}Ca, ^{48}Ca, ^{90}Zr, ^{114}Sn and ^{208}Pb. For a doubly closed shell nucleus such as oxygen, for example, this requires the self-consistent solution of our equations for 6 Dirac orbitals – the $1s_{1/2}$, $1p_{1/2}$ and $1p_{3/2}$ states of the protons and neutrons. The central Coulomb interaction has been taken into account for the protons.

The numerical calculation was carried out using the techniques described in Part I. The resulting charge density for ^{16}O is shown in Fig.37 (dotted curve) in comparison with the experimental data [199] (hatched area) and QHD [2]. In this calculation we used the parameters given in Table 2 for $R_B^0 = 0.8$ fm. However, as the central density of ^{16}O was a little high we increased the model-dependent slope of the scalar density $C(\sigma)$ and the coupling constant $g_\sigma(\sigma)$ (i.e. the parameter a in Eqs.(313) and (315)) by 10% to obtain the result shown. The corresponding effect on the saturation energy and density of nuclear matter is very small: $\rho_0 \rightarrow 0.1496$ fm^{-3} and the energy per nucleon becomes -15.65 MeV. In Fig.38, we also show the scalar and vector fields corresponding to the charge density of ^{16}O that was shown in Fig.37. Using the same parameter set one also finds a very reasonable fit to the charge density of ^{40}Ca, ^{48}Ca, ^{90}Zr, ^{114}Sn and ^{208}Pb.

To conclude this initial investigation of finite nuclei let us consider single particle binding energies of the protons and neutrons in ^{40}Ca, presented in Table 4, in comparison with the results of QHD and the experimental data [205]. Because of the smaller scalar and vector field strengths in the present model, compared with QHD, the spin orbit splitting tends also to be smaller – perhaps only $\frac{2}{3}$ of the experimentally observed splittings. In this context it is interesting to show the sensitivity of the present model to just one feature of the underlying structure of the nucleon, namely the mass of the confined quark. As an example, we consider the case $m_q = 300MeV$, which is a typical constituent quark mass. For $m_q = 300$ MeV and $R_0 = 0.8$ fm, the coupling constants required to fit the saturation properties of nuclear matter are $g_\sigma^2/4\pi = 6.84$ and $g_\omega^2/4\pi = 8.51$, and the effective nucleon mass (at saturation) and the incompressibility become 674 MeV and 334 MeV, respectively. Using these parameters one finds that the charge densities of finite nuclei are again reproduced very well (without any need to vary the slope parameter "a" – $a = 3.9 \times 10^{-4}$). From the table, one can see that a heavier quark mass gives a spectrum closer to that of QHD – as discussed by Saito and Thomas in Ref.[190] – and in better agreement with the observed spin orbit splittings. In conclusion we notice one more point: the $2s_{1/2}$ and $1d_{3/2}$ levels are inverted compared with the experimental data. This may be connected with the effect of rearrangement, which is not considered here.

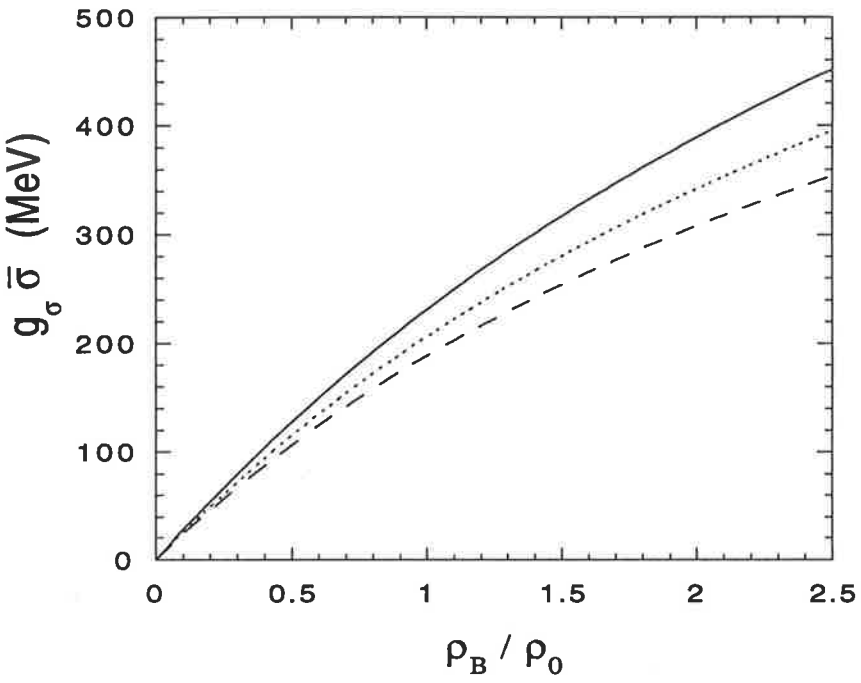

Figure 33: Mean-field values of the σ meson for various bag radii as a function of ρ_B. The solid, dotted and dashed curves show $g_\sigma \overline{\sigma}$ for $R_B^0 = 0.6$, 0.8 and 1.0 fm, respectively. The quark mass is chosen to be 5 MeV.

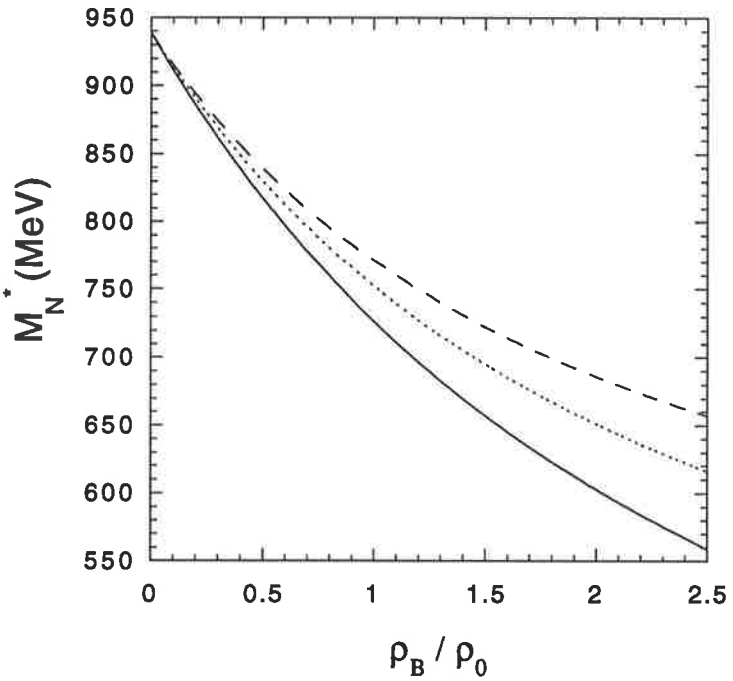

Figure 34: Effective nucleon mass (m_q=5MeV). The solid, dotted and dashed curves show $g_\sigma \overline{\sigma}$ for $R_B^0 = 0.6$, 0.8 and 1.0 fm, respectively. The quark mass is chosen to be 5 MeV.

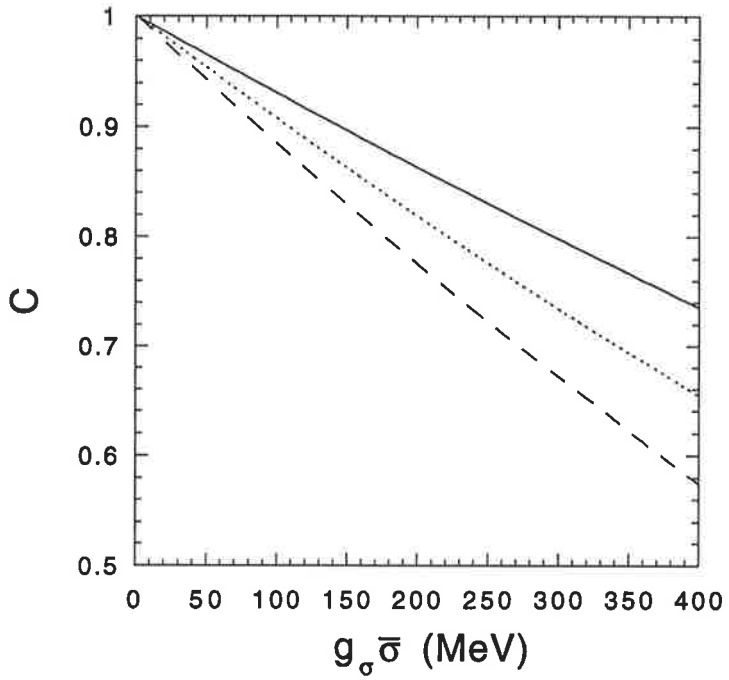

Figure 35: Scalar density ratio, $C(\overline{\sigma})$, as a function of $g_\sigma \overline{\sigma}$ ($m_q = 5$ MeV). The solid, dotted and dashed curves show $g_\sigma \overline{\sigma}$ for $R_B^0 = 0.6$, 0.8 and 1.0 fm, respectively. The quark mass is chosen to be 5 MeV.

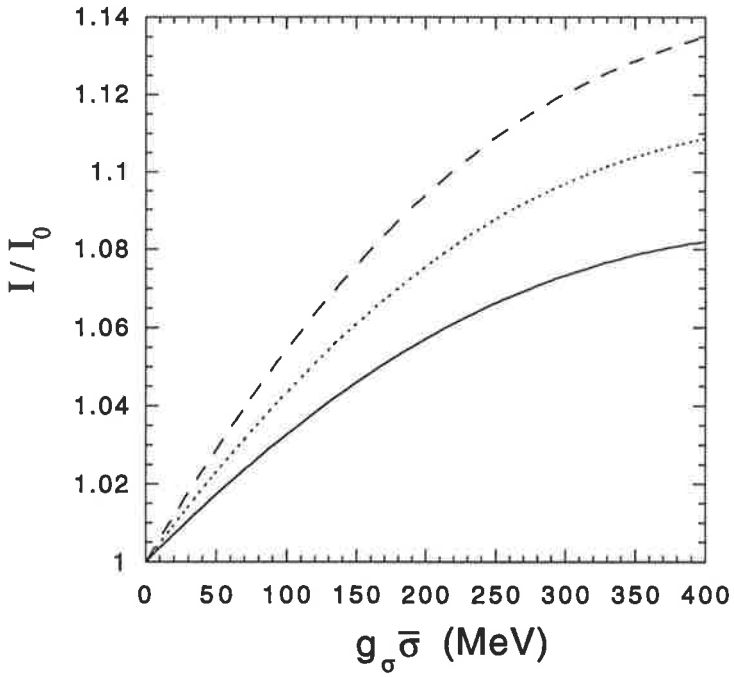

Figure 36: The ratio of $I(\overline{\sigma})$ to I_0 ($m_q = 5$ MeV). The solid, dotted and dashed curves show $g_\sigma \overline{\sigma}$ for $R_B^0 = 0.6$, 0.8 and 1.0 fm, respectively. The quark mass is chosen to be 5 MeV.

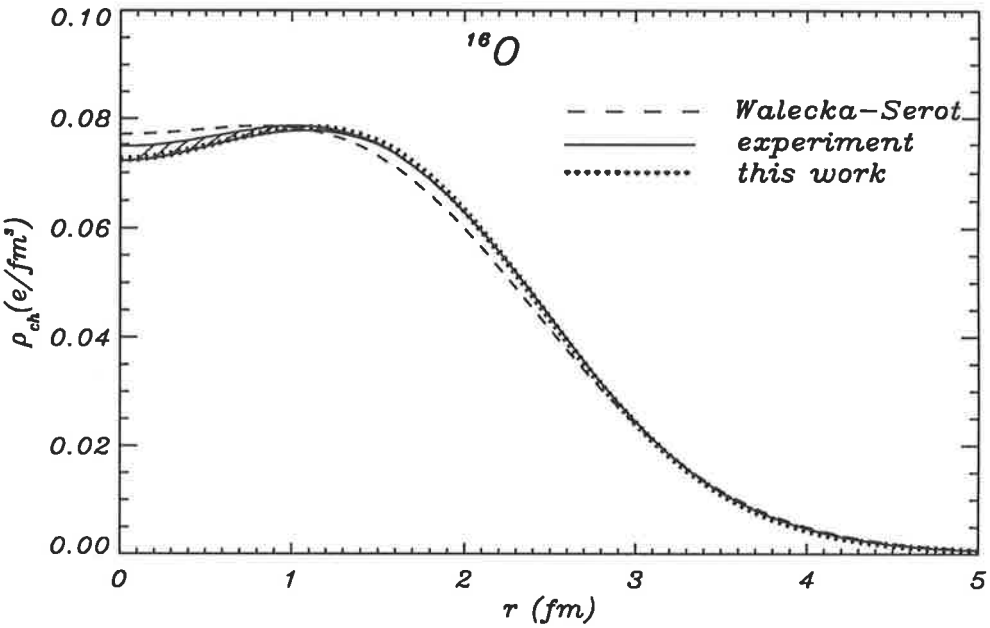

Figure 37: The charge density of ^{16}O in QHD and the present model, compared with the experimental distribution [205].

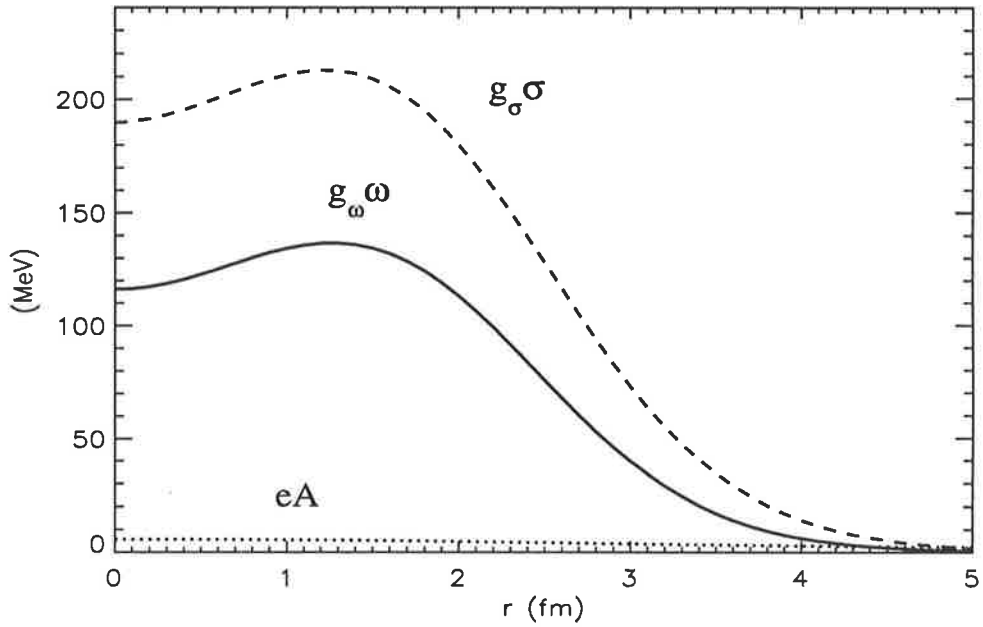

Figure 38: Scalar, vector and coulomb potentials for ^{16}O in the present model.

^{16}O								
Shell	neutron				proton			
	QHD	QMC(5)	QMC(300)	Expt.	QHD	QMC(5)	QMC(300)	Expt.
$1s_{1/2}$	41.4	34.8	36.9	47.0	37.2	32.7	30.7	40±8
$1p_{3/2}$	20.6	19.0	19.7	21.8	16.7	15.8	15.1	18.4
$1p_{1/2}$	12.6	17.0	16.2	15.7	8.9	12.3	13.1	12.1

Table 3: Predicted proton and neutron spectra of ^{16}O compared with QHD and the experimental data [205]. QMC(5, 300) means the present model with $R_0 = 0.8$ fm and $m_q = 5$ and 300 MeV, respectively. All energies are in MeV.

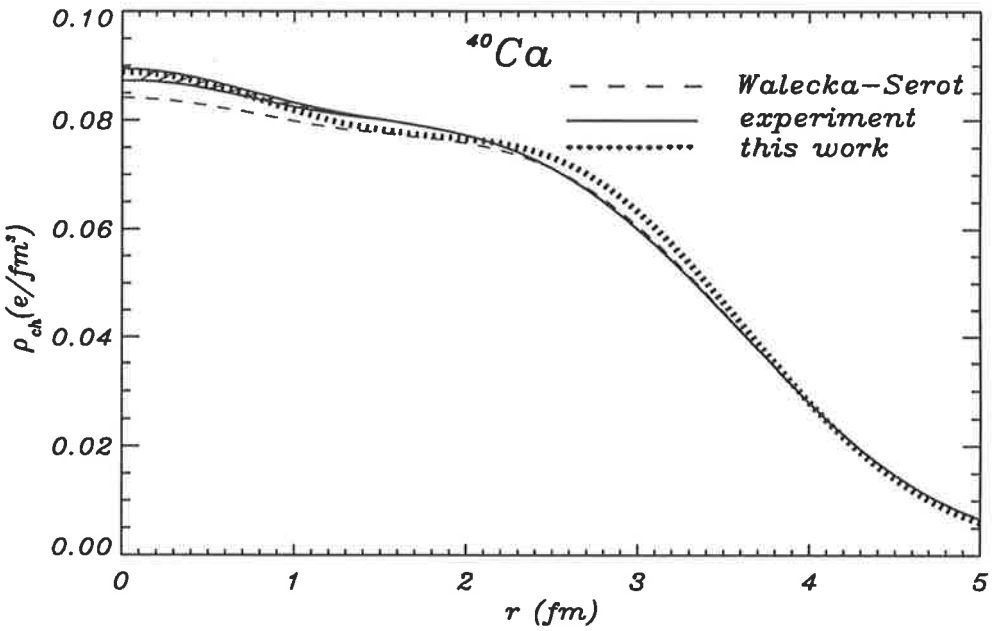

Figure 39: The charge density of ^{40}Ca in QHD and the present model, compared with the experimental distribution [205].

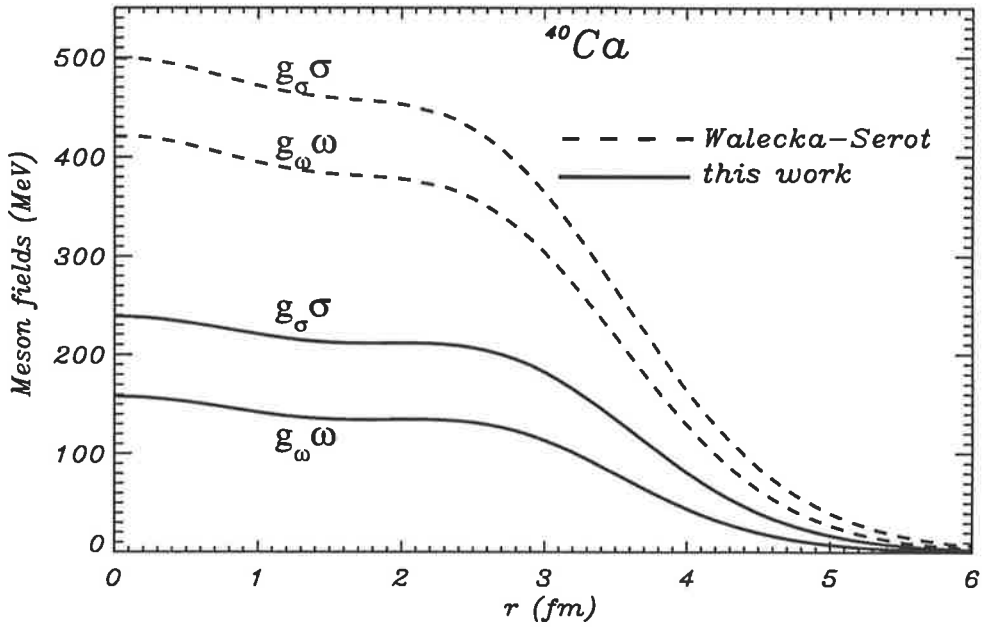

Figure 40: Scalar and vector potentials for ^{40}Ca in the present model and QHD.

^{40}Ca								
Shell	neutron				proton			
	QHD	QMC(5)	QMC(300)	Expt.	QHD	QMC(5)	QMC(300)	Expt.
$1s_{1/2}$	54.9	43.5	47.1	51.9	46.7	35.5	38.9	50±10
$1p_{3/2}$	38.6	32.7	35.0	36.6	30.8	25.0	27.2	34±6
$1p_{1/2}$	33.1	30.8	31.5	34.5	25.3	23.0	23.7	34±6
$1d_{5/2}$	22.6	20.6	22.0	21.6	15.2	13.2	14.6	15.5
$2s_{1/2}$	14.6	15.0	15.2	18.9	7.4	7.6	7.9	10.9
$1d_{3/2}$	14.1	17.1	15.9	18.4	6.8	9.7	8.4	8.3

Table 4: Predicted proton and neutron spectra of ^{40}Ca compared with QHD and the experimental data [205]. QMC(5, 300) means the present model with $R_0 = 0.8$ fm and $m_q = 5$ and 300 MeV, respectively. All energies are in MeV.

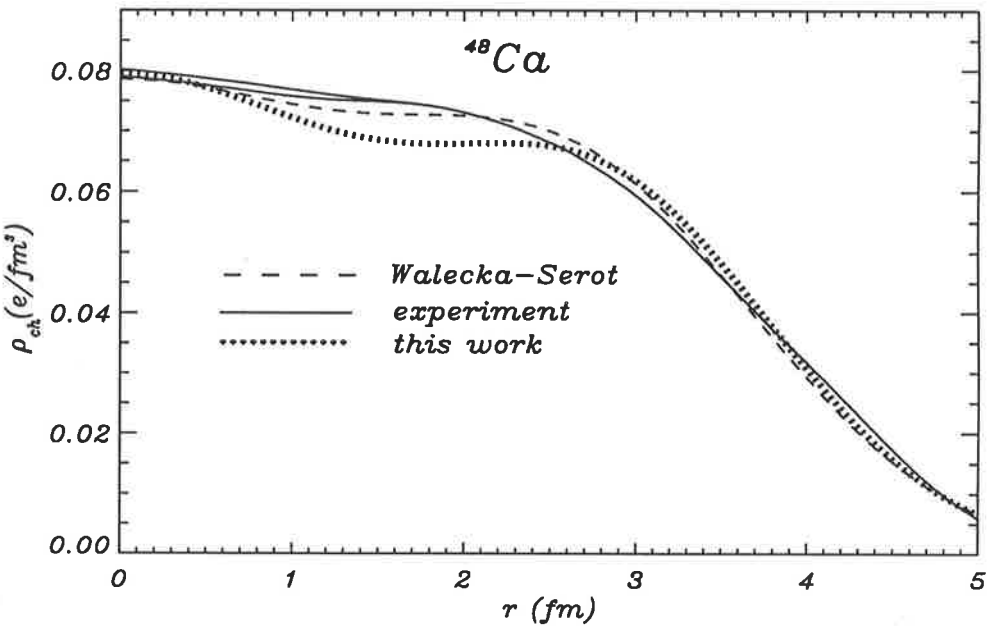

Figure 41: The charge density of ^{48}Ca in QHD and the present model, compared with the experimental distribution [205].

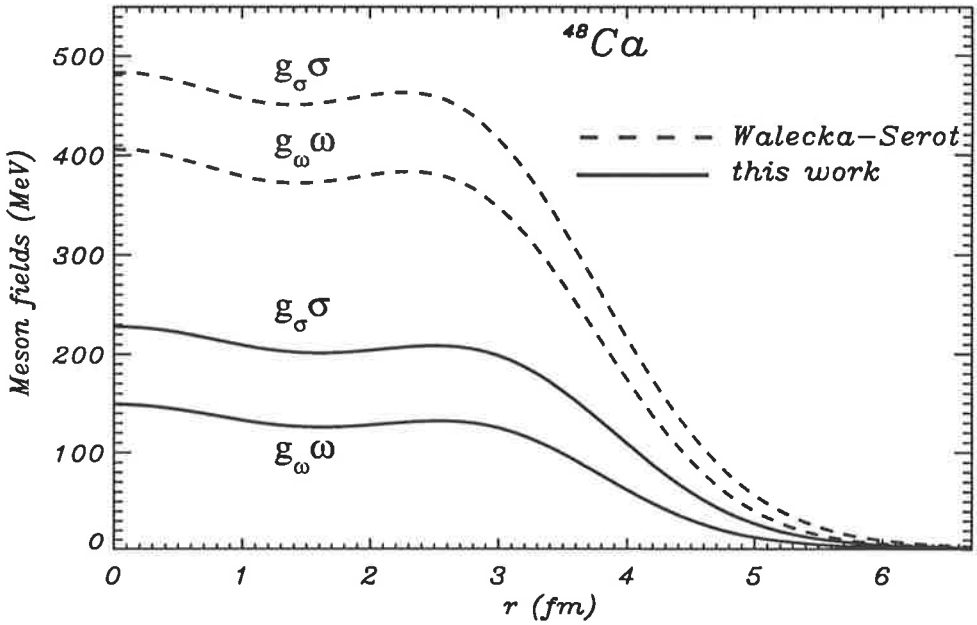

Figure 42: Scalar and vector potentials for ^{48}Ca in the present model and QHD.

^{48}Ca						
Shell	neutron			proton		
	QHD	QMC(5)	Expt.	QHD	QMC(5)	Expt.
$1s_{1/2}$	56.7	42.4		53.0	40.5	55±9
$1p_{3/2}$	40.8	31.6		38.6	30.9	35±7
$1p_{1/2}$	36.7	30.8		34.2	30.0	35±7
$1d_{5/2}$	24.7	19.8	16	23.2	19.6	20
$2s_{1/2}$	16.3	16.0	12.4	13.1	13.7	15.8
$1d_{3/2}$	16.8	18.1	12.4	15.0	17.8	15.3
$1f_{7/2}$	9.7	7.6	9.9			

Table 5: Predicted proton and neutron spectra of ^{48}Ca compared with QHD and the experimental data [205]. QMC(5) means the present model with $R_0 = 0.8$ fm and $m_q = 5$ MeV. All energies are in MeV.

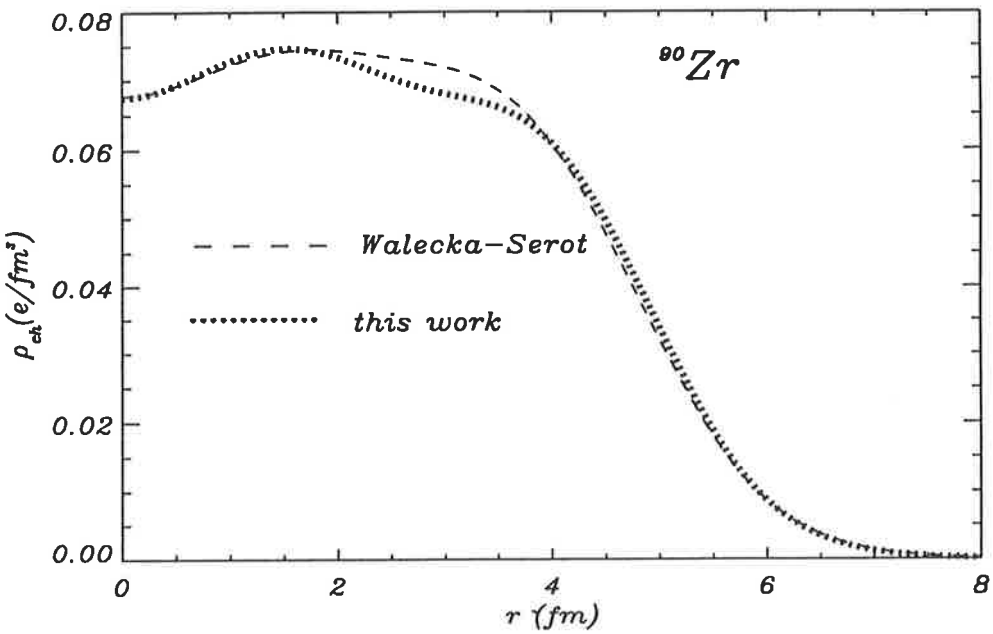

Figure 43: The charge density of ^{90}Zr in QHD and the present model.

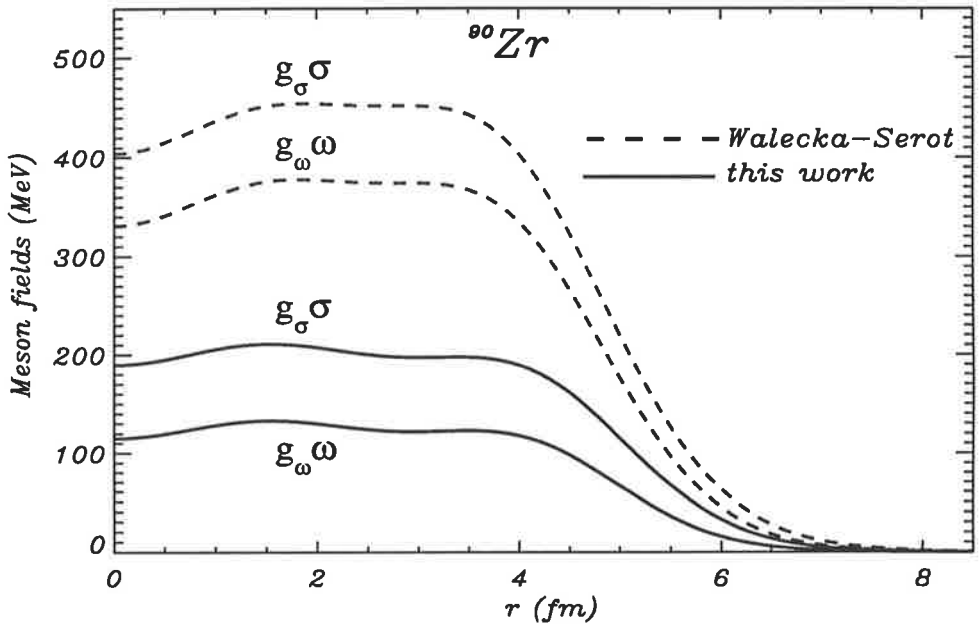

Figure 44: Scalar and vector potentials for ^{90}Zr in the present model and QHD.

^{90}Zr						
Shell	neutron			proton		
	QHD	QMC(5)	Expt.	QHD	QMC(5)	Expt.
$1s_{1/2}$	62.6	46.6		52.4	37.8	54±8
$1p_{3/2}$	51.0	38.9		42.0	31.3	43±8
$1p_{1/2}$	48.8	38.4		39.5	30.7	43±8
$1d_{5/2}$	38.2	30.0		30.1	23.1	27±8
$1d_{3/2}$	33.2	29.0		24.9	22.0	27±8
$2s_{1/2}$	30.3	26.4		21.0	18.0	27±8
$1f_{7/2}$	25.1	20.2		17.6	13.8	
$2p_{3/2}$	16.0	15.4	13.1	7.0	7.0	
$1f_{5/2}$	17.3	18.5	13.5	9.6	12.0	
$2p_{1/2}$	14.1	14.8	12.6	5.1	6.5	
$1g_{9/2}$	12.3	9.9	12.0			

Table 6: Predicted proton and neutron spectra of ^{90}Zr compared with QHD and the experimental data [205]. QMC(5) means the present model with $R_0 = 0.8$ fm and $m_q = 5$ MeV. All energies are in MeV.

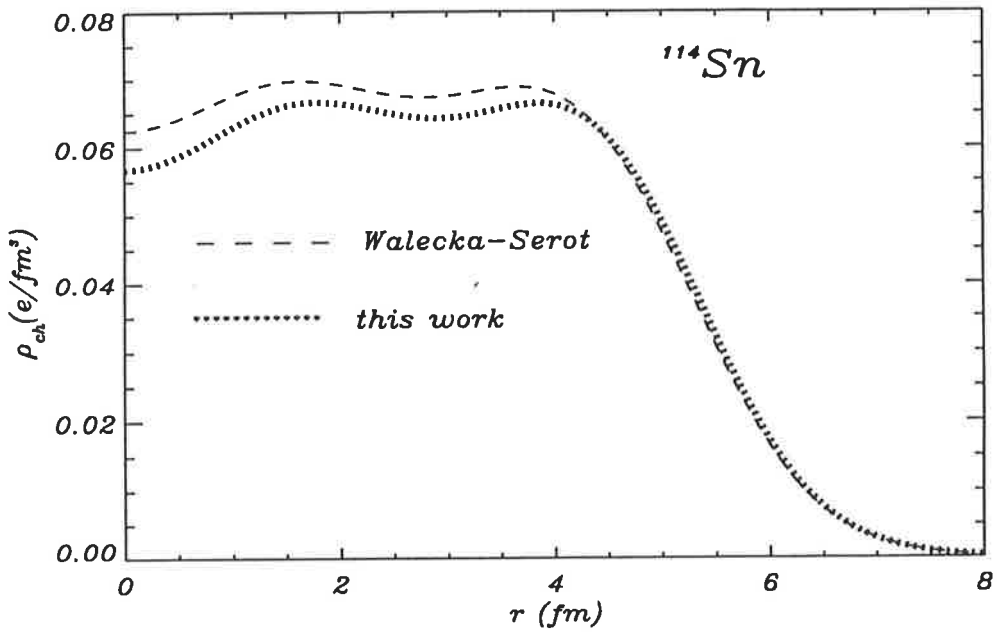

Figure 45: The charge density of ^{114}Sn in QHD and the present model.

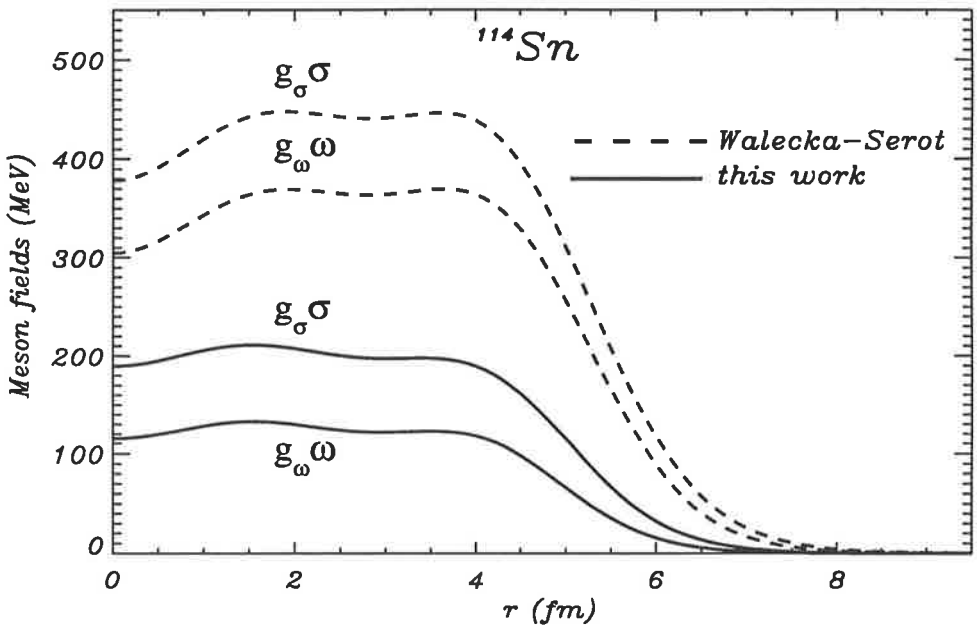

Figure 46: Scalar and vector potentials for ^{114}Sn in the present model and QHD.

^{114}Sn						
Shell	neutron			proton		
	QHD	QMC(5)	Expt.	QHD	QMC(5)	Expt.
$1s_{1/2}$	63.3	46.6		52.4	37.8	
$1p_{3/2}$	53.2	40.1		42.9	31.7	
$1p_{1/2}$	51.7	39.8		41.3	31.4	
$1d_{5/2}$	41.9	32.6		32.0	24.3	
$1d_{3/2}$	38.0	31.8		28.0	23.5	
$2s_{1/2}$	35.4	29.4		24.4	20.1	
$1f_{7/2}$	30.1	24.1		20.4	15.8	
$2p_{3/2}$	20.9	18.9		10.7	10.2	
$1f_{5/2}$	23.5	22.7		13.7	14.4	
$2p_{1/2}$	19.4	18.5		9.2	9.8	
$1g_{9/2}$	18.2	14.8		8.7	6.6	
$2d_{5/2}$	8.2	8.6				
$1g_{7/2}$	9.1	12.8				

Table 7: Predicted proton and neutron spectra of ^{114}Sn compared with QHD and the experimental data [205]. QMC(5) means the present model with $R_0 = 0.8$ fm and $m_q = 5$ MeV. All energies are in MeV.

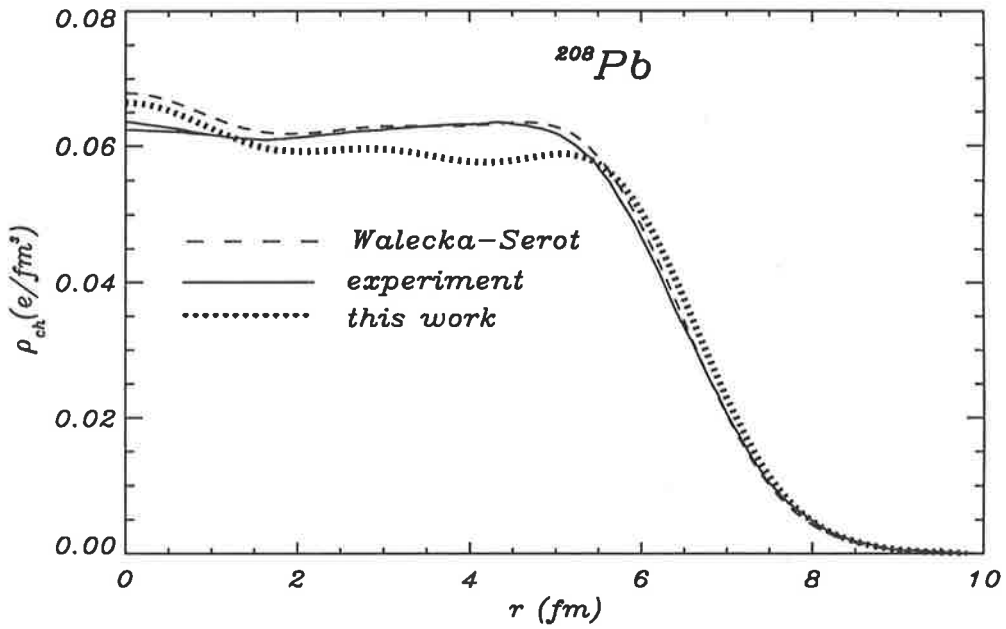

Figure 47: The charge density of ^{208}Pb in QHD and the present model, compared with the experimental distribution [205].

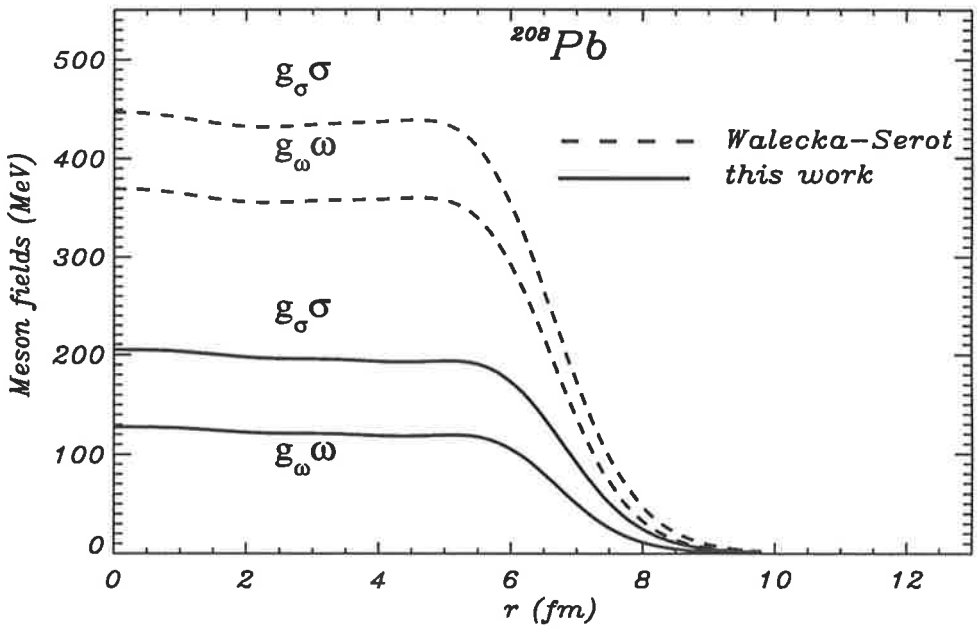

Figure 48: Scalar and vector potentials for ^{208}Pb in the present model and QHD.

^{208}Pb						
Shell	neutron			proton		
	QHD	QMC(5)	Expt.	QHD	QMC(5)	Expt.
$1s_{1/2}$	64.7	45.9		51.9	36.3	
$1p_{3/2}$	57.9	41.6		45.8	32.4	
$1p_{1/2}$	57.1	41.4		44.9	32.2	
$1d_{5/2}$	49.6	36.3		38.1	27.4	
$1d_{3/2}$	47.7	35.9		35.9	26.9	
$2s_{1/2}$	44.0	33.5		31.4	23.9	
$1f_{7/2}$	40.4	30.1		29.2	21.4	
$2p_{3/2}$	32.3	25.7		20.2	16.3	
$1f_{5/2}$	36.8	29.4		25.4	20.6	
$2p_{1/2}$	30.8	25.4		18.7	16.0	
$1g_{9/2}$	30.5	23.3		19.7	14.7	
$2d_{5/2}$	20.9	17.6		9.2	8.3	9.7
$1g_{7/2}$	25.0	22.1		14.0	13.5	11.4
$1h_{11/2}$	20.4	15.8		9.9	7.3	9.4
$2d_{3/2}$	18.7	17.0		7.0	7.7	8.4
$3s_{1/2}$	17.9	15.7		5.9	5.9	8.0
$2f_{7/2}$	10.4	9.3	9.7			
$1h_{9/2}$	12.8	14.1	10.8			
$1i_{13/2}$	10.3	7.8	9.0			
$2f_{5/2}$	7.8	8.6	7.9			
$3p_{3/2}$	7.3	6.9	8.3			
$3p_{1/2}$	6.4	6.6	7.4			

Table 8: Predicted proton and neutron spectra of ^{208}Pb compared with QHD and the experimental data [205]. QMC(5) means the present model with $R_0 = 0.8$ fm and $m_q = 5$ MeV. All energies are in MeV.

17 Conclusion and Outlook.

This thesis has been built around the MIT bag model as a theoretical tool in studying some phenomena in nuclear and particle physics.

To begin, the bag model was invented twice: in 1967 by Bogoliubov and in 1974 by a group of scientists from Massachussets Institute of Technology. It very soon became widely acclaimed as a tool for studying various systems of quarks and gluons.

In the first Chapters we reviewed the mathematical apparatus of the MIT bag model by deriving basic formulas in as general a form as possible, thoroughly describing the most difficult details. Here we also showed how the bag model can play a role in nuclear physics, in particular, its significance in the development of the new direction in this field, the Quark Meson Coupling model. This provides a description of the interactions of nucleons using the fundamental degrees of freedom, namely the quarks and gluons.

We applied the bag model to the question of charge symmetry of parton distributions by considering all possible CVS contributions, namely - the difference of the masses of the proton and neutron, the difference of masses of the intermediate states, the dependence of the bag wave function on the quark mass and the difference in the bag radius between the proton and neutron. To our surprise we found that the fractional differences between distributions of up quarks in the neutron and down quarks in the proton can be as large as 10% for intermediate values of Bjorken x. It would be quite important to test this result experimentally and though this seems to be quite difficult, due to the absence of a free nucleon target. We showed how one could extract the necessary information from the Drell-Yan process. Experimental results might also shed light on the question of whether it is necessary to review the parameters of the Standard Model to include the effect of charge symmetry breaking.

In the following Chapters we extended our investigations of charge symmetry violation in the valence quark distributions of the nucleon to the case of the pion. In the aim to find the experimental verification of our results we found that it is possible to separate the pion and nucleon CSV terms through the analysis of the Drell-Yan processes in the interaction of π^+ and π^- with deuterium and hydrogen. It seems that providing experimentalists with such an information should encourage them to carry out the measurements.

Continuing consideration of the Drell-Yan processes we came across the possibility of using combinations of measurements of pions on deuterium in order to extract pion sea quark distributions. To estimate the background screening we evolved the charge symmetry violating terms to find that it is still possible to get reliable information from experiments.

The third part of this work was completely devoted to the development of the QMC model, where the MIT bag model also played an important role. Starting with a hybrid model, in which quarks confined in nucleon bags interact through the exchange of scalar and vector mesons, we have shown that the Born-Oppenheimer approximation leads naturally to a generalization of QHD with a density dependent scalar coupling. The physical origin of this density dependence, which provides a new saturation mechanism for nuclear matter, is the relatively rapid increase of the lower Dirac component of the wavefunction of the confined, light quark. We confirm the original discovery of Guichon [3] that, once the scalar and vector coupling constants are chosen to fit the observed saturation properties of nuclear matter, the extra, internal degrees of freedom lead to an incompressibility that is consistent with experiment.

In the case of finite nuclei we have derived a set of coupled differential equations which must be solved self-consistently but which are not much more difficult to solve than the relativistic Hartree equations of QHD. Initial results are quite promising but a full

numerical study is a subject for further work.

The successful generalisation of the quark-meson coupling model to finite nuclei opens a tremendous number of opportunities. For example, earlier results for the Okamoto-Nolen-Schiffer anomaly [62], the nuclear EMC effect [195], the charge-symmetry violating correction to super-allowed Fermi beta-decay [194] and so on, can now be treated in a truly quantitative way.

It will be very interesting to explore the connection between the density dependence of the variation of the effective σ-nucleon coupling constant, which arises so naturally here, with the variation found empirically in earlier work. We note, in particular, that while our numerical results depend on the particular model chosen here (namely, the MIT bag model), the qualitative features which we find (such as the density dependent decrease of the scalar coupling) will apply in any model in which the nucleon contains light quarks and the attractive N-N force is a Lorentz scalar. Of course, it will be important to investigate the degree of variation in the numerical results for other models of nucleon structure.

We could list many other directions for future theoretical work: for the replacement of the MIT bag by a model respecting PCAC (e.g. the cloudy bag model [200]), the replacement of σ-exchange by two-pion exchange, the replacement of ω exchange by nucleon overlap at short distance, the inclusion of the density dependence of the meson masses themselves [191, 201] and so on. On the practical side, we stress that the present model can be applied to all the problems for which QHD has proven so attractive, with very little extra effort. It will also be interesting to explore its phenomenological consequences in this way.

Appendix

Here we want to demonstrate that the center of mass correction to the bag energy is essentially independent of the external scalar field. (Since the vector fields do not alter the quark structure of the nucleon we need not consider them.) To avoid the difficulties associated with the confinement by a sharp boundary, we consider a model where the quark mass grows quadratically with the distance from the center of the bag. This is justified because we do not look for the c.m. correction itself but only for its dependence on the external field. Moreover, after the strength of the confining mass has been adjusted to reproduce the lowest eigenfrequency of the bag, we have found that the corresponding wave functions are rather similar to those for the bag.

To estimate the c.m. correction we also make the assumption that the quark number is a good quantum number, which allows us to formulate the problem in the first quantized form. This amounts to neglecting the effect of quark-antiquark excitation and is therefore not a very strong constraint.

Thus the model is defined by the following first-quantized Hamiltonian:

$$H_B = \sum_{i=1,N} \gamma_0(i)[\vec{\gamma}(i)\cdot\vec{p}_i + m(\vec{r}_i)], \quad \vec{p}_i = -i\vec{\nabla}_i, \tag{316}$$

with

$$m(\vec{r}) = m^* + Kr^2, \tag{317}$$

where m^* is the mass of the quark in the presence of the external scalar field.

By assumption, N is a number, so we can define intrinsic coordinates $(\vec{\rho},\vec{\pi})$ by

$$\vec{\pi}_i = \vec{p}_i - \frac{\vec{P}}{N}, \quad \vec{P} = \sum_i \vec{p}_i, \quad \sum_i \vec{\pi}_i = 0, \tag{318}$$

$$\vec{\rho}_i = \vec{r}_i - \vec{R}, \quad \vec{R} = \frac{1}{N}\sum_i \vec{r}_i, \quad \sum_i \vec{\rho}_i = 0. \tag{319}$$

Then we can write the Hamiltonian in the form:

$$H_B = H_{intr.} + H_{CM}, \tag{320}$$

$$H_{intr.} = \sum_i \gamma_0(i)[\vec{\gamma}(i)\cdot\vec{\pi}_i + m(\vec{\rho}_i)], \tag{321}$$

$$H_{CM} = \frac{\vec{P}}{N}\cdot\sum_i \gamma_0(i)\vec{\gamma}(i) + \sum_i \gamma_0(i)[m(\vec{r}_i) - m(\vec{\rho}_i)]. \tag{322}$$

This separation into an intrinsic and a c.m. Hamiltonian is correct because:

1. $H_{intr.}$ commutes with $\vec{P}$ and $\vec{R}$,
2. One has $[H_{CM},\vec{R}] = -i\sum_i \gamma_0(i)\vec{\gamma}(i)$. Since for a Dirac particle $\gamma_0\vec{\gamma}$ is the velocity, one can identify the RHS of the previous equation with the time derivative of $\vec{R}$, which is consistent.

The fact that the c.m. Hamiltonian depends on the intrinsic coordinates is not a surprise because the separation is only complete in certain special cases.

We now look for the intrinsic energy of the bag, writing

$$H_{intr.} = H_B - H_{CM}. \tag{323}$$

All that we know are the eigenstates of H_B but we can consider H_{CM} as a correction of order $1/N$ with respect to the leading term in the bag energy. Therefore we estimate its effect in first order perturbation theory, that is

$$E_{intr.} = E_B - \langle B|H_{CM}|B\rangle = E_B - E_{CM}, \tag{324}$$

where $|B\rangle$ is the eigenstate of H_B with energy E_B. We must therefore evaluate

$$\begin{aligned} E_{CM} &= \langle B|\frac{\vec{P}}{N}\cdot\sum_j \gamma_0(j)\vec{\gamma}(j) + \sum_i \gamma_0(i)\left[m(\vec{r}_i) - m(\vec{r}_i - \vec{R})\right]|B\rangle \\ &= \langle B|\frac{\vec{P}}{N}\cdot\sum_j \gamma_0(j)\vec{\gamma}(j) + 2K\vec{R}\cdot\sum_i \gamma_0(i)\vec{r}_i - KR^2\sum_i \gamma_0(i)|B\rangle. \end{aligned} \tag{325}$$

(Note that there are no ordering problems as long as N is a number). Let $|\alpha\rangle$ be the one body solutions, that is (in units such that $R_B = 1$)

$$\gamma_0[\vec{\gamma}\cdot\vec{p} + m(\vec{r})]\phi_\alpha = \Omega_\alpha\phi_\alpha. \tag{326}$$

If we assume that $|B\rangle$ has all the quarks in the lowest mode then elementary techniques for many-body systems lead to the results

$$\begin{aligned} \langle B|\frac{\vec{P}}{N}\cdot\sum_j \gamma_0(j)\vec{\gamma}(j)|B\rangle &= \Omega_0 - \langle 0|\gamma_0(m^\star + Kr^2)|0\rangle, \\ \langle B|\vec{R}\cdot\sum_i \gamma_0(i)\vec{r}_i|B\rangle &= \langle 0|\gamma_0 r^2|0\rangle, \\ \langle B|R^2\sum_i \gamma_0(i)|B\rangle &= \frac{1}{N}\langle 0|\gamma_0 r^2|0\rangle + \left(1 - \frac{1}{N}\right)\langle 0|\gamma_0|0\rangle\langle 0|r^2|0\rangle. \end{aligned} \tag{327}$$

so that we get

$$\begin{aligned} E_{CM} &= \Omega_0 - m^\star\langle 0|\gamma_0|0\rangle + K\left(1 - \frac{1}{N}\right)\left(\langle 0|\gamma_0 r^2|0\rangle - \langle 0|\gamma_0|0\rangle\langle 0|r^2|0\rangle\right) \\ &= \Omega_0 - m^\star\langle 0|\gamma_0|0\rangle + K\left(\langle 0|\gamma_0 r^2|0\rangle - \langle 0|\gamma_0|0\rangle\langle 0|r^2|0\rangle\right) + O(1/N). \end{aligned} \tag{328}$$

Note that we keep only the leading term in $1/N$. This is consistent with our initial approximation according to which E_{CM} is computed as a correction of order $1/N$ with respect to the leading term in the bag energy.

To proceed we need to evaluate the single particle matrix elements which appear in the expression for E_{CM}. To determine the wave function we solve Eq.(326) numerically and adjust the constant K to give $\Omega_0 = 2.04$ - i.e. the lowest energy level of the free bag, in units such that $R_B = 1$. We found $K = 1.74$.

Then we compute E_{CM} numerically according to Eq.(328), as a function of $m^\star$. The result is shown in Fig.49, where we also plot the value of Ω_0. One can see that in the range $-1.5 < m^\star < 0$, which certainly contains the possible values of $m^\star$ in the case of finite real nuclei, the value of E_{CM} is almost constant. For instance at $m^\star = -1$, E_{CM} differs from its free value by only 6%. Furthermore, its variation is clearly negligible with respect to that of Ω_0. Thus, for practical purposes, it is a very reasonable approximation to ignore the dependence of E_{CM} on the external field.

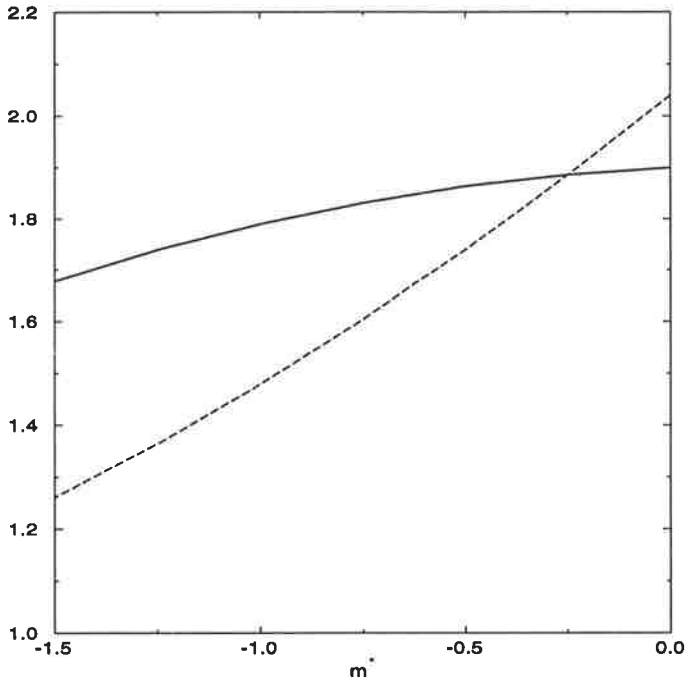

Figure 49: Dependence of E_{CM} (full line) and Ω_0 (dashed line) on $m^\star$.

References

[1] T. DeGrand, R.L. Jaffe, K. Johnson and J. Kiskis, *Phys. Rev.* **D12**, 2060 (1975);

[2] B.D. Serot and J.D. Walecka, *Adv. Nucl. Phys.* vol.**16** (1986);

[3] P.A.M. Guichon, *Phys. Lett.* **B200**, 235 (1988);

[4] M. Gell-Mann and Y. Ne'eman, *The Eightfold Way*, Benjamin, New York (1964);

[5] G. Zweig, CERN preprint 8419/TH 412 (1964);

[6] S.J. Brodsky and S.D. Drell, Phys. Rev. **D22**, 2236 (1980);

[7] J.G. Pati and A. Salam, *Phys. Rev.* **D10**, 275 (1974);

[8] J.C. Pati, A. Salam and J. Strathdee, *Phys. Lett.* **B58**, 265 (1975);

[9] H. Terazawa, *Phys. Rev.* **D22**, 184 (1980);

[10] O.W. Greenberg, *Phys. Rev. Lett* **35**, 1120 (1975);

[11] G.R. Kalbleish and B.C. Fowler, *Nuovo Cimento* **19A**, 173 (1974);

[12] E. Novak, J. Sucher and C.H. Woo, *Phys. Rev.* **D16**, 2874 (1974);

[13] H. Hararim, *Phys. Lett.* **86B**, 83 (1979);

[14] M.A. Shupe, *Phys. Lett.* **86B**, 87 (1979);

[15] J.G. Taylor, *Phys. Lett.* **88B**, 291 (1979);

[16] W.K.H. Panofsky, Rapporteurs talk, in International Conference on High Energy Physics, Vienna, ed. J. Prentki and J. Steinberger (CERN Geneva);

[17] E.D. Bloom et al., *Phys. Rev. Lett.* **23**, 930 (1969);

[18] M. Breidenbach et. al., *Phys. Rev. Lett.* **23**, 935 (1969);

[19] P.N. Bogolioubov, *Ann. Inst. Henry Poincaré* **8**, 163 (1974);

[20] V.N. Gribov, *Physica Scripta* **T15**, 164 (1987);

[21] V.N. Gribov, LU TP 91/7 (Mar 1991), Orsay lectures LPTHE Orsay 92/60 (June 1993) and LPTHE Orsay 94/20 (Feb. 1994);

[22] A. Chodos, B.L. Jaffe, K. Johnson, C.B. Thorn and V.F. Weisskopf, *Phys. Rev.* **D9**, 3471 (1974);

[23] A. Chodos, B.L. Jaffe, K. Johnson and C.B. Thorn, *Phys. Rev.* **D10**, 2599 (1974);

[24] A.W. Thomas, *Adv. Nucl. Phys.* **13**, 1 (1984);

[25] A. Chodos and C.B. Thorn, *Phys. Rev.* **D12**, 2733 (1975);

[26] T. Inoue and T. Maskawa, *Prog. Th. Phys.* **54**, 1833 (1975);

[27] M.V. Barnhill, W.K. Cheng, and A. Halprin, *Phys. Rev.* **D20**, 727 (1979);

[28] G.E. Brown and M. Rho, *Phys. Lett.* **82B**, 177 (1979);

[29] N.G. Deshpande, D.A. Dicus, K. Johnson, V.L. Teplitz, *Phys. Rev.* **D15**, 1885 (1977);

[30] W.A. Bardeen, M.S. Chanowitz, S.D Drell, M. Weinstein, and T.M. Yan, *Phys. Rev.* **D11**, 1094 (1975);

[31] M. Creutz, *Phys. Rev.* **D10**, 1749 (1974);

[32] R. Friedberg and T.D. Lee, *Phys. Rev.* **D18**, 2623 (1978);

[33] T.D. Lee, *Phys. Rev.* **D19**, 1802 (1979);

[34] T. Degrand, *University of Toronto*, 1980;

[35] J.F. Donoghue and K. Johnson, *Phys. Rev.* **D21**, 1975 (1980);

[36] C.W. Wong, *Phys. Rev.* **D24**, 1416 (1981);

[37] J.D. Bjorken and S.D. Drell *Relativistic Quantum Mechanics*, McGraw-Hill Book Company, 1964;

[38] V.B. Berestecky, E.M. Lifshic, L.P. Pitaevsky, Quantum Electrodynamics, 1989

[39] T. Barnes, *Nucl. Phys.* **B152**, 171 (1979)

[40] T. Barnes and F.E. Close, *Nucl. Phys.* **B198**, 380 (1982)

[41] K. Saito, A.W. Thomas *Nuclear Physics* **A574**, 659 (1994);

[42] M. Gell-Mann and Y. N'eman, *The Eightfold Way* Benjamin, New York (1964);

[43] H. Yukawa, *Proc. Phys.-Math. Soc. Jpn. Ser.3* **17**, 48 (1935);

[44] A. Proca, *J. Phys. Rad* **7**, 347 (1936); see also N. Kemmer, *Proc. R. Soc. London Ser.A*, **166**, 127 (1938);

[45] A.E.S. Green and T. Sawada, *Rev. Mod. Phys.* **39**, 594 (1967);

[46] D. Gogny, *Nuclear Physics of Electromagnetic Interactions*, Lecture Notes in Physics, Vol 108;

[47] J.W. Negele and D. Vautherin, *Phys. Rev.* **C5**, 1472 (1972);

[48] D. Vautherin and Brink, *Phys. Rev.* **C5**, 626 (1972);

[49] A.L. Fetter and J.D. Walecka, *Quantum Theory of Many-Particle Systems*, McGraw-Hill, New-York (1971);

[50] J.D. Walecka, *Ann. Phys. (N.Y.)* **83**, 497 (1974);
see also L.D. Miller and A.E.S. Green, *Phys. Rev.* **C5**, 241 (1972);
as well as S.A. Chin, Ann. Phys. (N.Y.) **108**, 301 (1977);

[51] C.J. Horowitz and B.D. Serot, *Nucl. Phys.* **A399**, 529 (1983);

[52] M.R. Anastasio, L.S. Selenza, W.S Pong and C.M. Shakin, *Phys. Rep.* **100**, 327 (1983);

[53] R.Brockman and R.Machkeidt, *Phys. Lett.* **149B**, 283 (1984);

[54] B. ter Haar and R. Malfliet, *Phys. Rep.* **149**, 207 (1987);

[55] C.J. Horowitz and B.D. Serot, *Nucl. Phys.* **A368**, 503 (1981);

[56] A.Bouyssy, J.-F. Mathiot , N. Van Giai and S. Marcos *Phys. Rev.* **C36**, 380 (1987);

[57] H.F. Boersma and R. Malfliet, *Phys. Rev.* **C49**, 233 (1994);

[58] H.F. Boersma and R. Malfliet, *Phys. Rev.* **C49**, 1495 (1994);

[59] S. Fleck, W. Bentz, K. Shimizu and K. Yazaki, *Nucl. Phys.*, **A510**, 731 (1990);

[60] L.N. Savushkin, *Sov. J. Nucl. Phys.* **30**, 340 (1979)

[61] K. Saito and A.W. Thomas, *Phys. Lett.* **B327**, 16 (1994);

[62] K. Saito and A. W. Thomas, *Phys. Lett.* **B335**, 17 (1994);

[63] K. Saito and A. W. Thomas, *Nucl. Phys.*, **A574**, 659 (1994);

[64] A.W. Thomas, University of Adelaide preprint: ADP-95-3/T170;

[65] M. K. Banerjee, Phys. Rev. **C45**, 1359 (1992);
E. Naar and M. C. Birse, J. Phys. **G19**, 555 (1993);

[66] R.G. Roberts, *The Structure of the Proton*, Cambridge University Press, 1990;

[67] F.J. Yndurain, *Quantum Chromodynamics*, Springer-Verlag, 1983;

[68] F.J. Yndurain, *The Theory of Quark and Gluon Interactions*, Springer-Verlag, 1992;

[69] T. Muta, *Foundations of Quantum chromodynamics*, World Scientific, 1987;

[70] R.L. Jaffe, *Deep Inelastic Scattering with Application to Nuclear Targets*, Wiley New York, 1985;

[71] Ta-Pei Cheng and Ling-Fong Li, *Gauge theory of elementary particle physics*, Oxford University Press, 1984;

[72] Chris Quigg, *Gauge Theories of the Strong, Weak and electromagnetic interactions*, The Benjamin/Cummings Publishing Company, 1983;

[73] J.D. Bjorken and E.A. Pachos, *Phys. Rev.* **185**, 1975 (1969);

[74] J.D. Bjorken, *Phys. Rev.* **179**, 1547 (1969);

[75] C.G. Callan and D.J. Gross, *Phys. Rev. Lett.* **22**, 156 (1969);

[76] A. Signal,A.W. Schreiber and A.W. Thomas, *Mod. Phys. Lett.* **A6**, 271 (1991);

[77] A. Schafer, *Phys. Lett.* **B208**, 175 (1988);

[78] H. Jung and L.S. Kisslinger, *Carnegie Mellon University*, 1992;

[79] A.I. Signal and A.W. Thomas, *Phys. Lett.* **B211**, 481 (1988);

[80] A.W. Schreiber and A.W. Thomas, *Phys. Lett.* **B215**, 141 (1988);

[81] R.I Jaffe, *Massachusetts Institute of Technology*, 1983;

[82] H. Meyer and P.J. Mulders, *National Institute for nuclear Physics and High Energy Physics*, 1990;

[83] W. Thirring, Acta Phys. Aus., Suppl. II, 183 (1966);

[84] E.M. Henley and G.A. Miller, *Phys. Lett.* **B251**, 453 (1990);

[85] G. Preparata, P.G. Ratcliffe and J. Soffer, *Phys. Rev. Lett.* **66**, 687 (1991);

[86] S. Kumano, *Phys. Rev.* **D43**, 59 (1991); S. Kumano and J.T. Londergan, *Phys. Rev.* **D44**, 717 (1991);

[87] A.D. Martin, W.J. Stirling and R.G. Roberts, *Phys. Lett.* **B252**, 653 (1990); S.D. Ellis and W.J. Stirling, *Phys. Lett.* **B256**, 258 (1991);

[88] W. Melnitchouk and A.W. Thomas, *Phys. Rev.* **D47**, 3783 (1993); V.R. Zoller, *Phys. Lett.* **B279**, 145 (1992); B. Badelek and J. Kwiecinski, *Nucl. Phys.* **B370**, 278 (1991);

[89] E.J. Eichten et al., *Nucl. Phys.* **B234**, 189 (1984);

[90] W. Melnitchouk, A.W. Thomas and A.I. Signal, *Zeit. Phys.* **340**, 85 (1991);

[91] M. Sawicki and J.P. Vary, *Phys. Rev. Lett.* **71**, 1320 (1993);

[92] K. Gottfried, *Phys. Rev. Lett.* **18**, 1174 (1967);

[93] R.P. Feynman and R.D. Field, *Phys. Rev.* **D15**, 2590 (1977);

[94] P. Amaudruz et al. (NMC Collaboration), *Phys. Rev. Lett.* **66**, 560 (1991);

[95] F.E. Close, "An Introduction to Quarks and Partons", (Academic, London, 1979); E. Leader and E. Predazzi, "Gauge theories and the New Physics" (Cambridge University Press, Cambridge, 1982);

[96] G.A. Miller, B.M.K. Nefkens and I. Šlaus, *Phys. Rep.* **194**, 1 (1990);

[97] M. Gell-Mann, R.J. Oakes and B. Renner, *Phys. Rev.* **175**, 2195 (1968); K.G. Wilson, *Phys.Rev.* **179**, 1499 (1969);

[98] J. Gasser and H. Leutwyler, *Phys.Rep.* **87**, 77 (1982).

[99] H. Leutwyler, *Nucl.Phys.* **B76**, 413 (1974); *Phys.Lett.* **B48**, 431 (1974);

[100] A.I. Vainshtein et al., *Sov. J. Nucl. Phys.* **27**, 1207 (1978);

[101] S. Narison and E. Rafael, *Phys.Lett.* **B103**, 57 (1981);

[102] R.L. Jaffe, *Phys. Rev.* **D11**, 1953 (1975).

[103] A. LeYaouanc et al., *Phys. Rev.* **D11**, 2636 (1975).

[104] J.S. Bell and A.J.G. Hey, *Phys. Lett.* **B74**, 77 (1978); J.S. Bell,A.C. Davis and J. Rafelski, *Phys. Lett.* **B78**, 67 (1979);

[105] R.J. Hughes, *Phys. Rev.* **D16**, 622 (1977); J.A. Bartelski, *Phys. Rev.* **D20**, 1229 (1979);

[106] L.S. Celenza and C.M. Shakin, *Phys. Rev.* **C27**, 1561 (1983); **C39**, 2477(E) (1989).

[107] C.J. Benesh and G.A. Miller, *Phys. Lett.* **B222**, 476 (1989); *Phys. Rev.* **D38**, 48 (1988);

[108] R. Parisi and G. Petronzio, *Phys. Lett.* **B62**, 331 (1976);

[109] A.I. Signal and A.W. Thomas, *Phys. Rev.* **D40**, 2832 (1989);

[110] A.W. Schreiber, A.W. Thomas and J.T. Londergan, *Phys. Rev.* **D42**, 2226 (1990).

[111] A.W. Schreiber, A.I. Signal, A.W. Thomas *Phys.Rev.* **D44**, 2653 (1991);

[112] F.E. Close and A.W. Thomas, *Phys. Lett.* **B212**, 227 (1988);

[113] R.P. Bickerstaff and A.W. Thomas, *Phys.Rev.* **D25**, 1869 (1982);

[114] V. Soni, *NPL-Theory-94-2*, 1995, HEP-PH-9505290;

[115] A.W. Schreiber, *Thesis*, Adelaide, 1990;

[116] E. Sather, *Phys. Lett.* **B274**, 433 (1992);

[117] G. Altarelli and G. Parisi, *Nucl. Phys.* **B126**, 298 (1977).

[118] S. Kumano and J.T. Londergan, *Comp. Phys. Comm.* **69**, 373 (1992);

[119] R. Kobayashi, S. Kumano and M. Konuma, *Department of Physics, Saga University*, SAGA-HE-63-94 (1994);

[120] W. Furmanski and R. Petronzio, *Nucl. Phys.* **B195**, 237 (1982);

[121] X. Song and J. Du, *Phys. Rev.* **D40**, 2177 (1989);

[122] G.P. Ramsey, *Comp. Phys.* **60**, 97 (1985);

[123] A.J. Buras, *Nucl. Phys.* **B125**, 125 (1977);

[124] A.J. Buras and K.J.F. Gaemers, *Nucl. Phys.* **B132**, 249 (1978);

[125] G. Parisi and N. Sourlas, *Nucl. Phys.* **B151**, 421 (1979);

[126] A. Gonzales-Arroyo and C. Lopez, *Nucl. Phys.* **B166**, 429 (1980);

[127] A. Gross, *Phys. Rev. Lett.* **8**, 3633 (1974);

[128] G. Parisi, *Phys. Lett.* **B43**, 207 (1973);

[129] A. Gonzalez-Arroyo, C. Lopez and F.G. Yndurain, *Nucl. Phys.* **B159**, 512 (1979);

[130] A. Gonzalez-Arroyo, C. Lopez and F.G. Yndurain, *Nucl. Phys.* **B153**, 161 (1979);

[131] A. Gonzalez-Arroyo, C. Lopez and F.G. Yndurain, *Nucl. Phys.* **B166**, 429 (1980);

[132] G.P. Ramsey, Ph.D thesis, Illinois Institute of Technology (1982);

[133] N. Cabibbo and R. Petronizo, *Nucl. Phys.* **B137**, 395 (1978);

[134] I.J.R. Aitchison and A.J.G. Hey, *Gauge Theories In Particle Physics*, Adam Hilger, Bristol and Philadelphia;

[135] J. Ellis and M.K. Gaillard, *Nucl. Phys.* **B150**, 141 (1979);

[136] G. Sterman and S. Libby, *Phys. Rev.* **D18**, 4737 (1978);

[137] J. Kubar-Andre and E.F. Paige, *Phys. Rev.* **D19**, 221 (1979);

[138] G. Altarelli, R.K. Ellis and G. Martinelli, *Nucl. Phys.* **B143**, 521 (1978);

[139] E.G. Floratos, C. Kounnas and R. Lacaze, *Nucl. Phys.* **B192**, 417 (1981);

[140] B. Humpert and W.L. van Neerven, *Nucl. Phys.* **B184**, 225 (1981);

[141] K. Harada and T. Muta, *Phys. Rev.* **D22**, 663 (1980);

[142] A.J. Smith, *Proceedings of Summer Institute on Particle Physics*, Stanford Report 198, 449;

[143] W. Melnitchouk, A.W. Thomas and A.I. Signal, *Zeit. Phys.* **340**, 85 (1991).

[144] M. Sawicki and J.P. Vary, *Phys. Rev. Lett.* **71**, 1320 (1993).

[145] P. Amaudruz et al. (NMC Collaboration), *Phys. Rev. Lett.* **66**, 560 (1991).

[146] J. Ashman et al. (EMC Collaboration), *Phys. Lett.* **B206**, 364 (1988); *Nucl. Phys.* **B328**, 1 (1990).

[147] B. Adeva et al. (SMC Collaboration), *Phys. Lett.* **B302**, 533 (1993); P. L. Anthony et al., *Phys. Rev. Lett.* **71**, 959 (1993).

[148] R. Windmolders, *Int. J. Mod. Phys.* **A7**, 639 (1992); S. D. Bass and A.W. Thomas, *J. Phys.* **G19**, 925 (1993).

[149] E. Sather, *Phys. Lett.* **B274**, 433 (1992).

[150] G. A. Miller, B. M. K. Nefkens and I. Šlaus, *Phys. Rep.* **194**, 1 (1990).

[151] A. W. Thomas and W. Melnitchouk, New Frontiers in Nuclear Physics: Proceedings of the 1993 JSPS.

[152] D. M. Alde et al., *Phys. Rev. Lett.* **64**, 2479 (1990).

[153] A. Bodek and J. L. Ritchie, *Phys. Rev.* **D23**, 1070 (1981).

[154] L. L. Frankfurt and M. I. Strikman, *Phys. Rep.* **160**, 235 (1988).

[155] R. P. Bickerstaff and A. W. Thomas, *J. Phys.* **G15**, 1523 (1989).

[156] W. Melnitchouk, A. W. Schreiber and A. W. Thomas, *Phys. Rev.***D49**, 1183 (1994).

[157] E. Naar and C. Birse, *Phys. Lett.* **B305**, 190 (1993).

[158] G. Farrar and D. Jackson, *Phys. Rev. Lett.* **35**, 1416 (1975).

[159] Y. Nambu and G. Jona-Lasinio, *Phys. Rev.***122**, 345 (1961); *ibid.* **124**, 246 (1961).

[160] T. Shigetani, K. Suzuki and H. Toki, *Phys. Lett.* **B308**, 383 (1993).

[161] T. Shigetani, K. Suzuki and H. Toki, *Nucl.Phys.* **A579** 413, (1994).

[162] P.N. Harriman, A.D. Martin, W.J. Stirling and R.G. Roberts, Phys. Rev. **D42**, 798 (1990); P.J. Sutton, R.G. Roberts, A.D. Martin and W.J. Stirling, Phys. Rev. **D45**, 2349 (1992).

[163] W. Melnitchouk, A. W. Schreiber and A. W. Thomas, *Phys.Lett.* **B335** 11, (1994).

[164] P.J. Sutton, R.G. Roberts, A.D. Martin and W.J. Stirling, *Phys. Rev.* **D45**, 2349 (1992).

[165] NA10 Collaboration, P. Bordalo et al., *Phys. Lett.* **B193**, 368 (1987).

[166] NA10 Collaboration, B. Betev et al., *Z. Phys.* **C28**, 9 (1985).

[167] E615 Collaboration, J.S. Conway et al., *Phys. Rev.* **D39**, 92 (1989).

[168] WA70 Collaboration, M. Bonesini et al., *Z. Phys.* **C37**, 535 (1988).

[169] NA3 Collaboration, J. Badier et al., *Z. Phys.* **C18**, 281 (1983).

[170] S.D. Drell and Tung-Yan, *Ann. Phys.* **66**, 578 (1971).

[171] CCFR Collaboration, K. Lang et al., *Phys. Lett.* **B317**, 655 (1993).
P.Z. Quintas et al., *Phys. Rev. Lett.* **71**, 1307 (1993).

[172] CCFR Collaboration, W. Leung et al., *Z. Phys.* **C33**, 483 (1987).
H. Rabinowitz et al., *Phys. Rev. Lett.***70**, 134 (1993).

[173] CDHSW Collaboration, H. Abramowitz et al., *Phys. Rev. Lett.* **57**, 298 (1986).
*Z. Phys.***C28**, 51 (1985).

[174] P.N. Harriman, A.D. Martin, W.J. Stirling and R.G. Roberts, *Phys. Rev.* **D42**, 798 (1990);

[175] A.D. Martin, R.G. Roberts and W.J. Stirling, ICHEP 653, (1994)

[176] CTEQ Collaboration, H.I. Lai, J. Botts, J. Huston, J.G. Morfin, J.F. Owens, J.W. Qiu, W.K. Tung and Weerts, *Phys.Rev.* **D51** 4763,(1995).

[177] E. Sather, *Phys. Lett.***B274**, 433 (1992).

[178] EMC Collaboration, J.J. Aubert et al., *Phys. Lett.***B123**, 275 (1983).

[179] M. Arneodo, *Phys. Rep.***240**, 301 (1994).

[180] D.F. Geesaman, K. Saito and A.W. Thomas, PHY-7963-ME-95, Mar 1995.

[181] R. B. Wiringa, V. Fiks and A. Fabrocini, Phys. Rev. **C38**, 1010 (1988);
C. J. Pethic and D. G. Ravenhall, Phil. Trans. Roy. Soc. Lond. **A341**, 17 (1992).

[182] T. T. S. Kuo, Z. Y. Ma and R. Vinh Mau, Phys. Rev. **C33**, 717 (1986);
C. Mahaux and R. Sartor, Adv. Nucl. Phys. **20**, 1 (1991);
W. H. Dickhoff and H. Müther, Rep. Prog. Phys. **55**, 1947 (1992);
A. Stadler *et al.*, Phys. Rev. **C51**, 2896 (1995).

[183] L. S. Celenza and C. M. Shakin, Relativistic Nuclear Physics: Theories of Structure and Scattering, Vol.2 of Lecture Notes in Physics (World Scientific, Singapore, 1986).

[184] C. J. Horowitz and B. D. Serot, Nucl. Phys. **A464**, 613 (1987);
R. Machleidt, Adv. Nucl. Phys. vol. **19**, 189 (1989);
G. Q. Li, R. Machleidt and R. Brockmann, Phys. Rev. **C46**, 2782 (1992);
T. Nikolaus, T. Hoch and D. G. Madland, Phys. Rev. **C46**, 1757 (1992);
H. Huber, F. Weber and M. Weigel, Phys. Lett. **B317**, 485 (1993);
H. F. Boersma and R. Malfliet, Phys. Rev. **C49**, 233 (1994); ibid. 1495.

[185] S. J. Wallace, Ann. Rev. Nucl. Part. Phys. vol.**16**, 1 (1987);
P. G. Reinhard, Rep. Prog. Phys. **52**, 439 (1989);
L. Ray, G. W. Hoffman and W. R. Cooker, Phys. Rep. **212**, 223 (1991).

[186] J. Dey *et al.*, Phys. Rev. **C44**, 2181 (1991);
R. Brockmann and H. Toki, Phys. Rev. Lett. **68**, 3408 (1992);
S. Haddad and M. Weigel, Phys. Rev. **C48**, 2740 (1993);
H. Fritz and H. Müther, Phys. Rev. **C49**, 633 (1994);
C. Fuchs *et al.*, nucl-th/9507044 (July, 1994);
H. Lenske and C. Fuchs, Phys. Lett. **B345**, 355 (1995).

[187] T. Matsui, in Proc. of the 9th Nishinomiya-Yukawa Memorial Symposium, ed. T. Suzuki (Nishinomiya, Japan, 1994), Universal Academy Press (Tokyo), p.221;
G. Q. Li, C. M. Ko and G. E. Brown,nucl-th/9504025 (1995);
R. Rapp,G. Chanfray and J. Wambach, hep-ph/9508353 (August 1995).

[188] W. Koenig *et al.*, HADES Collaboration, in Proc. Workshop on Dilepton production in Heavy Ion Collisions, ed. H. Bokemeyer (GSI, Darmstadt, 1994) p.225;
G. Agakichiev *et al.*, CERES Collaboration, CERN preprint PPE/95-26 (1995).

[189] T. Muto *et al.*, Prog. Theor. Phys. Suppl. **112**, 221 (1993);
G. E. Brown, Nucl. Phys. **A574**, 217 (1994);
L. Engvik *et al.*, nucl-th/9509016 (Sept. 1995).

[190] K. Saito and A. W. Thomas, Phys. Lett. **B327**, 9 (1994);
Phys.Rev. **C52** 2789, (1995).

[191] K. Saito and A. W. Thomas, Phys. Rev. **C51**, 2757 (1995).

[192] S. Fleck *et al.* Nucl. Phys. **A510**, 731 (1990);
M. K. Banerjee, Phys. Rev. **C45**, 1359 (1992);
E. Naar and M. C. Birse, J. Phys. **G19**, 555 (1993).

[193] K. Okamoto, Phys. Lett. **11**, 150 (1964);
J. A. Nolen, Jr. and J. P. Schiffer, Ann. Rev. Nucl. Sci. **19**, 471 (1969);
S. Shlomo, Rep. Prog. Phys. **41**, 957 (1978);
G. A. Miller, B. M. K. Nefkens and I. Šlaus, Phys. Rep. **194**, 1 (1990).

[194] K. Saito and A. W. Thomas, Phys.Lett. **B363** 157, (1995)
A. W. Thomas and K. Saito, Proc. of the international conference on Weak and Electromagnetic Interactions in Nuclei (WEIN '95), Osaka, June 1995, Japan, nucl-th/9507010 (1995).

[195] K. Saito, A. Michels and A. W. Thomas, Phys. Rev. **C46**, R2149 (1992);
A. W. Thomas, K. Saito and A. Michels, Aust. J. Phys. **46**, 3 (1993);
K. Saito and A. W. Thomas, Nucl. Phys. **A574**, 659 (1994).

[196] P. A. Seeger and W. M. Howard, Nucl. Phys. **A238**, 491 (1975).

[197] J. P. Blaizot, D. Gogny and B. Grammaticos, Nucl. Phys. **A265**, 315 (1976);
V. R. Pandaripande and R. B. Wiringa, Rev. Mod. Phys. **51**, 821 (1979);
M. Brack, C. Guet and H. B. Håkansson, Phys. Rep. **123**, 275 (1985);
J. M. Cavedon *et al.*, Phys. Rev. Lett. **58**, 195 (1987);
M. M. Sharma *et al.*, Phys. Rev. **C38**, 2562 (1988);
J. P. Blaizot *et al.*, Nucl. Phys. **A591**, 435 (1995).

[198] P. A. M. Guichon *et al.*, to be published.

[199] I. Sick and J. S. McCarthy, Nucl. Phys. **A150**, 631 (1970).

[200] A. W. Thomas, Adv. Nucl. Phys. **13**, 1 (1984);
S. Théberge *et al.*, Phys. Rev. **D22** (1980) 2838; **D23**, 2106(E) (1981).

[201] K. Saito, T. Maruyama and K. Soutome, Phys. Rev. **C40**, 407 (1989);
H.-C. Jean, J. Piekarewicz and A. G. Williams, Phys. Rev. **C49**, 1981 (1994);
H. Shiomi and T. Hatsuda, Phys. Lett. **B334**, 281 (1994).

[202] H. Goldstein, Classical Mechanics, Addison-Wesley, Mento Park Ca USA, 212 (1968).

[203] J. Achtzehnter and Wilets, Phys. Rev. **C38**, 5 (1988).

[204] J.D. Jackson, Classical Electrodynamics, J. Wilew & Sons, New York, 364 (1967).

[205] B. Frois *In Proceedings of the International Conference on Nuclear Physics*, Bologna, 1983, Vol 2, 221.

List of publications

1) CHARGE ASYMMETRY OF PARTON DISTRIBUTIONS.
By E.N. Rodionov, A.W. Thomas (Adelaide U.), J.T. Londergan (Indiana U.). Published in Mod.Phys.Lett.A9:1799-1806,1994

2) DRELL-YAN PROCESSES AS A PROBE OF CHARGE SYMMETRY VIOLATION IN THE PION AND THE NUCLEON.
By J.T. Londergan (Indiana U.), G.T. Carvey (Los Alamos), G.Q. Liu, E.N. Rodionov, A.W. Thomas (Adelaide U).
Published in Phys.Lett.B340:115-121,1994

3) PROBING THE PION SEA WITH PI D DRELL-YAN PROCESSES.
By J.T. Londergan (Indiana U.), G.Q. Liu, E.N. Rodionov, A.W. Thomas (Adelaide U.). Published in Phys.Lett.B361:110-114,1995

4) THE ROLE OF NUCLEON STRUCTURE IN FINITE NUCLEI.
By Pierre A.M. Guichon (DAPNIA, Saclay), Koichi Saito (Tohoku Coll., Pharmacy), Evgenii Rodionov, Anthony W. Thomas (Adelaide U.).
Nucl.Phys.A601:349-379,1996

Rodionov, E.N., Thomas, A.W. and Londergan, J.T. (1994). Charge asymmetry of parton distributions. *Modern Physics Letters A*, 9(19), 1799-1806.

PHYSICS LETTERS B

Physics Letters B 340 (1994) 115–121

Drell–Yan processes as a probe of charge symmetry violation in the pion and the nucleon

J.T. Londergan [a], G.T. Garvey [b], G.Q. Liu [c], E.N. Rodionov [c], A.W. Thomas [c]

[a] *Department of Physics and Nuclear Theory Center, Indiana University, Bloomington, IN 47408, USA*
[b] *Los Alamos National Laboratory, Los Alamos, NM 87544, USA*
[c] *Department of Physics and Mathematical Physics, University of Adelaide, Adelaide S.A. 5005, Australia*

Received 8 June 1994; revised manuscript received 4 September 1994
Editor: H. Georgi

ELSEVIER

ELSEVIER

1 December 1994

PHYSICS LETTERS B

Physics Letters B 340 (1994) 115–121

Drell–Yan processes as a probe of charge symmetry violation in the pion and the nucleon

J.T. Londergan [a], G.T. Garvey [b], G.Q. Liu [c], E.N. Rodionov [c], A.W. Thomas [c]

[a] *Department of Physics and Nuclear Theory Center, Indiana University, Bloomington, IN 47408, USA*
[b] *Los Alamos National Laboratory, Los Alamos, NM 87544, USA*
[c] *Department of Physics and Mathematical Physics, University of Adelaide, Adelaide S.A. 5005, Australia*

Received 8 June 1994; revised manuscript received 4 September 1994
Editor: H. Georgi

Abstract

We extend earlier investigations of charge symmetry violation in the valence quark distributions of the nucleon, and make similar estimates for the pion. The sensitivity of pion-induced Drell–Yan measurements to such effects is then examined. It is shown that combinations of π^+ and π^- data on deuterium and hydrogen are sensitive to these violations, and that the pion and nucleon charge symmetry violating terms separate as a function of x_π and x_N respectively. We estimate the background terms which must be evaluated to extract charge symmetry violation.

At the present time the flavor structure of the nucleon is a topic of intense interest [1–8]. This is largely a consequence of unexpected experimental results, such as the discovery by the New Muon Collaboration (NMC) of a violation of the Gottfried sum-rule [9] and the so-called "proton spin crisis" [10–12] of EMC. There have also been recent theoretical calculations of the violation of charge symmetry in the valence quark distributions of the nucleon [13,14].

In most nuclear systems, charge symmetry is obeyed to within about one percent [15], so one would expect small charge symmetry violation [CSV] in parton distributions. The theoretical calculations suggest that there is a CSV part of the "minority" valence quark distributions (d^p or u^n), with a slightly smaller violation in the "majority" valence distributions (u^p or d^n). Although both CSV contributions are rather small in absolute magnitude, the *fractional* charge symmetry violation in the minority valence quark distributions $r_{\min}(x) \equiv 2(d^p(x) - u^n(x))/(d^p(x) + u^n(x))$ can be large, because at large momentum fraction x, $d^p(x)/u^p(x) \ll 1$. Rodionov et al. [14] predicted charge symmetry violation as large as 5–10% for the ratio $r_{\min}(x)$, in the region $x > 0.5$. The relative size of these CSV effects might require a change in the standard notation for parton distributions [16] in this region; in addition, Sather [13] showed that CSV effects of this magnitude could significantly alter the value of the Weinberg angle extracted from neutral and charged current neutrino interactions.

Since (in this particular region of Bjorken x) we predict fractional CSV violations as large as 5–10%, it is important to explore experiments which would be sensitive to the relative minority quark distributions in the neutron and proton. Observation of a CSV effect at this level would reinforce confidence in our ability to relate quark models to measured quark–parton distributions – and hence to use deep inelastic scattering as a real probe of the non-perturbative aspects of hadron structure [17]. Drell–Yan processes have proven to be

SSDI 0370-2693(94)01237-7

a particularly useful source of information on the antiquark distributions in nuclei [18]. If one uses beams of pions, and concentrates on the region where Bjorken x of the target quarks is reasonably large, then the annihilating quarks will predominantly come from the nucleon and the antiquarks from the pion. Furthermore, for $x \gtrsim 0.4$ to good approximation the nucleon consists of three valence quarks, and the pion is a quark–antiquark valence pair – in particular, π^+ contains a valence $\bar{d}$ and π^- a valence $\bar{u}$. Comparison of Drell–Yan processes induced by π^+ and π^- in this kinematic region will provide a good method of separately measuring d and u quark distributions in the nucleon.

Consider the Drell–Yan process in which a quark with momentum fraction x_1 in a deuteron annihilates with an anti-quark of momentum fraction x_2 in a π^+. Provided that $x_1, x_2 \geq 0.4$, to minimize the contribution from sea quarks, this will be the dominant process. Neglecting sea quark effects, the Drell–Yan cross section will be proportional to:

$$\sigma^{\mathrm{DY}}_{\pi^+ D} \sim \tfrac{1}{9}(d^p(x_1) + d^n(x_1))\bar{d}^{\pi^+}(x_2) \,. \tag{1}$$

The corresponding cross section for $\pi^- D$ is:

$$\sigma^{\mathrm{DY}}_{\pi^- D} \sim \tfrac{4}{9}(u^p(x_1) + u^n(x_1))\bar{u}^{\pi^-}(x_2) \,, \tag{2}$$

so that if we construct the ratio, $R^{\mathrm{DY}}_{\pi D}$:

$$R^{\mathrm{DY}}_{\pi D}(x_1, x_2) = \frac{4\sigma^{\mathrm{DY}}_{\pi^+ D} - \sigma^{\mathrm{DY}}_{\pi^- D}}{(4\sigma^{\mathrm{DY}}_{\pi^+ D} + \sigma^{\mathrm{DY}}_{\pi^- D})/2} \,, \tag{3}$$

only charge symmetry violating (CSV) terms contribute. In fact, defining

$$\delta d = d^p - u^n, \quad \delta u = u^p - d^n \,,$$
$$\delta\bar{d}^{\pi} = \bar{d}^{\pi^+} - \bar{u}^{\pi^-} \,, \tag{4}$$

(and recalling that charge conjugation implies $\bar{d}^{\pi^+} = d^{\pi^-}$ etc.) we find that, to first order in the small CSV terms, the Drell–Yan ratio becomes:

$$R^{\mathrm{DY}}_{\pi D}(x_1, x_2) = \left(\frac{\delta d - \delta u}{u^p + d^p}\right)(x_1) + \left(\frac{\delta\bar{d}^{\pi}}{\bar{d}^{\pi^+}}\right)(x_2) \,,$$
$$= R^N_{\pi D}(x_1) + R^{\pi}(x_2) \,. \tag{5}$$

Eq. (5) is quite remarkable in that only CSV quantities enter, and there is a separation of the effects associated with the nucleon and the pion. Because $R^{\mathrm{DY}}_{\pi D}$ is a ratio of cross sections one expects a number of systematic errors to disappear – although the fact that different beams (π^+ and π^-) are involved means that not all such errors will cancel. This certainly needs further investigation, since R^{DY} is obtained by almost complete cancellation between terms in the numerator. The largest "background" term, contributions from nucleon or pion sea, will be estimated later in this letter. However we note that Eq. (5) is not sensitive to differences between the parton distributions in the free nucleon and those in the deuteron [19–22]. For example, if the parton distributions in the deuteron are related to those in the neutron and proton by

$$q_i^D(x) = (1 + \epsilon(x))(q_i^p(x) + q_i^n(x)) \,, \tag{6}$$

then by inspection Eq. (5) will be unchanged. Any correction to the deuteron structure functions which affects the proton and neutron terms identically will cancel in R^{DY}.

It should not be necessary to know absolute fluxes of charged pions to obtain an accurate value for R^{DY}. The yield of J/ψ's from π^+–D and π^-–D can be used to normalize the relative fluxes, since the J/ψ's are predominantly produced via gluon fusion processes. The gluon structure functions of the π^+ and π^- are identical, so the relative yield should be unity to within 1%.

Next we turn to the predictions for the charge symmetry violating terms, δd, δu and $\delta\bar{d}^{\pi}$ which appear in Eq. (5). For the former two there has been an extensive discussion by Sather [13] and Rodionov et al. [14] from which there is at least a theoretical consensus that the magnitude of δd is somewhat larger than δu. This is easy to understand because the dominant source of CSV is the mass difference of the residual di-quark pair when one quark is hit in the deep-inelastic process. For the minority quark distribution the residual di-quark is uu in the proton, and dd in the neutron. Thus, in the difference, $d^p - u^n$, the up–down mass difference enters twice. Conversely, for the majority quark distributions the residual di-quark is a ud-pair in both proton and neutron, so there is no contribution to CSV.

In Fig. 1(a) we show the predicted CSV terms for the majority and minority quark distributions in the nucleon, as a function of x, calculated for the simple MIT bag model [14,23,24]. There are, of course, more sophisticated quark models available but the similarity of the results obtained by Naar and Birse [25] using the color dielectric model suggests that similar results would be obtained in any relativistic model based on

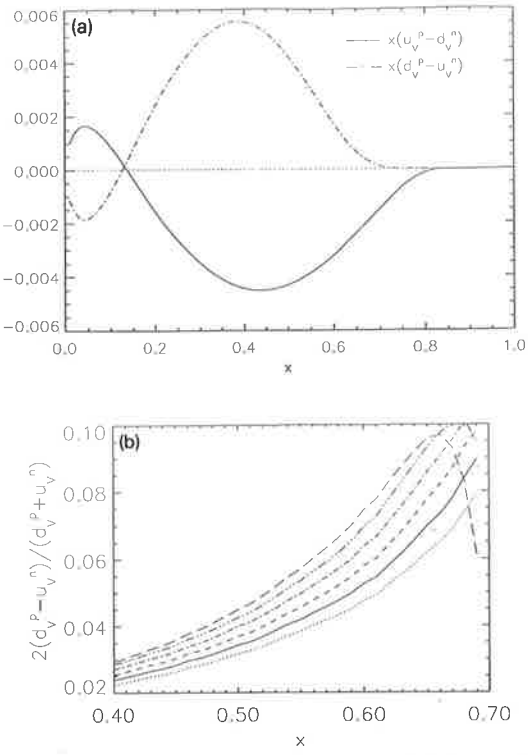

Fig. 1. (a) Predicted charge symmetry violation (CSV), calculated using the MIT bag model. Dashed curve: "minority" quark CSV term, $x\delta d(x) = x(d^p(x) - u^n(x))$; solid curve: "majority" quark CSV term, $x\delta u(x) = x(u^p(x) - d^n(x))$. (b) Fractional minority quark CSV term, $\delta d(x)/d^p(x)$, vs. x, as a function of the average di-quark mass $\bar{m}_d = (m_{uu} + m_{dd})/2$. The di-quark mass difference is fixed at $\delta m_d = m_{dd} - m_{uu} = 4$ MeV. From top to bottom, the curves correspond to average di-quark mass $\bar{m}_d = 850$, 830, 810, 790, 770, and 750 MeV. The curves have been evolved to $Q^2 = 10$ GeV^2. This quantity is the nucleonic CSV term for the Drell–Yan ratio $R^{DY}_{\pi N}$ of Eq. (11).

confined current quarks. The bag model parameters are listed in this figure. The mean di-quark masses are chosen as 600 MeV for the $S = 0$ case, and 800 MeV for the $S = 1$ case (note that for the minority quark distributions the di-quark is always in an $S = 1$ state). The di-quark mass difference, $m_{dd} - m_{uu}$, is taken to be 4 MeV, a rather well determined difference in the bag model. We note that δu is opposite in sign to δd and, therefore, these two terms add constructively in the Drell–Yan ratio R^{DY} of Eq. (5).

In Fig. 1(b) we show the fractional change in the minority quark CSV term, $2(d^p - u^n)/(d^p + u^n)$ vs. x for several values of the intermediate mean di-quark mass. Although the precise value of the minority quark CSV changes with mean di-quark mass, the size is always roughly the same and the sign is unchanged. This shows that "smearing" the mean di-quark mass will not dramatically diminish the magnitude of the minority quark CSV term (the mean di-quark mass must be roughly 800 MeV in the $S = 1$ state to give the correct N–Δ mass splitting).

In Fig. 2 we show the nucleon CSV contribution, $R^N_{\pi D}(x_1)$, calculated using the same bag model. As is customary in these bag model calculations, this term is calculated at the bag model scale (0.5 GeV for $R = 0.8$ fm) and then evolved to higher Q^2 using the QCD evolution equations [26]. As the main uncertainty in our calculation is the mean di-quark mass (the splitting between $S = 0$ and $S = 1$ is kept at 200 MeV [27]), the results are shown for several values of this parameter. In the region $0.4 \leq x \leq 0.7$, we predict R^N will be always positive, with a maximum value of about 0.015. For $x > 0.7$ the struck quark has a momentum greater than 1 GeV which is very unlikely in a mean-field model like the bag. As a consequence the calculated valence distributions for the bag model tends to be significantly smaller than the measured distributions in this region. In these circumstances one cannot regard the large, relative charge symmetry violation found in this region as being reliable and we prefer not to show it. It would be of particular interest to add q–q correlations which are known to play an important role as $x \to 1$ [28].

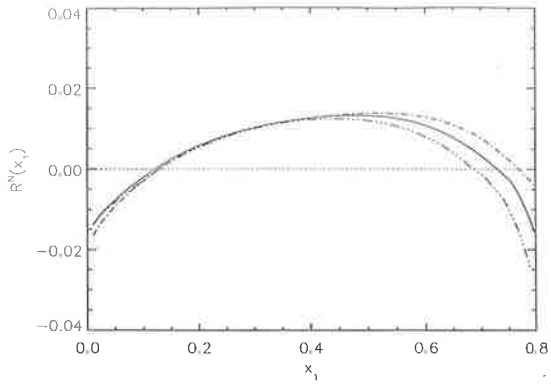

Fig. 2. Contributions from various sources to the nucleonic charge symmetry breaking term $R^{DY}_{\pi D}$ of Eq. (5), evolved to $Q^2 = 10$ GeV^2, for pion-induced Drell–Yan ratios on deuterons. Unless otherwise specified, parameters are: $m_d = m_u = 0$ MeV; $M^{(n)} = M^{(p)} = 938.27$ MeV; $R^{(n)} = R^{(p)} = 0.8$ fm; $\delta m_d = m_{dd} - m_{uu} = 4$ MeV. Curves represent different values of average di-quark mass. Dash–dot: $\bar{m}_d = 750$ MeV; solid: 800 MeV; dash–triple-dot: 850 MeV.

For the pion, calculations based on the MIT bag model are really not appropriate. In particular, the light pion mass means that center of mass corrections are very large, and of course bag model calculations do not recognize the pion's Goldstone nature. On the other hand the model of Nambu and Jona-Lasinio (NJL) [29] is ideally suited to treating the structure of the pion, and there has been recent work, notably by Toki and collaborators, in calculating the structure function of the pion (and other mesons) in this model [30,31]. The essential element of their calculation was the evaluation of the so-called handbag diagram for which the forward Compton amplitude is:

$$T_{\mu\nu} = i \int \frac{d^4k}{(2\pi)^4} \mathrm{Tr}\left[\gamma_\mu Q \frac{1}{\not{k}} \gamma_\nu Q T_- \right] + (T_+ \text{ term}) , \quad (7)$$

where

$$T_- = S_F(k-q, M_1) g_{\pi qq} \tau_+ i\gamma_5 S_F(k-p-q, M_2) \times g_{\pi qq} \tau_- i\gamma_5 S_F(k-q, M_1) , \quad (8)$$

represents the contribution with an anti-quark of mass M_2 as spectator to the absorption of the photon (of momentum q) by a quark. In Eq. (8) $g_{\pi qq}$ is the pion–quark coupling constant, Q the charge of the struck quark, p the momentum of the target meson, and S_F the quark propagator. T_+ is the corresponding term where the quark is a spectator and the anti-quark undergoes a hard collision. As in our bag model studies this model was used to determine the leading twist structure function at some low scale (0.25 GeV in this case), and then evolved to high-Q^2 using the Altarelli–Parisi equations [26]. The agreement between the existing data and the calculations for the pion and kaon obtained in Ref. [30] was quite impressive.

In the light of the successful application of the NJL model to the structure functions of the pion and the kaon, where the dominant parameter is the mass difference between the constituent strange and non-strange quarks (assumed to be about 180 MeV), it seems natural to use the same model to describe the small difference $\delta\bar{d}^\pi$ (cf. Eq. (4)) arising from the 3 MeV constituent mass difference of the u and d [15]. We have carried out such a calculation. Fig. 3 shows the pionic contribution to the CSV Drell–Yan ratio, $R^\pi(x_2)$, corresponding to this mass difference and an average non-strange quark mass of 350 MeV – as used in Refs. [30,31]. The dashed curve is the result at the bag scale, and the solid curve shows the result evolved to $Q^2 = 10$ GeV^2. For $x_2 > 0.3$, we predict that R^π will be positive and increase monotonically, reaching a value of about 0.01 at $x_2 = 0.8$ and increasing to about 0.02 as $x_2 \to 1$. (We note that there is some ambiguity in translating the usual Euclidean cutoff in the NJL model into the cutoff needed for deep inelastic scattering. In order to study charge symmetry violation we are particularly concerned to start with a model that gives a good description of the normal pion structure function. For this reason we have chosen to follow the method used in Ref. [30] rather than Ref. [31].)

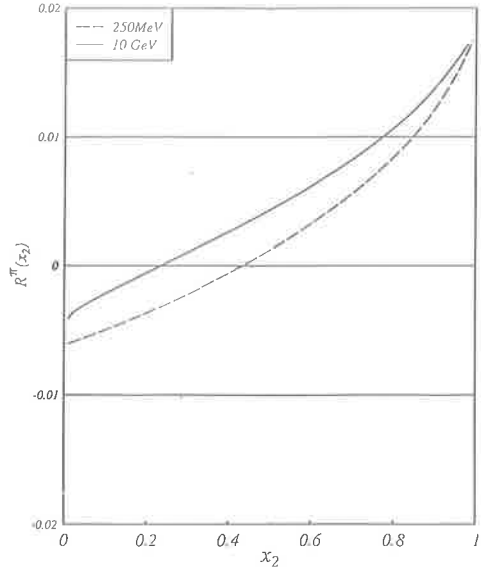

Fig. 3. Calculation of the pion CSV contribution R^π of Eq. (5), using the model of Refs. [30,31], for average nonstrange quark mass 350 MeV, and mass difference $m_d - m_u = 3$ MeV. Dashed curve: R^π evaluated at the bag scale, $\mu = 250$ MeV; solid curve: the same quantity evolved to $Q^2 = 10$ GeV^2.

Up to this point we have neglected the nucleon and pion sea quark contributions. Since the Drell–Yan ratios arising from CSV are very small (viz. Figs. 2 and 3), even small contributions from sea quarks could make a substantial effect. The dominant contribution will arise from interference between one sea quark and one valence quark. Assuming charge symmetry for the quark distributions, and using the same form for the quark and antiquark distributions in the pion, the sea-valence contribution to the Drell–Yan ratio of Eq. (5) has the form

$$R^{\rm SV}_{\pi D}(x_1, x_2) = \frac{3\sigma^{\rm SV}_{\pi D}(x_1, x_2)}{\{\frac{4}{9}\bar{d}^{\pi}_{v}(x_2)[u^{p}_{v}(x_1)+d^{p}_{v}(x_1)]+\frac{5}{2}\sigma^{\rm SV}_{\pi D}(x_1, x_2)\}};$$

$$\sigma^{\rm SV}_{\pi D}(x_1, x_2) \equiv \tfrac{5}{9}\{2\pi_v(x_2)u^{p}_{s}(x_1) + \pi_s(x_2)[u^{p}_{v}(x_1)+d^{p}_{v}(x_1)]\}\,. \quad (9)$$

Unlike the CSV contributions of Eq. (5), the sea-valence term does not separate. In Fig. 4 we show the sea-valence term as a function of x_1 and x_2 using recent phenomenological nucleon and pion parton distributions [32] [1]. The sea-valence contribution, although extremely large at small x, decreases rapidly as x increases. For $x \geq 0.5$, the sea-valence term is no larger than the CSV "signal". With accurate phenomenological nucleon and pion quark distributions, it should be possible to calculate this contribution reasonably accurately (the main uncertainty is the magnitude of the pion sea). For smaller values ($x_1 \approx x_2 \approx 0.4$), where the background dominates, we could use the data to normalize the pion sea contribution; we should then be able to predict the sea-valence term rather accurately for larger x values, where the CSV contributions become progressively more important. We could also exploit the very different dependence on x_1 and x_2 of the background and CSV terms. We conclude that the CSV terms could be extracted even in the presence of a sea-valence "background". We emphasize that our proposed Drell–Yan measurement would constitute the first direct observation of charge symmetry violation for these quark distributions.

The Drell–Yan CSV ratio $R^{\rm DY}_{\pi D}$ of Eq. (5) is the sum of the nucleon CSV term of Fig. 2 and the pion term of Fig. 3, at the respective values of Bjorken x. Since both quantities are positive, they will add to give the experimental ratio. Despite the fact that the fractional minority quark CSV term is as large as 10% (cf. Fig. 1(b)), the nucleonic CSV ratio $R^{N}_{\pi D}$ is more like 1–2%. This is because δd in Eq. (5) is divided by $u^p + d^p$ and since $d^p(x) \ll u^p(x)$ at large x the nucleon CSV term is significantly diminished. A much larger ratio could be obtained by comparing the π^+–p and "π^-–n" Drell–Yan processes through the ratio:

$$R^{\rm DY}_{\pi N}(x_1, x_2) = \frac{4\sigma^{\rm DY}_{\pi^+ p} + \sigma^{\rm DY}_{\pi^- p} - \sigma^{\rm DY}_{\pi^- D}}{(4\sigma^{\rm DY}_{\pi^+ p} - \sigma^{\rm DY}_{\pi^- p} + \sigma^{\rm DY}_{\pi^- D})/2}\,. \quad (10)$$

To first order in the small CSV quantities, this ratio can be written:

$$R^{\rm DY}_{\pi N}(x_1, x_2) = \frac{\delta d}{d^p}(x_1) + \left(\frac{\delta \bar{d}^{\pi}}{\bar{d}^{\pi^+}}\right)(x_2)\,, = R^{N}_{\pi N}(x_1) + R^{\pi}(x_2)\,. \quad (11)$$

Once again, the ratio separates completely in x_1 and x_2, and the pion CSV term is identical with Eq. (5). However, the nucleon CSV term is much larger – in fact, it is precisely the ratio given in Fig. 1(b) – so we expect CSV effects at the 5–10% level for this quantity.

Some care will need to be taken to normalize cross sections since one is comparing Drell–Yan processes on protons and deuterons. This should be feasible by bombarding both hydrogen and deuterium targets simultaneously with charged pion beams. Eq. (11) assumes that deuteron structure functions are just the sum of the free nucleon terms; if we include corrections in the form of Eq. (6), we obtain an additional first-order correction

$$\delta R^{\rm DY}_{\pi N}(x_1) = -\epsilon(x_1)\left(\frac{u^p + d^p}{d^p}\right)(x_1)\,. \quad (12)$$

This preserves the separation into nucleonic and pionic CSV terms, but depends on "EMC" changes in the deuteron structure functions relative to free proton and neutron distributions, and on the u/d ratio of proton distributions. For large x, $u(x)/d(x) \gg 1$, so the EMC term could be significant even for small values of $\epsilon(x)$. For $x \sim 0.5$, where $u^p/d^p \approx 4$, if $\epsilon(x)$ is as large as -0.02 then $\delta R^{\rm DY}_{\pi N}(x=0.5) \approx 0.10$. At larger x the EMC contribution could be even bigger, and might conceivably dominate the CSV terms. Since all terms (pion and nucleon CSV, and EMC) are predicted to have the same sign in the region $0.3 < x < 0.8$ (we expect $\epsilon(x) < 0$ in this region), the ratio $R^{\rm DY}_{\pi N}$ could be as large as 0.3. In view of this sensitivity to the EMC term, it is important that accurate calculations be carried out of Fermi motion and binding corrections for the deuteron, including possible flavor dependence of such corrections. Melnitchouk, Schreiber and Thomas [22,33] have recently studied the contributions to $\epsilon(x)$ in the deuteron.

[1] We used the nucleon parton distribution HMRS(B), and pion fit 3, for which the pion sea carries 10% of the pion's momentum at $Q^2 = 4$ GeV^2.

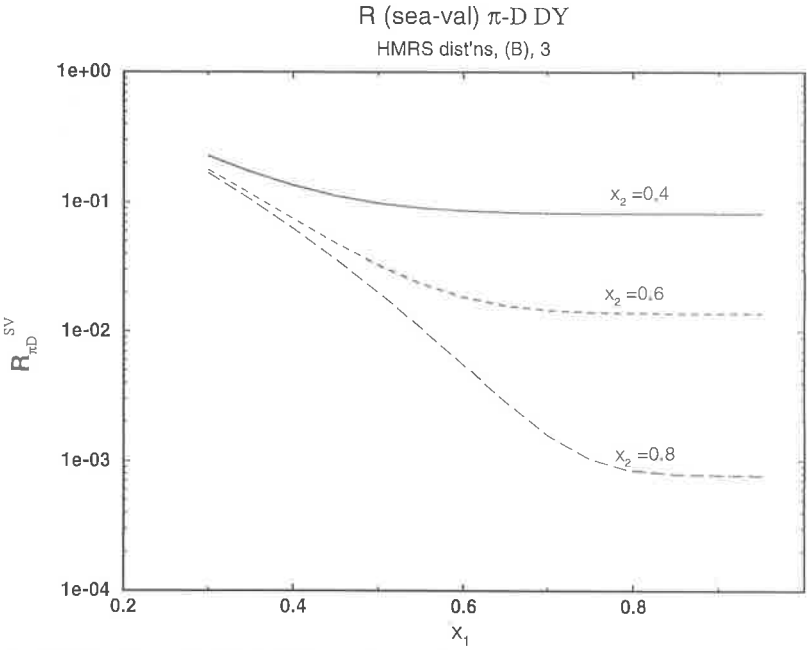

Fig. 4. The sea-valence contribution $R_{\pi D}^{SV}$ to pion-induced Drell–Yan ratios on deuterons, as a function of nucleon x_1. Solid curve: pion $x_2 = 0.4$; dashed curve: $x_2 = 0.6$; long-dashed curve: $x_2 = 0.8$. This quantity was calculated using nucleon and pion parton distributions of Ref. [32].

We have also calculated the sea-valence contribution to the Drell–Yan ratio $R_{\pi N}^{DY}$. Relative to the deuteron measurement, we predict a CSV contribution which increases by about a factor 5. The sea-valence background also increases by about the same factor. So our remarks about the sea-valence background and the CSV "signal" are equally valid for these Drell–Yan processes.

In conclusion, we have shown that by comparing the Drell–Yan yield for π^+ and π^- on nucleons or deuterons, one might be able to extract the charge symmetry violating [CSV] parts of *both* pion and nucleon. We discussed two different linear combinations of π^+ and π^- induced Drell–Yan cross sections, which produce a result directly proportional to the CSV terms. Furthermore, we found that the ratio of Drell–Yan cross sections *separates* completely into two terms, one of which ($R^N(x_N)$) depends only on the nucleon CSV, and the other ($R^\pi(x_\pi)$) depends on the pion CSV contribution. Thus if this ratio can be accurately measured as a function of x_N and x_π, both the nucleon and pion CSV terms might be extracted. The largest background should arise from terms involving one sea quark and one valence quark. Such contributions, although relatively large, should be predicted quite accurately, and may be subtracted off through their very different behavior as a function of nucleon and pion x. As the x_1 and x_2 values of interest for the proposed measurements are large ($x > 0.5$), a beam of 40–50 GeV pions will produce sufficiently massive dilepton pairs that the Drell–Yan mechanism is applicable. A flux of more than 10^9 pions/s is desirable, which may mean that the experiment is not feasible until the new FNAL Main Ring Injector becomes operable.

This work was supported by the Australian Research Council. One of the authors (JTL) was supported in part by the US NSF under research contract NSF-PHY91-08036.

References

[1] A.D. Martin, W.J. Stirling and R.G. Roberts, Phys. Lett. B 252 (1990) 653;
S.D. Ellis and W.J. Stirling, Phys. Lett. B 256 (1991) 258.

[2] A. Signal, A.W. Schreiber and A.W. Thomas, Mod. Phys. Lett. A 6 (1991) 271.
[3] E.M. Henley and G.A. Miller, Phys. Lett. B 251 (1990) 453.
[4] G. Preparata, P.G. Ratcliffe and J. Soffer, Phys. Rev. Lett. 66 (1991) 687.
[5] S. Kumano, Phys. Rev. D 43 (1991) 59;
S. Kumano and J.T. Londergan, Phys. Rev. D 44 (1991) 717.
[6] W. Melnitchouk and A.W. Thomas, Phys. Rev. D 47 (1993) 3783;
V.R. Zoller, Phys. Lett. B 279 (1992) 145;
B. Badelek and J. Kwiecinski, Nucl. Phys. B 370 (1991) 278.
[7] W. Melnitchouk, A.W. Thomas and A.I. Signal, Zeit. Phys. 340 (1991) 85.
[8] M. Sawicki and J.P. Vary, Phys. Rev. Lett. 71 (1993) 1320.
[9] P. Amaudruz et al. (NMC Collaboration), Phys. Rev. Lett. 66 (1991) 560.
[10] J. Ashman et al. (EMC Collaboration), Phys. Lett. B 206 (1988) 364; Nucl. Phys. B 328 (1990) 1.
[11] B. Adeva et al. (SMC Collaboration), Phys. Lett. B 302 (1993) 533;
P.L. Anthony et al., Phys. Rev. Lett. 71 (1993) 959.
[12] R. Windmolders, Int. J. Mod. Phys. A 7 (1992) 639;
S.D. Bass and A.W. Thomas, J. Phys. G 19 (1993) 925.
[13] E. Sather, Phys. Lett. B 274 (1992) 433.
[14] E. Rodionov, A.W. Thomas and J.T. Londergan, University of Adelaide preprint: ADP-93-222/T139; to appear in Int. J. Mod. Phys. Lett. (1994).
[15] G.A. Miller, B.M.K. Nefkens and I. Šlaus, Phys. Rep. 194 (1990) 1.
[16] F.E. Close, An Introduction to Quarks and Partons (Academic, London, 1979);
E. Leader and E. Predazzi, Gauge theories and the New Physics (Cambridge University Press, Cambridge, 1982).
[17] A.W. Thomas and W. Melnitchouk, University of Adelaide preprint: ADP-93-217/T135, to appear in Proc. JSPS-INS Spring School (World Scientific, Singapore, 1994).
[18] D.M. Alde et al., Phys. Rev. Lett. 64 (1990) 2479.
[19] A. Bodek and J.L. Ritchie, Phys. Rev. D 23 (1981) 1070.
[20] L.L. Frankfurt and M.I. Strikman, Phys. Rep. 160 (1988) 235.
[21] R.P. Bickerstaff and A.W. Thomas, J. Phys. G 15 (1989) 1523.
[22] W. Melnitchouk, A.W. Schreiber and A.W. Thomas, Phys. Rev. D 49 (1994) 1183.
[23] A. Chodos et al. Phys. Rev. D 10 (1974) 2599.
[24] A.I. Signal and A.W. Thomas, Phys. Rev. D 40 (1989) 2832; A.W. Schreiber, A.W. Thomas and J.T. Londergan, Phys. Rev. D 42 (1990) 2226.
[25] E. Naar and C. Birse, Phys. Lett. B 305 (1993) 190.
[26] G. Altarelli and G. Parisi, Nucl. Phys. B 126 (1977) 298.
[27] F.E. Close and A.W. Thomas, Phys. Lett. B 212 (1988) 227.
[28] G. Farrar and D. Jackson, Phys. Rev. Lett. 35 (1975) 1416.
[29] Y. Nambu and G. Jona-Lasinio, Phys. Rev. 122 (1961) 345; 124 (1961) 246.
[30] T. Shigetani, K. Suzuki and H. Toki, Phys. Lett. B 308 (1993) 383.
[31] T. Shigetani, K. Suzuki and H. Toki, Tokyo Metropolitan University preprint: TMU-NT940101 (1994).
[32] P.N. Harriman, A.D. Martin, W.J. Stirling and R.G. Roberts, Phys. Rev. D 42 (1990) 798;
P.J. Sutton, R.G. Roberts, A.D. Martin and W.J. Stirling, Phys. Rev. D 45 (1992) 2349.
[33] W. Melnitchouk, A.W. Schreiber and A.W. Thomas, University of Adelaide preprint: ADP-93-227/T143, to appear in Phys. Lett. (1994).

PHYSICS LETTERS B

Physics Letters B 361 (1995) 110–114

Probing the pion sea with π–D Drell-Yan processes

J.T. Londergan [a,1], G.Q. Liu [b,2], E.N. Rodionov [b,3], A.W. Thomas [b,4]

[a] *Department of Physics and Nuclear Theory Center, Indiana University, Bloomington, IN 47408, USA*

[b] *Department of Physics and Mathematical Physics, University of Adelaide, Adelaide, SA 5005, Australia*

Received 5 July 1995

Editor: H. Georgi

ELSEVIER

PHYSICS LETTERS B

Aims and Scope
Physics Letters B ensures the rapid publication of letter-type communications in the fields of Nuclear Physics/Intermediate Energy Physics, High Energy Physics and Field Theory.

Abstracted/indexed in:
Current Contents: Physical, Chemical & Earth Sciences; INSPEC; Physics Briefs.

Subscription Information 1995
PHYSICS LETTERS A (ISSN 0375-9601) and PHYSICS LETTERS B (ISSN 0370-2693) will each be published weekly. For 1995 13 volumes, volumes 198–210 (78 issues altogether) of Physics Letters A have been announced. For 1995 24 volumes, volumes 341–364 (96 issues altogether) of Physics Letters B have been announced. The subscription prices for these volumes are available upon request from the Publisher. PHYSICS REPORTS (ISSN 0370-1573) will be published approximately weekly. For 1995 12 volumes, volumes 252–263 (72 issues altogether) of Physics Reports have been announced.

The subscription price for these volumes is available upon request from the Publisher.
A combined subscription to the 1995 issues of Physics Letters A, Physics Letters B and Physics Reports is available at a reduced rate.
Subscriptions are accepted on a prepaid basis only and are entered on a calendar year basis. Issues are sent by SAL (Surface Air Lifted) mail wherever this service is available. Airmail rates are available upon request. Please address all enquiries regarding orders and subscriptions to:

Elsevier Science B.V.
Order Fulfilment Department
P.O. Box 211, 1000 AE Amsterdam
The Netherlands
Tel.: +31 20 4853642, Fax: +31 20 4853598

Claims for issues not received should be made within six months of our publication (mailing) date.

U.S mailing notice – Physics Letters B (ISSN 0370-2693) is published weekly by Elsevier Science B.V., P.O. Box 211, 1000 AE Amsterdam, The Netherlands. Annual subscription price in the USA is US$ 4863.00 (valid in North, Central and South America only), including air speed delivery. Second class postage paid at Jamaica, NY 11431.
USA POSTMASTERS: Send address changes to Physics Letters B, Publications Expediting, Inc., 200 Meacham Avenue, Elmont, NY 11003.
AIRFREIGHT AND MAILING in the USA by Publications Expediting, Inc., 200 Meacham Avenue, Elmont, NY 11003.

♾ The paper used in this publication meets the requirements of ANSI/NISO 239.48-1992 (Permanence of Paper).

Printed in The Netherlands

North-Holland, an imprint of Elsevier Science

ELSEVIER

2 November 1995

PHYSICS LETTERS B

Physics Letters B 361 (1995) 110–114

Probing the pion sea with π–D Drell-Yan processes

J.T. Londergan [a,1], G.Q. Liu [b,2], E.N. Rodionov [b,3], A.W. Thomas [b,4]

[a] *Department of Physics and Nuclear Theory Center, Indiana University, Bloomington, IN 47408, USA*

[b] *Department of Physics and Mathematical Physics, University of Adelaide, Adelaide, SA 5005, Australia*

Received 5 July 1995

Editor: H. Georgi

Abstract

Pion sea quark distributions are relatively poorly determined. We show that combinations of π^+ and π^- Drell-Yan measurements on deuterium allow the pion sea distribution to be extracted. The contribution from the sea of the pion is comparable with that from its valence quarks and hence the experiment should be quite sensitive to the fraction of the pion momentum carried by the sea. We estimate the charge symmetry violating [CSV] contributions to these processes, and show that pion sea distributions could still be extracted in the presence of CSV terms.

PACS: 13.60.Hb; 12.40.Gg; 12.40.Vv

Deep inelastic lepton-nucleon scattering measurements, together with Drell-Yan and prompt photon data, enable us to establish the valence and sea quark distributions for nucleons. Recently Sutton et al. [1] have used Drell-Yan and prompt photon data to extract pion structure functions. They used Drell-Yan pion-nucleus data from the CERN NA10 [2,3] and FNAL E615 [4] experiments, and prompt photon data from the WA70 [5] and NA3 [6] Collaborations. Although the pion valence quark distributions can be constrained reasonably well by existing data, there are relatively few constraints on the pion sea distribution. Presently there is insufficient experimental Drell-Yan data for the process $\pi^{\pm}N \rightarrow \mu^+\mu^- X$, for $x_\pi \leq 0.2$, to determine unambiguously the pion sea quark distribution.

In this letter we point out that the pion sea can be extracted rather directly, by comparing Drell-Yan processes induced by charged pions on an isoscalar target such as deuterium. This work follows from recent papers [7,8] where we have examined charge symmetry violation [CSV] in nucleon and pion structure functions, and we have shown that certain combinations of pion-deuteron and pion-nucleon Drell-Yan cross sections are very sensitive to CSV effects.

In Drell-Yan processes [9], a quark (antiquark) of a certain flavor in the projectile annihilates an antiquark (quark) of the same flavor in the target, producing an intermediate photon which later decays into a μ^+–μ^- pair. For nucleon-nucleus events, the antiquark is necessarily part of the sea, so all Drell-Yan events involve at least one sea quark. Since a pion has one valence quark and one valence antiquark, various combinations of valence and sea quarks are possible for pion-nucleus Drell-Yan processes. However, combinations of positively and negatively charged pions

[1] E-mail: londergan@iucf.indiana.edu.

[2] E-mail: gliu@physics.adelaide.edu.au.

[3] E-mail: erodiono@physics.adelaide.edu.au.

[4] E-mail: athomas@physics.adelaide.edu.au.

SSDI 0370-2693(95)01132-3

(on isoscalar targets) allow the valence-valence interactions to be separated in a straightforward way.

Assuming a deuteron target, Drell-Yan cross sections for positive and negative pions have the form

$$\sigma_{\rm DY}^{\pi^+ D}(x,x_\pi) = \left[\tfrac{1}{9}q_v^\pi(x_\pi)+\tfrac{5}{9}q_s^\pi(x_\pi)\right]\left[u_v^p(x)+d_v^p(x)\right] + \left[\tfrac{10}{9}q_v^\pi(x_\pi)+\tfrac{1}{9}(20+4\kappa)q_s^\pi(x_\pi)\right]q_s^N(x)\,,$$

$$\sigma_{\rm DY}^{\pi^- D}(x,x_\pi) = \left[\tfrac{4}{9}q_v^\pi(x_\pi)+\tfrac{5}{9}q_s^\pi(x_\pi)\right]\left[u_v^p(x)+d_v^p(x)\right] + \left[\tfrac{10}{9}q_v^\pi(x_\pi)+\tfrac{1}{9}(20+4\kappa)q_s^\pi(x_\pi)\right]q_s^N(x)\,.$$

In Eq. (1) we assumed the validity of charge symmetry, i.e. $d^n(x) = u^p(x)$, $u^n(x) = d^p(x)$, etc. With this assumption, we can write all processes in terms of parton distributions in the proton. In addition, for the pion sea we assumed SU(3) symmetry, i.e. the up, down and strange quark sea distributions in the pion are equal ($u_s^\pi = d_s^\pi = s^\pi = q_s^\pi$). Finally, for the nucleon we assumed $q_s^N(x) \equiv \frac{1}{2}[u_s(x)+d_s(x)] = s(x)/\kappa$, where the fraction of the strange sea is chosen to reproduce the experimental ratio of dimuon events to single-muon events in neutrino-induced reactions [10–12] at the scale $Q^2 = Q_0^2 = 4$ GeV^2.

Under these assumptions, the valence-valence contribution for $\pi^- - D$ Drell-Yan processes is four times that for $\pi^+ - D$, while the sea-valence and sea-sea contributions are equal. Consequently, if we form the linear combinations

$$\Sigma_s^{\pi D} = 4\sigma_{\rm DY}^{\pi^+ D} - \sigma_{\rm DY}^{\pi^- D}\,,$$
$$\Sigma_v^{\pi D} = -\sigma_{\rm DY}^{\pi^+ D} + \sigma_{\rm DY}^{\pi^- D}\,, \qquad (1)$$

Σ_s contains no valence-valence contribution (it contains only sea-valence and sea-sea terms), while Σ_v contains only a valence-valence term. In terms of sea and valence distributions (for pion and proton), these quantities have the form

$$\Sigma_s^{\pi D} = \tfrac{10}{3}q_v^\pi(x_\pi)q_s^N(x) + \tfrac{5}{3}q_s^\pi(x_\pi)\left[u_v^p(x)+d_v^p(x)\right] + \tfrac{1}{3}(20+4\kappa)q_s^\pi(x_\pi)q_s^N(x)\,,$$
$$\Sigma_v^{\pi D} = \tfrac{1}{3}q_v^\pi(x_\pi)\left[u_v^p(x)+d_v^p(x)\right]. \qquad (2)$$

This means that if one measures π^+ and π^- Drell-Yan cross sections on the deuteron, and constructs the quantities Σ_s and Σ_v, then the valence-valence pion-nucleon parton distributions can be extracted from Σ_v, and the pion and/or nucleon sea can be obtained from Σ_s. Since the nucleon and pion valence distributions are reasonably well known, one should be able to predict the quantity Σ_v rather accurately.

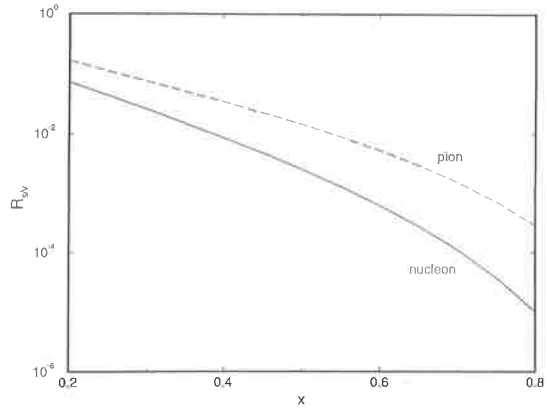

Fig. 1. (a) Predicted sea/valence ratios for pion and nucleon. Dashed curve: $r_{sv}^\pi(x)$; solid curve: $r_{sv}^N(x)$, vs. momentum fraction x, as given by Eq. (3). Nucleon parton distributions are HMRS(B) parameterization of Ref. [13]; pion distributions are those of fit 3 from Sutton et al., Ref. [1].

If one defines the sea-to-valence ratios for the pion and nucleon,

$$r_{sv}^N(x) \equiv [u_s^p(x)+d_s^p(x)]/[u_v^p(x)+d_v^p(x)]\,,$$
$$r_{sv}^\pi(x) \equiv q_s^\pi(x)/q_v^\pi(x)\,, \qquad (3)$$

then we have

$$R_{s/v}(x,x_\pi) \equiv \Sigma_s^{\pi D}/\Sigma_v^{\pi D} = 5\,r_{sv}^N(x)+5\,r_{sv}^\pi(x_\pi)+(10+2\kappa)\,r_{sv}^\pi(x_\pi)\,r_{sv}^N(x)\,, \qquad (4)$$

Although this does not "separate" entirely into pieces depending only on x or x_π it is relatively easy to isolate the piece depending on the pion sea by measuring $R_{s/v}$ at reasonably large x, where r_{sv}^N becomes quite small. Furthermore, if one assumes that the nucleon valence and sea are known, together with the pion valence distributions, then $R_{s/v}$ will be quite sensitive to the relative magnitude of the pion sea.

In Fig. 1 we show the predicted ratios $r_{sv}^\pi(x)$ and $r_{sv}^N(x)$. The sea-to-valence ratio drops off rapidly with increasing x. In Fig. 1 we have used the HMRS(B)

solution for the nucleon quark distributions [13] together with pion fit 3 of Sutton et al. [1]; for this pion parton distribution the sea carries 10% of the pion's momentum at $Q^2 = 4$ GeV^2. At large x, the nucleon sea/valence ratio $r_{sv}^N(x)$ is considerably smaller than the pion sea/valence ratio. This is because the nucleon sea of Harriman et al. [13] falls off very rapidly with increasing x [like $(1-x)^{9.75}$, relative to u_v^p which falls off like $(1-x)^{4.07}$]. Therefore as x increases, $r_{sv}^N(x)$ falls off very rapidly, and much faster than the pion sea/valence ratio. One can check this by measuring Σ_v. Assuming that one knows both the pion and nucleon valence distributions, one should be able to predict the magnitude of Σ_v, and its dependence on both x and x_π. Once this has been verified, one can use $R_{s/v}$ to determine the pion sea quark distribution.

In Fig. 2 we show predictions for $R_{s/v}$ vs. x_π, for three values of nucleon momentum fraction $x \in (0.3, 0.4$ and $0.6)$. At each value of x, we show curves corresponding to four different pion parton distributions of Sutton et al. [1]. These correspond to different fits to the NA10 Drell-Yan data [2,3], where the pion sea carries from 5% to 20% of the pion's momentum at $Q^2 = Q_0^2 = 4$ GeV^2 (i.e., these are fits 2–5 of Ref. [1]). The predicted ratio $R_{s/v}$ is quite large: e.g., for $x = x_\pi = 0.3$, $R_{s/v}$ varies from around 0.4 to 1.0 depending on the momentum fraction carried by the sea. Furthermore, $R_{s/v}$ is extremely sensitive to the momentum fraction carried by the pion sea. The quantity $R_{s/v}$ is more or less linear in this momentum fraction; the difference between a parton distribution where 5% of the pion's momentum is carried by the sea, and one where 20% of the momentum is carried by pion sea quarks, is almost a factor of 4 in $R_{s/v}$.

Thus even qualitative measurements of $R_{s/v}$ should be able to differentiate between pion parton distributions where the sea carries different fractions of the pion's momentum. Even for values of x_π as large as 0.5, where the pion sea/valence ratio is about 0.01, the quantity $R_{s/v}$ is still relatively large (about $0.3 \rightarrow 0.4$ for $x = x_\pi = 0.3$), and varies significantly depending on which pion sea one chooses.

In Fig. 3 we show the quantity $R_{s/v}$ vs. x_π, for three values of nucleon momentum fraction x (0.3, 0.4 and 0.6). As in Fig. 2, the four different curves correspond to pion structure functions where the sea carries different fractions of the pion's momentum. Fig. 3 differs from Fig. 2 in that we use the CTEQ(3M) [14] nu-

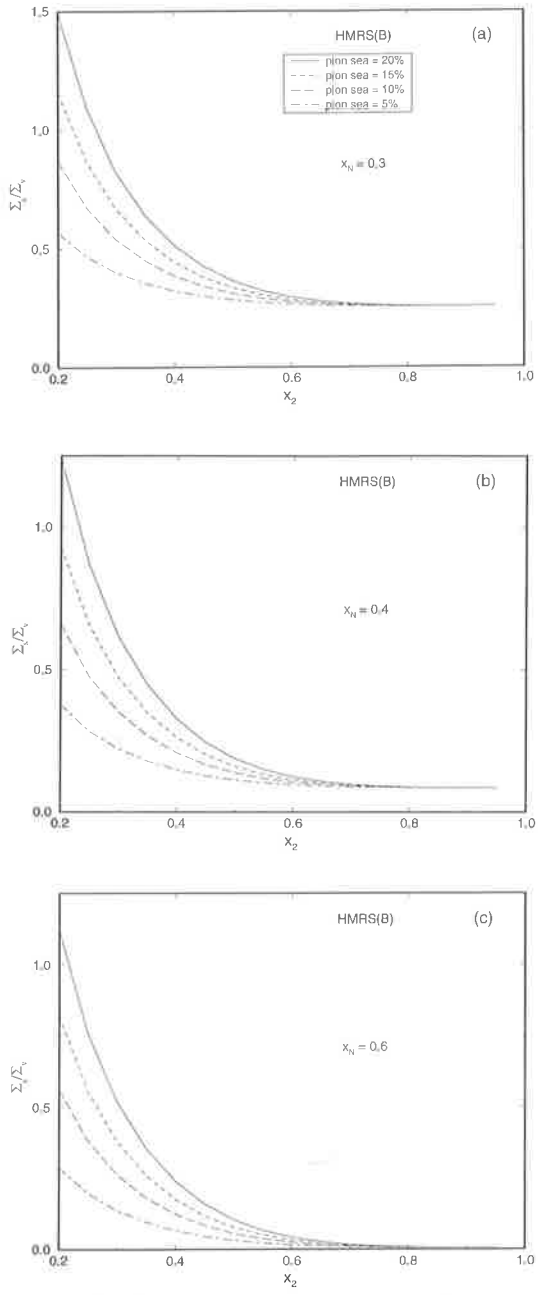

Fig. 2. Predicted sea/valence term $R_{s/v}$ of Eq. (4), vs. the pion momentum fraction $x_2 \equiv x_\pi$, for various pion sea quark distributions, which vary according to the fraction of the pion's momentum carried by the pion sea. Solid curve: pion sea carries 20% of the pion's momentum; dashed curve: pion sea of 15%; long-dashed curve: pion sea of 10%; dot-dashed curve: pion sea of 5%. (a) Nucleon momentum fraction $x_N = 0.3$; (b) $x_N = 0.4$; (c) $x_N = 0.6$. Parton distributions are those of Fig. 1.

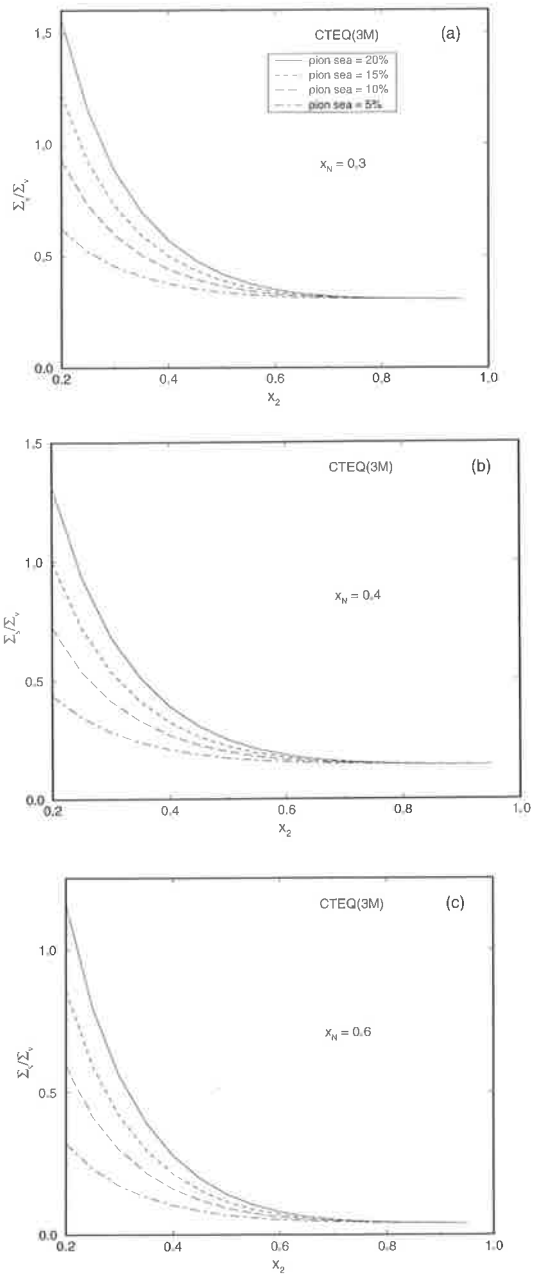

Fig. 3. Sea/valence ratio $R_{s/v}$, using the same notation as that in Fig. 2. Nucleon distributions are the CTEQ(3M) distributions of Ref. [14].

cleon structure functions, rather than the HMRS(B) structure functions of Fig. 2. Although there are some minor quantitative differences between Figs. 2 and 3, it is clearly straightforward to differentiate experimentally between the various pion sea distributions. In both Figs. 2 and 3, the quantity $R_{s/v}$ allows one to extract the pion sea distribution, and $R_{s/v}$ is extremely sensitive to the fraction of the pion momentum carried by the sea.

The Drell-Yan ratio given in Eq. (4) was derived assuming charge symmetry for the nucleon and pion structure functions. In a recent paper [8] we estimated charge symmetry violation [CSV] for both nucleon and pion (see also Ref. [15]) and found that the "minority" CSV term δd was surprisingly large. If we include CSV terms, then to lowest order in charge symmetry violation the sea/valence ratio $R_{s/v}$ will acquire additional terms

$$\delta R_{s/v} = \frac{4}{3}\left[\frac{\delta d_v(x) - \delta u_v(x)}{d_v(x) + u_v(x)}\right] - r^{\pi}_{sv}(x_\pi)\left[\frac{\delta u_v(x) + \frac{4}{3}\delta d_v(x)}{d_v(x) + u_v(x)}\right] - \delta\bar{d}_\pi(x_\pi)\left[8r^N_{sv}(x) - \frac{4}{3}\right], \quad (5)$$

where we define the charge symmetry violating terms for the nucleon and pion,

$$\delta d_v(x) \equiv d^p_v(x) - u^n_v(x),$$
$$\delta u_v(x) \equiv u^p_v(x) - d^n_v(x),$$
$$\delta\bar{d}_\pi(x) \equiv \bar{d}^{\pi^+}_v(x) - \bar{u}^{\pi^-}_v(x). \quad (6)$$

In Fig. 3 we have already included the CSV contributions to $R_{s/v}$. In Fig. 4, we show the CSV contributions $\delta R_{s/v}$ for $\pi - D$ Drell-Yan processes, assuming various values for the momentum fraction carried by the pion sea. Comparing Fig. 4 with Fig. 3 shows that, for reasonably small values of x_π, charge symmetry violation makes a quite a small contribution – of the order of 1–2% percent of $R_{s/v}$. This relative contribution grows with increasing x_π, so that for $x_\pi \approx 0.5$ the contribution is of the order of 10%. Clearly, it should be possible to extract the pion sea from such measurements even in the presence of charge symmetry violating amplitudes for both nucleon and pion. Finally, the magnitude of the CSV contributions depends very weakly on the fraction of the pion momentum carried by the sea.

These results should hold for Drell-Yan processes induced by π^+ and π^- on any isoscalar target, such as ^{12}C or ^{16}O. Furthermore, EMC effects (shifts in the

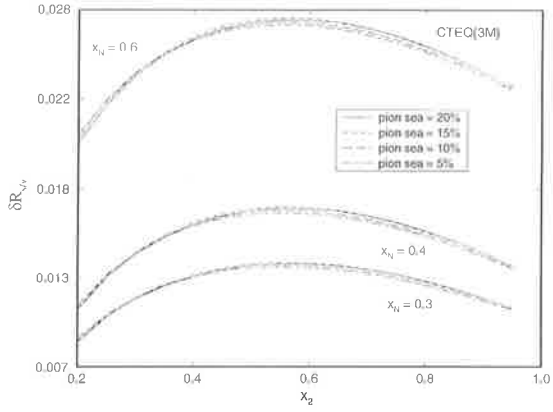

Fig. 4. Charge-symmetry violating [CSV] contributions $\delta R_{s/v}$ to the sea/valence ratio $R_{s/v}$, as given in Eq. (5). Nucleon and pion parton distributions are those of Fig. 3, and CSV contributions are those of Ref. [8].

quark distributions between free nucleons and nuclei) [16–18] will not affect the quantity $R_{s/v}$, provided EMC effects are the same for up and down quarks (and protons and neutrons). Such corrections would be the same for both numerator and denominator of $R_{s/v}$, and would cancel.

This work was supported by the Australian Research Council. One of the authors [J.T.L.] was supported in part by the US NSF under research contract NSF-PHY94-08843.

References

[1] P.J. Sutton, A.D. Martin, R.G. Roberts and W.J. Stirling, Phys. Rev. D 45 (1992) 2349.
[2] NA10 Collaboration, P. Bordalo et al., Phys. Lett. B 193 (1987) 368.
[3] NA10 Collaboration, B. Betev et al., Z. Phys. C 28 (1985) 9.
[4] E615 Collaboration, J.S. Conway et al., Phys. Rev. D 39 (1989) 92.
[5] WA70 Collaboration, M. Bonesini et al., Z. Phys. C 37 (1988) 535.
[6] NA3 Collaboration, J. Badier et al., Z. Phys. C 18 (1983) 281.
[7] E. Rodionov, A.W. Thomas and J.T. Londergan, Intern. J. Mod. Phys. Lett. A 9 (1994) 1799.
[8] J.T. Londergan, G.T. Garvey, G.Q. Liu, E. Rodionov and A.W. Thomas, Phys. Lett. B 340 (1994) 115.
[9] S.D. Drell and Tung-Mow Yan, Ann. Phys. 66 (1971) 578.
[10] CCFR Collaboration, K. Lang et al., Phys. Lett. B 317 (1993) 655;
P.Z. Quintas et al., Phys. Rev. Lett. 71 (1993) 1307.
[11] CCFR Collaboration, W. Leung et al., Z. Phys. C 33 (1987) 483;
H. Rabinowitz et al., Phys. Rev. Lett. 70 (1993) 134.
[12] CDHSW Collaboration, H. Abramowitz et al., Phys. Rev. Lett. 57 (1986) 298; Z. Phys. C 28 (1985) 51.
[13] P.N. Harriman, A.D. Martin, W.J. Stirling and R.G. Roberts, Phys. Rev. D 42 (1990) 798.
[14] CTEQ Collaboration, H.L. Lai, J. Botts, J. Huston, J.G. Morfin, J.F. Owens, J.W. Qiu, W.K. Tung and H. Weerts, preprint HEP-PH-9410404, unpublished.
[15] E. Sather, Phys. Lett. B 274 (1992) 433.
[16] EMC Collaboration, J.J. Aubert et al., Phys. Lett. B 123 (1983) 275.
[17] M. Arneodo, Phys. Rep. 240 (1994) 301.
[18] D.F. Geesaman, K. Saito and A.W. Thomas, ADP-95-13/T174, Ann. Rev. Nucl. Part. Sci. (1995), to appear.